

Succulence and Crassulacean Acid Metabolism in the Genus *Clusia*

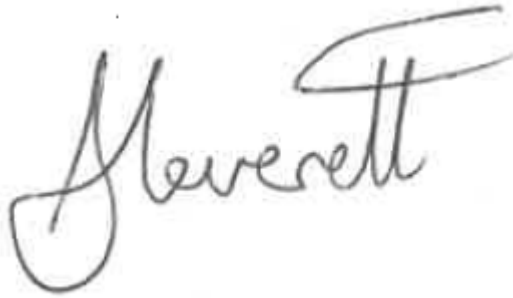
Alistair Patrick Leverett

Doctor of Philosophy

School of Natural and Environmental Sciences

November 2019

I hereby certify that this thesis is the result of my own investigations and that no part of it has been submitted for any degree other than the Doctor of Philosophy at Newcastle University. All references to the work of others are duly acknowledged.

A handwritten signature in cursive script, reading "Alistair Patrick Leverett". The signature is written in black ink on a white background.

Alistair Patrick Leverett

Abstract

Succulent plants can be found across the world in semi-arid and seasonally dry ecosystems. Succulent anatomy exists in different forms; either via large chlorenchyma cells, specialised water-storage tissue called hydrenchyma, or some combination of the two. In addition, succulent chlorenchyma tissue is often accompanied by Crassulacean acid metabolism (CAM); an altered form of photosynthesis which minimises transpirational water loss.

By comparing the hydrenchyma to the large photosynthetic chlorenchyma cells, it was shown that only succulence in the hydrenchyma provides capacitance to the leaf. In addition, the degree to which succulence and CAM contribute to leaf turgor loss point (TLP) was explored. The presence of hydrenchyma drives the TLP up, whereas the presence of CAM does not. To develop this, the ecological significance of hydrenchyma and CAM was tested, by investigating how these adaptations affect species' climatic niches. CAM, and not hydrenchyma, is an important adaptation for species ability to inhabit arid environments. As hydrenchyma and CAM were deemed to be playing discretely different, non-overlapping roles in both the physiology and ecology of CAM, it was expected that they would have different impacts on the vascular architecture of *Clusia*. Vein density was significantly lower in CAM leaves, whilst hydrenchyma has no impact, suggesting that the lower diel stomatal conductance of CAM plants requires less hydraulic conductance to replace lost water, but that the capacitance generated by hydrenchyma does not have this effect. Finally, as CAM plays an ecologically important role in species distributions, but does not affect the TLP, it was hypothesised that the relevance of this adaptation lies outside of maintaining cell turgor during drought. Accordingly, the CAM drought response was characterised by higher photosynthetic assimilation and mitochondrial respiration rates, suggesting that the purpose of CAM is to sustain metabolic rates during drought, rather than prevent drops in water potentials.

Acknowledgements

I would like to first and foremost thank my supervisor, Professor Anne Borland for her invaluable advice and assistance in completing this PhD. Annie has allowed me to have autonomy in my research, whilst also providing me regular and sound advice. I have been lucky to have such a supportive supervisor and teacher, and I know I will continue to benefit from this experience well beyond the completion of my PhD.

I would also like to thank Dr. Klaus Winter for his advice and support during my internship at the Smithsonian Tropical Research Institute. I have definitely been infected by Klaus' passion for *Clusia*, and really appreciated finding out all the history (and gossip) of research into this genus.

I would also like to thank Helen Martin, Aurelio Virgo and Milton Garcia for their technical assistance in the lab, both in Newcastle and Panama. In addition, I would like to thank Sammy Logan for his help transporting *Clusia* branches back from Cockle Park Farm to Newcastle University campus. Sammy has been extremely patient with me and given more lifts than I can count, without which I would not have been able to complete my research. Finally, I would like to thank Jorge Aranda for his assistance in identifying *Clusia* species in the field. About half the branches I collected were not actually *Clusia*, so without Jorge, this research would not have been possible.

In addition, I would like to thank all the researchers with whom I have collaborated over the last 4 years. I would particularly like to thank Samantha Hartzell, with whom regular skype calls have sparked many ideas and experiments, which span multiple chapters of this thesis. Working with Samantha to parameterise the PHOTO3 model was extremely enjoyable and I hope that it is the first of many collaborations. In addition, I would like to thank Richard Tillett for assembling the transcriptomes of *C. pratensis* and *C. tocuchensis*, and Won Yim for his bioinformatics advice.

I would also like to thank the undergraduate/masters student researchers who have worked on *Clusia* projects whilst I have been at Newcastle. Working with Kate Ferguson during the summer of 2017, Thomas Corner over the fall of 2018 and Adam Rasmussen Arda over the summer of 2019 has been a pleasure.

Finally, I would like to thank my friends Niall Convoy and Danny Cowan Turner for putting up with me going on about pressure volume curves on the walk home to Heaton. Their blank expressions were signals that I need to do better at explaining my thoughts (or maybe talk about something else when I'm not at work).

Table of Contents

CHAPTER 1. GENERAL INTRODUCTION.....	1
1.1 IDENTIFYING PHYSIOLOGICAL ADAPTATIONS TO DROUGHT	1
1.2 SUCCULENT ANATOMY	3
1.2.1 Leaf Anatomy of Eudicots.....	3
1.2.2 Succulence is a Complex Morphological Syndrome, Not a Simple Trait	6
1.2.3 Succulent Tissue Contains Large Cells to Store Water	6
1.2.4 Low Internal Air Space Associated With Succulent Anatomy is an Adaptive Trait...	9
1.2.5 Succulent Anatomy in <i>Clusia</i> is Very Diverse	10
1.3 HYDRAULIC ADAPTATIONS ASSOCIATED WITH SUCCULENT ANATOMY.....	11
1.3.1 Succulent Anatomy Provides Greater Water Stores.....	11
1.3.2 Saturated Water Content – a Simple Quantification of ‘Succulence’	11
1.3.3 Measuring Leaf Water Potential – Scholander Pressure Bomb.....	12
1.3.4 Pressure Volume Curves	14
1.3.5 The Turgor Loss Point.....	17
1.3.6 The Osmotic Potential at Full Turgor – a Proxy for the Turgor Loss Point	19
1.3.7 The Effect of Succulent Anatomy on the Turgor Loss Point.....	19
1.3.8 Hydraulic Capacitance.....	20
1.3.9 Bulk Modulus of Cell Wall Elasticity	22
1.3.10 Beyond PV Curves: Hydraulic Conductance	26
1.3.11 Vein Length per Leaf Area has a Large Effect on K_{leaf}	27
1.3.12 Vein Density in Three Dimensions: IVD:VED Ratios Determine the Efficiency of Hydraulic Conductance	27
1.3.13 Conduit Diameter Affects Species’ Loss of Hydraulic Conductance	28
1.4 METABOLIC ADAPTATIONS ASSOCIATED WITH SUCCULENT ANATOMY	30
1.4.1 Crassulacean Acid Metabolism; a Metabolic Adaptation in All-Cell Succulent Tissue	30
1.4.2 Nocturnal Accumulation of Citrate in Crassulacean Acid Metabolism	31
Box 1. Measuring Crassulacean Acid Metabolism I: Titratable Acidity, Malic and Citric Acid.....	32
1.4.3 The Role of Anatomy - Crassulacean Acid Metabolism Relies on Large Chlorenchyma Cells.....	33
1.4.4 Crassulacean Acid Metabolism Relies on Succulent Chlorenchyma, Not Hydrenchyma.....	34
1.4.5 Consequences of CAM – Higher Internal Carbon Concentrations	35
1.4.6 Succulent Anatomical Traits Affect Internal Carbon Concentration	36
1.4.7 Four Diel Phases of Gas Exchange in Plants Exhibiting Crassulacean Acid Metabolism.....	37
Box 2. Measuring Crassulacean Acid Metabolism II: Infrared Gas Analysers.....	40
1.4.8 Ecophysiological Consequences of Crassulacean Acid Metabolism – Reduced Transpiration and Stomatal Conductance	40
1.4.9 Ecophysiological Consequences of CAM – Increased Carbon Gain During Drought.....	43
1.4.10 Water Use Efficiency – Why Does it Matter?.....	46
1.4.11 Effect of Crassulacean Acid Metabolism on Species Climatic Distributions	47
1.4.12 Diversity of Crassulacean Acid Metabolism Phenotypes.....	47
1.4.13 Phases II III and IV; Variability in the Contribution of Diurnal Gas Exchange.....	48
1.4.14 Phase I; Variability in the Contribution of Nocturnal Gas Exchange.....	49

1.4.15 Crassulacean Acid Metabolism: A Continuous Trait, but a Discrete Phenotype ..	52
1.4.16 Facultative Crassulacean Acid Metabolism	53
1.4.17 Crassulacean Acid Metabolism in <i>Clusia</i> – A History	54
1.4.18 Crassulacean Acid Metabolism in <i>Clusia</i> – A Uniquely Diverse Genus.....	54
1.4.19 Crassulacean Acid Metabolism in <i>Clusia</i> – Reliance on Succulent Palisade Mesophyll Cells	55
Box 3. Measuring Crassulacean Acid Metabolism III: RNA-seq With Next Generation Sequencing	57
Questions Addressed in this Thesis, by Chapter:	58
References	59

CHAPTER 2. DISSECTING CAPACITANCE AND CRASSULACEAN ACID METABOLISM; TWO DISTINCT ADAPTATIONS TO DROUGHT IN THE GENUS *CLUSIA* 79

2.1 INTRODUCTION.....	79
2.2 MATERIALS AND METHODS	82
2.2.1 Species Studied.....	82
2.2.2 Plant Growth Conditions	82
2.2.3 Characterising Photosynthetic Physiology	83
2.2.4 Measurement of Saturated Water Content (SWC), Leaf Dry Mass per Area (LMA) and Water Mass per Area (WMA).....	84
2.2.5 Anatomical Measurements	85
2.2.6 Pressure Volume Curves	85
2.2.7 Statistics.....	86
2.2.8 PHOTO3 Model Parameterisation.....	86
2.3 RESULTS	88
2.4 DISCUSSION.....	99
2.5 CONCLUSIONS AND FUTURE CONSIDERATIONS	109
2.6 REFERENCES	110

CHAPTER 3. THE ROLE OF HYDRENCHYMA AND CRASSULACEAN ACID METABOLISM IN DETERMINING THE TURGOR LOSS POINT IN *CLUSIA* 115

3.1 INTRODUCTION.....	115
3.2 MATERIALS AND METHODS	120
3.2.1 Species Studied.....	120
3.2.2 Plant Growth Conditions	123
3.2.3 Pressure-Volume Curves.....	123
3.2.4 Anatomical Measurements	125
3.2.5 Determining Osmotic Potential at Full Turgor (π_0) for Field-Grown Plants.....	125
3.2.6 Titratable Acidity.....	126
3.2.7 Determining the Impact of Osmotic Potential (π_0) at Full Turgor and Bulk Modulus of Elasticity (ϵ) on the Turgor Loss Point.....	126
3.2.8 Statistics.....	127
3.3 RESULTS	128
3.3.1 Crassulacean Acid Metabolism Does not Affect the Turgor Loss Point in <i>Clusia</i> ..	128
3.3.2 Hydrenchyma Depth Affects the Turgor Loss Point in <i>Clusia</i>	132
3.3.3 Contribution of Osmotic Potential at Full Turgor (π_0) and Bulk Modulus of Elasticity (ϵ) to the Turgor Loss Point in <i>Clusia</i>	132
3.3.4 Changes to Bulk Modulus of Elasticity (ϵ) can Affect the Turgor Loss Point in Highly Succulent Species.....	133

3.3.5 Field Measurements	137
3.4 DISCUSSION	142
3.4.1 Summary of Findings	142
3.4.2 Crassulacean Acid Metabolism (CAM) Does not Affect the Turgor Loss Point.....	142
3.4.3 Investment in Hydrenchyma Raises the Turgor Loss Point.....	143
3.4.4 Osmotic Potential at Full Turgor (π_0), not Bulk Modulus of Cell Elasticity (ϵ) is the Mechanism by Which Hydrenchyma Affects the Turgor Loss Point	143
3.4.5 Quantifying the 'Phenotypic Space'; How Best to Interpret This Analysis?	144
3.4.6 Osmotic Potential at Full Turgor (π_0) Can Be Used as a Proxy for the Turgor Loss Point, for Field Measurements	145
3.5 CONCLUSIONS AND FUTURE CONSIDERATIONS.....	147
3.6 REFERENCES	148

CHAPTER 4. FUNCTIONAL ECOLOGY AND PHYSIOLOGY OF HYDRENCHYMA IN *CLUSIA*...153

4.1 INTRODUCTION	153
4.2 MATERIALS AND METHODS	157
4.2.1 Climatic Niche Determination.....	157
4.2.2 Field Collections and Anatomical Measurements.....	157
4.2.3 Laboratory Plant Growth Conditions.....	158
4.2.4 Dissections and Anatomical Images.....	158
4.2.5 Titratable Acidity and Osmolality	159
4.2.6 Gas Exchange.....	159
4.2.7 Diel Changes in Relative Water Content	159
4.2.8 Measurement of Saturated Water Content.....	160
4.2.9 Statistics and Graphs.....	160
4.3 RESULTS	161
4.3.1 Aridity Predicts the Occurrence of Crassulacean Acid Metabolism (CAM) but not of Hydrenchyma in <i>Clusia</i>	161
4.3.2 Species in the Cloud Forests in Panama are Characterised by Deep Hydrenchyma	161
4.3.3 Validation of Dissection Method.....	165
4.3.4 Titratable Acidity.....	165
4.3.5 The Osmotic Potential Remains Stable and Low in Hydrenchyma Tissue.....	168
4.3.6 The Water Content of the Hydrenchyma Mirrors Gas Exchange of a C_3 and CAM Species.....	168
4.3.7 Saturated Water Content (SWC) is Higher in the Hydrenchyma Than the Chlorenchyma.....	169
4.4 DISCUSSION	172
4.4.1 Aridity does not Determine Interspecific Variability in Hydrenchyma Depth in <i>Clusia</i>	172
4.4.2 The Physiology of Hydrenchyma: Validation of Method.....	182
4.4.3 The Physiology of Hydrenchyma: Maintenance of a Stable Osmotic Potential and Absence of Crassulacean Acid Metabolism.....	182
4.4.4 Long Term Aridity Does Affect Interspecific Variation in Crassulacean Acid Metabolism.....	185
4.5 CONCLUSIONS	186
4.6 REFERENCES	187

CHAPTER 5. LEAF VASCULAR ADAPTATIONS ASSOCIATED WITH CRASSULACEAN ACID METABOLISM AND SUCCULENCE IN *CLUSIA* 193

5.1 INTRODUCTION.....	193
5.1.1 <i>Leaves: the Site of Water Loss From Trees</i>	193
5.1.2 <i>Veins are Important for Conducting Water</i>	194
5.1.3 <i>Vein Length per Leaf Area (VLA) Determines Hydraulic Conductance</i>	195
5.1.4 <i>Measuring Vein Density in Three Dimensions</i>	196
5.1.5 <i>Conduit Dimensions Effect Embolism Formation</i>	198
5.2 MATERIALS AND METHODS	199
5.2.1 <i>Species Studied</i>	199
5.2.2 <i>Plant Growth Conditions</i>	199
5.2.3 <i>Photosynthetic Gas Exchange</i>	199
5.2.4 <i>Vein Length per Leaf Area (VLA) and Vein to Epidermal Surface (VED)</i>	199
5.2.5 <i>Cross-Sectional Vessel Area</i>	201
5.2.6 <i>Statistics</i>	201
5.3 RESULTS	202
5.3.1 <i>Crassulacean Acid Metabolism is Associated with Lower Vein Length per Leaf Area (VLA)</i>	202
5.3.2 <i>Crassulacean Acid Metabolism is Associated with Fewer Vein Endings</i>	202
5.3.3 <i>Thicker Leaves, Associated With Crassulacean Acid Metabolism, Require Vascular Overinvestment</i>	206
5.3.4 <i>Crassulacean Acid Metabolism Does Not Impact Vessel Sizes</i>	207
5.4 DISCUSSION.....	211
5.4.1 <i>Summary of Findings</i>	211
5.4.2 <i>Low Vein Length per Leaf Area (VLA) in Species Doing Crassulacean Acid Metabolism</i>	211
5.4.3 <i>Overinvestment in Veins in Species Doing Crassulacean Acid Metabolism</i>	216
5.4.4 <i>Crassulacean Acid Metabolism and Vessel Size; no Relationship Exists</i>	220
5.4.5 <i>Towards a Complete Anatomical Characterisation of <i>Clusia</i></i>	220
5.5 REFERENCES	222

CHAPTER 6. CRASSULACEAN ACID METABOLISM ALLOWS PLANTS TO MAINTAIN HIGHER CORE METABOLIC RATES DURING DROUGHT, IN *CLUSIA* 228

6.1 INTRODUCTION.....	228
6.1.1 <i>Global Warming is Killing Trees</i>	228
6.1.2 <i>Tree Mortality: Hydraulic Failure vs Carbon Starvation</i>	228
6.1.3 <i>Avoiding Drought Induced Mortality: Crassulacean Acid Metabolism</i>	229
6.1.4 <i>Does Crassulacean Acid Metabolism Curtail Carbon Starvation During Drought?</i>	231
6.2 MATERIALS AND METHODS	234
6.2.1 <i>Plant Growth Conditions</i>	234
6.2.2 <i>Gas Exchange</i>	235
6.2.3 <i>Nocturnal Oxygen Consumption</i>	235
6.2.4 <i>Malate and Citrate Assays</i>	236
6.2.5 <i>Biological Sampling and RNA Sequencing</i>	237
6.2.6 <i>De novo Transcriptome Assembly</i>	237
6.2.7 <i>Homolog Identification and Transcriptome Annotation</i>	237

6.2.8 Transcript Quantification, Differential Expression and Comparison of Two <i>Clusia</i> Species.....	238
6.2.9 Gene Ontology (GO) Enrichment Analysis.....	238
6.3 RESULTS	239
6.3.1 Long Term Gas Exchange – Newcastle, UK	239
6.3.2 Short Term Gas Exchange – Oak Ridge National Laboratory, USA.....	241
6.3.3 Nocturnal Oxygen Consumption	241
6.3.4 Diel Malate and Citrate Concentrations.....	242
6.3.5 RNA-seq: Transcript Annotation	247
6.3.6 Identification and Expression of ‘Core-CAM Genes’	247
6.3.7 Gene Ontology Enrichment.....	251
6.4 DISCUSSION	255
6.4.1 Summary of Findings.....	255
6.4.2 Phenotypic Characterisation of <i>Clusia pratensis</i> and <i>C. tocuchensis</i>	256
6.4.3 Maintenance of Photosynthetic Physiology During Drought	256
6.4.4 Maintenance of Respiratory Physiology During Drought.....	262
6.4.5 Identifying ‘Core-CAM Genes’ in the <i>Clusia</i> Transcriptome.....	262
6.4.6 Gene Ontology Enrichment Detects Signature of Increased Respiratory Rate.....	263
6.5 CONCLUSIONS AND FUTURE WORK	269
6.6 REFERENCES	270
CHAPTER 7. GENERAL DISCUSSION	277
7.1 ADVANTAGES OF <i>CLUSIA</i> AS A MODEL GENUS	277
7.1.1 Physiological Diversity in <i>Clusia</i>	277
7.1.2 Dissecting Hydrenchyma and Chlorenchyma Tissues	278
7.2 LIMITATIONS OF USING <i>CLUSIA</i> AS A MODEL GENUS.....	280
7.2.1 Latex	280
7.2.2 Cuticular Wax.....	282
7.3 CONCLUSIONS	284
7.3.1 The Ecophysiology of Succulent Hydrenchyma Tissue	284
7.3.2 The Ecophysiology of Succulent Chlorenchyma Tissue and Crassulacean Acid Metabolism.....	285
7.4 FUTURE WORK.....	287
7.5 REFERENCES	289
APPENDIX A. GENE ONTOLOGY ENRICHMENT FROM UPREGULATED GENES IN EACH <i>CLUSIA</i> SPECIES.....	292
APPENDIX B. <i>CLUSIA</i> LEAVES HAVE VERY LOW CUTICULAR CONDUCTANCE (G_{MIN})	303
REFERENCES	306

TABLE OF FIGURES

CHAPTER 1. GENERAL INTRODUCTION	1
FIG. 1.1) TISSUE LAYERS IN A CROSS SECTION OF <i>CLUSIA FLUMINENSIS</i> . SCALE BAR = 1 MM.	5
FIG. 1.2) HYDRENCHYMA DO NOT HAVE CHLOROPLASTS.....	8
FIG. 1.3) SCHEMATIC DIAGRAM OF A PRESSURE BOMB.....	13
FIG. 1.4) WATER POTENTIAL DROPS IN TWO PHASES AS A LEAF DEHYDRATES.	16
FIG. 1.5) THE RELATIONSHIP BETWEEN LEAF WATER POTENTIAL (Ψ_{LEAF}) AND RWC CAN BE EXPLAINED BY TWO LINEAR FUNCTIONS.	18
FIG. 1.6) THE RELATIONSHIP BETWEEN BULK TURGOR PRESSURE (P) AND RWC IS EXPLAINED BY A LINEAR FUNCTION, UP TO THE TURGOR LOSS POINT (TLP).....	25
FIG. 1.7) THE FOUR PHASES OF GAS EXCHANGE TYPICAL OF PLANTS ENGAGED IN CAM.	39
FIG. 1.8) EXTREMELY WEAK CAM CAN BE DETECTED FROM A NON-FLAT NIGHT TIME CO ₂ EFFLUX RATE. ...	51
CHAPTER 2. DISSECTING CAPACITANCE AND CRASSULACEAN ACID METABOLISM; TWO DISTINCT ADAPTATIONS TO DROUGHT IN THE GENUS <i>CLUSIA</i>	79
FIG. 2.1) STRONG CAM PLANTS HAVE MORE WATER IN THEIR LEAVES, BUT DO NOT HAVE HIGHER SATURATED WATER CONTENT (SWC).	89
FIG. 2.2) CONSTITUTIVE CAM SPECIES HAVE THICKER LEAVES, BUT DO NOT HAVE HIGHER SATURATED WATER CONTENTS (SWC).	90
FIG. 2.3) THERE ARE TWO FORMS OF SUCCULENT ANATOMY IN <i>CLUSIA</i>	92
FIG. 2.4) ALL-CELL AND WATER-STORAGE SUCCULENCE ARE ANATOMICALLY INDEPENDENT.....	93
FIG. 2.5) HYDRENCHYMA TISSUE DEPTH, NOT PALISADE DEPTH CONTRIBUTES TO SATURATED WATER CONTENT (SWC).	95
FIG. 2.6) HYDRENCHYMA CELL SIZE, NOT PALISADE CELL SIZE CONTRIBUTES TO SATURATED WATER CONTENT (SWC).	96
FIG. 2.7) SATURATED WATER CONTENT (SWC) PREDICTS CAPACITANCE, WITH A LINEAR MIXED EFFECT MODEL.....	98
FIG. 2.8) HYDRENCHYMA TISSUE DEPTH, NOT PALISADE DEPTH CONTRIBUTES TO CAPACITANCE.....	101
FIG. 2.9) HYDRENCHYMA CELL SIZE, NOT PALISADE CELL SIZE CONTRIBUTES TO CAPACITANCE.....	102
FIG. 2.10) ELASTICITY IN THE CELL WALLS OF HYDRENCHYMA CONFERS HYDRAULIC CAPACITANCE.	105
FIG. 2.11) CRASSULACEAN ACID METABOLISM PREVENTS WATER LOSS, HYDRENCHYMA DOES NOT.....	108
CHAPTER 3. THE ROLE OF HYDRENCHYMA AND CRASSULACEAN ACID METABOLISM IN DETERMINING THE TURGOR LOSS POINT IN <i>CLUSIA</i>	115
FIG. 3.1) SPECIES THAT EMPLOY CRASSULACEAN ACID METABOLISM DO NOT HAVE DIFFERENT TURGOR LOSS POINT TO C ₃ RELATIVES, IN <i>CLUSIA</i>	121
FIG. 3.2) DEEPER HYDRENCHYMA TISSUE RAISES THE TURGOR LOSS POINT IN <i>CLUSIA</i>	122
FIG. 3.3) THE OSMOTIC POTENTIAL AT FULL TURGOR, ALONE, IS A STRONG DETERMINANT OF THE TURGOR LOSS POINT IN <i>CLUSIA</i>	124
FIG. 3.4) OSMOTIC POTENTIAL AT FULL TURGOR, NOT THE BULK MODULUS OF ELASTICITY HAS THE POTENTIAL TO AFFECT THE TURGOR LOSS POINT IN <i>C. TOCUCHENSIS</i> AND <i>C. ALATA</i>	129
FIG. 3.5) OSMOTIC POTENTIAL AT FULL TURGOR, NOT THE BULK MODULUS OF ELASTICITY HAS THE POTENTIAL TO AFFECT THE TURGOR LOSS POINT IN <i>C. GRANDIFLORA</i> AND <i>C. MULTIFLORA</i>	130
FIG. 3.6) OSMOTIC POTENTIAL AT FULL TURGOR, NOT THE BULK MODULUS OF ELASTICITY HAS THE POTENTIAL TO AFFECT THE TURGOR LOSS POINT IN <i>C. LANCEOLATA</i> AND <i>C. ARIPOENSIS</i>	131

FIG. 3.7) OSMOTIC POTENTIAL AT FULL TURGOR, NOT THE BULK MODULUS OF ELASTICITY HAS THE POTENTIAL TO AFFECT THE TURGOR LOSS POINT IN <i>C. PRATENSIS</i> AND <i>C. MINOR</i>	134
FIG. 3.8) OSMOTIC POTENTIAL AT FULL TURGOR, NOT THE BULK MODULUS OF ELASTICITY HAS THE POTENTIAL TO AFFECT THE TURGOR LOSS POINT IN <i>C. ROSEA</i> AND <i>C. FLUMINENSIS</i>	135
FIG. 3.9) OSMOTIC POTENTIAL AT FULL TURGOR, NOT THE BULK MODULUS OF ELASTICITY HAS THE POTENTIAL TO AFFECT THE TURGOR LOSS POINT IN <i>C. HILARIANA</i>	136
FIG. 3.10) <i>ANACAMPSEROS LANCEOLATA</i> IS AN ALL-CELL SUCCULENT.....	138
FIG. 3.11) ELASTICITY DOES CONTRIBUTE TO THE TURGOR LOSS POINT IN OTHER SUCCULENT SPECIES.....	139
FIG. 3.12) HYDRENCHYMA, BUT NOT CRASSULACEAN ACID METABOLISM INFLUENCES THE OSMOTIC POTENTIAL AT FULL TURGOR (Π_0), IN FIELD GROWN TREES IN GAMBOA, PANAMA.....	141

CHAPTER 4. FUNCTIONAL ECOLOGY AND PHYSIOLOGY OF HYDRENCHYMA IN *CLUSIA*...153

FIG. 4.1) ARIDITY DOES NOT PREDICT THE OCCURRENCE OF HYDRENCHYMA, BUT IT DOES PREDICT THE OCCURRENCE OF CAM IN <i>CLUSIA</i>	163
FIG. 4.2) <i>CLUSIA</i> SPECIES IN CLOUD FOREST ECOSYSTEM HAVE SIGNIFICANTLY DEEPER HYDRENCHYMA TISSUE TO THOSE LIVING IN LOWLAND SEASONALLY DRY FOREST IN PANAMA.....	166
FIG. 4.3) SPECIES IN CLOUD FOREST ECOSYSTEM HAVE DEEPER HYDRENCHYMA TISSUE THAN THOSE LIVING IN LOWLAND SEASONALLY DRY FOREST IN PANAMA.....	167
FIG. 4.4) <i>CLUSIA ALATA</i> AND <i>C. TOCUCHENSIS</i> HAVE DEEP HYDRENCHYMA TISSUE.....	170
FIG. 4.5) THE METHOD FOR DISSECTING THE HYDRENCHYMA SUCCESSFULLY SEPARATES THIS TISSUE FROM THE PALISADE.....	171
FIG. 4.6) CRASSULACEAN ACID METABOLISM OCCURS IN THE CHLORENCHYMA AND NOT THE HYDRENCHYMA IN <i>C. ALATA</i>	173
FIG. 4.7) CRASSULACEAN ACID METABOLISM DOES NOT OCCUR IN THE CHLORENCHYMA OR THE HYDRENCHYMA IN <i>C. TOCUCHENSIS</i>	174
FIG. 4.8) <i>CLUSIA ALATA</i> HYDRENCHYMA MAINTAINS A STABLE OSMOTIC POTENTIAL WHICH IS HIGHER THAN CHLORENCHYMA.....	175
FIG. 4.9) <i>CLUSIA TOCUCHENSIS</i> HYDRENCHYMA MAINTAINS A STABLE OSMOTIC POTENTIAL WHICH IS HIGHER THAN CHLORENCHYMA.....	176
FIG. 4.10) <i>CLUSIA ALATA</i> AND <i>C. TOCUCHENSIS</i> HAVE DISTINCT PHOTOSYNTHETIC PHYSIOLOGIES.....	179
FIG. 4.11) <i>CLUSIA ALATA</i> AND <i>C. TOCUCHENSIS</i> HAVE DISTINCT STOMATAL CONDUCTANCE PROFILES.....	180
FIG. 4.12) DIEL FLUCTUATIONS IN HYDRENCHYMA RELATIVE WATER CONTENT (RWC) ARE DIFFERENT IN C_3 AND CAM SPECIES.....	181
FIG. 4.13) SATURATED WATER CONTENT (SWC) IS HIGHER IN THE HYDRENCHYMA THAN THE CHLORENCHYMA.....	184

CHAPTER 5. LEAF VASCULAR ADAPTATIONS ASSOCIATED WITH CRASSULACEAN ACID METABOLISM AND SUCCULENCE IN *CLUSIA*193

FIG. 5.1) VEINS DEVELOP IN ONE PLANE IN <i>CLUSIA</i> LEAVES.....	203
FIG. 5.2) SCHEMATIC DIAGRAM DEPICTING THE EFFECT OF IVD:VED RATIO ON WATER MOVEMENT INTO THE MESOPHYLL.....	204
FIG. 5.3) LEAF TISSUE USED FOR DETERMINING MAJOR VLA.....	205
FIG. 5.4) IMAGES USED TO MEASURE MINOR VLA.....	205
FIG. 5.5) CONSTITUTIVE CAM SPECIES HAVE LOWER VEIN DENSITIES.....	208
FIG. 5.6) SPECIES THAT DO CRASSULACEAN ACID METABOLISM HAVE A GREATER MAJOR : MINOR VLA RATIO.....	209
FIG. 5.7) CRASSULACEAN ACID METABOLISM SPECIES HAVE FEWER VEIN TERMINI.....	210
FIG. 5.8) CAM SPECIES OVERINVEST IN VASCULATURE.....	213
FIG. 5.9) CAM SPECIES OVERINVEST IN VASCULATURE.....	214

FIG. 5.10) VASCULAR OVERINVESTMENT IS AN ADAPTATION TO LEAF THICKNESS, AND NOT HYDRENCHYMA DEPTH.....	215
FIG. 5.11) EXAMPLE IMAGES USED TO MEASURE MIDRIB XYLEM VESSELS.....	217
FIG. 5.12) SPECIES THAT EMPLOY CAM PHOTOSYNTHESIS DURING DROUGHT HAVE NOT EVOLVED NARROWER XYLEM VESSELS, IN THEIR MIDRIBS.	218
FIG. 5.13) SPECIES THAT EMPLOY CAM PHOTOSYNTHESIS DURING DROUGHT HAVE NOT EVOLVED NARROWER XYLEM VESSELS, IN THEIR PETIOLES.	219
CHAPTER 6. CRASSULACEAN ACID METABOLISM ALLOWS PLANTS TO MAINTAIN HIGHER CORE METABOLIC RATES DURING DROUGHT, IN <i>CLUSIA</i>.....	228
FIG. 6.1) CRASSULACEAN ACID METABOLISM PREVENTS STOMATAL CLOSURE DURING DROUGHT AND ENSURES A POSITIVE CARBON BALANCE.....	240
FIG. 6.2) GAS EXCHANGE PROFILES OF <i>C. PRATENSIS</i> AND <i>C. TOCUCHENSIS</i> DURING DROUGHT.....	244
FIG. 6.3) THE INDUCTION OF CRASSULACEAN ACID METABOLISM DURING DROUGHT IS ACCOMPANIED BY IN AN INCREASED NOCTURNAL RESPIRATORY RATE.	245
FIG. 6.4) THE INDUCTION OF CRASSULACEAN ACID METABOLISM DURING DROUGHT IS ACCOMPANIED BY IN AN INCREASED NOCTURNAL RESPIRATORY RATE.	246
FIG. 6.5) DROUGHT INDUCES NOCTURNAL MALATE ACCUMULATION IN THE FACULTATIVE CAM SPECIES, <i>C. PRATENSIS</i>	249
FIG. 6.6) DROUGHT INDUCES NOCTURNAL CITRATE ACCUMULATION IN THE FACULTATIVE CAM SPECIES, <i>C. PRATENSIS</i>	250
FIG. 6.7) THREE ANNOTATION METHODS EXHIBITED SIMILAR SUCCESS RATES, BASED ON NUMBER OF TRANSCRIPTS ANNOTATED.....	253
FIG. 6.8) PEPC TRANSCRIPT ABUNDANCE INCREASES WITH THE INDUCTION OF CRASSULACEAN ACID METABOLISM.	258
FIG. 6.9) PEPCK TRANSCRIPT ABUNDANCE INCREASES WITH THE INDUCTION OF CRASSULACEAN ACID METABOLISM.	259
FIG. 6.10) NADP-ME TRANSCRIPT ABUNDANCE INCREASES WITH THE INDUCTION OF CRASSULACEAN ACID METABOLISM.	260
FIG. 6.11) ALMT TRANSCRIPT ABUNDANCE INCREASES WITH THE INDUCTION OF CRASSULACEAN ACID METABOLISM.	261
CHAPTER 7. GENERAL DISCUSSION.....	277
FIG. 7.1) LATEX EXUDATE EMERGING FROM THE CUT PETIOLE OF A <i>CLUSIA ROSEA</i> LEAF.	281
FIG. 7.2) THICK, IMPERMEABLE WAXY CUTICLES ARE DIFFICULT TO INFILTRATE IN <i>CLUSIA</i> LEAVES.	283
APPENDIX A. GENE ONTOLOGY ENRICHMENT FROM UPREGULATED GENES IN EACH <i>CLUSIA</i> SPECIES	292
APPENDIX B. <i>CLUSIA</i> LEAVES HAVE VERY LOW CUTICULAR CONDUCTANCE (G_{MIN}).....	303
FIG. A.2) <i>CLUSIA</i> EXHIBITS VERY LOW G_{MIN} VALUES, IN COMPARISON WITH DATA COLLECTED FROM A META-ANALYSIS OF ALL MEASURED SPECIES.....	305

Table of Tables

TABLE 1.1) TRANSPIRATION RATES OF A C ₃ AND CAM SPECIES OF <i>CLUSIA</i>	42
TABLE 1.2) WELL-CHARACTERISED SPECIES STUDIED IN THIS THESIS.....	56
TABLE 2.1) HYDRAULIC CAPACITANCE VALUES FOR HIGH AND LOW CAPACITANCE SCENARIOS, USED IN PHOTO3 MODEL.....	107
TABLE 2.2) PHOTOSYNTHETIC PARAMETERS USED IN PHOTO3 MODEL.	107
TABLE 2.3) SHARED HYDRAULIC VALUES USED FOR PARAMETERISING THE PHOTO3 MODEL.	107
TABLE 3.1) DERIVATIVE OF THE SLOPE AT THE POINT WHERE THE TRUE VALUE FOR Π_0 OR E INTERSECTS THE SIMULATED DATA	140
TABLE 6.1) COMPARISON OF ORTHOFINDER (USING 9 TRANSCRIPTOMES) WITH CONDITIONAL ORTHOLOGY ASSIGNMENT TOOL.....	254
TABLE 6.2) GO TERMS ENRICHED IN THE CORE-CAM GENES SIGNIFY CHANGES TO MITOCHONDRIA.	266
TABLE 6.3) GO TERMS ENRICHED IN THE CORE-CAM GENES SIGNIFY CHANGES TO RESPIRATION.	267
TABLE A.1) SIGNIFICANTLY ENRICHED 'CELLULAR COMPARTMENT' GO TERMS IN GENES UPREGULATED AFTER 20 DAYS OF DROUGHT IN <i>C. PRATENSIS</i>	293
TABLE A.2) SIGNIFICANTLY ENRICHED 'CELLULAR COMPARTMENT' GO TERMS IN GENES UPREGULATED AFTER 22 DAYS OF DROUGHT IN <i>C. TOCUCHENSIS</i>	294
TABLE A.3) SIGNIFICANTLY ENRICHED 'BIOLOGICAL PROCESS' GO TERMS IN GENES UPREGULATED AFTER 20 DAYS OF DROUGHT IN <i>C. PRATENSIS</i>	295
TABLE A.4) SIGNIFICANTLY ENRICHED 'BIOLOGICAL PROCESS' GO TERMS IN GENES UPREGULATED AFTER 22 DAYS OF DROUGHT IN <i>C. TOCUCHENSIS</i>	300

Table of Equations

Equation 1.1	14
Equation 1.2	15
Equation 1.3	15
Equation 1.4	20
Equation 1.5	21
Equation 1.6	23
Equation 1.7	23
Equation 1.8	26
Equation 2.1	84
Equation 2.2	84
Equation 2.3	84
Equation 2.4	85
Equation 2.5	86
Equation 2.6	86
Equation 3.1	119
Equation 4.1	160
Equation 4.2	160
Equation 5.1	201

Abbreviations

%	Percent
μL	Microliters
μmol	Micromole
ABA	Abscisic Acid
ALMT	Aluminium-Activated Malate Transporter
ATP	Adenine Triphosphate
BP	Biological Process
C ₃	Photosynthesis Carboxylated by Rubisco
CA	Carbonic Anhydrase
CAM	Crassulacean Acid Metabolism
CC	Cellular Compartment
CCM	Carbon Concentrating Mechanism
C _{FT}	Capacitance at Full Turgor
cm	Centimetre
CO ₂	Carbon Dioxide
C _{TLP}	Capacitance after the Turgor Loss Point
DNA	Deoxynucleic acid
E	Transpiration
FMA	Leaf Fresh Mass per Area
g	Grams
G	G Force
g _{min}	Cuticular Conductance
GO	Gene Ontology
H ⁺	Proton
Ha	Hectare
Hz	Hertz
IAS	Internal Air Space
IRGA	Infrared Gas Analyser
IVD	Intervein Distance
K	Hydraulic Conductance
L _{mes} /area	Mesophyll Area Exposed to Internal Air Space
m	Metre
MDH	Malate Dehydrogenase
microCT	X-ray Microtomography
ml	Millilitre
mm	millimetre
mMol	Millimole
Mol	Mole
MPa	Mega Pascal
NAD	Nicotinamide Adenine Dinucleotide
NAD-ME	Nicotinamide Adenine Dinucleotide - Malic Enzyme
NADP	Nicotinamide Adenine Dinucleotide Phosphate
NADP-ME	Nicotinamide Adenine Dinucleotide Phosphate - Malic Enzyme
NGS	Next Generation Sequencing

NSC	Non Structural Carbohydrate
O ₂	Oxygen
°C	Degrees Centigrade
ORF	Open Reading Frame
ORNL	Oak Ridge National Laboratory
π	Osmotic Potential
π _o	Osmotic Potential at Full Turgor
P	Turgor Pressure
P50	50 Percent Loss of Conductance
PEP	Phosphoenolpyruvate
PEPC	Phosphoenolpyruvate Carboxylase
PEPCK	Phosphoenolpyruvate Carboxykinase
PFD	Photon Flux Density
pH	Potential of Hydrogen
PLC	Percentage Loss of Conductance
PV curves	Pressure Volume Curve
RD	Read Depth
RNA	Ribonucleic Acid
RNA-seq	The Sequencing of a Transcriptome
RPK	Reads per Killobase Million
Rubisco	Ribulose Bisphosphate Carboxylase Oxygenase
RWC	Relative Water Content
s	Second
SWC	Saturate Water Content
TA	Titrateable Acidity
tDT	Tonoplast Dicarboxylate Transporter
TLP	Turgor Loss Point
TPM	Tags Per Million
VED	Vein to Lower Epidermal Distance
VLA	Vein Length per Leaf Area
VPD	Vapour Pressure Deficit
w/v	weight by volume
WMA	Leaf Water Mass per Area
WUE	Water Use Efficiency
Ψ	Water Potential
ΔH ⁺	Dawn - Dusk Difference in Proton Concentration
ε	Bulk Modulus of Cell Wall Elasticity

Chapter 1. General Introduction

1.1 Identifying Physiological Adaptations to Drought

The advent of global warming, due to the emission of greenhouse gasses, is expected to cause more frequent and severe drought events to ecosystems, worldwide (Sheffield and Wood, 2008; Choat et al., 2018). In order to prepare for increased aridity, it is imperative that scientists develop a thorough understanding of the adaptations that plants currently employ to evade and tolerate drought in nature. A strong knowledge of how plants have adapted their physiology to survive drought will aid predictions of how ecosystems will change over the next century (Trueba et al., 2019). Beyond this, identifying successful adaptations to drought can be informative of which species will be best able to survive and provide valuable ecosystem services, if introduced into an environment (Winter and Holtum 2014). Finally, concerns about the availability of water over the next century have led many to speculate that the future will require the development of more drought resistant plants for food and biofuel crops (Borland et al., 2015; Leakey et al., 2019). The increasing use of genetic engineering will allow scientists to create such crops, but this will rely on a robust understanding of how naturally occurring plants have adapted to drought, in order to predict which traits will provide benefits when modified.

One approach to understand which traits are physiologically important adaptations to drought is to conduct comparative analyses (Scoffoni et al., 2016b). By comparing closely related, but physiologically diverse species it is possible to understand how trait variation affects the plant drought response. The genus *Clusia* is comprised up of approximately 400 species, which live as either hemiepiphytes or free-standing terrestrial trees (Lüttge and Duarte, 2007). The gross morphology of all *Clusia* species is relatively similar, as every species has woody stems, with opposite, entire leaves (Lüttge 1999; Lüttge and Duarte, 2007). Despite *Clusia* containing species that share the same 'morphotype', one trait does vary considerably across this genus; leaf thickness, which can range from approximately 0.5 – 3 mm (Barrera Zambrano et al., 2014, also see Chapter 2 of this thesis). The variation in leaf thickness in *Clusia* is the consequence of different succulent anatomical adaptations (Barrera Zambrano et al., 2014; see section 1.2.5), which in turn are suspected to contribute to radical differences

in the hydraulic (see section 1.3) and metabolic physiology (see section 1.4) of these plants during drought. Based on these considerations, the scope of this thesis is:

To investigate the effect of succulent anatomy on the hydraulic and metabolic physiology of leaves in the genus *Clusia*

1.2 Succulent Anatomy

1.2.1 Leaf Anatomy of Eudicots

The anatomy of all eudicot leaves is comprised of vascular networks, epidermal and mesophyll tissues (Esau, 1965). The role of plant vasculature is to conduct water and sugars across the leaf to meet the energy and water requirements of the plant, whereas the primary purpose of the mesophyll tissue is to perform photosynthesis; harnessing the light energy to fix atmospheric CO₂ and synthesise sugars (Sack and Scoffoni, 2013). The mesophyll of eudicots is often made up of several tissue layers (Fig. 1.1). The adaxial surface is comprised of epidermal cells, making up a layer that can be 1 or more cells thick (Esau, 1965). The adaxial epidermis of some taxa contains pores in the leaf flanked by two guard cells, called stomata. However, amphistomaty (the presence of stomata on the adaxial as well as the abaxial surface of the leaf) is far rarer than hypostomaty (stomata only on the abaxial surface) (Drake et al., 2019). The tissue layer below the epidermis is the palisade, a row of densely-packed rod shaped cells that harvest light entering from above (Fig. 1.1). Palisade cells typically appear as 'I' shaped rods, although in some species, such as *Viburnum awabuki*, multiple 'rods' are joined laterally and appear as 'H' shaped cells (Chatelet et al., 2013). Below the palisade is the spongy mesophyll; a layer of sparsely spaced, spheroid-shaped cells (John et al., 2013). The sparse arrangement of spongy mesophyll cells means this tissue layer has high internal air space (IAS), and consequently a large proportion of cellular surface area is exposed to the air cavities in the leaf (John et al., 2017). By having a large portion of cellular surface area exposed to IAS, spongy mesophyll can uptake CO₂ that is entering the leaf from the atmosphere (Tomás et al., 2013). The size of palisade and spongy mesophyll cells are often allometrically linked. For example, a study of 14 phylogenetically diverse angiosperm species found that the size of palisade cells correlated strongly with the size of the spongy mesophyll cells (John et al., 2013). However, outliers do exist, such as *Clusia alata* (Clusiaceae) (Barrera Zambrano et al., 2014) and *Peperomia camptotricha* (Piperaceae) (Ting et al., 1997) which have large palisade and spongy mesophyll cells, respectively, without corresponding changes to cell sizes in other tissues. Adding to the diversity of mesophyll anatomies, are taxa that lack differentiated palisade and spongy mesophyll layers, and instead have uniform circular chlorenchyma cells. For example, in the genus *Kalanchoë* (Crassulaceae), whilst some species have differentiated palisade and spongy mesophyll, most have mesophyll tissue comprised of tightly packed,

uniform spherical cells (Abdel-Raouf, 2012). Irrespective of the anatomy of the mesophyll, the most abaxial tissue layer on the lower surface of a leaf is the abaxial epidermis (Esau 1965). Abaxial epidermal layers invariably contain stomata, which can open and close, thus controlling the movement of gases into and out of the IAS (Drake et al., 2019).

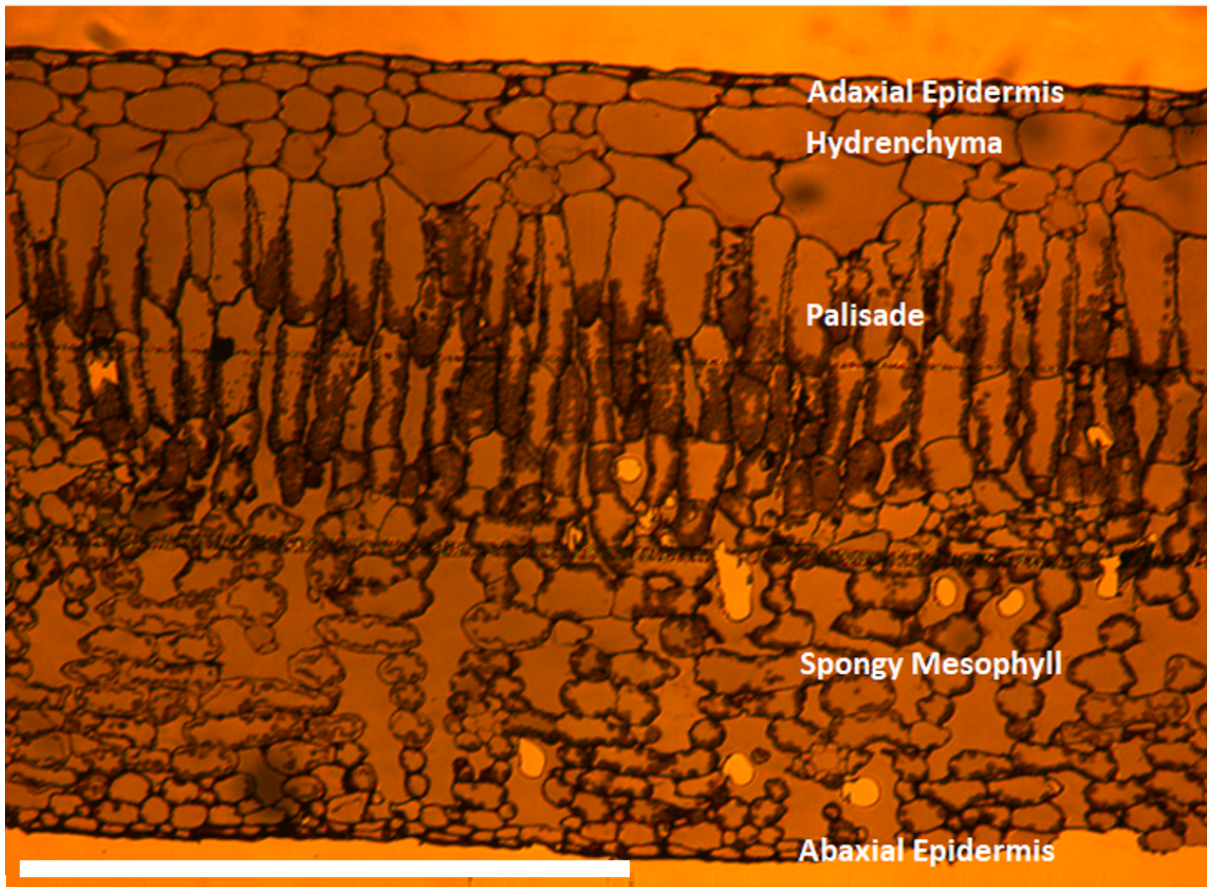


Fig. 1.1) Tissue layers in a cross section of *Clusia fluminensis*. Scale bar = 1 mm.

1.2.2. Succulence is a Complex Morphological Syndrome, Not a Simple Trait

Succulence describes anatomical adaptations that result in the storage of large volumes of water somewhere in the body of a plant (Ogburn and Edwards, 2010; 2012; Males, 2017b). Succulence can occur in stems, such as the fleshy cladodes of *Opuntia ficus-indica* (Cactaceae), or the woody tissue of *Beaucarnea gracilis* (Asparagaceae) (Ogburn and Edwards, 2010). In addition, several thousand species of leaf-succulents exist, which are defined by their storage of large volumes of water in the leaf tissue. It is important to note that succulence is not a categorical variable; there is no cut off point after which more water storage makes a species 'a succulent' (Ogburn and Edwards, 2010). In fact, even describing leaf succulence as a continuous variable, whilst sometimes valuable (see section 1.3.2), should be treated with caution. This is because succulence is often achieved not through the employment of a single trait, but rather several coordinated anatomical changes (Males 2017b). Therefore, succulence is better considered a complex syndrome, made up of multiple, distinct succulent anatomies (described in section 1.2.3). This thesis attempts to describe specific succulent anatomical adaptations, described below, rather than succulence *per se*, in order to understand how these anatomical adaptations influence the hydraulic and metabolic physiology of leaves.

1.2.3 Succulent Tissue Contains Large Cells to Store Water

A commonality of succulent anatomy in leaves is the development of large cells, which provide increased tissue depth in order to store water (Males, 2017b). One way succulent anatomy can develop is through the evolution of large photosynthetic chlorenchyma cells. For example, in the genus *Kalanchoë*, the tightly packed mesophyll layer is made up of swollen cells that can hold large volumes of water (Smith and Lüttge, 1985; Griffiths et al., 2008; Abdel-Raouf, 2012). Furthermore, in taxa with well-defined palisade and spongy mesophyll tissues, large succulent cells can evolve in a specific layer. For example, succulent anatomy is found in the spongy mesophyll, but not the palisade cells in *Peperomia* (Piperaceae) (Gibeaut and Thomson, 1989). The development of large chlorenchyma cells, which is often described as 'all-cell' succulence, allows plants to store water without the need to develop specialised water storage tissue. However, the development of specialised water storage tissue, which is

distinct from the chlorenchyma, is an alternative way in which plants have evolved leaf-succulence. Water storage tissue, called hydrenchyma, is a convergent adaptation found across the tracheophytes (Kaul 1977; Gibeaut and Thomson, 1989; Nowak and Martin, 1997; Borland et al., 1998; Chiang et al., 2013, Barrera Zambrano et al., 2014; Males 2018). Hydrenchyma tissue is typically made up of large, spheroid or cuboid cells with thin cell walls. Hydrenchyma tissue can exist as an adaxial epidermal layer, as in *Peperomia*, *Clusia* and *Pitcairnia* (Bromeliaceae) (Gibeaut and Thomson, 1989; Borland et al., 1998; Males 2017a). In contrast, some species develop a sub-mesophyllous hydrenchyma tissue, at the centre of the leaf, as seen in *Agave* (Agavaceae) and *Aloe* (Asphodelaceae) (Smith et al., 1987; Grace et al., 2015; Ahl et al., 2019). Hydrenchyma is often described as achlorophyllous (Fig. 1.2), although some species do contain small numbers of chloroplasts in this tissue (Nishio and Ting, 1987). Nevertheless, the primary function of hydrenchyma is not photosynthesis; this tissue exists to provide a specialised storage tissue, thereby allowing leaves to hold greater volumes of water. Hence, in contrast to swollen chlorenchyma cells, the development of deep hydrenchyma tissue in leaves is known as 'storage-succulence'.

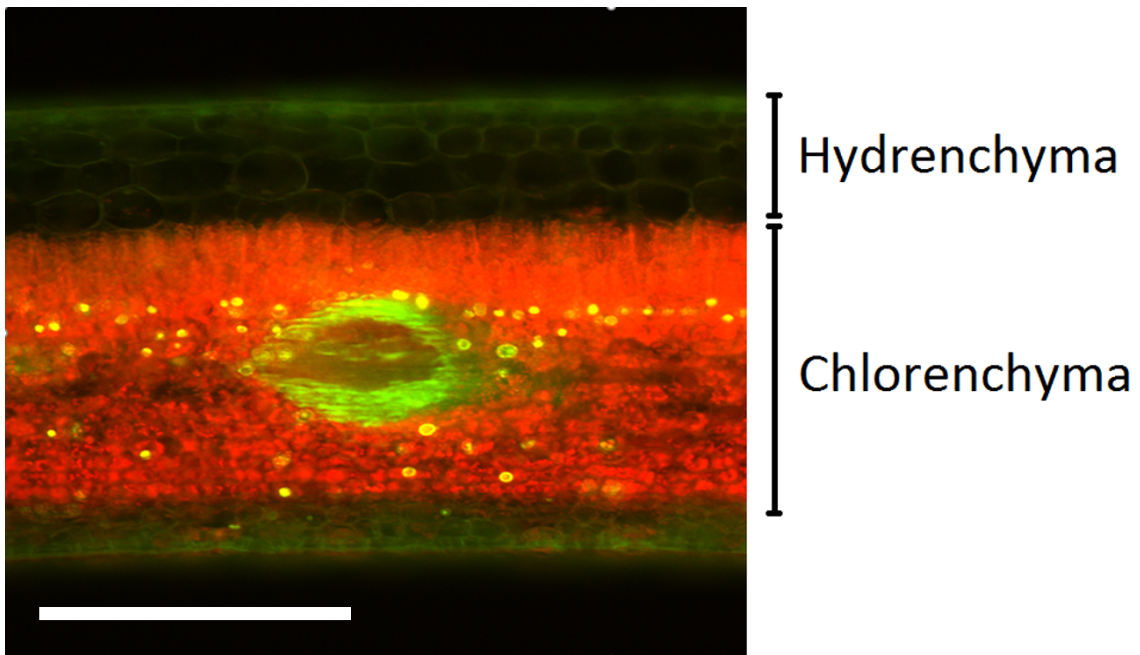


Fig. 1.2) Hydrenchyma do not have chloroplasts. Hand-cut section of *C. multiflora* imaged under a fluorescent microscope. Chlorenchyma tissue fluoresces due to the presence of chlorophyll, whereas adaxial hydrenchyma does not, because chloroplasts are absent from this tissue. Scale bar = 0.5 mm.

1.2.4 Low Internal Air Space Associated With Succulent Anatomy is an Adaptive Trait

One anatomical trait often found in species with high degrees of all-cell or water-storage succulence is a low IAS. Low IAS is often attributed to large succulent cells packing tightly together and hence minimising the fraction of air space in the leaf. However, many species without succulent anatomy, such as *Gentianella amarella* (Gentianaceae), *Antennaria umbrinella* (Asteraceae) and *Bistorta officinalis* (Polygonaceae) have very low IAS values (below 6 %). In addition, *Arabidopsis thaliana* (Brassicaceae) mutants, created to have large, swollen chlorenchyma cells do not appear to have low IAS (Lim et al., 2018). Taken together, these observations show that control of IAS can be independent of cell size. Therefore, the low IAS associated with succulent anatomy cannot simply be explained as an evolutionary spandrel (i.e. a by-product of large cells), as this trait has been selected for in taxa with succulent species (Gould and Lewontin, 1979).

Most studies of IAS, such as those referenced in the previous paragraph, have focused on porosity, which is the percentage of total leaf content made up by air. Porosity can be measured by measuring the percentage of anatomical sections made up by air space, or by vacuum infiltrating leaves with water and measuring any changes in mass (Smith and Heuer, 1981; Barrera Zambrano et al., 2014; Males 2018). Low porosity decreases the mesophyll cell surface exposed to IAS ($L_{mes}/area$), meaning less area is available for the exchange of gases (a full discussion of the consequences of low $L_{mes}/area$ are provided in section 1.4.6). In addition, recent advances in imaging leaf anatomy in three dimensions, such as x-ray microcomputed tomography (microCT), have shown that low porosity increases IAS tortuosity, a parameter that can only be measured when considering anatomy in 3 dimensions. Tortuosity is defined as the path length a gas must follow when diffusing across the IAS, divided by the Euclidean distance. Alongside lower porosity, succulent anatomy is associated with higher IAS tortuosity in leaves. Therefore, the low IAS in succulent tissues is not only associated with reduced porosity, as both $L_{mes}/area$ and tortuosity are also significantly different in succulent tissues.

1.2.5 Succulent Anatomy in *Clusia* is Very Diverse

In some taxa only one form of succulent anatomy (i.e. large chlorenchyma and hydrenchyma cells) is present. For example, species within the Crassulaceae have typically evolved succulent anatomy in the form of large chlorenchyma cells, whereas in some Aizoaceae, the development of hydrenchyma predominates (Ripley et al., 2013). Consequently, Ripley et al., (2013) categorised these two families as all-cell and storage-succulents, respectively. However, many taxa cannot be categorised so easily, because both large succulent chlorenchyma and hydrenchyma cells can develop, even in the same species. For example, in the family Bromeliaceae, large, succulent cells have evolved in both the chlorenchyma and hydrenchyma, as both tissue layers contribute to increasing water storage in the leaf. At a higher taxonomic resolution, species in the genus *Clusia* have evolved succulence with either large chlorenchyma, deep hydrenchyma or a combination of the two (Popp et al., 1987; Borland et al., 1998; Barrera Zambrano et al., 2014). The percentage of total leaf depth made up by hydrenchyma ranges from ~ 5-30 % in this genus, meaning some species develop deep hydrenchyma whereas others do not. In the chlorenchyma, all-cell succulent anatomy occurs predominantly in the palisade tissue layer. A large range of palisade cell sizes exist in *Clusia*, meaning the percentage of total leaf depth made up by this tissue ranges from 25-45 %. In contrast, the spongy mesophyll makes up ~ 50 % of leaf depth in every species in *Clusia*. The lack of succulent anatomy in the spongy mesophyll is associated with large IAS in *Clusia*, whereas the palisade and hydrenchyma cells are tightly packed together and have low IAS porosity. Importantly, all-cell and storage-succulence are independent in *Clusia*, as no correlation exists between the size of chlorenchyma and hydrenchyma cells in this genus (Barrera Zambrano et al., 2014; also see reanalysis of data from Barrera Zambrano et al., (2014) in Chapter 2 of this thesis). This makes *Clusia* an ideal model for investigating the physiological consequences of succulent anatomy, as it is possible to conduct comparative analyses to dissect the roles of hydrenchyma from those of large palisade cells, within closely related species.

1.3 Hydraulic Adaptations Associated With Succulent Anatomy

1.3.1 Succulent Anatomy Provides Greater Water Stores

One fundamental reason that plants are believed to evolve succulent anatomy is to provide water stores for use during periods of drought; more investment in water-storage hydrenchyma tissue or enlarged chlorenchyma cells means a greater volume of stored water is present inside plant organs (Ogburn and Edwards, 2010). Therefore, a comprehensive study of succulence in *Clusia* would be incomplete without an investigation into the water relations and hydraulic physiology of the leaves in this genus. To this end, several methodologies exist to measure biophysical properties that each contribute to the hydraulic response to drought. These methods, and the parameters they measure are outlined below:

1.3.2 Saturated Water Content – a Simple Quantification of ‘Succulence’

‘Succulence’ is a complex syndrome made up of many anatomical traits, such as large hydrenchyma and/or chlorenchyma cells and low IAS (see section 1.2.3). These anatomical adaptations have the combined effect of increasing the water content in a leaf or stem tissue. Therefore, it is often beneficial to quantify the water stores in a given species, in addition to the anatomical changes associated with the succulent syndrome. Several different methods have been employed to describe the water stores in succulent leaves. Some studies have quantified succulent water stores by measuring the leaf fresh mass per area (FMA) (Griffiths et al., 2008; Barrera Zambrano et al., 2014), or measuring the mass of water per leaf area (WMA), (Males and Griffiths 2017). However, some species, can have thick mesophyll tissues without any large succulent cells, and others can have large succulent cells without deep, thick leaves (Nowak and Martin, 1997; Ogburn and Edwards, 2010; John et al., 2014). To overcome this limitation, succulence is often quantified using the saturated water content (SWC), which is a unitless parameter calculated by dividing the mass of water by the dry mass of a tissue (Ogburn and Edwards, 2012; Ogburn and Edwards, 2013; Ripley et al., 2013; Males and Griffiths, 2017). SWC is often higher in species with larger, succulent cellular anatomy because the ratio of water to biomass will be higher. Furthermore, SWC appears to correlate with species’ hydraulic capacitance (capacitance is discussed in more detail in section 1.3.8),

meaning that SWC is a physiologically meaningful parameter that relates to species' ability to buffer themselves against drought. It is important to note that whilst SWC provides a physiologically meaningful quantitative estimate of succulence, this value is an average for the whole leaf. Therefore, SWC does not assess succulence as a syndrome made up of multiple anatomical adaptations. As such, no information currently exists about the relative role of all-cell and water-storage succulence on the SWC of leaves.

1.3.3 Measuring Leaf Water Potential – Scholander Pressure Bomb

Integral to the hydraulic study of leaves is the pressure bomb (Scholander et al., 1965), a device that measures the water potential (Ψ_{leaf} : i.e. the free energy of water) of leaves. To measure the water potential using a pressure bomb, a leaf is cut at the petiole and sealed into a chamber, such that only the cut petiole is exposed to the outside world (Fig. 1.3). By applying external pressure to the inside of the chamber with compressed gas, water is forced out of the cells across semi-permeable plasma membranes and moves into the veins and up towards the cut petiole. The point at which the pressure inside the chamber is equal in magnitude to the negative water potential inside the leaf (a point called the balancing pressure), bubbles of water become visible emerging from the cut petiole. Thus, by gradually increasing the pressure inside the chamber it is possible to measure the water potential of the leaf.

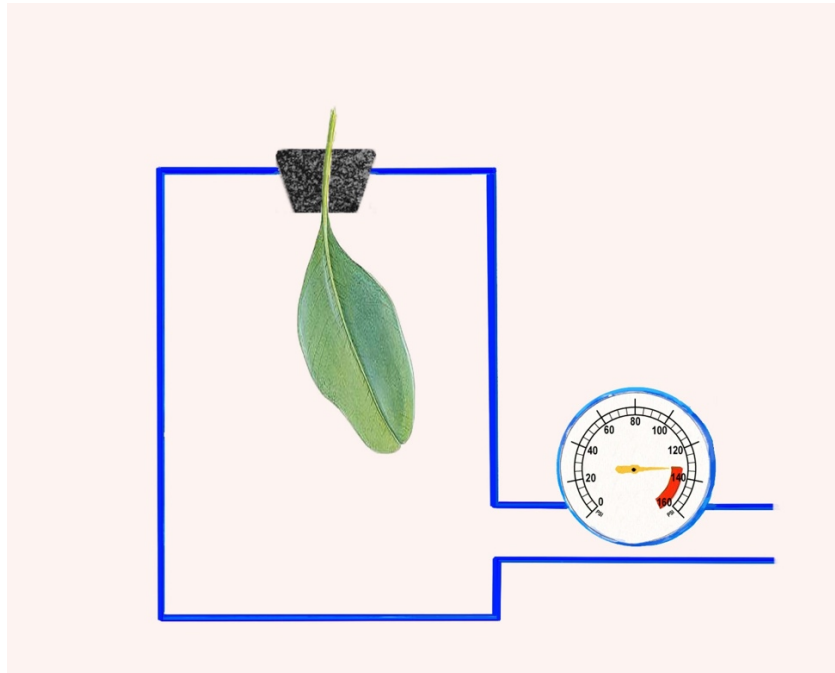


Fig. 1.3) Schematic diagram of a pressure bomb. A leaf is sealed inside the chamber, so that only the cut petiole is exposed. External pressure is applied using compressed gas. When water droplets emerge from the cut petiole, the pressure in the leaf is equal in magnitude to the water potential of the leaf.

In a well hydrated leaf, assuming that the differential effect of gravity on leaf water potential is negligible, Ψ_{leaf} is determined by two factors: the osmotic potential (π) and the turgor pressure (P). Osmotic potential is a term that describes the contribution of osmotically active dissolved solutes to the free energy of water. The maximum osmotic potential possible is that of pure water, which has an osmotic potential of 0 MPa, therefore the osmotic potential inside a leaf is always negative (Beadle et al., 1985). If a greater concentration of osmolytes are dissolved, the water has less free energy and hence the osmotic potential is lower (more negative). Turgor pressure, on the other hand, is a positive pressure inside a leaf, which contributes to the final water potential. Turgor is the consequence of water moving into cells, by osmosis, which causes the plasma membrane to swell and push against the surrounding cell walls (Beadle et al., 1985; Zhang et al., 2016). This positive pressure increases the water potential of the leaf, but is never greater in magnitude than the negative osmotic potential. Hence, like the osmotic potential, the water potential of a leaf is always negative. Based on the aforementioned considerations, the water potential of a leaf can be described by the equation:

Equation 1.1

$$\psi_{\text{leaf}} = \pi + P$$

Where π is the osmotic potential and P is the turgor pressure.

1.3.4 Pressure Volume Curves

Measuring Ψ_{leaf} can be a valuable way to understand the drought stress a plant is experiencing. For example, if water transfer between the soil and roots is possible, then during periods of stomatal closure, Ψ_{leaf} will equilibrate with Ψ_{soil} ; hence Ψ_{leaf} can be used to describe the degree of drought stress a plant is experiencing (Buckley, 2019). However, interspecific comparisons are most valuable when they describe species' capacity to tolerate and/or prevent stress, rather than the stress a plant is experiencing under specific conditions (Hochberg et al., 2018). To explore interspecific variation, a pressure bomb can be used to construct 'pressure-volume curves' (PV curves). This technique, described below, allows scientists to measure six traits pertaining to the hydraulic physiology of leaves.

Central to constructing PV curves is the sequential measurement of Ψ_{leaf} on the same leaf, as it dehydrates. To measure the degree of leaf dehydration, the relative water content (RWC) is calculated. RWC is calculated as:

Equation 1.2

$$RWC = \frac{FM - DM}{FM_{FT} - DM} \times 100$$

Where FM is fresh mass during the dry-down experiment, DM is the dry mass and FM_{FT} is the fresh mass at full turgor, for fully hydrated leaves. By calculating 100-RWC, it is possible to determine the percentage water loss, as an estimate of how dehydrated a leaf is. As water is lost from a well hydrated leaf, the osmolyte concentration will increase due to their being lower aqueous solvent volume. Therefore, as a leaf dehydrates π will become more negative. In conjunction, the initial loss of water from a leaf will decrease cell turgor; lower water availability means less positive pressure is generated from plasma membranes pushing against cell walls. Since both π and P decrease during early stages of leaf drought, Ψ_{leaf} will drop sharply (Fig. 1.4). However, eventually enough water will be lost that P decreases to zero, as more severe drought will mean insufficient water is available to generate any turgor pressure. Once $P = 0$, Equation 1.1 can be expressed as:

Equation 1.3

$$\psi_{\text{leaf}} = \pi$$

The consequence of this is that following the loss of turgor, Ψ_{leaf} drops less rapidly, as a falling value for P can no longer contribute to this trend (Fig 1.4). Together, these considerations cause the drop in Ψ_{leaf} to occur in two phases: an initial rapid decline in Ψ_{leaf} , followed by a slower drop (Fig. 1.5). The two phases of declining Ψ_{leaf} can both be represented by straight lines, because both π and P drop linearly with declining RWC. Analysis of these linear changes can yield a great deal of information about the hydraulic physiology of a leaf. The physiological parameters that can be derived from PV curves and their ecological significance is discussed below.

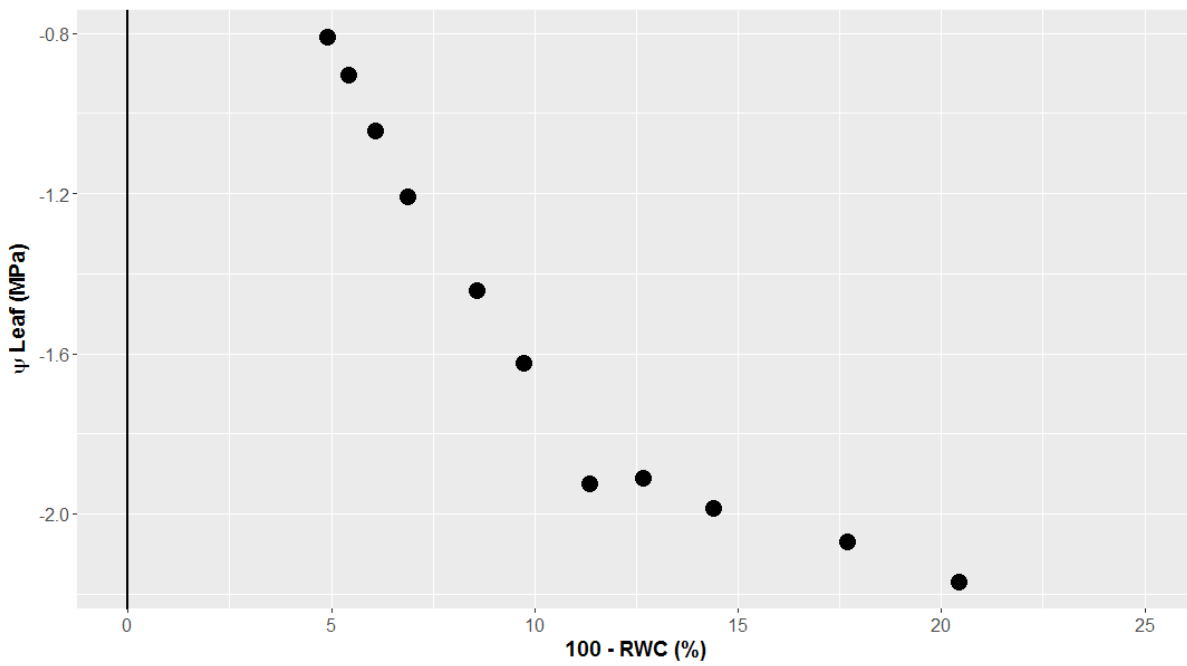


Fig. 1.4) Water potential drops in two phases as a leaf dehydrates. Graph shows drop in water potential (Ψ_{leaf}) against dehydration level of a leaf (100-RWC). Two phase of water loss can be seen to occur: an initial, steep drop in Ψ_{leaf} due to declining π and P, and a more gradual drop when P = 0 and $\Psi_{\text{leaf}} = \pi$.

1.3.5 The Turgor Loss Point

As seen in Fig. 1.4 and Fig. 1.5, as a leaf dehydrates, an inflection point exists where the initial sharp decline in Ψ_{leaf} becomes more gradual. This inflection point is the consequence of P falling to zero in the leaf, at which point $\Psi_{\text{leaf}} = \pi$ (Equation 1.1 and Equation 1.3). Therefore, this inflection point is known as the turgor loss point (TLP), as the cells are no longer able to maintain any positive turgor pressure in the leaf (Bartlett et al., 2012b). The TLP in many species causes wilting, i.e. leaves become flaccid and often bend over (Tyree and Hammel, 1972; Trueba et al., 2019). However, not all species display a visible wilting phenotype as some leaves maintain their gross rigidity even in the absence of cell turgor. Once the inflection point from the loss of turgor is identified on a PV curve graph, the value of Ψ_{leaf} and RWC at which this occurs can be measured (see the straight lines going to the x and y axes in Fig. 1.5). Consequently, the TLP can be described both in terms of the water potential or the RWC that causes a loss of turgor (TLP_{Ψ} and TLP_{RWC} , respectively).

The loss of turgor in a leaf is coordinated with a decline in stomatal gas exchange (Box 2) and efficient hydraulic conductance (Section 1.3.10) during drought (Brodribb and Holbrook, 2003; Brodribb et al., 2003; Nolan et al., 2017; Griffin-Nolan et al., 2019). Therefore, the extent to which turgor can be maintained as a leaf dehydrates is instrumental to a species' ability to maintain basic physiological functions during drought (Trueba et al., 2019). Both TLP_{Ψ} and TLP_{RWC} are estimates of drought tolerance; the former describes the extent to which a species can withstand low water potentials and the latter represents the ability to withstand low water contents (Bartlett et al., 2012a; Bartlett et al., 2012b). Whilst both TLP_{Ψ} and TLP_{RWC} represent drought tolerance, a global meta-analysis found that the former was best predicted by species' environmental conditions; species that experience more drought *in situ* tend to have lower TLP_{Ψ} and therefore can tolerate more negative water potentials (Bartlett et al., 2012b). In addition, seasonal variation in TLP_{Ψ} appears to be low in tropical trees (Bartlett et al., 2014; Maréchaux et al., 2017), meaning that this physiological parameter can be measured at any time of the year and still provide a meaningful estimate of the species capacity to tolerate drought.

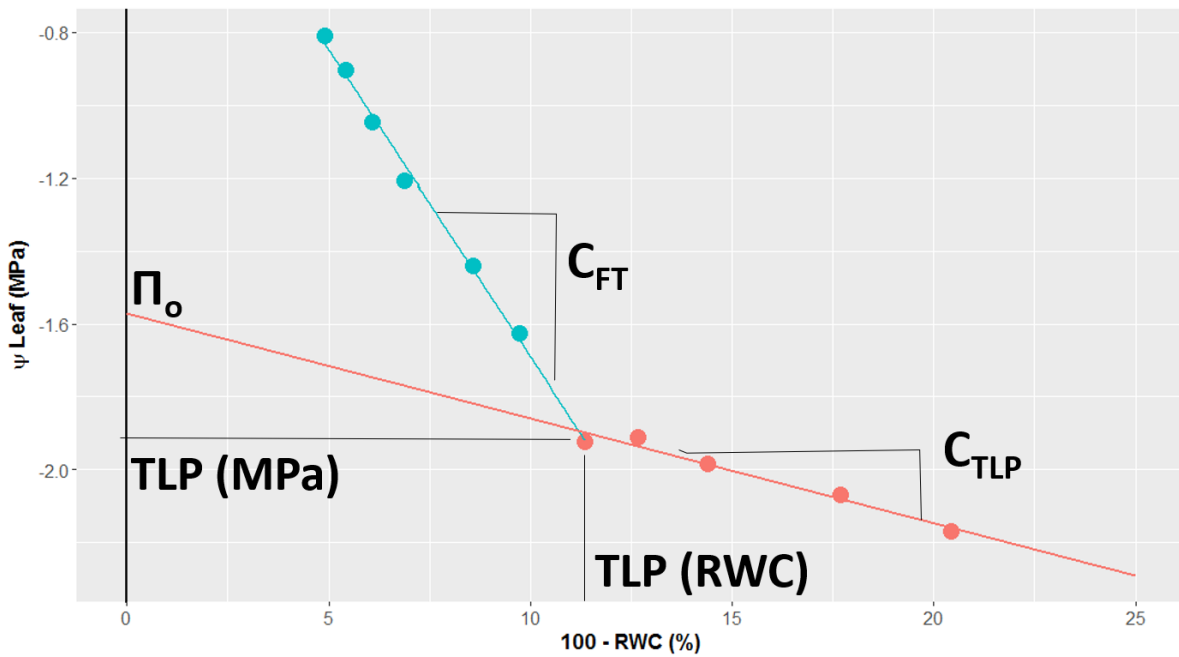


Fig. 1.5) The relationship between leaf water potential (Ψ_{leaf}) and RWC can be explained by two linear functions. The inflection point between these two straight lines, where the blue and red lines meet, is the turgor loss point (TLP). Blue line represents falling Ψ_{leaf} before the TLP. This sharp drop in Ψ_{leaf} in the blue line is the consequence of both osmotic potential (π) and turgor pressure (P) falling as the leaf dehydrates. At RWC values below the TLP, the red line shows a more gradual drop in Ψ_{leaf} , that is caused only by falling π , as $P = 0$. This red line can be extrapolated back to higher RWC values to calculate π before the TLP. Extrapolating the line to the y axis calculates the osmotic potential at full hydration (π_o). Relative capacitance is calculated as the gradient between Ψ_{leaf} and RWC, and can be calculated before or after the TLP (C_{FT} and C_{TLP} , respectively).

1.3.6 The Osmotic Potential at Full Turgor – a Proxy for the Turgor Loss Point

After leaves dehydrate to the TLP, the gradual drop in Ψ_{leaf} is the sole consequence of dropping π (Equation 1.3). Because this gradual drop occurs linearly, it is possible to use a linear regression to extrapolate the value of π at any RWC, even when the leaf is hydrated and still has cell turgor. This is demonstrated by the red line in Fig. 1.5, which extends from the TLP to the y axis. By extrapolating all the way back to the y axis, where RWC = 100 %, it is possible to calculate the osmotic potential at full hydration (π_o). The value of π_o is determined by the osmolality (i.e. the concentration of osmotically active solutes and ions) in the fully hydrated leaf (Beadle et al., 1985). The value of π_o correlates strongly with TLP_{Ψ} (Bartlett et al 2012a). This is clear if one considers the entire red line in Fig. 1.5: if the value of π_o drops, and the gradient of the line remains the same, then the TLP_{Ψ} will fall to the same extent (i.e. the TLP_{Ψ} will fall by the same number of MPa). As a result, species accumulate osmolytes in order to acquire an π_o value that will in turn determine the TLP_{Ψ} (Bartlett et al., 2012b). Due to the mechanistic relationship between π_o and TLP_{Ψ} , these parameters correlate tightly across species. The relationship between π_o and TLP_{Ψ} exists in tropical and temperate trees species, woody shrubs in arid ecosystems, herbaceous species in grassland meadows and even succulent taxa (Bartlett et al., 2012a; Bartlett et al., 2012b; Griffin-Nolan et al., 2019). The ubiquity of this relationship has one major technical advantage: π_o , which can be measured in minutes using an osmometer, can be used as a proxy for TLP_{Ψ} , which takes 1 – 9 days to measure using PV curves (Bartlett et al., 2012a). Consequently, many researchers have started using π_o to estimate the TLP_{Ψ} for large numbers of species (Maréchaux et al., 2015; Males and Griffiths, 2017; Maréchaux et al., 2017; Medeiros et al., 2019; Méndez-Alonzo et al., 2019).

1.3.7 The Effect of Succulent Anatomy on the Turgor Loss Point

The precise role that each form of succulent anatomy has on the TLP has not been well documented, presumably because it is technically difficult to generate PV curves on large, fleshy leaves (Ogburn and Edwards, 2010). It is known that epiphytic species, which are often characterised by succulent anatomy typically have high TLP_{Ψ} (or π_o) values; meaning they are more vulnerable to negative water potentials than terrestrial relatives (Martin et al., 2004; Males and Griffiths, 2018). It has been suggested that this is due to the presence of deep

hydrenchyma tissue (Martin et al., 2004; Silvera and Lasso, 2016), although no studies have robustly shown the presence of deeper hydrenchyma in epiphytes (Katia Silvera, personal communication). As hydrenchyma is known, in limited cases, to have higher (less negative) values of π_o (Schmidt and Kaiser, 1987; Smith et al., 1987; Nobel, 2006) a greater investment in this tissue may cause species to have higher TLP_{Ψ} and be more vulnerable to drought. The contribution of enlarged chlorenchyma cells to the TLP_{Ψ} is even less understood; hence it is not known if all-cell succulent anatomy affects the TLP_{Ψ} in the same way as hydrenchyma, or even at all. Despite the lack of research into the role of succulent anatomy in determining the TLP_{Ψ} , succulent species are often described as ‘drought avoiders’, as they are thought to have limited ability to maintain cell turgor when tissue has become sufficiently dehydrated to cause plant water potentials to fall (Ogburn and Edwards, 2010; Males 2017b). For example, analysis of 25 species in the Caryophyllales found that high SWC, which was used as a quantitative metric for succulence, correlated with high (less negative) values of TLP_{Ψ} (Ogburn and Edwards, 2012). Rather than evolving an ability to withstand low internal water potentials, succulent anatomy is considered an adaptation to prevent plants from experiencing negative water potentials altogether. However, the relative contribution of succulent anatomy in the hydrenchyma and chlorenchyma to this avoidance strategy remains unclear.

1.3.8 Hydraulic Capacitance

How can plants avoid experiencing negative water potentials during periods of low rainfall? Typically, this feat is achieved by the process of hydraulic capacitance, which describes a species ability to buffer the water potential in leaves or stems in response to water loss (Beadle et al., 1985; Ogburn and Edwards, 2012). Hydraulic capacitance in a leaf is the ratio of changing water loss (the drop in RWC) to changing Ψ_{leaf} , described by the equation:

Equation 1.4

$$C = \frac{\Delta RWC}{\Delta \Psi_{leaf}}$$

Thus, capacitance is the linear gradient between RWC and Ψ_{leaf} . Because the relationship between RWC and Ψ_{leaf} is described by two straight lines (see the blue and red lines in Fig. 1.5), hydraulic capacitance for a species can be calculated both before and after the TLP.

A greater slope between RWC and Ψ_{leaf} means the leaf experiences more severe drops to water potential when water loss occurs. For example, if two leaves both lose 10 % of their RWC before the TLP is reached, but they experience a 1 MPa and a 2 MPa drop in Ψ_{leaf} , respectively, the former has higher capacitance as it is better able to buffer Ψ_{leaf} during drought. However, this example somewhat oversimplifies true plant physiology, because comparing two leaves that have lost 10 % of their RWC does not account for the absolute volume of water that is being lost (Ogburn and Edwards, 2010). In reality, a 10 % water loss from the massive leaves of *Agave deserti* and the thin leaves of *Encelia farinosa* (Asteraceae) are physiologically distinct phenomena, due to these species having substantially different initial water contents (Nobel and Jordan, 1983). To overcome this issue, the relative capacitance described in Equation 1.4 is converted to an absolute capacitance by the equation:

Equation 1.5

$$\text{Absolute Capacitance} = C \times WMA/18$$

Where WMA is the water mass per leaf area in a fully hydrated leaf and 18 is the molar mass of water. Equation 1.5 calculates absolute capacitance by combining the ability to buffer Ψ_{leaf} against drops in RWC, with the volume of water stored in well hydrated leaves, thereby providing a valuable parameter that describes a species' ability to avoid experiencing dangerous negative water potentials.

Capacitance is believed to be an integral component of the ecophysiological strategy of succulent plants (Ogburn et al., 2010; Males 2017b). A study of 25 species in the Carophyllales found that plants with greater water stores (determined by measuring SWC) had substantially higher capacitance (Ogburn and Edwards, 2012). This study measured relative capacitance (Equation 1.4), because some species were so fleshy that they had lost the abaxial/adaxial axis in the leaves, and hence measurement of WMA was not possible.

Nevertheless, the large water stores in succulent cells invariably cause leaves to have higher WMA and is therefore likely to increase the absolute capacitance (Equation 1.5). In addition, evidence from storage-succulents in the genus *Peperomia* has shown that ionic salts can move from the hydrenchyma to the chlorenchyma during drought, establishing an osmotic gradient between the two tissues which drives the movement of water into the photosynthetic cells (Schmidt and Kaiser, 1987). As such, the hydrenchyma is thought to buffer the water potential of the chlorenchyma and therefore provide substantial capacitance to the leaf. It is not known if large chlorenchyma cells that define all-cell succulence are also providing capacitance to the leaf, although this is often assumed, due to the storage of water in these tissues.

Accordingly, a study on *Kalanchoë daigremontiana* (Crassulaceae), which is made up of relatively homogeneous large chlorenchyma cells with no hydrenchyma tissue, found that this species exhibits large values of capacitance, presumably due to the water reserves found in this species with ‘all-cell’ succulent anatomy (Smith and Nobel, 1985). However, every species in the genus *Kalanchoë* exhibit some degree of ‘all-cell’ succulence (Griffiths et al., 2008) and as such it is not possible to directly assess the affect that this anatomical adaptation has on capacitance within a genus. In addition, measurements of *Kalanchoë daigremontiana*, over a 24-hour cycle, in the absence of any drought treatment found large fluctuations in Ψ_{leaf} . Furthermore, even under well-watered conditions, *K. daigremontiana* transiently loses cell turgor during the night, due to water loss from the leaf. Therefore, whilst ‘all-cell’ succulence appears to provide high levels of capacitance, it is unclear if this is sufficient to buffer the leaf against water loss. To better understand if this is the case, it is valuable to investigate capacitance of species within genera that vary in their commitment to chlorenchyma-based succulent anatomy. Only then will it be possible to provide more generalised understanding of the role that ‘all-cell’ succulent anatomy plays in the capacitance of leaves.

1.3.9 Bulk Modulus of Cell Wall Elasticity

The final parameter that can be calculated from PV curves is the bulk modulus of cell wall elasticity (ϵ). Section 1.3.6 described the calculation of π_o ; by fitting a linear regression to describe how Ψ_{leaf} and RWC correlate (after the TLP, when $\Psi_{\text{leaf}} = \pi$) it is possible to extrapolate the value of π in fully hydrated leaves (Beadle et al., 1985). In fact, it is possible to

use this linear regression to calculate π at any RWC. Therefore, Equation 1.1 can be rearranged as:

Equation 1.6

$$P = \psi_{leaf} - \pi$$

to calculate the linear drop in turgor pressure as a leaf dehydrates (Fig. 1.6). The relationship between positive turgor pressure and drops in RWC approximate a stress/strain relationship, meaning that the bulk modulus of elasticity can be calculated by:

Equation 1.7

$$\varepsilon = \frac{\Delta P}{\Delta RWC}$$

If a species has very rigid cell walls, changes to RWC will have a greater impact on P, as the force of the plasma membrane will not cause any conformational changes (strain) to the cell walls and a high positive turgor pressure will be established. Therefore, a high value of ε is caused by rigid, inflexible cell walls (Saito et al., 2006). In contrast, if the cell walls are highly flexible, the effect of changing RWC on cell turgor will be dampened and ε will be low.

The role of ε in the physiology of succulent tissues is inherently tied to capacitance. Highly flexible cell walls allow cells to readily inflate and deflate, in coordination with the water status of the leaf (Ogburn and Edwards, 2010; Males 2017b). The inflation and deflation of cells facilitates the free movement of water into tissues that need rehydration. Hydrenchyma, which are known to have thinner cell walls than chlorenchyma cells, are believed to achieve their high capacitance in part due to their flexible cell walls. The ability of hydrenchyma to readily deflate in *Tillandsia ionantha* (Bromeliaceae) means Ψ_{leaf} and chlorenchyma cell size can be maintained for approximately 25 days after the cessation of watering, allowing this species to continue to photosynthesise during drought (Nowak and Martin, 1997). Likewise, the hydrenchyma of *Agave deserti* can deflate so much that this tissue reaches its TLP, but in doing so the chlorenchyma is kept hydrated (Schulte and Nobel, 1989). In some species with succulent anatomy, flexibility allows cell walls to morph into a folded pattern during drought. This occurs in the hydrenchyma of *Aloe helenae* (Ahl et al., 2019) and in the central tissue of

Pyrrhosia piloselloides (Ong et al., 1992; although this study does not report if it is hydrenchyma or chlorenchyma tissue). The fact that cell walls in succulent tissues can fold in a regular pattern during dehydration, rather than a random cell buckling due to weak points (Zhang et al., 2016), suggests that this phenomenon is adaptive; it is likely that succulent tissue have evolved highly flexible cell walls, in order to control the movement of water out of cells to provide capacitance during periods of drought.

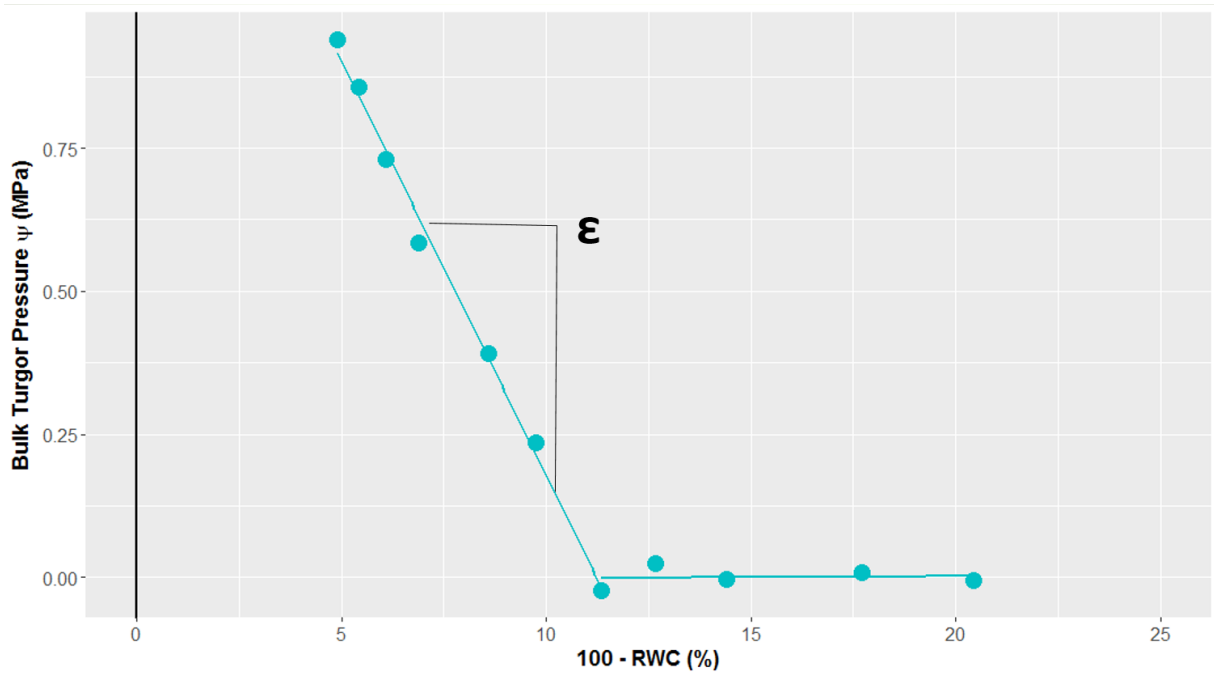


Fig. 1.6) The relationship between bulk turgor pressure (P) and RWC is explained by a linear function, up to the turgor loss point (TLP). After The TLP, P = 0. The gradient between P and RWC before the TLP represents the bulk modulus of cell wall elasticity.

1.3.10 Beyond PV Curves: Hydraulic Conductance

The physiological parameters presented thus far can all be measured using PV curves, a method that uses the dehydration of detached leaves on a lab bench. PV curves are extraordinarily informative, as they describe the physiology of leaves as water is lost, but this method does not address the movement of water across the leaf (Sack and Tyree, 2005; Sack and Holbrook, 2006; Sack and Scoffoni, 2013). Water enters the leaf via xylem conduits at the petiole, and moves from the central midrib to smaller veins. Typically, the midrib, and the two orders of veins that branch off this (i.e. the first, second and third order veins) are known collectively as major veins (Scoffoni et al., 2011; Sack and Scoffoni, 2013; Zhang et al., 2016). The smaller, fine veins that can branch off from these (fourth to seventh order veins) are known as the minor veins. One primary role of this vein network is to conduct water inside dead xylem conduits for use by the mesophyll tissue. After water exits the veins, it is conducted across the mesophyll along the cell walls (apoplastic pathway), through cells and across the plasma membranes (symplastic pathway) or evaporates as gas and diffuses across the IAS (gas pathway) (Buckley 2016; Sack et al., 2016; Scoffoni et al., 2017). Therefore, the flow of water across a leaf relies on movement across both vascular and non-vascular regions. The combined efficiency of water movement across an entire leaf can be described by the equation:

Equation 1.8

$$K_{leaf} = \frac{E}{\Delta\psi_{leaf}}$$

Where E is transpiration and $\Delta\psi_{leaf}$ is the difference in water potential across the leaf (Sack and Tyree, 2005; Sack and Holbrook, 2006). K_{leaf} can be calculated by measuring the flow of water into or out of the leaf (Brodribb and Holbrook, 2003; Brodribb and Holbrook, 2004; Blackman and Brodribb, 2011; Scoffoni et al., 2011; Males and Griffiths, 2018), as an estimate of E , and dividing this value by the water potential inside the leaf minus the water potential of the solution entering the leaf. K_{leaf} provides an overview of the combined efficiency of the vascular and non-vascular pathways in the movement of water across the leaf. In addition, by sequentially measuring K_{leaf} as a leaf dehydrates and ψ_{leaf} falls, it is possible to determine the percentage loss of conductivity (PLC). The ψ_{leaf} at which a 50 % loss of conductivity occurs

(P50) is often used as a metric to describe species ability to withstand low water potentials (Brodribb and Holbrook, 2003; Sack et al., 2016).

1.3.11 Vein Length per Leaf Area has a Large Effect on K_{leaf}

K_{leaf} describes the combined effect of vascular and non-vascular hydraulic conductance and is therefore determined by several different anatomical parameters, such as mesophyll cell sizes and cell wall thickness. Interestingly, the diameter of xylem conduits does not appear to influence the maximal K_{leaf} , suggesting that the flow of water is not limited by the width of xylem conduits, but rather by the ability of water to reach and move through the lateral portions of the mesophyll (Scoffoni et al., 2016a). The extension of veins into the lamina is determined by vein density (Scoffoni et al., 2011; Sack and Scoffoni, 2013). Vein density, also known as vein length per leaf area (VLA), contributes significantly to K_{leaf} ; comparisons of both phylogenetically diverse and closely related species found a positive correlation between VLA and K_{leaf} (Scoffoni et al., 2016b; Scoffoni et al., 2017). High VLA values can increase K_{leaf} in two ways: a more extensive vein network can efficiently conduct water further into the leaf, and more closely packed veins reduce the distance water must move across the non-vascular pathways in order to exit the leaf. Together, these effects mean that VLA has a strong impact on K_{leaf} .

1.3.12 Vein Density in Three Dimensions: IVD:VED Ratios Determine the Efficiency of Hydraulic Conductance

Measurements of VLA consider the veins in only two dimensions; VLA is measured as the number of veins in a given area of lamina. However, it is often also valuable to consider the arrangement of veins in relation to the depth of the mesophyll, as water exiting veins will also have to move through the mesophyll to reach stomata (Zwieniecki and Boyce, 2014). Theoretical and empirical measurements have found that for most angiosperms, the intervein distance (IVD is the reciprocal of VLA) is approximately equal in size to the vein to epidermal distance (VED) (Noblin et al., 2008). Any IVD:VED ratio < 1 would mean insufficient water is supplied to mesophyll tissue to replace that lost via transpiration. An IVD:VED ratio > 1 is thought to only produce superfluous veins that do not increase the efficiency with which lost

water is replaced. That $IVD \approx VED$ is believed to be an integral adaptation that led to the radiation of angiosperms across into all ecosystems across the globe, as this coordinated anatomy is the most efficient way a species can conduct water across the leaf (Zwieniecki and Boyce, 2014). However, more recently, research on eucalypts and Bromeliaceae have found the occurrence of species with IVD:VED ratios > 1 , meaning some species appear to ‘overinvest’ in vasculature (de Boer et al., 2016; Males 2017a). High IVD:VED ratios are predominantly found in species with thick leaves, leading authors to suggest that increased hydraulic resistance in the apoplastic pathway of thick leaves requires species to ‘overinvest’ in their vasculature. As leaf thickness is often associated with succulent anatomy, it is possible that species with increased tissue succulence could benefit from IVD:VED ratios > 1 . This may explain why species with high tissue succulence often develop multiple planes of veins in the leaf, often described as 3D venation (Balsammo and Uribe, 1988; Ogburn and Edwards, 2013). As leaves become thicker, species must increase their three dimensional vein density in order to compensate for the greater hydraulic resistance that is caused by longer apoplastic pathways.

1.3.13 Conduit Diameter Affects Species’ Loss of Hydraulic Conductance

As with K_{leaf} , variation in the PLC is strongly influenced by the anatomy of the leaf. However, in contrast to K_{leaf} , a species’ PLC is strongly influenced by xylem conduit diameter (Scoffoni et al., 2016a). Water moves through xylem conduits due to the pulling force of transpiration, meaning xylem water exists under negative tensions. When xylem tensions increase, during drought, the water enters a metastable state and can spontaneously change phase from a liquid to a gas (Brodrribb et al., 2016; Choat et al., 2018; Rodriguez-Dominguez et al., 2018). These gaseous embolisms cause breaks in the contiguity of the xylem sap, meaning that water proximal to these bubbles is no longer pulled into the distal parts of the leaf. Observations from microCT scanning in 12 phylogenetically diverse species found that wide conduit diameters are more vulnerable to the formation of emboli, and hence cause species to lose hydraulic conductance more readily (Scoffoni et al., 2016a). Congruent with this finding, observations of emboli formation across the entire leaf lamina, by detecting the differential refraction of light through water and gas in veins, found that bubbles originate in the major veins, and extend into smaller, minor veins (Brodrribb et al., 2016). Major veins are

populated by wider conduits, which are thought to cause the high vulnerability to low water potentials in midribs and petioles. Exactly what causes wide xylem conduits to be more vulnerable to seeding embolisms is not fully understood. However, it is suspected that wide xylem vessels have larger pits (the pores that connects two parallel conduits) and that these large pits are more vulnerable to cracks and damage that can seed the formation of an embolism (Lens et al., 2013; Scoffoni et al., 2016a). However, more data is required to better test this hypothesis. Nevertheless, xylem conduit diameter is an important determinant of a species' vulnerability to the formation of gaseous emboli and the loss of hydraulic conductance that these bubbles cause.

1.4 Metabolic Adaptations Associated With Succulent Anatomy

1.4.1 *Crassulacean Acid Metabolism; a Metabolic Adaptation in All-Cell Succulent Tissue*

Species with large chlorenchyma cells often exhibit a modified form of photosynthesis (Osmond 1978; Barrera Zambrano et al., 2014; Borland et al., 2015; Niechayev et al., 2019), known as Crassulacean acid metabolism (CAM). CAM serves to increase plant water use efficiency (WUE = carbon gained per water lost) thereby enabling plants to survive in semiarid and seasonally dry environmental niches (see section 1.4.8 to 1.4.10 for more detail on the ecophysiological consequences of CAM). CAM is an altered version of C₃ photosynthesis, characterised by the assimilation and storage of atmospheric carbon during the night, for use during the following day (Borland et al., 2014). As such, CAM is often described as a cycle, with temporally distinct stages or phases over a 24-hour period (Winter 2019). The CAM metabolic cycle is defined by two stages (note that these two 'stages' describe the metabolism, and not the four phases of gas exchange often exhibited by CAM plants, which are discussed later). The first stage of CAM occurs at night, during which CO₂ is converted by carbonic anhydrase (CA) to HCO₃⁻, which is then combined with phosphoenolpyruvate (PEP), via the enzyme PEP carboxylase (PEPC) to form oxaloacetate (OAA) (Miszalski et al., 2001; Taybi et al., 2004). Following this, OAA is converted to malic acid via the enzyme malate dehydrogenase (MDH), and imported into the vacuole for storage. The import of malic acid is believed to be driven by aluminium activated malate importers (ALMT) (Hafke et al., 2003; Angeli et al., 2013, Wai et al., 2017). During the day the second stage of the CAM cycle occurs, in which stored malic acid is decarboxylated to produce CO₂ for use as the substrate for light-powered photosynthesis (Dever et al., 2015). The export of malic acid may occur passively, although some evidence points towards tonoplast dicarboxylate transporter (tDT) as a putative export channel (Wai et al., 2017). Following the movement of malic acid into the cytosol, it is decarboxylated by either nicotinamide adenine dinucleotide dependent malic enzyme (NAD-ME), nicotinamide adenine dinucleotide phosphate dependent malic enzyme (NADP-ME), or phosphoenolpyruvate carboxykinase (PEPCK) in combination with MDH (Borland et al., 1998; Miszalski et al., 2001; Taybi et al., 2004). The type of CAM that a plant employs is typically categorised by the decarboxylating enzyme used (Shameer et al., 2018); with NAD-ME/NADP-ME type CAM being used predominantly by the Agavaceae, Cactaceae and Crassulaceae and

PEPCK type CAM being used by the Bromeliaceae, Clusiaceae and Euphorbiaceae (Niechayev et al., 2019). The use of alternative decarboxylating enzymes in different forms of CAM highlights the metabolic diversity of this adaptation.

1.4.2 Nocturnal Accumulation of Citrate in Crassulacean Acid Metabolism

Adding to the metabolic diversity of CAM is the overnight accumulation of citric acid in some, but not all, species (Kornas et al., 2009). Citric acid accumulation has been studied the most in *Clusia* (Popp yet al., 1987; Borland et al., 1992; Borland et al., 1993; Borland et al., 1998; Kornas et al., 2009), but it has also been observed in the Bromeliaceae (Pereira et al., 2017) and in *Talinum triangulare* (Talinaceae) (Brilhaus et al., 2016). The precise role of citric acid in the CAM cycle is uncertain as many species can undertake CAM without the overnight accumulation of citric acid, demonstrating that this metabolite is not integral to the CAM cycle. In addition, some species that can upregulate the CAM cycle in response to environmental stimuli (see Section 1.4.16 on facultative CAM) exhibit a decrease in overnight citrate accumulation in conjunction with increased CAM expression (Borland et al., 1993). It has been hypothesised that citrate may be playing a photoprotective role; that this metabolite provides CO₂ to maintain rates of photosynthesis during high light intensity to prevent damage from excess chlorophyll excitation (Lüttge 1999). However, studies of *Clusia minor* and *C. alata* found that overnight citrate accumulation went down when plants were exposed to high light levels (Franco et al., 1994; Kornas et al., 2009). Consequently, the precise role of citrate in the CAM cycle has remained enigmatic. Recently, a flux balance analysis model was built to describe the CAM cycle, by constraining a diel C₃ metabolic model so that CO₂ assimilation could only occur at night (Cheung et al., 2014). This model correctly predicted malic acid as the overnight storage molecule for carbon, but also found some nocturnal accumulation of citric acid. The role of citric acid was twofold: it functioned to provide CO₂ for photosynthesis in the day and it also, like in C₃ plants, acted as a carbon skeleton for amino acid synthesis. Therefore, this model predicted that citric acid is used both within and outside the CAM cycle, which might shed some light onto why the function of this metabolite in CAM plants has been so difficult to determine.

**Box 1. Measuring Crassulacean Acid Metabolism I:
Titratable Acidity, Malic and Citric Acid**

One consequence of nocturnal malic and/or citric acid accumulation is that plants engaged in CAM exhibit overnight drops in pH due to the accumulation of acids in the vacuole. The nocturnal accumulation of acid provides a simple means with which to investigate the presence and/or strength of CAM. By measuring titratable acidity (TA) in tissues, it is possible to determine the acid content of a leaf or stem segment. If CAM is occurring in a tissue, significantly higher TA should be present at dawn than at dusk. However, TA might not necessarily reflect the flux through CAM, as it is a bulk measure of acid content, and cannot differentiate between malic and citric acids. For example, *Clusia* has some of the highest dawn-dusk differences in acid content, despite these species exhibiting lower nocturnal CO₂ assimilation than *Kalanchoë* and *Agave* (Griffiths et al., 2008; Abraham et al, 2016). The high dawn-dusk TA values in *Clusia* have largely been attributed to the nocturnal accumulation of citric acid alongside malic acid (Lüttge 1999). Therefore, it is important to mention that comparisons of dawn-dusk TA values should only be made between closely related species (for example within the same genus) and should be treated as a rough estimation of CAM. Nevertheless, the ease with which TA values can be measured makes this technique a valuable method for assessing CAM. A more robust method for assessing the extent of CAM is to directly measure malic and citric acid concentrations, using spectrophotometer-based enzyme assays (Borland et al., 1993). Direct measurements of malic and citric acid provide a more detailed understanding of how different fluxes through the CAM cycle are influencing nocturnal acidification of the vacuole.

1.4.3 The Role of Anatomy - Crassulacean Acid Metabolism Relies on Large Chlorenchyma Cells

If plants exhibit a large flux through the CAM cycle leading to high rates of night time CO₂ assimilation, they will need space to store the nocturnally accumulated malic and/or citric acid, for use the following day (Nelson et al., 2005; Nelson and Sage, 2008; Barrera Zambrano et al., 2014). As described above, the night stage of the CAM cycle is characterised by malic acid import into the vacuole. Consequently, plants that exhibit strong CAM phenotypes require large vacuoles to house the acids generated by the CAM cycle. Species that can undertake CAM invariably exhibit some degree of all-cell tissue succulence, as large chlorenchyma cells are required to host these large vacuoles. Comparisons of phylogenetically diverse species found that CAM occurs more in species with larger, tightly packed chlorenchyma cells (Nelson et al., 2005; Nelson and Sage, 2008). In closely related species, the importance of all-cell succulence for CAM is also clear; CAM occurs more in species with large chlorenchyma cells in the Bromeliaceae, and in photosynthetically diverse genera such as *Clusia* and *Yucca* (Barrera Zambrano et al., 2014; Heyduk et al., 2016a; Males 2018). Whilst not every species with succulent chlorenchyma cells does CAM (Heyduk et al., 2016b), CAM does rely on succulent chlorenchyma, as interspecific variability in the use of CAM is determined by the large cells that provide space for the nocturnal storage of malic acid.

Further evidence pointing to the important role large succulent cells play in the CAM cycle comes from comparisons between different tissues in the same species, as even within a single leaf CAM relies on large succulent cells. In *Clusia*, the palisade cells are much larger in species exhibiting CAM than in their C₃ relatives, whereas spongy mesophyll cell size does not vary as much between species (a linear regression found $p = 0.1$, Barrera Zambrano et al., 2014). Interestingly, in *Clusia rosea*, PEPC protein is most abundant in the large palisade cells, suggesting that this is the primary site at which CAM exists within the leaf. Whilst CAM is known to occur across the entire chlorenchyma in *Clusia* (Borland et al., 1998), it is believed to be stronger in the palisade than the spongy mesophyll due to the former having larger cells (Barrera Zambrano et al., 2014). Furthermore, work on *Peperomia camptotricha* (Piperaceae) investigated overnight malate accumulation, enzyme activity of PEPC, PEPCCK and NADP-ME and attempted to measure *in situ* mRNA and protein abundance of PEPC in different tissue layers in the leaf. These experiments pointed towards CAM occurring predominantly in the

chlorophyll-containing hydrenchyma and the spongy mesophyll; the tissues made up of large, succulent cells in *P. camptotricha* (Nishio and Ting, 1985; Ting et al., 1994). The final example of CAM occurring only in the succulent tissue within a single leaf comes from *Camellia oleifera* (Theaceae), a small tree species from China (Yuan et al., 2012). A fungal pathogen, *Exobasidium vexans*, is known to infect *C. oleifera* and cause the development of succulent leaves that perform CAM. Some infected leaves do not develop succulence in a uniform pattern across the lamina, instead forming patches of succulent and non-succulent tissue in the same leaf. In these 'patchy' leaves CAM only occurs in the areas that are succulent, demonstrating that swollen cellular anatomy is integral to the functioning of this metabolic adaptation. Taken together, these examples of CAM occurring predominantly or even exclusively in the succulent tissues within a single leaf provide further evidence for the importance of large cells to the nocturnal storage of organic acids that define this metabolic adaptation.

1.4.4 Crassulacean Acid Metabolism Relies on Succulent Chlorenchyma, Not Hydrenchyma

It is worth mentioning that CAM is predominantly found in all-cell succulent tissue, as CAM requires the photosynthetic machinery present in chlorenchyma cells to assimilate CO₂ generated from the decarboxylation of malic acid reserves in the day. Therefore, achlorophyllous hydrenchyma cells are believed to be incapable of hosting the CAM cycle. However, direct observations of the absence of CAM in hydrenchyma are rare and often inferred by the fact that no chlorophyll exists in this tissue (Borland et al., 1998). Measurements of CAM (or absence thereof) in the leaf hydrenchyma have thus far been limited to thick-leaved species, that are amenable to dissections. Studies that made direct measurements of *Aloe arborescens* and *Agave deserti* found that no nocturnal acid accumulation occurred in the central hydrenchyma, as CAM was restricted to the succulent chlorenchyma tissue (Kluge et al., 1979; Smith et al., 1987). In addition, immunostaining for PEPC in *Clusia minor* found that this enzyme was present in the chlorenchyma cells but absent from the adaxial hydrenchyma (Borland et al., 1998). In contrast, in *Peperomia camptotricha* (discussed above) the hydrenchyma appears to accumulate acid overnight, indicating CAM is occurring in this tissue (Nishio and Ting, 1987). The hydrenchyma in *P. camptotricha* is not

truly achlorophyllous; it does contain some chloroplasts and can therefore make use of CO₂ produced from the decarboxylation of malic acid in the day. However, it is also possible that CO₂ from the decarboxylation of the CAM cycle in the hydrenchyma is being used by the palisade layer below, which can have high chloroplast density incorporated into crystalline druses, in the genus *Peperomia* (Horner et al., 2012). Whilst direct measurements of acid accumulation in the hydrenchyma are sparse, anatomical measurements show that investment in hydrenchyma is independent of CAM, in both the family Bromeliaceae (Males 2018) and the genus *Clusia* (Barrera Zambrano et al., 2014). In both taxa, CAM is associated with increased chlorenchyma cell size, but no such relationship exists between CAM and the hydrenchyma. Therefore, whilst CAM can sometimes occur in hydrenchyma tissue, as in *P. camptotricha*, this metabolic adaptation is largely independent of this water storage tissue.

1.4.5 Consequences of CAM – Higher Internal Carbon Concentrations

The discussion so far has focused on *how* the CAM cycle functions, but little attention has been given to *why* many species with large succulent chlorenchyma cells perform this altered form of photosynthesis. One important consequence of CAM in succulent leaves is to elevate the internal CO₂ concentration during the day, when light is available to power photosynthesis (Lüttge, 2002). By decarboxylating malate stores to provide carbon for photosynthesis, plants that do CAM can raise their internal CO₂ concentrations far higher than is possible in C₃ plants. The enzyme that catalyses the first step in day-time CO₂ assimilation, ribulose bisphosphate carboxylase oxygenase (Rubisco), also has affinity for O₂ which causes it to catalyse a wasteful oxygenase reaction, termed photorespiration (South et al., 2019). By increasing the internal CO₂ concentration, CAM plants maximise the carboxylase function and minimise the wasteful photorespiratory contribution of Rubisco (Shameer et al., 2018). This has meant that evolutionary changes to Rubisco are less constrained in plants exhibiting CAM; elevated internal CO₂ concentrations allow for the evolution of changes to Rubisco, even if these changes decrease the specificity of this enzyme to CO₂ (Griffiths et al., 2008). Hence, by acting as a carbon concentrating mechanism (CCM), CAM frees plants from the need to undertake wasteful photorespiration.

1.4.6 Succulent Anatomical Traits Affect Internal Carbon Concentration

The carbon concentrating capacity achieved from CAM is further increased by succulent anatomy itself (Nolan and Sage, 2008; Earles et al., 2018). As outlined above, large chlorenchyma cells that characterise all-cell succulent anatomy are often associated with low IAS porosity, $L_{mes}/area$ and high tortuosity. Low IAS porosity and high tortuosity restrict the movement of gases in the air phase within the leaf, and low $L_{mes}/area$ minimises the movement of gases between the liquid and gaseous phases at the surface of cells. As the low IAS space associated with large chlorenchyma cells restricts the movement of gases, species exhibiting all-cell succulence can minimise the mesophyll conductance to CO_2 (i.e. the moles of CO_2 that can move horizontally across a leaf each second at a given partial pressure of CO_2). Plants with large chlorenchyma cells have some of the lowest mesophyll conductance values recorded, and this has largely been attributed to the tight packing of cells and low IAS (Maxwell et al., 1997). In a C_3 plant, low mesophyll conductance would limit photosynthesis, as it would slow the movement of CO_2 from the stomata to the chloroplasts (Maxwell et al., 1997; Tomás et al., 2013). However, in a CAM plant, the CO_2 that is fixed by Rubisco during the day is generated from the decarboxylation of organic acids *inside* the photosynthetic cells in the leaf. Therefore, a low mesophyll conductance is beneficial as it limits the escape of CO_2 from the cells, thereby maximising the concentration of CO_2 available to Rubisco in the chloroplasts (Nolan and Sage, 2008). Hence a synergy exists between the CAM cycle and the low IAS conferred from tightly packed, large succulent chlorenchyma cells; together these adaptations increase the chloroplastic CO_2 concentration in the day.

Whilst the low IAS in succulent chlorenchyma tissue reduces mesophyll conductance in leaves, greater investment in hydrenchyma tissue (i.e. storage succulence) does not have the same effect. Despite hydrenchyma tissue having extremely low IAS, storage-succulence is thought to have little to no effect on mesophyll conductance. This is evidenced in the Aizoaceae, where greater investment in non-photosynthetic water storage hydrenchyma has no effect on mesophyll conductance (Ripley et al., 2013). The likely reason for this is that neither adaxial epidermal nor central hydrenchyma tissues make up part of the pathway through which CO_2 moves when travelling from the stomata to the chloroplasts. Consequently, the low IAS of these water-storage tissues do not affect mesophyll

conductance. This further demonstrates the different effects all-cell and water storage succulence have on the metabolic physiology of leaves; large chlorenchyma cells decrease mesophyll conductance and increase the concentration of CO₂ in CAM plants, whereas the hydrenchyma tissue has no effect on mesophyll conductance and is not believed to contribute to internal CO₂ concentrations.

1.4.7 Four Diel Phases of Gas Exchange in Plants Exhibiting Crassulacean Acid Metabolism

Whilst increased internal CO₂ concentrations is a defining characteristic of CAM, this alone does not explain the ecophysiological benefit of this altered form of photosynthesis. The main benefit conferred by CAM is a higher WUE, due to more moles of carbon being assimilated per mole of water lost from transpiration (Winter et al., 2005; Borland et al., 2014; 2015). To understand the way that CAM confers such high WUE it is necessary to describe the altered diel gas exchange profile that occurs due to CAM (Osmond 1978). The gas exchange profile of plants engaged in CAM is typically made up of four temporally separated phases (Fig. 1.7). The first phase (phase I) occurs at night, during which atmospheric CO₂ is assimilated by CA and PEPC enzymes. During phase I, plants undertaking CAM keep their stomata open so that CO₂ can diffuse into the leaf. Open stomata also cause water to be lost, as H₂O escapes through these open pores in the leaf (Sipes and Ting, 1985; Smith and Lüttge, 1985; Borland et al., 1993; Griffiths et al., 2008). Once malic acid has accumulated towards the end of the night, PEPC activity usually decreases and Rubisco becomes the main carboxylation enzyme for CO₂ assimilation (Borland et al., 2014), although in some taxa, including *Clusia* PEPC remains active in the morning (Taybi et al., 2004). In the morning phase II occurs, during which stomata are open for a brief period so that atmospheric CO₂ can be assimilated by Rubisco. The following phase, phase III, occurs during the middle of the day and is characterised by stomatal closure. During phase III, when light is available to the plant, decarboxylation of malic acid produces CO₂ which is assimilated by Rubisco and feeds into the Calvin cycle, behind closed stomata (Borland et al., 2014). Therefore, despite photosynthesis functioning in the leaf, phase III is characterised by little, or even zero net gas exchange across the stomata (Zotz and Winter, 1993; Winter et al., 2009; Holtum et al., 2017). Finally, towards the end of the day, phase IV occurs, during which stomata reopen and atmospheric CO₂ is assimilated by

Rubisco again (Borland et al., 2018). It is important to mention that the four phases of gas exchange described here are not observed in every plant that exhibits CAM. These phases should be considered a framework, with many plants exhibiting variations to one or more of these phases (for example the absence of phases II and IV are common). Variations to the gas exchange profile are discussed later (see Section 1.4.12).

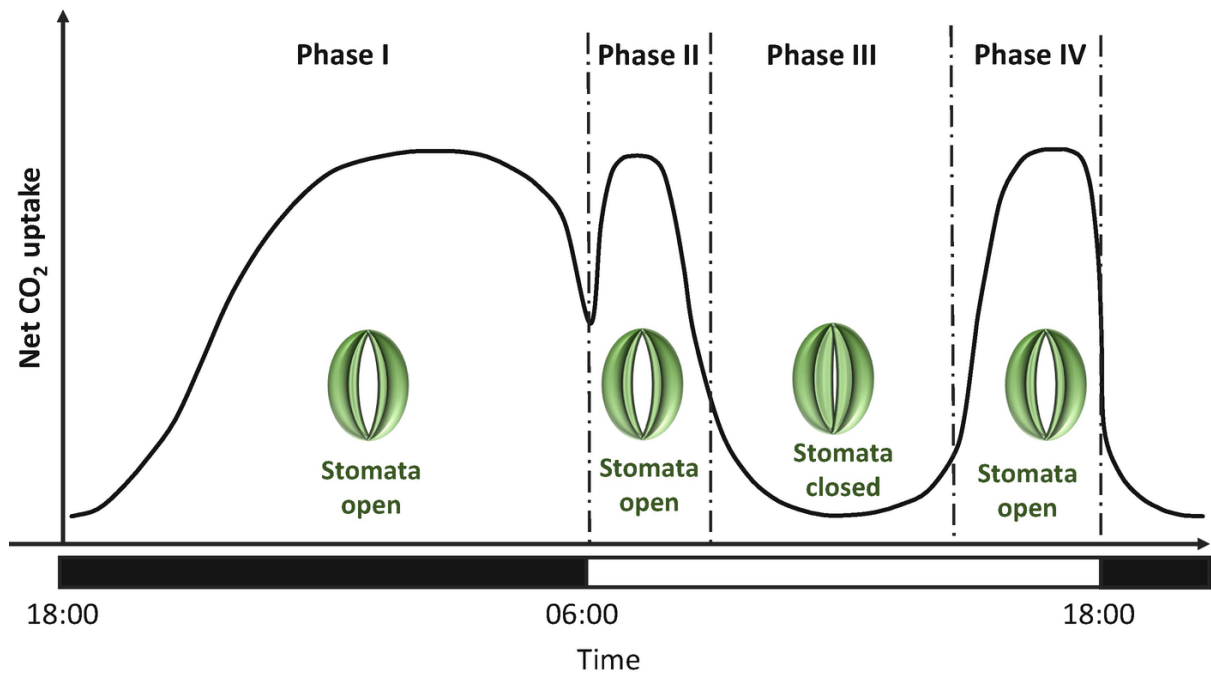


Fig. 1.7) The four phases of gas exchange typical of plants engaged in CAM. During the night, when PEPC is assimilating CO₂, the stomata are open during phase I. At the beginning of the morning the stomata remain open for phase II, during which Rubisco is the primary carboxylation enzyme for CO₂ assimilation. In the middle of the day, phase III is characterised by stomatal close, as atmospheric CO₂ assimilation falls close to zero. During Phase III the plant uses Rubisco to fix CO₂ generated from the decarboxylation of organic acids, such as malate. Finally, in the evening, phase IV occurs, during which stomata re-open and atmospheric CO₂ is fixed again by Rubisco. The consequence of this diel pattern of gas exchange is that stomata are closed during the middle of the day, when the air is hottest and driest, thereby minimising water loss, whilst maintaining CO₂ assimilation. Image taken from Borland et al., (2018).

Box 2. Measuring Crassulacean Acid Metabolism II: Infrared Gas Analysers

Infrared gas analysers (IRGA) are an integral tool to measure the photosynthetic assimilation and water loss occurring on a leaf. Typical IRGA systems work by measuring the absorbance of infrared light by a gas mixture. By comparing gas that has passed over the surface of a leaf to a reference (normally atmospheric air), it is possible to determine the rate of CO₂ assimilation and H₂O loss that has occurred due to the leaf; i.e. the gas exchange from the leaf. Typical IRGA systems, such as the BINOS-100 IRGA (Heinz Walz GmbH, Effeltrich, Germany) and the LI-6400XT IRGA (LiCOR, Lincoln, NE, USA) have cuvettes that can be clipped on to a leaf (Barrera Zambrano et al., 2014; Males and Griffiths 2018). Automatic measurements, typically every 15-30 minutes, can then determine the diel gas exchange profile of the leaf. Some labs have specialised cuvettes for the measurements of stems (Winter and Holtum, 2015) or whole plant canopies (Winter et al., 2008; Winter et al., 2009; Winter and Holtum, 2011), but these are often custom-made for each species.

1.4.8 Ecophysiological Consequences of Crassulacean Acid Metabolism – Reduced Transpiration and Stomatal Conductance

A major consequence of the four phases of gas exchange in plants that do CAM is the inverted pattern of stomatal opening, as stomata are open at night and closed during the middle of the day. Lower temperatures and higher humidity at night decrease the vapour pressure deficit plants experience (VPD is the difference in vapour pressure between the inside and outside of the leaf). Lower VPD values decrease the rate of water loss through stomata, and hence minimise transpiration. By opening the stomata at night rather than during the day, plants engaged in CAM can continue to assimilate CO₂ without opening their stomata in the hottest, driest portion of the day. Using infrared gas analysers (IRGA – see Box 2), estimates of diel transpiration can be measured, which have demonstrated that CAM considerably reduces the water loss from leaves (Smith and Lüttge, 1985; Zotz et al., 1994). To assess longer term rates of transpiration (> 1 day) potted plants need to be weighed to determine water loss. Few reports exist to compare the transpiration rates associated with C₃ and CAM photosynthesis over long periods of time. However, by reanalysing data presented in Winter et al., (2005), Table 1.1 shows the transpiration over a 9-month period for *Clusia*

valerioi (C₃) and *C. rosea* (CAM). These data are imperfect as transpiration here is standardised by the average plant dry mass over the 9 months (i.e. the mean dry mass over the growing season). Transpiration averaged by total leaf area would be a more accurate method, but unfortunately leaf area is not reported in this study. Nevertheless, *C. valerioi* clearly exhibits a far higher transpiration rate than *C. rosea*, demonstrating that CAM effects plants by minimising water loss over long periods of time. Therefore both diel and long-term transpiration rates are lower due to CAM, which contributes to the high WUE of plants with this metabolic adaptation.

Table 1.1) Transpiration rates of a C₃ and CAM species of *Clusia*. Data calculated from data in Winter et al., (2005).

Species	Physiotype	Dry mass (g)	Transpiration (g H ₂ O g ⁻¹ dry mass)
<i>Clusia valerioi</i>	C ₃	31.5	452.7
<i>Clusia rosea</i>	CAM	34.0	158.4

1.4.9 Ecophysiological Consequences of CAM – Increased Carbon Gain During Drought

Whilst CAM is often thought to increase WUE by minimising transpiration, this metabolic adaptation may also have considerable impact on the carbon acquisition of plants. Atmospheric carbon gain has received a great deal more attention in the study of CAM than transpirational water loss, as many papers report diel CO₂ assimilation without addressing the corresponding transpiration rates that occur (Borland et al., 1992; Borland et al., 1993; Roberts et al., 1996; Borland et al., 1998; Lüttge 1999; Griffiths et al., 2008; Winter et al., 2008; Winter et al., 2009; Winter and Holtum, 2011; Winter and Holtum, 2014; Heyduk et al., 2016b; Boxall et al., 2017; Holtum et al., 2017; Winter et al., 2018; Heyduk et al., 2019a). Precisely how CAM contributes to the carbon budget of a plant is not well established. Flux balance analysis modelling predicted that the ATP consumption and reducing power required by CAM is similar to those of C₃ plants during the day (Shameer et al., 2018). At night, however, CAM requires approximately 3-fold higher ATP and NADPH than C₃ photosynthesis, and this higher energy demand relies on greater respiratory fluxes through the mitochondria. Congruent with predictions from flux balance analysis modelling, genes functioning in mitochondrial biosynthesis exhibit higher steady-state transcript abundance at night in the constitutive CAM species *Agave americana* and *Yucca aloifolia* (Abraham et al., 2016; Heyduk et al., 2019b). Despite requiring greater rates of respiratory metabolism to function, CAM might not necessarily have a negative effect plant productivity. The same flux balance analysis model described earlier predicted the energetic cost of CAM could theoretically be overcome by low levels of photorespiration (Shameer et al., 2018). As CAM confers higher internal CO₂ concentrations (Section 1.4.5), less wasteful photorespiration is believed to occur during the day, which allows plants to offset the energy requirements of CAM at night. However, it is important to note that whilst decreases in photorespiratory losses to CO₂ assimilation could theoretically offset the energetic cost of CAM, the cost of CAM to productivity predicted by Shameer et al., (2018) ranged from 0 to 40 %, depending on the carbohydrate stores and decarboxylation enzyme used. Put simply, CAM can theoretically occur at no additional energetic cost (relative to that of C₃ photosynthesis), but most versions of this metabolic cycle are likely to confer a considerable penalty to plant productivity. This is evidenced in *Clusia*, as well-watered plants that do CAM (*C. rosea*) assimilate less CO₂ over 24 hours than those doing C₃ photosynthesis (*C. aripoensis*) (Borland et al., 1998).

The modelling efforts described above did not consider the effect of drought when comparing the energy requirements of CAM relative to C₃ photosynthesis. Whilst it is likely that CAM decreases plant productivity under well-watered conditions, it is possible that under periods of drought, when negative water potentials and/or low leaf water contents are causing stomatal closure, CAM may increase productivity. In all vascular plants, when leaves perceive drought, they initiate stomatal closure (Brodribb and Holbrook, 2003; Males and Griffiths, 2018; Trueba et al., 2019), which drastically decreases transpiration to protect the stems and roots from dangerous low water potentials. However, stomatal closure restricts photosynthesis, as CO₂ can no longer move through the pores in the leaf and consequently cannot reach the chloroplasts. Therefore, drought imposes a considerable energetic penalty to plants. One study found no difference in the water potential at which 50 % loss in stomatal conductance to water occurred (P50_s), between terrestrial C₃ and CAM species of Bromeliaceae (Males and Griffiths, 2018), suggesting that the stomata of plants engaged in CAM are as sensitive to drought as those of C₃ relatives. However, this study measured P50_s during the day for C₃ species and at night for species that do CAM, and therefore assumes that the time of the day has no impact on stomatal aperture. More recently, gas exchange analysis from *Kalanchoë pinnata* (Crassulaceae) demonstrated that sudden drought, induced by cutting the petiole to prevent water entering the leaf, caused a sharp decline in diurnal stomatal aperture, with gas exchange falling to zero within hours of the petiole being cut (Winter 2019 – Fig. 4). Nocturnal gas exchange, however, persisted for the remaining 6 nights, until the end of the experiment. Therefore, it appears that nocturnal stomatal sensitivity to drought is less severe than diurnal sensitivity, even in the same leaf. The significance of this is that the nocturnal gas exchange associated with CAM may be less sensitive to negative water potentials than the diurnal stomatal opening observed in C₃ plants. If this is the case, CAM plants should be able to maintain stomatal opening and net gas exchange and photosynthetic assimilation to a greater extent than C₃ plants when droughted. Accordingly, drought has been observed to cause a slight increase to the diel CO₂ assimilation of a *Clusia* species that constitutively undertakes CAM (*C. rosea*), whereas the same drought treatment causes a substantial decline to assimilation to a species with only a tiny capacity for CAM during drought (*C. aripoensis*) (Borland et al., 1998). Therefore, it is possible that when experiencing drought, CAM increases the photosynthetic assimilation of CO₂ in plants.

There are some examples where CAM increases the carbon acquisition of plants, even under well-watered conditions. An extreme example of this is in aquatic lycopod ferns belonging to the genus *Isoetes* (Isoetaceae). *Isoetes* species live in ponds or streams and consequently do not experience drought as a part of their natural life cycle, and the presence of CAM in this genus is believed to be purely for carbon acquisition (Keeley and Busche, 1984). In freshwater ecosystems the respiration rates of other plants and animals are highest at night, and therefore nocturnal environmental CO₂ concentrations are far higher than those observed during the day. In *Isoetes*, the nocturnal phase I of CAM allows assimilation to occur when CO₂ is most abundant, thereby increasing plant productivity. CAM is also believed to be an adaptation to maximise diel assimilation in epiphytic Bromeliaceae species, living in cloud forest ecosystems in Panama (Pierce et al., 2002). *Aechmea dactylina* (CAM) and *Werauhia capitata* (C₃) live in high-elevation montane forests, which experience high cloud cover and correspondingly low, and highly fluctuating sunlight. By undertaking CAM, *A. dactylina* can temporally uncouple CO₂ uptake from sunlight availability, as assimilation occurs predominantly during the night. As a result, *A. dactylina* exhibits high diurnal internal concentrations of CO₂, which subsequently allow this species to maximise rubisco-mediated carboxylation during transient periods of sunlight availability, when cloud cover is momentarily reduced. In contrast, *W. capitata* gains CO₂ for photosynthesis via open stomata when sunlight is available, causing Rubisco to be substrate-limited, due to stomatal and mesophyll resistance. Therefore, the use of CAM allows epiphytic Bromeliaceae species to achieve higher diel CO₂ assimilation rates, in this high elevation ecosystem. These examples, from a freshwater aquatic ecosystem and a high elevation cloud forest are characterised by a high availability of water. The presence of CAM in these ecosystems is evidence that this metabolic adaptation can occur to maximise the CO₂ acquisition of plants. Therefore, the high WUE of CAM plants can occur from reduced water loss, increased carbon gain or a combination of the two.

1.4.10 Water Use Efficiency – Why Does it Matter?

The high WUE generated by CAM can have multiple effects on plant physiology that each prevent plant death during periods of drought. To understand how high WUE aids plants, it is necessary to describe the causes of plant death during exposure to drought. Researchers investigating plant death, particularly the death of trees, have developed a framework to describe the different ways in which plants die. At early stages of drought, stomatal closure and a loss in hydraulic conductance in leaves will precede any damage to stems and roots (Choat et al., 2018; Rodriguez-Dominguez et al., 2018). Following this, water potentials will slowly drop until they eventually reach values low enough to cause emboli to form in the stem (Choat et al., 2018). The difference between the water potential at which stomata shut and stem conduits embolise, known as the hydraulic safety margin, is very small in most species, meaning plants have very little time to adjust their physiology upon experiencing drought (Choat et al., 2012). After the water potential in the stem falls below the hydraulic safety margin, and emboli form, the plant will start to experience hydraulic failure, as bubbles in the stem conduits break the transpiration stream and prevent water from reaching the leaves, even after rain events (Brodribb and Cochard, 2009). Analogous to K_{leaf} , K_{stem} and K_{root} represent the efficiency with which water can flow across an organ at a certain water potential (See Section 1.3.10 for more detail on hydraulic conductance). A substantial drop in K_{stem} and/or K_{root} can cause plants to die. In addition, during drought stomatal closure stops the assimilation of CO_2 and subsequently prevents photosynthesis from regenerating non-structural carbohydrate (NSC) stores. This leads to a process of carbon starvation, defined as partial depletion of NSC stores, leading to plant death (Hartmann 2015). The consequence of carbon starvation is the slowing of metabolic rates during drought. For example, in *Pinus edulis* (Pinaceae), nocturnal respiratory rates drop due to carbon starvation as plants start to die (Sevanto et al., 2014). Hydraulic failure and carbon starvation have typically been described as two discrete causes of plant death (McDowell et al., 2008). However, recently scientists have emphasised the fact that carbon starvation has the potential to affect hydraulic failure (Hartmann 2015). For example, when attempting to refill embolised xylem conduits, plants are thought to use sugars from the phloem to generate an osmotic gradient that drives the movement of water (Brodersen et al., 2010; Nardini et al., 2011). If NSC supplies are depleted,

this process will slow, and hence carbon starvation will contribute to the hydraulic failure of a plant. Therefore, it is likely that an interaction between carbon starvation and hydraulic failure causes plant health to decline and ultimately results in death. To prevent plant death, a high WUE is extremely beneficial. As described earlier, the high WUE of CAM plants is generated by either low transpiration rates, high CO₂ assimilation (during drought) or a combination of the two. Therefore, by increasing WUE, CAM has the potential to minimise both hydraulic failure and carbon starvation; providing synergistic protective mechanisms against the effect of drought on plant survival.

1.4.11 Effect of Crassulacean Acid Metabolism on Species Climatic Distributions

As CAM increases WUE to minimise plant mortality during drought, it is unsurprising that plants exhibiting CAM phenotypes are distributed in hot, dry environments. Terrestrial plants doing some form of CAM have radiated into semi-arid regions around the world, including (but not limited to) the Sonoran Desert, The South African Karoo and the Australian deserts (Arakaki et al., 2011; Valente et al., 2014; Holtum et al., 2016). Climatic niche modelling of orchids in the subtribe Eulophiinae (Orchidaceae) and for the Bromeliaceae found that, in terrestrial species, CAM occurs in dry, hot environmental niches, characterised by low aridity indexes (Bone et al., 2015; Males and Griffiths, 2017). In addition, investigations in *Clusia* found that CAM is particularly rare at high altitudes (Holtum et al., 2004). CAM is also common in wetter tropical ecosystems but is predominantly found in species inhabiting epiphytic niches; as life in the canopy is characterised by sporadic and low water availability (Crayn et al., 2004; Silvera et al., 2009; Chiang et al., 2013; Silvera and Lasso, 2016). Therefore, by increasing the WUE of plants, CAM allows survival in more arid, inhospitable ecological niches.

1.4.12 Diversity of Crassulacean Acid Metabolism Phenotypes

The diversity of CAM phenotypes was touched on earlier, with reference to the different decarboxylation enzymes that can be employed and the presence/absence of citrate. There is also a great deal of diversity in gas exchange profiles realised by plants employing the CAM pathway. The four phases of CAM, described above, are a general framework for

considering the diel gas exchange of CAM, but many variations to this profile do exist. The diversity of CAM phenotypes, and their relationships to environmental conditions and succulent anatomy are considered below.

1.4.13 Phases II III and IV; Variability in the Contribution of Diurnal Gas Exchange

Whilst CAM is typically characterised by night-time opening and day time closure of stomata, phases II and IV are often present, during which external CO₂ is primarily assimilated directly by Rubisco in the day. The contribution of phases II and IV to diel gas exchange are affected considerably by water availability, and these phases can often disappear when plants experience drought (Winter 2019). Phase IV is particularly sensitive to drought stress, as late afternoon stomatal opening that defines this phase often disappears days after the cessation of watering (Winter et al., 2008; Winter et al., 2009, Winter and Holtum, 2014). Even under well-watered conditions, the stomatal opening during phases II and/or IV can be low or even zero in some taxa, such as in the genus *Agave* (Smith et al., 1987; Schulte and Nobel, 1989; Abraham et al., 2016), and *Clusia hilariana* (Barrera Zambrano et al., 2014). It is worth mentioning that some species may exhibit phases II and IV for such short times that the resolution of some gas exchange experiments is not able to detect them (Heyduk et al., 2016a). In taxa that do exhibit phases II and IV under well-watered conditions, a great deal of variability exists in the length of these day-time phases and consequently how much they contribute to the total diel gas exchange of the plant. For example, a comparison of two all-cell succulent species in the genus *Kalanchoë* (Crassulaceae) found that in the more succulent species, *K. daigremontiana*, phases II and IV were shorter than in the less succulent *K. pinnata* (Griffiths et al., 2008). Thus, in *Kalanchoë*, the contribution of day-time stomatal opening to the total diel gas exchange, appears to be determined, in part, by tissue succulence. This is likely due to larger chlorenchyma cells providing a greater space for the nocturnal storage of organic acids by the CAM cycle. As almost twice as much nocturnal acidification occurs in *K. daigremontiana*, greater stores of organic acids will be available for decarboxylation in the day, which will increase the internal CO₂ concentration and extend stomatal closure in phase III, thereby minimising phases II and IV. Finally, some species maintain gas exchange during the middle of the day, and therefore do not exhibit the midday closure of stomata that

characterises phase III. For example, *Clusia minor* (Clusiaceae) and *Erycina pusilla* (Orchidaceae) both assimilate CO₂ during the night, but keep their stomata open in the middle of the day under well-watered conditions (Borland et al., 1993; Heyduk et al., 2019a). Therefore, like phases II and IV, phase III (or a lack thereof) affects how much day-time stomatal gas exchange varies between different species engaged in CAM.

1.4.14 Phase I; Variability in the Contribution of Nocturnal Gas Exchange

The nocturnal gas exchange of the CAM cycle, phase I, is typically characterised by assimilation of CO₂, which enters the leaf via open stomata to be fixed by CA and PEPC. Like phases II, III and IV (henceforth called the day phases), a great deal of variability exists in the intensity and duration of nocturnal CO₂ fixation. Like the day phases drought can sometimes cause a decrease in phase I CO₂ assimilation, such as in *Agave deserti* which decreases both the maximal CO₂ assimilation and the duration of nocturnal stomatal opening in the dry season (Schulte and Nobel, 1989). However, many species respond to drought by increasing their nocturnal CO₂ assimilation. For example, *Clusia alata* and *C. rosea*, both exhibit all four phases of CAM under well-watered conditions, but upon drought treatment CO₂ assimilation drops to zero in the day phases, whereas phase I assimilation increases (Barrera Zambrano et al., 2014). In addition to this example, several species can induce CAM and nocturnal CO₂ assimilation in response to drought, even when CAM was absent in these species under well-watered conditions, via a process termed facultative CAM (a more detailed discussion of facultative CAM is provided below in section 1.4.16). Therefore, the extent to which plants assimilate CO₂ at night is highly dependent on environmental conditions.

Not all variability in nocturnal CO₂ assimilation is the consequence of environmental conditions. A huge amount of variability exists in species' capacity to nocturnally assimilate CO₂; this variability is thought to be under genetic control rather than determined by the environmental conditions *per se*. There is, in fact, a complete spectrum of nocturnal gas exchange phenotypes that exist between that of C₃ photosynthesis and the 'typical' phase I, depicted in Fig. 1.7. A true C₃ species can be recognised by a relatively constant respiration rate throughout the night (Fig. 1.8) (Winter 2019). Therefore, even slight increases to the net nocturnal CO₂ assimilation can be indicative of some low flux through the CAM cycle. For

example, at the very low end of the 'CAM spectrum', are species such as *Calandrinia creethiae* (Montiaceae), *Sesuvium portulacastrum* (Aizoaceae) and *Erycina crista-galli* (Orchidaceae) in which CAM does not generate a positive nocturnal CO₂ assimilation rate (Holtum et al., 2017; Winter et al., 2018; Heyduk et al., 2019a). For these species, CAM causes the assimilation of CO₂ at night, but at a rate that is lower than the production of CO₂ from respiration (Fig. 1.8). CAM can be identified in these species by the curve in the nocturnal CO₂ assimilation rate as the night progresses. Other species, such as *Talinum triangulare* (Talinaceae) and *Clusia aripoensis* are able to surpass the compensation point for respiration, but only achieve low nocturnal rates of CO₂ assimilation (< 1 μmol m⁻² s⁻¹ for both) due to low flux through the CAM cycle (Borland et al., 1992; Barrera Zambrano et al., 2014; Winter et al., 2014; Brilhaus et al., 2016). Higher fluxes through the CAM cycle cause a greater nocturnal CO₂ assimilation rate, as seen in *Clusia alata*, *Agave americana* and *Kalanchoë fedtschenkoi*, which can achieve CO₂ assimilation rates of approx. between 3-5 μmol m⁻² s⁻¹ (Barrera Zambrano et al., 2014; Abraham et al., 2016; Boxall et al., 2017). Therefore, like the day phases of CAM, considerable variation exists in species' capacity to assimilate CO₂ during phase I.

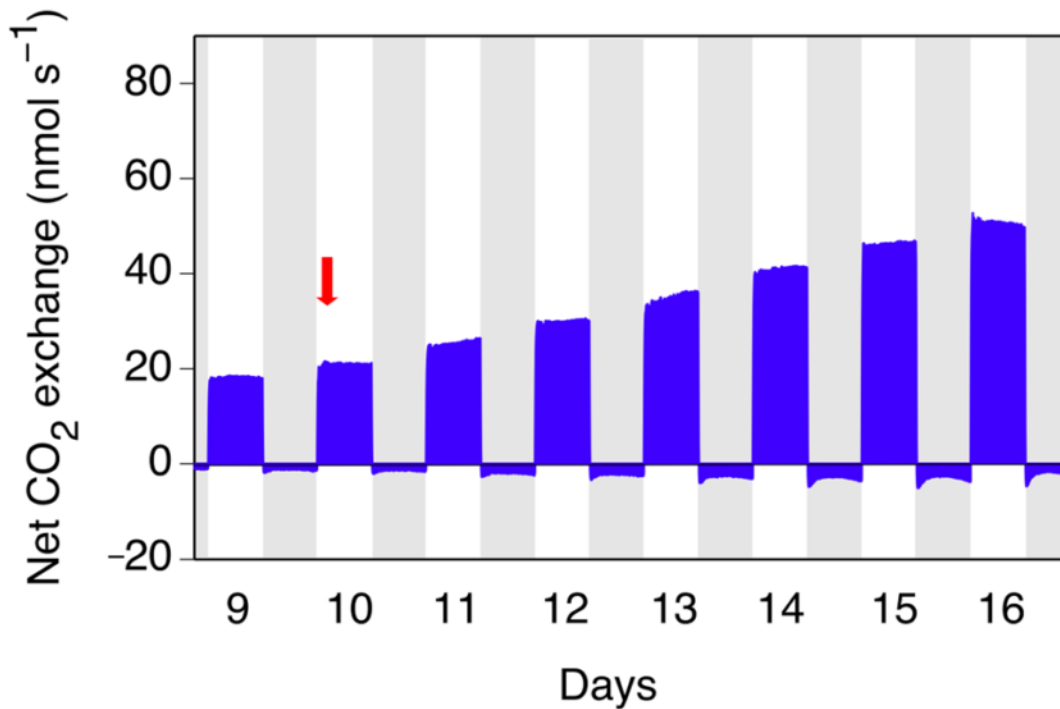


Fig. 1.8) Extremely weak CAM can be detected from a non-flat night time CO₂ efflux rate. These data are taken from Holtum et al., (2017), and depict the effect of days 7 days of drought treatment to the gas exchange of *Calandrinia creethiae*. Prior to drought treatment, (Day 9) the respiration rate remains relatively constant throughout the night. However, the induction of CAM can be seen from the night prior to day 14, by the curved nocturnal gas exchange profile. This is the consequence of very weak CAM expression.

1.4.15 Crassulacean Acid Metabolism: A Continuous Trait, but a Discrete Phenotype

The variability in all the four phases of gas exchange of CAM (Section 1.4.7) have one major consequence: the ratio of nocturnal to diurnal CO₂ assimilation for any species falls somewhere on a continuous spectrum. At one end of this spectrum are obligate C₃ species, which achieve all of their photosynthetic assimilation in the light. At the other extreme are plants that obtain all of their CO₂ from nocturnal assimilation, and are therefore described as 'full CAM' (Winter 2019). In reality most CAM causes a gas exchange profile somewhere in the middle; thus, it is often more convenient to categorise CAM as 'weak' or 'strong', depending on how much of the total assimilation is done at night. Calculating the percentage of photosynthesis done at night is a valuable parameter to quantify the strength of the CAM phenotype a plant is exhibiting (Barrera Zambrano et al., 2014). By measuring the strength of CAM, it is possible to move beyond thinking about CAM as a discrete, categorical variable (Winter et al., 2015), and instead recognise that variability in this form of altered metabolism is continuous (Winter 2019). It is important to note that whilst CAM can be quantified as a continuous trait, the photosynthetic phenotype a species exhibits cannot. This may seem paradoxical at first, but it is the consequence of phenotypic plasticity in many species that are able to undertake CAM. The strength of CAM in any plant is determined not only by the capacity of that species to assimilate CO₂ at night, but also by the environmental conditions the plant is experiencing. For example, it is possible to quantify the strength of CAM in *Clusia pratensis* under certain environmental conditions (Winter et al., 2014), but it is not possible to quantify the strength of CAM in this species (or any species) in and of itself. To complicate things, the phenotypic plasticity each species is able to achieve varies hugely (Barrera Zambrano et al., 2014; Winter and Holtum, 2014; Holtum et al., 2017). Therefore, any quantitative interspecific comparisons must take into account the conditions of the plant when CAM was measured. Often this is not possible, due to the constraints of certain experimental designs, in which case the phenotype of a species is best categorised as a discrete variable. In this thesis, the phenotypes of each species are described as obligate C₃, facultative CAM (see sections 1.4.18 and 1.4.19 for more detail), or constitutive CAM. These phenotypic categories are represented graphically by the colours blue, yellow and green, respectively.

1.4.16 Facultative Crassulacean Acid Metabolism

Many species exhibit C₃ or CAM physiology under all environmental conditions. These phenotypes, known respectively as obligate C₃ and constitutive CAM, may exhibit some slight changes to their diel gas exchange profiles upon experiencing stress, but cannot exhibit a switch in the dominant photosynthetic mode that is used for CO₂ assimilation. Put simply, obligate C₃ and constitutive CAM species are not able to switch their photosynthetic mode in response to environmental stresses (Winter et al., 2014). Many species, however, do change their photosynthetic physiology in response to environmental cues, in a process called facultative CAM. Facultative CAM is a form of phenotypic plasticity, whereby plants can initiate nocturnal acid accumulation in response to environmental stimuli. Critically, facultative CAM is defined as a reversible induction of CAM and is distinct from the irreversible developmental induction of CAM that occurs during many species' ontogeny (Winter et al., 2008; Aragón et al., 2012; Winter and Holtum, 2014; Dever et al., 2015). The cause of the switch from C₃ to CAM differs across taxa, but invariably involves a drop in water availability to the plant. In the halophyte *Mesembryanthemum crystallinum* (Aizoaceae), CAM can be induced by both salinity and drought, as these stress treatments both lower the water potential of the soil and hence restrict the free energy of water available to the plant (Taybi and Cushman, 1999). A screening of 50 species in the Aizoaceae found many examples of CAM induction in response to drought and/or salt stress, demonstrating that facultative CAM is relatively common across this family (Winter 2019). Salt stress can induce CAM in *M. crystallinum*, however for many genera, such as *Clusia*, *Calandrinia*, *Talinum*, *Sedum* (Crassulaceae) and *Portulaca* (Portulacaceae), facultative CAM has only been reported to occur in response to drought stress (Franco et al., 1991; Borland et al., 1992; Winter and Holtum 2011; Winter and Holtum 2014; Brilhaus et al., 2016; Wai et al., 2019). In these genera, withholding water from the plants increases nocturnal CO₂ assimilation whilst simultaneously decreasing diurnal stomatal opening, thereby switching the plants' physiology from C₃ to CAM. Other environmental conditions, such as light and availability of nutrients in the soil have been showed to influence the speed and intensity of the switch into CAM for some species (Franco et al., 1991; Borland et al., 1992; Winter and Holtum 2011). However, all species that can facultatively upregulate CAM are able to do so in response to drought, demonstrating that facultative CAM is first and foremost a drought response, across all taxa.

1.4.17 Crassulacean Acid Metabolism in *Clusia* – A History

The diversity of leaf succulence in *Clusia* was discussed in Section 1.2.5. An equal degree of diversity is seen in the photosynthetic physiology of *Clusia*, as weak, strong, facultative and constitutive CAM phenotypes, as well as obligate C₃ photosynthesis exists in this genus. The occurrence of CAM in *Clusia* was, arguably, first observed by Alexander von Humboldt in 1800 (translated in Lüttge 2002). von Humboldt recognised that in the day, leaves of the constitutive CAM species *C. rosea* did not produce any gases (i.e. there was no gas exchange due to stomatal closure during phase III). However, the lack of diurnal gas exchange in *Clusia* was not directly attributed to CAM until Tinoco Ojanguren and Vazquez Yanes (1983) demonstrated that *C. lundelli* exhibited nocturnal CO₂ assimilation. This report was not cited in the subsequent *Science* paper in 1985 that claimed to be the first identification of CAM in the genus (Ting et al., 1985). Following these initial studies, measurements of titratable acidity, malic acid assays (Box 1) and gas exchange (Box 2) identified CAM in tens of other *Clusia* species (Popp et al., 1987; Borland et al., 1993; Zotz and Winter, 1993; Roberts et al., 1996). The abundance of weak, facultative and constitutive CAM in so many *Clusia* species led some to question if obligate C₃ phenotypes actually existed in the genus (Grams et al., 1998), although more comprehensive screening found that C₃ photosynthesis is in fact more common than CAM (Holtum et al., 2004; Gustafsson et al., 2007).

1.4.18 Crassulacean Acid Metabolism in *Clusia* – A Uniquely Diverse Genus

As mentioned above, *Clusia* is extremely diverse; every different form of CAM can be found in this genus. Under well-watered conditions, the complete spectrum of photosynthetic physiologies exists, from C₃, in *C. articulata* and *C. tocuchensis* (Borland et al., 1992; Grams et al., 1998; Barrera Zambrano et al., 2014; Borland et al., 2018); to weak CAM in *C. minor* and *C. uvitana* (Borland et al., 1993; de Mattos et al., 1998; Holtum et al., 2004; Winter and Holtum, 2014) and strong (constitutive) CAM in *C. alata* and *C. fluminensis* (Roberts et al., 1996; Kornas et al., 2009). In addition, a great deal of diversity exists in species' capacity to facultatively express CAM. Whilst some species, such as *C. multiflora* cannot induce CAM (Grams et al., 1998; Taybi et al., 2004), a number are able to turn on this carbon concentrating mechanism (CCM) in response to drought. Species such as *C. lanceolata* and *C. aripoensis* are

able to switch from a C₃ to a weak CAM phenotype (Roberts et al., 1996; Barrera Zambrano et al., 2014). *Clusia pratensis*, which is perhaps the 'purest' example of facultative CAM in the genus, can switch from a C₃ to a strong CAM physiology during drought stress (Winter et al., 2005; Winter et al., 2008; Winter and Holtum, 2014). Finally, *C. minor* and *C. uvitana* alter between weak and strong CAM depending on water availability (Borland et al., 1992; Winter and Holtum, 2014). Therefore, both the 'strength' of CAM phenotypes and the capacity for phenotypic plasticity varies considerably in *Clusia*.

1.4.19 Crassulacean Acid Metabolism in *Clusia* – Reliance on Succulent Palisade Mesophyll Cells

The most comprehensive phenotyping effort in *Clusia* was performed by Barrera Zambrano et al., (2014). These authors measured diel gas exchange rates for nine species of *Clusia* under both well-watered and drought-treated conditions. Integration of these gas exchange curves allowed measurement of the percentage of photosynthetic assimilation done at night for each species (i.e. the strength of CAM), in each condition. Due to variable levels of facultative CAM in *Clusia* the phenotypes for each species in this study are best described categorically, as obligate C₃, facultative CAM or constitutive CAM (See Section 1.4.15 for discussion of CAM as a continuous or discrete trait). This study also found that the strength of CAM in well-watered conditions correlates significantly with palisade mesophyll size, presumably because larger palisade cells are able to store greater quantities of malic and/or citric acid. Importantly, the strength of CAM was unrelated to cell succulence in the hydrenchyma, as this tissue is not believed to perform CAM in *Clusia*. Therefore, Barrera Zambrano et al., (2014) were able to provide the first link between succulent anatomy and physiology in this diverse genus. To develop these findings, this thesis makes extensive use of these reported gas exchange data, to understand how different forms of succulent anatomy affects the water relations and hydraulic physiology of leaves.

Table 1.2) Well-characterised species studied in this thesis. Physiotypes were determined from Barrera Zambrano et al., 2014, except for *C. pratensis* and *C. fluminensis*, which are physityped in Winter and Holtum, 2014 and Roberts et al., 1996, respectively. Phylogenetic position was determined from Gustafsson et al., 2007.

Species	Physiotype	Phylogenetic Position
<i>Clusia grandiflora</i>	Obligate C ₃	Sect. Chlamydoclusia
<i>Clusia tocuchensis</i>	Obligate C ₃	Sect. Anadrogyne
<i>Clusia multiflora</i>	Obligate C ₃	Sect. Anadrogyne
<i>Clusia aripoensis</i>	Facultative CAM	Omphalantha Complex
<i>Clusia lanceolata</i>	Facultative CAM	Sect. Phloianthera
<i>Clusia pratensis</i>	Facultative CAM	Sect. Retinostemon
<i>Clusia minor</i>	Facultative CAM	Sect. Retinostemon
<i>Clusia rosea</i>	Constitutive CAM	Sect. Chlamydoclusia
<i>Clusia fluminensis</i>	Constitutive CAM	Sect. Cordylandra
<i>Clusia hilariana</i>	Constitutive CAM	Sect. Phloianthera
<i>Clusia alata</i>	Constitutive CAM	NA

Box 3. Measuring Crassulacean Acid Metabolism III: RNA-seq With Next Generation Sequencing

Recently, a great deal of emphasis has been directed towards understanding the genetics of CAM, using next generation sequencing (NGS) technologies. The most common NGS technique is RNA-seq, a process that quantifies the RNA abundance of every expressed gene (the transcriptome) in a sample (Wang et al., 2009). All RNA-seq investigations work by sequencing short fragments of mRNA, called reads, and aligning these to a complete reference sequence. When a genome is available this will be used as the reference sequence, as it will contain nearly all the protein-coding genes in a species (Ming et al., 2015; Wai et al., 2017; Yang et al., 2017, Wai et al., 2019). Alternatively, the genome of a closely related species can sometimes be used, if enough genetic homology exists (Strickler et al., 2012; Brillhaus et al., 2016). However, the process of *de novo* RNA-seq, i.e. the transcriptomic analysis of species without a reference genome (Suget-Groba et al., 2010; Grabherr et al., 2011), is particularly popular for researching CAM, as it allows scientists to analyse phylogenetically diverse non-model organisms (Abraham et al., 2016; Heyduk et al., 2019a; Heyduk et al., 2019b). The initial step in any RNA-seq experiment is the extraction and reverse translation of mRNA to produce complementary DNA molecules (Wang et al., 2009). NGS platforms then employ a 'sequencing-by-synthesis' technique, meaning the DNA is sequenced as it is amplified, in order to read the code of nucleic acids. DNA chains, typically 80-500 base pairs long, are synthesised, in the presence of fluorescent nucleic acid monomers, such that incorporation of a fluorescent monomer in the amplification process is detected and recorded. This process generates billions of short digital sequences, called reads, which can be used for the *de novo* assembly of a transcriptome. If reads originate from overlapping regions of the same mRNA transcript, they will share part of their sequence. These regions of shared sequences can be used to join reads together, using De Bruijn graphs, into longer sequences called contigs, which are better estimations of whole mRNA molecules (Strickler et al., 2012). Hence the production of contigs represents an estimate of the transcriptome of a sample, as it reflects all the genes that have non-zero steady-state transcript abundance.

Having assembled the transcriptome of a species, the next step is to quantify gene expression. If a genome is available then reads are aligned to open reading frames, whereas in *de novo* RNA-seq reads are aligned to contigs. Whilst counting the number of reads per contig gives some information about the steady-state mRNA abundance of a gene, this is heavily skewed by the contig length, as longer contigs will produce more reads. In addition, read counts are also skewed by read depth, which is the difference in how much mRNA is extracted per sampling effort (Wagner et al., 2012). To overcome these skews, read counts are standardised by calculating the metric 'transcripts per million' (TPM). To calculate TPM, read counts for each gene are first divided by the length of each contig, to calculate the reads per kilobase (RPK). This standardises the read count of each gene by the length of the contig for that gene. Following this, all the RPK values in a sample are summed and divided by 1,000,000, to determine the read depth (RD) of that sample. Finally, the RPK of for each contig is divided by RD, so that each gene is standardised for read depth, giving an estimate of mRNA steady state abundance as TPM.

By calculating TPM for every contig in a *de novo* transcript assembly it becomes possible to estimate steady-state mRNA abundance for every expressed gene in a sample. By doing this, scientists can compare mRNA abundance of any gene under different conditions, time points or developmental stages of a plant, even in non-model organisms (Wai et al., 2017; Heyduk et al., 2019a; Heyduk et al., 2019b). In addition, because RNA-seq quantifies the entire transcriptome, it is possible to identify broad-scale biological processes or cellular compartments that experience transcriptomic changes between two sampling efforts. Broad-scale phenomena are uncovered from RNA-seq data using gene ontology (GO) enrichment analyses (Huang et al., 2009; Wai et al., 2019). To undertake GO enrichment, each gene is assigned GO terms, which describe the function or subcellular location of the protein product of that gene. In *de novo* data sets, from non-model organisms, GO terms are typically allocated based on sequence homology with model organisms. GO terms that are more abundant in a set of genes (for example genes that are upregulated in response to drought) than they would be by chance alone are therefore considered to be 'enriched'. Therefore, gene ontology enrichment analysis allows CAM researchers to achieve both targeted investigations into genes of interest and the identification of novel processes associated with this metabolic adaptation.

Questions Addressed in this Thesis, by Chapter:

1. Do large chlorenchyma cells provide hydraulic capacitance in addition to hosting the CAM cycle?
2. Does hydrenchyma tissue or CAM have a greater effect on a species' turgor loss point, and hence their ability to tolerate low water potentials?
3. Does hydrenchyma tissue or CAM contribute more to species' climatic niche distributions?
4. Does low transpirational water loss due to CAM influence the vascular architecture of *Clusia* leaves?
5. Is CAM in *Clusia* an adaptation to prevent the metabolic symptoms of carbon starvation during drought?

References

- Abdel-Raouf, H. S. (2012). Anatomical traits of some species of Kalanchoë (Crassulaceae) and their taxonomic value. *Annals of Agricultural Sciences*, 57(1), 73–79.
<http://doi.org/10.1016/j.aoas.2012.03.002>
- Abraham, P. E., Yin, H., Borland, A. M., Weighill, D., Lim, S. D., De Paoli, H. C., ... Yang, X. (2016). Transcript, protein and metabolite temporal dynamics in the CAM plant Agave. *Nature Plants*, 2(December), 1–10. <http://doi.org/10.1038/nplants.2016.178>
- Ahl, L. I., Mravec, J., Jørgensen, B., Rudall, P. J., Rønsted, N., & Grace, O. M. (2019). Dynamics of intracellular mannan and cell wall folding in the drought responses of succulent Aloe species. *Plant Cell and Environment*, (March), 1–14. <http://doi.org/10.1111/pce.13560>
- Aragón, C., Carvalho, L., González, J., Escalona, M., & Amancio, S. (2012). The physiology of ex vitro pineapple (*Ananas comosus* L. Merr. var MD-2) as CAM or C3 is regulated by the environmental conditions. *Plant Cell Reports*, 31(10), 757–769.
<http://doi.org/10.1007/s00299-013-1493-3>
- Arakaki, M., Christin, P.-A., Nyffeler, R., Lendel, A., Eggli, U., Ogburn, R. M., ... Edwards, E. J. (2011). Contemporaneous and recent radiations of the world's major succulent plant lineages. *Proceedings of the National Academy of Sciences*, 108(20), 8379–8384.
<http://doi.org/10.1073/pnas.1100628108>
- Balsamo, R. A., & Uribe, E. G. (1988). Leaf anatomy and ultrastructure of the Crassulacean-acid-metabolism plant *Kalanchoë daigremontiana*. *Planta*, 173(2), 183–189.
<http://doi.org/10.1007/BF00403009>
- Barrera Zambrano, V. A., Lawson, T., Olmos, E., Fernández-García, N., & Borland, A. M. (2014). Leaf anatomical traits which accommodate the facultative engagement of crassulacean acid metabolism in tropical trees of the genus *Clusia*. *Journal of Experimental Botany*, 65(13), 3513–23. <http://doi.org/10.1093/jxb/eru022>

- Bartlett, M. K., Scoffoni, C., Ardy, R., Zhang, Y., Sun, S., Cao, K., & Sack, L. (2012a). Rapid determination of comparative drought tolerance traits: Using an osmometer to predict turgor loss point. *Methods in Ecology and Evolution*, 3(5), 880–888.
<http://doi.org/10.1111/j.2041-210X.2012.00230.x>
- Bartlett, M. K., Scoffoni, C., & Sack, L. (2012b). The determinants of leaf turgor loss point and prediction of drought tolerance of species and biomes: A global meta-analysis. *Ecology Letters*, 15(5), 393–405. <http://doi.org/10.1111/j.1461-0248.2012.01751.x>
- Bartlett, M. K., Zhang, Y., Kreidler, N., Sun, S., Ardy, R., Cao, K., & Sack, L. (2014). Global analysis of plasticity in turgor loss point, a key drought tolerance trait. *Ecology Letters*, 17(12), 1580–1590. <http://doi.org/10.1111/ele.12374>
- Beadle, C. L., Ludlow, M. M., & Honeysett, J. L. (1985). Water Relations. In J. Coombs, D. O. Hall, S. P. Long, & J. M. O. Scurlock (Eds.), *Techniques in Bioproductivity and Photosynthesis* (2nd ed., pp. 50–61). Pergamon.
- Blackman, C. J., & Brodribb, T. J. (2011). Two measures of leaf capacitance: Insights into the water transport pathway and hydraulic conductance in leaves. *Functional Plant Biology*, 38(2), 118–126. <http://doi.org/10.1071/FP10183>
- Bone, R. E., Smith, J. A. C., Arrigo, N., & Buerki, S. (2015). A macro-ecological perspective on crassulacean acid metabolism (CAM) photosynthesis evolution in Afro-Madagascan drylands: Eulophiinae orchids as a case study. *New Phytologist*, 208(2), 469–481.
<http://doi.org/10.1111/nph.13572>
- Borland, A. M., Griffiths, H., Broadmeadow, M. S. J., Fordham, M. C., & Maxwell, C. (1993). Short-term changes in carbon-isotope discrimination in the C3-CAM intermediate *Clusia minor* L. growing in Trinidad. *Oecologia*, 95(3), 444–453.
<http://doi.org/10.1007/BF00321001>
- Borland, A. M., Griffiths, H., Maxwell, C., Broadmeadow, M. S. J., Griffiths, N. M., & Barnes, J. D. (1992). On the ecophysiology of the Clusiaceae in Trinidad: expression of CAM in *Clusia minor* L. during the transition from wet to dry season and characterization of

- three endemic species. *New Phytologist*, 122(2), 349–357.
<http://doi.org/10.1111/j.1469-8137.1992.tb04240.x>
- Borland, A. M., Hartwell, J., Weston, D. J., Schlauch, K. a., Tschaplinski, T. J., Tuskan, G. a., ... Cushman, J. C. (2014). Engineering crassulacean acid metabolism to improve water-use efficiency. *Trends in Plant Science*, 19(5), 327–338.
<http://doi.org/10.1016/j.tplants.2014.01.006>
- Borland, A. M., Leverett, A., Hurtado-Castano, N., Hu, R., & Yang, X. (2018). Functional Anatomical Traits of the Photosynthetic Organs of Plants with Crassulacean Acid Metabolism. In W. W. Adams III & I. Terashima (Eds.), *The Leaf: A Platform for Performing Photosynthesis* (1st ed., pp. 281–305). http://doi.org/10.1007/978-3-319-93594-2_10
- Borland, A. M., Técsi, L. I., Leegood, R. C., & Walker, R. P. (1998). Inducibility of crassulacean acid metabolism (CAM) in *Clusia* species; physiological/biochemical characterisation and intercellular localization of carboxylation and decarboxylation processes in three species which exhibit different degrees of CAM. *Planta*, 205(3), 342–351.
<http://doi.org/10.1007/s004250050329>
- Borland, A. M., Wulschleger, S. D., Weston, D. J., Hartwell, J., Tuskan, G. a., Yang, X., & Cushman, J. C. (2015). Climate-resilient agroforestry: physiological responses to climate change and engineering of crassulacean acid metabolism (CAM) as a mitigation strategy. *Plant, Cell & Environment*, 38, 1833–1849. <http://doi.org/10.1111/pce.12479>
- Boxall, S. F., Dever, L. V, Knerova, J., Gould, P. D., & Hartwell, J. (2017). Phosphorylation of Phosphoenolpyruvate Carboxylase is Essential for Maximal and Sustained Dark CO₂ Fixation and Core Circadian Clock Operation in the Obligate Crassulacean Acid Metabolism Species *Kalanchoë fedtschenkoi*. *The Plant Cell*, 29(10):2519-2536.
<http://doi.org/10.1105/tpc.17.00301>
- Brilhaus, D., Bräutigam, A., Mettler-Altmann, T., Winter, K., & Weber, A. P. M. (2016). Reversible Burst of Transcriptional Changes during Induction of Crassulacean Acid Metabolism in *Talinum triangulare*. *Plant Physiology*, 170(1), 102–122.
<http://doi.org/10.1104/pp.15.01076>

- Brodersen, C. R., McElrone, A. J., Choat, B., Matthews, M. A., & Shackel, K. A. (2010). The dynamics of embolism repair in xylem: In vivo visualizations using high-resolution computed tomography. *Plant Physiology*, *154*(3), 1088–1095.
<http://doi.org/10.1104/pp.110.162396>
- Brodribb, T. J., & Holbrook, N. M. (2004). Diurnal depression of leaf hydraulic conductance in a tropical tree species. *Plant, Cell and Environment*, *27*(7), 820–827.
<http://doi.org/10.1111/j.1365-3040.2004.01188.x>
- Brodribb, T. J., Holbrook, N. M., Edwards, E. J., & Gutiérrez, M. V. (2003). Relations between stomatal closure, leaf turgor and xylem vulnerability in eight tropical dry forest trees. *Plant, Cell and Environment*, *26*(3), 443–450. <http://doi.org/10.1046/j.1365-3040.2003.00975.x>
- Brodribb, T. J., & Holbrook, N. M. (2003). Stomatal Closure during Leaf Dehydration, Correlation with Other Leaf Physiological Traits. *Plant Physiology*, *132*(4), 2166–2173.
<http://doi.org/10.1104/pp.103.023879>
- Brodribb, T. J., & Cochard, H. (2009). Hydraulic failure defines the recovery and point of death in water-stressed conifers. *Plant Physiology*, *149*(1), 575–584.
<http://doi.org/10.1104/pp.108.129783>
- Brodribb, T. J., Skelton, R. P., Mcadam, S. A. M., Bienaimé, D., Lucani, C. J., & Marmottant, P. (2016). Visual quantification of embolism reveals leaf vulnerability to hydraulic failure. *New Phytologist*, *209*(4), 1403–1409. <http://doi.org/10.1111/nph.13846>
- Buckley, T. N. (2015). The contributions of apoplastic, symplastic and gas phase pathways for water transport outside the bundle sheath in leaves. *Plant, Cell and Environment*, *38*(1), 7–22. <http://doi.org/10.1111/pce.12372>
- Buckley, T. N. (2019). How do stomata respond to water status? *New Phytologist*.
<http://doi.org/10.1111/nph.15899>
- Chatelet, D. S., Clement, W. L., Sack, L., Donoghue, M. J., & Edwards, E. J. (2013). The evolution of photosynthetic anatomy in *Viburnum* (Adoxaceae). *International Journal of Plant Sciences*, *174*(9), 1277–1291. <http://doi.org/10.1086/673241>

- Cheung, C. Y. M., Poolman, M. G., Fell, D. A., Ratcliffe, R. G., & Sweetlove, L. J. (2014). A Diel Flux Balance Model Captures Interactions between Light and Dark Metabolism during Day-Night Cycles in C3 and Crassulacean Acid Metabolism Leaves. *Plant Physiology*, *165*(2), 917–929. <http://doi.org/10.1104/pp.113.234468>
- Chiang, J. M., Lin, T. C., Luo, Y. C., Chang, C. Te, Cheng, J. Y., & Martin, C. E. (2013). Relationships among rainfall, leaf hydrenchyma, and Crassulacean acid metabolism in *Pyrosia lanceolata* (L.) Fraw. (Polypodiaceae) in central Taiwan. *Flora*, *208*(5–6), 343–350. <http://doi.org/10.1016/j.flora.2013.04.007>
- Choat, B., Brodribb, T. J., Brodersen, C. R., Duursma, R. A., López, R., & Medlyn, B. E. (2018). Triggers of tree mortality under drought. *Nature*, *558*(7711), 531–539. <http://doi.org/10.1038/s41586-018-0240-x>
- Choat, B., Jansen, S., Brodribb, T. J., Cochard, H., Delzon, S., Bhaskar, R., ... Zanne, A. E. (2012). Global convergence in the vulnerability of forests to drought. *Nature*, *491*(V), 752–5. <http://doi.org/10.1038/nature11688>
- Crayn, D. M., Winter, K., & Smith, J. A. C. (2004). Multiple origins of crassulacean acid metabolism and the epiphytic habit in the Neotropical family Bromeliaceae. *Proceedings of the National Academy of Sciences of the United States of America*, *101*(10), 3703–3708. <http://doi.org/10.1190/segam2015-5905882.1>
- De Angeli, A., Zhang, J., Meyer, S., & Martinoia, E. (2013). AtALMT9 is a malate-activated vacuolar chloride channel required for stomatal opening in *Arabidopsis*. *Nature Communications*, *4*, 1804–1810. <http://doi.org/10.1038/ncomms2815>
- de Boer, H. J., Drake, P. L., Wendt, E., Price, C. A., Schulze, E.-D., Turner, N. C., ... Veneklaas, E. J. (2016). Apparent Overinvestment in Leaf Venation Relaxes Leaf Morphological Constraints on Photosynthesis in Arid Habitats. *Plant Physiology*, *172*(4), 2286–2299. <http://doi.org/10.1104/pp.16.01313>
- de Mattos, E. A., Herzog, B., & Luttge, U. (1999). Chlorophyll fluorescence during CAM-phases in *Clusia minor* L. under drought stress. *Journal of Experimental Botany*, *50*(331), 253–561. <http://doi.org/10.1093/jxb/50.331.253>

- Dever, L. V., Boxall, S. F., Kneřová, J., & Hartwell, J. (2015). Transgenic Perturbation of the Decarboxylation Phase of Crassulacean Acid Metabolism Alters Physiology and Metabolism But Has Only a Small Effect on Growth. *Plant Physiology*, *167*, 44–59. <http://doi.org/10.1104/pp.114.251827>
- Drake, P. L., de Boer, H. J., Schymanski, S. J., & Veneklaas, E. J. (2019). Two sides to every leaf: water and CO₂ transport in hypostomatous and amphistomatous leaves. *New Phytologist*, *222*(3), 1179–1187. <http://doi.org/10.1111/nph.15652>
- Earles, J. M., Theroux-Rancourt, G., Roddy, A. B., Gilbert, M. E., McElrone, A. J., & Brodersen, C. R. (2018). Beyond Porosity: 3D Leaf Intercellular Airspace Traits That Impact Mesophyll Conductance. *Plant Physiology*, *178*(1), 148–162. <http://doi.org/10.1104/pp.18.00550>
- Esau, K. (1965). *Anatomy of Seed Plants* (1st ed.). John Wiley & Sons.
- Franco, A. C., Ball, E., & Lüttge, U. (1991). The influence of nitrogen, light and water stress on CO₂ exchange and organic acid accumulation in the tropical C₃-CAM tree, *Clusia minor*. *Journal of Experimental Botany*, *42*(5), 597–603. <http://doi.org/10.1093/jxb/42.5.597>
- Gibeaut, D. M., & Thomson, W. W. (1989). Leaf Ultrastructure of *Peperomia obtusifolia*, *P. camptotricha*, and *P. scandens*. *Botanical Gazette*, *150*(2), 108–114.
- Gould, S. J., & Lewontin, R. C. (1979). The spandrels of San Marco and the Panglossian paradigm: a critique of the adaptationist programme. *Proceedings of the Royal Society of London - Biological Sciences*, *205*(1161), 581–598. <http://doi.org/10.1098/rspb.1979.0086>
- Grabherr, M. G., Haas, B. J., Yassour, M., Levin, J. Z., Thompson, D. A., Amit, I., ... Regev, A. (2011). Full-length transcriptome assembly from RNA-Seq data without a reference genome. *Nature Biotechnology*, *29*(7), 644–652. <http://doi.org/10.1038/nbt.1883>
- Grace, O. M., Buerki, S., Symonds, M. R. E., Forest, F., Van Wyk, A. E., Smith, G. F., ... Rønsted, N. (2015). Evolutionary history and leaf succulence as explanations for medicinal use in aloes and the global popularity of *Aloe vera*. *BMC Evolutionary Biology*, *15*(1), 1–12. <http://doi.org/10.1186/s12862-015-0291-7>

- Grams, T. E. E., Herzog, B., & Lüttge, U. (1998). Are there species in the genus *Clusia* with obligate C3 photosynthesis? *Journal of Plant Physiology*, *152*(1), 1–9.
[http://doi.org/10.1016/S0176-1617\(98\)80094-1](http://doi.org/10.1016/S0176-1617(98)80094-1)
- Griffin-Nolan, R. J., Ocheltree, T. W., Mueller, K. E., Blumenthal, D. M., Kray, J. A., & Knapp, A. K. (2019). Extending the osmometer method for assessing drought tolerance in herbaceous species. *Oecologia*, *189*(2), 353–363. <http://doi.org/10.1007/s00442-019-04336-w>
- Griffiths, H., Robe, W. E., Girnus, J., & Maxwell, K. (2008). Leaf succulence determines the interplay between carboxylase systems and light use during Crassulacean acid metabolism in *Kalanchoë* species. *Journal of Experimental Botany*, *59*(7), 1851–1861.
<http://doi.org/10.1093/jxb/ern085>
- Gustafsson, M., Winter, K., & Bittrich, V. (2007). Diversity, Phylogeny and Classification of *Clusia*. In U. Lüttge (Ed.), *Clusia A Woody Neotropical Genus of Remarkable Plasticity and Diversity* (pp. 95–116). Springer-Verlag Berlin Heidelberg. Retrieved from
http://link.springer.com/chapter/10.1007/978-3-540-37243-1_7
- Hafke, J. B., Hafke, Y., Smith, J. A. C., Lüttge, U., & Thiel, G. (2003). Vacuolar malate uptake is mediated by an anion-selective inward rectifier. *Plant Journal*, *35*(1), 116–128.
<http://doi.org/10.1046/j.1365-313X.2003.01781.x>
- Hartmann, H. (2015). Carbon starvation during drought-induced tree mortality – are we chasing a myth? *Journal of Plant Hydraulics*, *2*(2008), 005.
<http://doi.org/10.20870/jph.2015.e005>
- Heyduk, K., Burrell, N., Lalani, F., & Leebens-Mack, J. (2016a). Gas exchange and leaf anatomy of a C3-CAM hybrid, *Yucca gloriosa* (Asparagaceae). *Journal of Experimental Botany*, *67*(5), 1369–1379. <http://doi.org/10.1093/jxb/erv536>
- Heyduk, K., Hwang, M., Albert, V., Silvera, K., Lan, T., Farr, K., ... Leebens-Mack, J. (2019a). Altered Gene Regulatory Networks Are Associated With the Transition From C3 to Crassulacean Acid Metabolism in *Erycina* (Oncidiinae: Orchidaceae). *Frontiers in Plant Science*, *9*(January), 1–15. <http://doi.org/10.3389/fpls.2018.02000>

- Heyduk, K., McKain, M. R., Lalani, F., & Leebens-Mack, J. (2016b). Evolution of a CAM anatomy predates the origins of Crassulacean acid metabolism in the Agavoideae (Asparagaceae). *Molecular Phylogenetics and Evolution*, *105*, 102–113. <http://doi.org/10.1016/j.ympev.2016.08.018>
- Heyduk, K., Ray, J. N., Ayyampalayam, S., Moledina, N., Borland, A., Harding, S. A., ... Leebens-Mack, J. (2019b). Shared expression of crassulacean acid metabolism (CAM) genes pre-dates the origin of CAM in the genus *Yucca*. *Journal of Experimental Botany*, (March). <http://doi.org/10.1093/jxb/erz105>
- Hochberg, U., Rockwell, F. E., Holbrook, N. M., & Cochard, H. (2018). Iso/Anisohdry: A Plant–Environment Interaction Rather Than a Simple Hydraulic Trait. *Trends in Plant Science*, *23*(2), 112–120. <http://doi.org/10.1016/j.tplants.2017.11.002>
- Holtum, J. A. M., Aranda, J., Virgo, A., Gehrig, H. H., & Winter, K. (2004). $\delta^{13}\text{C}$ values and crassulacean acid metabolism in *Clusia* species from Panama. *Trees*, *18*, 658–668. <http://doi.org/10.1007/s00468-004-0342-y>
- Holtum, J. A. M., Hancock, L. P., Edwards, E. J., Crisp, M. D., Crayn, D. M., Sage, R., & Winter, K. (2016). Australia lacks stem succulents but is it depauperate in plants with crassulacean acid metabolism (CAM)? *Current Opinion in Plant Biology*, *31*(April), 109–117. <http://doi.org/10.1016/j.pbi.2016.03.018>
- Holtum, J. A. M., Hancock, L. P., Edwards, E. J., & Winter, K. (2017). Facultative CAM photosynthesis (crassulacean acid metabolism) in four species of *Calandrinia*, ephemeral succulents of arid Australia. *Photosynthesis Research*, *134*(1), 17–25. <http://doi.org/10.1007/s11120-017-0359-x>
- Horner, H. T. (2012). *Peperomia* leaf cell wall interface between the multiple hypodermis and crystal-containing photosynthetic layer displays unusual pit fields. *Annals of Botany*, *109*(7), 1307–1315. <https://doi.org/10.1093/aob/mcs074>
- Huang, D. W., Sherman, B. T., & Lempicki, R. A. (2009). Bioinformatics enrichment tools: Paths toward the comprehensive functional analysis of large gene lists. *Nucleic Acids Research*, *37*(1), 1–13. <http://doi.org/10.1093/nar/gkn923>

- John, G. P., Scoffoni, C., Buckley, T. N., Villar, R., Poorter, H., & Sack, L. (2017). The anatomical and compositional basis of leaf mass per area. *Ecology Letters*, *20*(4), 412–425. <http://doi.org/10.1111/ele.12739>
- John, G. P., Scoffoni, C., & Sack, L. (2013). Allometry of cells and tissues within leaves. *American Journal of Botany*, *100*(10), 1936–1948. <http://doi.org/10.3732/ajb.1200608>
- Kaul, R. B. (1977). The Role of the Multiple Epidermis in Foliar Succulence of Peperomia (Piperaceae). *Botanical Gazette*, *138*(2), 213–218.
- Keeley, J. E., & Busch, G. (1984). Carbon assimilation characteristics of the aquatic CAM plant, *Isoetes howellii*. *Plant Physiology*, *76*(2), 525–530. <http://doi.org/10.1104/pp.76.2.525>
- Kluge, M., Knapp, I., Kramer, D., Schwerdtner, I., & Ritter, H. (1979). Crassulacean Acid Metabolism (CAM) in Leaves of *Aloe arborescens* Mill: Comparative Studies of the Carbon Metabolism of Chlorenchym and Central Hydrenchym. *Planta*, *145*(4), 357–363.
- Kornas, A., Fischer-Schliebs, E., Lüttge, U., & Miszalski, Z. (2009). Adaptation of the obligate CAM plant *Clusia alata* to light stress: Metabolic responses. *Journal of Plant Physiology*, *166*(17), 1914–1922. <http://doi.org/10.1016/j.jplph.2009.06.005>
- Leakey, A. D. B., Ferguson, J. N., Pignou, C. P., Wu, A., Jin, Z., Hammer, G. L., & Lobell, D. B. (2019). Water Use Efficiency as a Constraint and Target for Improving the Resilience and Productivity of C3 and C4 Crops. *Annual Review of Plant Biology*, *70*(1), 781–808. <https://doi.org/10.1146/annurev-arplant-042817-040305>
- Lens, F., Tixier, A., Cochard, H., Sperry, J. S., Jansen, S., & Herbette, S. (2013). Embolism resistance as a key mechanism to understand adaptive plant strategies. *Current Opinion in Plant Biology*, *16*, 287–292. <http://doi.org/10.1016/j.pbi.2013.02.005>
- Lim, S. D., Yim, W. C., Liu, D., Hu, R., Yang, X., & Cushman, J. C. (2018). A *Vitis vinifera* basic helix–loop–helix transcription factor enhances plant cell size, vegetative biomass and

reproductive yield. *Plant Biotechnology Journal*, 16(9), 1595–1615.

<https://doi.org/10.1111/pbi.12898>

Lüttge, U. (1999). One morphotype, three physiotypes: Sympatric species of *Clusia* with obligate C3 photosynthesis, obligate CAM and C3-CAM intermediate behaviour. *Plant Biology*, 1(2), 138–148. <http://doi.org/10.1111/j.1438-8677.1999.tb00237.x>

Lüttge, U. (2002). CO₂-concentrating: consequences in crassulacean acid metabolism. *Journal of Experimental Botany*, 53(378), 2131–2142. <http://doi.org/10.1093/jxb/erf081>

Lüttge, U., & Duarte, H. M. (2007). Morphology, Anatomy, Life Forms and Hydraulic Architecture. In U. Lüttge (Ed.), *Clusia A Woody Neotropical Genus of Remarkable Plasticity and Diversity* (1st ed., pp. 17–30). Springer.

Males, J. (2017a). Adaptive variation in vein placement underpins diversity in a major Neotropical plant radiation. *Oecologia*, 185(3), 375–386. <http://doi.org/10.1007/s00442-017-3956-7>

Males, J. (2018). Concerted anatomical change associated with crassulacean acid metabolism in the Bromeliaceae. *Functional Plant Biology*, 45(7), 681–695. <http://doi.org/10.1071/fp17071>

Males, J. (2017b). Secrets of succulence. *Journal of Experimental Botany*, 68(9), 2121–2134. <http://doi.org/10.1093/jxb/erx096>

Males, J., & Griffiths, H. (2018). Economic and hydraulic divergences underpin ecological differentiation in the Bromeliaceae. *Plant Cell and Environment*, 41(1), 64–78. <http://doi.org/10.1111/pce.12954>

Males, J., & Griffiths, H. (2017). Functional types in the Bromeliaceae: relationships with drought-resistance traits and bioclimatic distributions. *Functional Ecology*, 31(10), 1868–1880. <http://doi.org/10.1111/1365-2435.12900>

- Maréchaux, I., Bartlett, M. K., Iribar, A., Sack, L., & Chave, J. (2017). Stronger seasonal adjustment in leaf turgor loss point in lianas than trees in an Amazonian forest. *Biology Letters*, 13(1). <http://doi.org/10.1098/rsbl.2016.0819>
- Maréchaux, I., Bartlett, M. K., Sack, L., Baraloto, C., Engel, J., Joetzjer, E., & Chave, J. (2015). Drought tolerance as predicted by leaf water potential at turgor loss point varies strongly across species within an Amazonian forest. *Functional Ecology*, 29(10), 1268–1277. <http://doi.org/10.1111/1365-2435.12452>
- Martin, C. E., Lin, T. C., Lin, K. C., Hsu, C. C., & Chiou, W. L. (2004). Causes and consequences of high osmotic potentials in epiphytic higher plants. *Journal of Plant Physiology*, 161(10), 1119–1124. <http://doi.org/10.1016/j.jplph.2004.01.008>
- Maxwell, K., Von Caemmerer, S., & Evans, J. R. (1997). Is a low internal conductance to CO₂ diffusion a consequence of succulence in plants with crassulacean acid metabolism? *Australian Journal of Plant Physiology*, 24(6), 777–786. <http://doi.org/10.1071/PP97088>
- Mcdowell, N., Pockman, W. T., Allen, C. D., David, D., Cobb, N., Kolb, T., ... Yezzer, E. A. (2008). Mechanisms of plant survival and mortality during drought: why do some plants survive while others succumb to drought? *New Phytologist*, 178, 719–739.
- Medeiros, C. D., Scoffoni, C., John, G. P., Bartlett, M. K., Inman-Narahari, F., Ostertag, R., ... Sack, L. (2019). An extensive suite of functional traits distinguishes Hawaiian wet and dry forests and enables prediction of species vital rates. *Functional Ecology*, 33(4), 712–734. <http://doi.org/10.1111/1365-2435.13229>
- Méndez-Alonzo, R., Ewers, F. W., Jacobsen, A. L., Pratt, R. B., Scoffoni, C., Bartlett, M. K., & Sack, L. (2019). Covariation between leaf hydraulics and biomechanics is driven by leaf density in Mediterranean shrubs. *Trees*, 33(2), 507–519. <http://doi.org/10.1007/s00468-018-1796-7>
- Ming, R., VanBuren, R., Wai, C. M., Tang, H., Schatz, M. C., Bowers, J. E., ... Yu, Q. (2015). The pineapple genome and the evolution of CAM photosynthesis. *Nature Genetics*, (November). <http://doi.org/10.1038/ng.3435>

- Nardini, A., Lo Gullo, M. A., & Salleo, S. (2011). Refilling embolized xylem conduits: Is it a matter of phloem unloading? *Plant Science*, *180*(4), 604–611.
<http://doi.org/10.1016/j.plantsci.2010.12.011>
- Nelson, E. a., & Sage, R. F. (2008). Functional constraints of CAM leaf anatomy: Tight cell packing is associated with increased CAM function across a gradient of CAM expression. *Journal of Experimental Botany*, *59*(7), 1841–1850. <http://doi.org/10.1093/jxb/erm346>
- Nelson, E. a., Sage, T. L., & Sage, R. F. (2005). Functional leaf anatomy of plants with crassulacean acid metabolism. *Functional Plant Biology*, *32*(5), 409–419.
<http://doi.org/10.1071/FP04195>
- Niechayev, N. A., Pereira, P. N., & Cushman, J. C. (2019). Understanding trait diversity associated with crassulacean acid metabolism (CAM). *Current Opinion in Plant Biology*, *49*, 74–85. <http://doi.org/10.1016/j.pbi.2019.06.004>
- Nishio, J. N., & Ting, I. P. (1987). Carbon Flow and Metabolic Specialization in the Tissue Layers of the Crassulacean Acid Metabolism Plant, *Peperomia camptotricha*. *Plant Physiology*, *84*(3), 600–604. <http://doi.org/10.1104/pp.84.3.600>
- Nobel, P. S. (2006). Parenchyma-chlorenchyma water movement during drought for the hemiepiphytic cactus *Hylocereus undatus*. *Annals of Botany*, *97*(3), 469–474.
<http://doi.org/10.1093/aob/mcj054>
- Nobel, P. S., & Jordan, P. W. (1983). Transpiration stream of desert species: Resistances and capacitances for a C₃, a C₄, and a CAM plant. *Journal of Experimental Botany*, *34*(10), 1379–1391. <http://doi.org/10.1093/jxb/34.10.1379>
- Noblin, X., Mahadevan, L., Coomaraswamy, I. A., Weitz, D. A., Holbrook, N. M., & Zwieniecki, M. A. (2008). Optimal vein density in artificial and real leaves. *Proceedings of the National Academy of Sciences of the United States of America*, *105*(27), 9140–9144.
<http://doi.org/10.1073/pnas.0709194105>
- Nolan, R. H., Fairweather, K. A., Tarin, T., Santini, N. S., Cleverly, J., Faux, R., & Eamus, D. (2017). Divergence in plant water-use strategies in semiarid woody species. *Functional Plant Biology*, *44*(11), 1134–1146. <http://doi.org/10.1071/FP17079>

- Nowak, E. J., & Martin, C. E. (1997). Physiological and Anatomical Responses to Water Deficits in the CAM Epiphyte *Tillandsia ionantha* (Bromeliaceae). *International Journal of Plant Sciences*, *158*(6), 818–826.
- Ogburn, R. M., & Edwards, E. J. (2010). The ecological water-use strategies of succulent plants. In J.-C. Kader & M. Delseny (Eds.), *Advances in Botanical Research* (1st ed., Vol. 55, pp. 179–225). Elsevier Ltd. <http://doi.org/10.1016/B978-0-12-380868-4.00004-1>
- Ogburn, R. M., & Edwards, E. J. (2013). Repeated origin of three-dimensional leaf venation releases constraints on the evolution of succulence in plants. *Current Biology*, *23*(8), 722–726. <http://doi.org/10.1016/j.cub.2013.03.029>
- Ogburn, R. M., & Edwards, E. J. (2012). Quantifying succulence: A rapid, physiologically meaningful metric of plant water storage. *Plant, Cell and Environment*, *35*(9), 1533–1542. <http://doi.org/10.1111/j.1365-3040.2012.02503.x>
- Ong, B.-L., Koh, C. K.-K., & Wee, Y.-C. (1992). Changes in Cell Wall Structure of *Pyrrhosia piloselloides* (L.) Price Leaf Cells During Water. *International Journal of Plant Sciences*, *153*(3), 329–332.
- Osmond, C. B. (1978). Crassulacean Acid Metabolism : a Curiosity. *Annual Review of Plant Physiology*, *29*, 379–414.
- Pereira, P. N., Smith, J. A. C., Purgatto, E., & Mercier, H. (2017). Proton and anion transport across the tonoplast vesicles in bromeliad species. *Functional Plant Biology*, *44*(6), 646–653. <http://doi.org/10.1071/FP16293>
- Pierce, S., Winter, K., & Griffiths, H. (2002). The role of CAM in high rainfall cloud forests: an in situ comparison of photosynthetic pathways in Bromeliaceae. *Plant, Cell and Environment*, *25*(2), 1181–1189. Retrieved from <http://onlinelibrary.wiley.com/doi/10.1046/j.1365-3040.2002.00900.x/pdf>
- Popp, M., Kramer, D., Lee, H., Diaz, M., Ziegler, H., & Liittge, U. (1987). Crassulacean acid metabolism in tropical dicotyledonous trees of the genus *Clusia*. *Trees*, *1*, 238–247.

- Ripley, B. S., Abraham, T., Klak, C., & Cramer, M. D. (2013). How succulent leaves of Aizoaceae avoid mesophyll conductance limitations of photosynthesis and survive drought. *Journal of Experimental Botany*, *64*(18), 5485–5496.
<http://doi.org/10.1093/jxb/ert314>
- Rodriguez-Dominguez, C. M., Carins Murphy, M. R., Lucani, C., & Brodribb, T. J. (2018). Mapping xylem failure in disparate organs of whole plants reveals extreme resistance in olive roots. *New Phytologist*, *218*(3), 1025–1035. <http://doi.org/10.1111/nph.15079>
- Sack, L., Buckley, T. N., & Scoffoni, C. (2016). Why are leaves hydraulically vulnerable? *Journal of Experimental Botany*, *67*(17), 4917–4919. <http://doi.org/10.1093/jxb/erw304>
- Sack, L., & Holbrook, N. M. (2006). Leaf Hydraulics. *Annual Review of Plant Biology*, *57*(1), 361–381. <http://doi.org/10.1146/annurev.arplant.56.032604.144141>
- Sack, L., & Scoffoni, C. (2013). Leaf venation : structure, function, development, evolution, ecology and applications in the past, present and future. *New Phytologist*, 983–1000.
<http://doi.org/10.1111/nph.12253>
- Sack, L., & Tyree, M. T. (2005). Leaf Hydraulics and Its Implications in Plant Structure and Function. In *Vascular Transport in Plants* (pp. 93–114). Elsevier Inc.
<http://doi.org/10.1016/B978-0-12-088457-5.50007-1>
- Saito, T., Soga, K., Hoson, T., & Terashima, I. (2006). The bulk elastic modulus and the reversible properties of cell walls in developing *Quercus* leaves. *Plant and Cell Physiology*, *47*(6), 715–725. <http://doi.org/10.1093/pcp/pcj042>
- Schmidt, J. E., & Kaiser, W. M. (1987). Response of the Succulent Leaves of *Peperomia magnoliaefolia* to Dehydration. *Plant Physiology*, *83*(1), 190–194.
<http://doi.org/10.1104/pp.83.1.190>
- Scholander, A. P. F., Hammel, H. T., Bradstreet, E. D., & Hemmingsen, E. A. (1965). Sap Pressure in Vascular Plants. *Science*, *148*(3668), 339–346.
- Schulte, P. J., & Nobel, P. S. (1989). Responses of a CAM Plant to Drought and Rainfall : Capacitance and Osmotic Pressure Influences on Water Movement. *Journal of*

Experimental Botany, 40(210), 61–70. Retrieved from

<http://jxb.oxfordjournals.org/lookup/doi/10.1093/jxb/40.1.61>

Scoffoni, C., Rawls, M., McKown, A., Cochard, H., & Sack, L. (2011). Decline of Leaf Hydraulic Conductance with Dehydration: Relationship to Leaf Size and Venation Architecture. *Plant Physiology*, 156(2), 832–843. <http://doi.org/10.1104/pp.111.173856>

Scoffoni, C., Albuquerque, C., Brodersen, C. R., Townes, S. V., John, G. P., Bartlett, M. K., ... Sack, L. (2017). Outside-Xylem Vulnerability, Not Xylem Embolism, Controls Leaf Hydraulic Decline during Dehydration. *Plant Physiology*, 173(2), 1197–1210. <http://doi.org/10.1104/pp.16.01643>

Scoffoni, C., Albuquerque, C., Brodersen, C. R., Townes, S. V., John, G. P., Cochard, H., ... Sack, L. (2016a). Leaf vein xylem conduit diameter influences susceptibility to embolism and hydraulic decline. *New Phytologist*, 213(3), 1076–1092. <http://doi.org/10.1111/nph.14256>

Scoffoni, C., Chatelet, D. S., Pasquet-Kok, J., Rawls, M., Donoghue, M. J., Edwards, E. J., & Sack, L. (2016b). Hydraulic basis for the evolution of photosynthetic productivity. *Nature Plants*, 2(6), 1–8. <http://doi.org/10.1038/nplants.2016.72>

Sevanto, S., McDowell, N. G., Dickman, L. T., Pangle, R., & Pockman, W. T. (2014). How do trees die? A test of the hydraulic failure and carbon starvation hypotheses. *Plant, Cell and Environment*, 37(1), 153–161. <http://doi.org/10.1111/pce.12141>

Shameer, S., Baghalian, K., Cheung, C. Y. M., Ratcliffe, R. G., & Sweetlove, L. J. (2018). Computational analysis of the productivity potential of CAM. *Nature Plants*, 4(3), 165–171. <http://doi.org/10.1038/s41477-018-0112-2>

Sheffield, J., & Wood, E. F. (2008). Global trends and variability in soil moisture and drought characteristics, 1950–2000, from observation-driven simulations of the terrestrial hydrologic cycle. *Journal of Climate*, 21(3), 432–458. <https://doi.org/10.1175/2007JCLI1822.1>

- Silvera, K., & Lasso, E. (2016). Ecophysiology and Crassulacean Acid Metabolism of Tropical Epiphytes. In G. Goldstein & L. S. Santiago (Eds.), *Tropical Tree Physiology* (6th ed., pp. 25–43). Springer.
- Silvera, K., Santiago, L. S., Cushman, J. C., & Winter, K. (2009). Crassulacean acid metabolism and epiphytism linked to adaptive radiations in the Orchidaceae. *Plant Physiology*, *149*(4), 1838–47. <http://doi.org/10.1104/pp.108.132555>
- Sipes, D. L., & Ting, I. P. (1985). Crassulacean Acid Metabolism and Crassulacean Acid Metabolism Modifications in *Peperomia camptotricha*. *Plant Physiology*, *77*(1), 59–63. <http://doi.org/10.1104/pp.77.1.59>
- Smith, J. A. C., & Lüttge, U. (1985). Day-night changes in leaf water relations associated with the rhythm of crassulacean acid metabolism in *Kalanchoë daigremontiana*. *Planta*, *163*(2), 272–282. <http://doi.org/10.1007/BF00393518>
- Smith, J. A. C., Schulte, P. J., & Nobel, P. S. (1987). Water Flow and Water Storage in Agave deserti: osmotic implications of Crassulacean Acid Metabolism. *Plant, Cell and Environment*, *10*, 639–648.
- Smith, J. A. C., & Heuer, S. (1981). Determination of the volume of intercellular spaces in leaves and some values for CAM plants. *Annals of Botany*, *48*(6), 915–917. <https://doi.org/10.1093/oxfordjournals.aob.a086200>
- South, P. F., Cavanagh, A. P., Liu, H. W., & Ort, D. R. (2019). Synthetic glycolate metabolism pathways stimulate crop growth and productivity in the field. *Science*, *363*(6422), 0–10. <http://doi.org/10.1126/science.aat9077>
- Strickler, S. R., Bombarely, A., & Mueller, L. a. (2012). Designing a transcriptome next-generation sequencing project for a nonmodel plant species. *American Journal of Botany*, *99*(2), 257–266. <http://doi.org/10.3732/ajb.1100292>
- Surget-Groba, Y., & Montoya-Burgos, J. I. (2010). Optimization of de novo transcriptome assembly from next-generation sequencing data. *Genome Research*, *20*(10), 1432–1440. <http://doi.org/10.1101/gr.103846.109>

- Taybi, T., & Cushman, J. C. (1999). Signaling events leading to Crassulacean acid metabolism induction in the common ice plant. *Plant Physiology*, *121*(2), 545–555.
- Taybi, T., Nimmo, H. G., & Borland, A. M. (2004). Expression of Phospho enol pyruvate Carboxylase and Phospho enol pyruvate Carboxylase Kinase Genes. Implications for Genotypic Capacity and Phenotypic Plasticity in the Expression of Crassulacean Acid Metabolism. *Plant Physiology*, *135*(May), 587–598.
<http://doi.org/10.1104/pp.103.036962.1>
- Ting, I. P., Lord, E. M., Sternberg, L. S. L., & DeNiro, M. J. (1985). Crassulacean Acid Metabolism in the Strangler *Clusia rosea* Jacq. *Science*, *229*(4717), 969–971.
- Ting, I. P., Patel, A., Sipes, D. L., Reid, P. D., & Walling, L. L. (1994). Differential expression of photosynthesis genes in leaf tissue layers of *Peperomia* as revealed by tissue printing. *American Journal of Botany*, *81*(4), 414–422. <http://doi.org/10.2307/2445490>
- Tinoco Ojanguren, C., & Vázquez Yanes, C. (1983). Especies CAM en la selva húmeda tropical de los tuxtlas, Veracruz. *Boletín de La Sociedad Botánica de México*, *45*(March 1983), 150–153.
- Tomás, M., Flexas, J., Copolovici, L., Galmés, J., Hallik, L., Medrano, H., ... Niinemets, Ü. (2013). Importance of leaf anatomy in determining mesophyll diffusion conductance to CO₂ across species: Quantitative limitations and scaling up by models. *Journal of Experimental Botany*, *64*(8), 2269–2281. <http://doi.org/10.1093/jxb/ert086>
- Trueba, S., Pan, R., Scoffoni, C., John, G. P., Davis, S. D., & Sack, L. (2019). Thresholds for leaf damage due to dehydration: declines of hydraulic function, stomatal conductance and cellular integrity precede those for photochemistry. *New Phytologist*, *223*(1), 134–149. <http://doi.org/10.1111/nph.15779>
- Tyree, M. T., & Hammel, H. T. (1972). The Measurement of the Turgor Pressure and the Water Relations of Plants by the Pressure-bomb Technique. *Journal of Experimental Botany*, *23*(February), 267–282. <http://doi.org/10.1093/jxb/23.1.267>
- Valente, L. M., Britton, A. W., Powell, M. P., Papadopoulos, A. S. T., Burgoyne, P. M., & Savolainen, V. (2014). Correlates of hyperdiversity in southern African ice plants

(Aizoaceae). *Botanical Journal of the Linnean Society*, 174(1), 110–129.

<http://doi.org/10.1111/boj.12117>

Wagner, G. P., Kin, K., & Lynch, V. J. (2012). Measurement of mRNA abundance using RNA-seq data: RPKM measure is inconsistent among samples. *Theory in Biosciences*, 131(4), 281–5. <http://doi.org/10.1007/s12064-012-0162-3>

Wai, C. M., VanBuren, R., Zhang, J., Huang, L., Miao, W., Edger, P. P., ... Ming, R. (2017). Temporal and spatial transcriptomic and microRNA dynamics of CAM photosynthesis in pineapple. *Plant Journal*, 92(1), 19–30. <http://doi.org/10.1111/tpj.13630>

Wai, C. M., Weise, S. E., Ozersky, P., Mockler, T. C., Michael, T. P., & VanBuren, R. (2019). Time of day and network reprogramming during drought induced CAM photosynthesis in *Sedum album*. *PLOS Genetics* (Vol. 15). <http://doi.org/10.1371/journal.pgen.1008209>

Wang, Z., Gerstein, M., & Snyder, M. (2009). RNA-Seq: a revolutionary tool for transcriptomics. *Nature Reviews. Genetics*, 10(1), 57–63. <http://doi.org/10.1038/nrg2484>

Winter, K., Garcia, M., & Holtum, J. a. M. (2008). On the nature of facultative and constitutive CAM: environmental and developmental control of CAM expression during early growth of *Clusia*, *Kalanchoë*, and *Opuntia*. *Journal of Experimental Botany*, 59(7), 1829–1840. <http://doi.org/10.1093/jxb/ern080>

Winter, K. (2019). Ecophysiology of constitutive and facultative CAM photosynthesis. *Journal of Experimental Botany*, *In pr.* <http://doi.org/10.1093/jxb/erz002>

Winter, K., Aranda, J., & Holtum, J. A. M. (2005). Carbon isotope composition and water-use efficiency in plants with crassulacean acid metabolism. *Functional Plant Biology*, 32(5), 381–388. <http://doi.org/10.1071/FP04123>

Winter, K., Garcia, M., & Holtum, J. A. M. (2009). Canopy CO₂ exchange of two neotropical tree species exhibiting constitutive and facultative CAM photosynthesis, *Clusia rosea* and *Clusia cylindrica*. *Journal of Experimental Botany*, 60(11), 3167–3177. <http://doi.org/10.1093/jxb/erp149>

- Winter, K., Garcia, M., Virgo, A., & Holtum, J. A. M. (2018). Operating at the very low end of the crassulacean acid metabolism spectrum: *Sesuvium portulacastrum* (Aizoaceae) . *Journal of Experimental Botany*, (December). <http://doi.org/10.1093/jxb/ery431>
- Winter, K., Holtum, J. A. M., & Smith, J. A. C. (2015). Crassulacean acid metabolism: a continuous or discrete trait? *The New Phytologist*, *208*(1), 73–8. <http://doi.org/10.1111/nph.13446>
- Winter, K., & Holtum, J. A. M. (2015). Cryptic crassulacean acid metabolism (CAM) in *Jatropha curcas*. *Functional Plant Biology*, *42*(8), 711–717. <http://doi.org/10.1071/FP15021>
- Winter, K., & Holtum, J. A. M. (2011). Induction and reversal of crassulacean acid metabolism in *Calandrinia polyandra*: Effects of soil moisture and nutrients. *Functional Plant Biology*, *38*(7), 576–582. <http://doi.org/10.1071/FP11028>
- Winter, K., & Holtum, J. A. M. (2014). Facultative crassulacean acid metabolism (CAM) plants: powerful tools for unravelling the functional elements of CAM photosynthesis. *Journal of Experimental Botany*, *65*(13), 3425–3441. <http://doi.org/10.1093/jxb/eru063>
- Yang, X., Hu, R., Yin, H., Jenkins, J., Shu, S., Tang, H., ... Tuskan, G. A. (2017). The *Kalanchoë* genome provides insights into convergent evolution and building blocks of crassulacean acid metabolism. *Nature Communications*, *8*(1). <http://doi.org/10.1038/s41467-017-01491-7>
- Yuan, M., Xu, F., Wang, S. D., Zhang, D. W., Zhang, Z. W., Cao, Y., ... Yuan, S. (2012). A single leaf of *Camellia oleifera* has two types of carbon assimilation pathway, C3 and crassulacean acid metabolism. *Tree Physiology*, *32*(2), 188–199. <http://doi.org/10.1093/treephys/tps002>
- Zhang, Y.-J., Rockwell, F. E., Graham, A. C., Alexander, T., & Holbrook, N. M. (2016). Reversible Leaf Xylem Collapse: A Potential “Circuit Breaker” against Cavitation. *Plant Physiology*, *172*(4), 2261–2274. <http://doi.org/10.1104/pp.16.01191>

- Zotz, G., & Winter, K. (1993). Short-Term Regulation of Crassulacean Acid Metabolism Activity in a Tropical Hemiepiphyte, *Clusia uvitana*. *Plant Physiology*, *102*(3), 835–841.
<http://doi.org/10.1104/pp.102.3.835>
- Zotz, G., Tyree, M. T., Cochard, H., & Cochard, H. (1994). Hydraulic architecture, water relations and vulnerability to cavitation of *Clusia uvitana* Pittier: a C3-CAM tropical hemiepiphyte. *New Phytologist*, *127*(2), 287–295.
- Zwieniecki, M. A., & Boyce, C. K. (2014). Evolution of a unique anatomical precision in angiosperm leaf venation lifts constraints on vascular plant ecology. *Proceedings of the Royal Society B: Biological Sciences*, *281*(1779), 20132829–20132829.
<http://doi.org/10.1098/rspb.2013.2829>

Chapter 2. Dissecting Capacitance and Crassulacean Acid Metabolism; Two Distinct Adaptations to Drought in the Genus *Clusia*

2.1 Introduction

Succulence is an adaptation in plants found across the world in arid, semi-arid and seasonally dry ecosystems (Arakaki et al., 2011; Males 2017). The succulence syndrome is defined by fleshy, water-filled tissue that are often assumed to buffer a plant against dehydration by providing hydraulic capacitance; allowing the plant to lose water without experiencing damaging drops to water potentials (Ogburn and Edwards, 2010; Males 2018). Plants can evolve succulence via the development of specialised water storage tissue called hydrenchyma (such as the gel of an *Aloe vera* leaf) (Grace et al., 2015; Ahl et al., 2019), enlarged photosynthetic chlorenchyma cells, or a combination of the two (Males 2018). In addition, the succulent syndrome is often characterised by a diel rhythm of acid accumulation in the chlorenchyma, a process known as Crassulacean acid metabolism (CAM) (Nelson et al., 2005; Borland et al., 2014; Yang et al., 2015). CAM allows plants to minimise water loss by inverting the diel cycle of stomatal opening (Borland et al., 2014). During the night, plants doing CAM open their stomata and assimilate carbon, fixing CO₂ into organic acids which are then stored in large vacuoles of succulent chlorenchyma cells (Borland et al., 2018, Winter, 2019). The following day, this organic acid is decarboxylated behind closed stomata to regenerate CO₂, which is fed into the Calvin cycle. The consequence of CAM is that stomata open more at night, when evapotranspirational demands are lower, and less during the day when the atmosphere is hotter and drier. Thus, like succulence, CAM is an adaptation to drought.

Despite it being known for over a century that CAM is found exclusively and frequently in succulent taxa (Richards, 1915), the precise hydraulic roles these adaptations play in the plant drought response have been hitherto indistinguishable, as they co-occur and are presumed to be under the same selection pressures (Ogburn and Edwards, 2010; Ripley et al., 2013; Edwards, 2019). When looking at phylogenetic analyses, it has become clear that the evolution of strong CAM (where CAM is expressed constitutively, and is the major mode of carbon acquisition), from a C₃-CAM intermediate (where CAM is weakly or transiently expressed, and C₃ is the major mode of carbon acquisition) is often substantially limited by

the evolution of larger, succulent chlorenchyma cells to store the organic acids that are produced at night (Edwards 2019). CAM and succulent chlorenchyma tissue are co-selected, and consequently it has not been possible to determine if large photosynthetic cells evolved specifically to store organic acids during the night phase of CAM, or if they originated to facilitate water storage and buffer leaves against water loss, with CAM being a side effect (Ripley et al., 2013; Edwards, 2019).

To answer this question, it is necessary to develop a robust physiological framework for describing how CAM and the different forms of succulent tissue each contribute to the plant drought response, with particular focus on bulk hydraulic capacitance: the ability of a plant tissue to buffer water potential during dehydration (Blackman and Brodribb, 2011). In recent years, comparative physiology has helped uncover some important traits associated with succulence beyond increased capacitance, such as the evolution of 3D venation and a lower osmotic potential at full turgor (Ogburn and Edwards, 2012; Ogburn and Edwards, 2013; Males and Griffiths 2017). However, these studies have typically made comparisons within plant families or even orders and have not been able to dissect the hydraulic properties of each individual component of the succulent syndrome; the large chlorenchyma cells that host the CAM cycle and the specialised water-storage hydrenchyma. Recent emphasis has argued for the use of closely related, physiologically diverse taxa to answer central questions about physiology (Scoffoni et al., 2016). To this end, the genus *Clusia* is an extremely powerful model to understand CAM and the different succulent anatomical adaptations, due to its high physiological and anatomical diversity. It has been known for 30 years that *Clusia* contains a complete spectrum of C₃, facultative and constitutive CAM species (Popp et al., 1987; Lüttge 1999; Holtum et al., 2004; Barrera Zambrano et al., 2014), but recent research has also pointed to the anatomical diversity in this genus. A study into the leaf anatomy of 9 species with different photosynthetic physiologies found that CAM is associated with large, succulent palisade cells (Barrera Zambrano et al., 2014). In addition, *Clusia* species vary in their development of hydrenchyma tissue; a trait which is independent of CAM and palisade size. Therefore, *Clusia* contains an unparalleled anatomical diversity, within a single genus, making it an ideal model for comparative analyses into the physiology of succulence. This study made use of the anatomical diversity in *Clusia* leaves, to investigate which form of succulent anatomy (hydrenchyma or enlarged chlorenchyma cells) provides greater hydraulic capacitance to the leaf. In addition, the newly developed PHOTO3 model was used to

investigate how CAM and capacitance each contribute to plant physiology during drought. The PHOT03 model was parameterised to simulate how high and low capacitance affects transpiration and water use efficiency in a C₃ and constitutive CAM plant, to explore how each adaptation contributes to the drought response of *Clusia*. Together, the data presented indicate that CAM-based and water-storage succulence play discretely different roles in the plant drought response, and should be considered distinct adaptations that make up the succulent syndrome.

2.2 Materials and Methods

2.2.1 Species Studied

This comparative study investigated all of the 9 species previously characterised by Barrera Zambrano et al., (2014). These are: C₃ species – *Clusia multiflora*, *C. tocuchensis* and *C. grandiflora*; C₃-CAM species – *C. lanceolata*, *C. aripoensis* and *C. minor*; and the constitutive CAM – *C. rosea*, *C. alata* and *C. hilariana*. These represent phylogenetically diverse spread of species, from multiple clades in the phylogeny, including sect. Anandrogynae, sect. Retinostemon, sect. Cordylandra and sect. Chlamydoclusia (Gustafsson et al., 2007, Barrera Zambrano et al., 2014 – and references therein). In addition, 2 other species were included. These are the C₃-CAM species, *C. pratensis* (Winter et al., 2008, Winter and Holtum, 2014) and the constitutive CAM species, *C. fluminensis* (Roberts et al., 1996).

2.2.2 Plant Growth Conditions

Plants used for pressure volume curve analyses and hand-cut anatomical sections were grown in glass houses at Cockle Park University Farm, Newcastle. Three to seven year old plants were grown in 10 L pots, containing a mix of loam-based compost (John Innes No. 2, Sinclair Horticulture Ltd, Lincoln, UK) and sand (3:1 v/v). The glass house was fitted with photosynthetic LED lights (Attis 5 LED plant growth light, PhytoLux, UK) allowing plants to receive a minimum 12 hour light day. Plants were kept at 25 degrees C during the day and 23 degrees C during the night and watered every 2 days.

Clusia pratensis and *C. fluminensis* plants were phenotyped under identical conditions, in the same growth room, as the studies described in Barrera Zambrano et al., (2014). Namely, plants were propagated from cuttings taken from mature trees grown in the glass house in Cockle Park Farm, Newcastle, initially harvested 3 to 4 internodes below the stem apical meristem and were cut just below the node, to facilitate root growth. Cuttings were transferred to 200 ml pots containing 2:1:1 soil (John Innes No. 2, Sinclair Horticulture Ltd, Lincoln, UK), perlite (Sinclair, UK) and sand, to allow drainage. Pots were placed in a thermal incubator that warmed the soil to 23 °C. The incubator was lined with sand that was watered every 2 days to ensure the soil remained wet and the air remained humid. Individual pots

were watered if, upon inspection they appeared too dry. Once plants had rooted they were transferred to pots containing a 3:1 mix of soil (John Innes No. 2, Sinclair Horticulture Ltd, Lincoln, UK) and sand. Plants were grown for 6 months following propagation under fluorescent lights (F100W/840, Polylux cool white, Light Emission Technology, New York, USA), which provided approx. $300 \mu\text{mol m}^{-2} \text{s}^{-1}$ PFD. Plants were kept at a relative humidity level of 65-75% and a temperature of 27 °C during the day and 18 °C at night.

2.2.3 Characterising Photosynthetic Physiology

Gas exchange profiles from Barrera Zambrano et al., (2014) were used to characterise species as either C_3 , facultative CAM or constitutive CAM. To phenotype *C. pratensis* and *C. fluminensis*, the same procedure was carried out as described in Barrera Zambrano et al., (2014), under the same environmental growth conditions. One week prior to starting the drought treatment, plants were watered every day to ensure that soil was saturated with water. One day prior to starting the drought treatment, plants were watered heavily, so that the trays containing pots contained approx. 2 cm of water. The following day, plants were moved from the aforementioned trays and a mature, fully expanded and light-exposed leaf was inserted into a compact mini cuvette system, Central Unit CMS-400 linked to a BINOS-100 infra-red gas analyser (Heinz Walz GmbH, Effeltrich, Germany). As described in Barrera Zambrano et al., (2014), the temperature of the cuvette tracked the temperature in the growth room and the gas flow through the cuvette was set to 400-500 ml min^{-1} . The rate of photosynthetic assimilation was recorded every 20 minutes for 14 days. DIAGAS software (Heinz Walz GmbH, Effeltrich, Germany) was used to calculate rates of net CO_2 uptake on a leaf area basis. An in-house R script was used to calculate the total 24 hour net CO_2 uptake, which was then used to determine the percentage of net CO_2 uptake occurring at night. These analyses were performed for well-watered plants and drought treated plants (days 1 and 9 after the cessation of watering, respectively). For each species data was generated for 3 biological replicates. Upon completion of this analysis it was shown that *C. pratensis* facultatively expresses CAM, and *C. fluminensis* constitutively expresses CAM, and these data were added to pre-existing gas exchange values for nine other species of *Clusia* (Barrera Zambrano et al., 2014).

2.2.4 Measurement of Saturated Water Content (SWC), Leaf Dry Mass per Area (LMA) and Water Mass per Area (WMA)

Plants analysed from the *Clusia* collection at Cockle Park, Newcastle University were sampled between May and June, 2018. One day prior to starting each experiment, branches were cut at 6-9 nodes from the apex and immediately recut underwater 2 nodes higher. From each branch, the third leaf from the apex was cut underwater and the leaf was incubated in deionised water, so that the cut petiole was fully submerged, and the lamina was not. Incubated leaves were sealed inside clear plastic bags, into which water was sprayed to maximise the humidity. Bagged leaves were then placed inside a plant growth chamber (SANYO Fitotron) for 24 hours (12 hour light period, day/night temp 25/19 °C) to allow leaves to rehydrate. Once leaves were rehydrated, they were dabbed dry and the fresh mass at full turgor (FM_{FT}) was immediately measured to the closest milligram. Leaves were then scanned using a flatbed scanner, and ImageJ was used to measure leaf area. Leaves were then dried in an oven at 75 °C for 48 hours and weighed to measure dry mass. Leaf dry mass per area (LMA) was calculated with the equation:

Equation 2.1

$$LMA = \frac{DM}{LA},$$

Where DM is dry mass and LA is leaf area. Water mass per area (WMA) was calculated as:

Equation 2.2

$$WMA = \frac{(FM_{FT} - DM)}{LA},$$

Where FM_{FT} is the fresh mass at full turgor, for fully hydrated leaves.

Saturated water content (SWC) was calculated using the equation:

Equation 2.3

$$SWC = \frac{WMA}{LMA}$$

For each species, 12 replicate leaves were measured.

2.2.5 Anatomical Measurements

High throughput measurements of tissue thickness were taken from hand-sectioned leaves. Lamina tissue was sectioned, using a razor blade, midway along the proximal-distal axis of the leaf. Sectioned tissue was imaged with a fluorescent microscope (Q-IMAGING, QICAM, fast 1394 camera, mounted on a Leica DMRB microscope). Images were used to measure the depth of hydrenchyma, palisade and spongy mesophyll tissue using ImageJ (NIH). For each image, three technical replicate measurements were recorded. For each species, 12 replicate leaves were measured. In addition to data for tissue depth, anatomical data on cell sizes, from resin-set sections was taken from Barrera Zambrano et al., (2014) and Borland et al., (2018) (n = 2-4).

2.2.6 Pressure Volume Curves

The bench drying method described by Tyree and Hammel (1972) was used to construct pressure volume curves. Sampling was done between November 2017 and March 2018. Plants were sampled and leaves were cut and incubated in the same way as described for the determination of LMA, WMA and SWC. After incubated rehydration for 24 hours, leaves were weighed to calculate fresh mass at full turgor. Leaf water potential (Ψ_l) and fresh mass were then measured, serially: leaves were placed in plastic bags to equilibrate, for 15 minutes, and sealed in a Scholander pressure-bomb (Scholander et al., 1965) to measure their water potential. Following this, leaves were immediately weighed to the nearest milligram. This was repeated for each leaf until it appeared damaged or water potential went up/could not be measured. After measurements of Ψ_l had finished, leaves were scanned using a flatbed scanner (hp Scanjet 5530 Photosmart Scanner, Hp, UK) and leaf area was measured using ImageJ (NIH). Leaves were then dried in an oven at 75 °C for 48h and weighed to determine the dry mass. With this it was possible to calculate the relative water content at any point in the serial dry-down data using the following equation:

Equation 2.4

$$RWC = \frac{FM - DM}{FM_{FT} - DM} \times 100$$

Where FM is fresh mass during the dry-down experiment, DM is the dry mass and FM_{FT} is the fresh mass at full turgor, for fully hydrated leaves.

For each replicate, the data was plotted using the pressure volume curve tool from Sack and Pasquet-Kok (2011). Bulk capacitance at full turgor C_{FT} was calculated according to the equation:

Equation 2.5

$$C_{FT} = \Delta RWC / \Delta \Psi_l \times (FM_{FT} / LA) / 18$$

Where LA is the leaf area in m^2 . The bulk modulus of cell wall elasticity, ϵ , was calculated using the equation:

Equation 2.6

$$\epsilon = \frac{\Delta P}{\Delta RWC}$$

Where P is turgor pressure. At the conclusion of the experiment, 6 biological replicates had been recorded per species.

2.2.7 Statistics

All statistics were performed using R version 3.4.1. Mixed effect modelling was performed using the package 'nlme' version 3.1-137. With all mixed effect modelling, assumptions of the statistical test were investigated, by inspecting residual vs fitted plots and normal Q-Q plots (plots not shown).

2.2.8 PHOT03 Model Parameterisation

To explore the effect of capacitance and CAM on transpiration and leaf water potentials during drought, the PHOT03 model, (Hartzell et al., 2018) was parameterised using *Clusia* data. The PHOT03 model estimates daily transpiration, and can be parameterised to simulate a C_3 or a CAM plant. In the PHOT03 model, stomatal conductance, and hence transpiration are estimated based on the leaf water potential. Therefore, by including different values of absolute capacitance, it was possible to explore how capacitance affected water loss, and how this compared to the effects that CAM had on transpiration. Four scenarios were simulated; C_3 –high capacitance, C_3 –low capacitance, CAM – high capacitance

and CAM – low capacitance. This work was done in collaboration with Samantha Hartzell, Princeton, USA, who designed the model. The maximum and minimum capacitance values measured in this chapter were used to parameterise the model (Table 2.1). The TLP was assumed to be -1.5 MPa, and to not differ between C₃ and CAM species (Chapter 3). In addition, maximum malic acid concentration, as well as maximum rate of malic acid storage flux (Chapter 6), were used to parameterise CAM photosynthesis in the model. Other parameters (Tables 2.2 and 2.3) were taken from the literature, from a previous attempt to model CAM in *Clusia* (Bartlett et al., 2014).

2.3 Results

It was predicted that saturated water content (SWC), which is a physiologically meaningful metric for describing succulence (Ogburn and Edwards, 2012), would correlate strongly with water mass per leaf area (WMA), and leaf thickness in *Clusia*. This prediction was based on the observation that, in *Clusia*, thicker leaves, with greater water contents occur primarily due to the presence of larger palisade cells, rather than more layers of cells in the leaf (Barrera Zambrano et al., 2014). However, this prediction did not hold true for the 11, physiologically diverse species of *Clusia* studied (Fig. 2.1). In fact, when considering all the species together no relationship existed between photosynthetic physiology and SWC, despite the constitutive CAM species having consistently higher WMA values than facultative CAM or obligate C₃ relatives. The same was true when looking at the relationship between leaf thickness and SWC (Fig. 2.2) There was, however, a clear and significant relationship between WMA and SWC when only comparing species with C₃ or C₃-CAM photosynthetic physiologies (blue and yellow dots, respectively, Fig. 2.1). Likewise, a significant correlation exists between the WMA and SWC values of the strong CAM species (green dots, Fig. 2.1). The lack of a significant relationship between SWC and WMA in the total data set is the result of the strong CAM species having higher WMA without a higher SWC (i.e. the gap between the blue/yellow dashed lines and the green dashed line). The reason for this is that strong CAM species have higher LMA (Fig. 2.1). Taken together, these data show that higher WMA causes leaves to have higher SWC, unless this high water content is associated with the evolution of a strong CAM physiology. Put differently, strong CAM species have a higher water content, but do not exhibit high SWC; the physiological characteristic typical of succulent plants (Ogburn and Edwards, 2012).

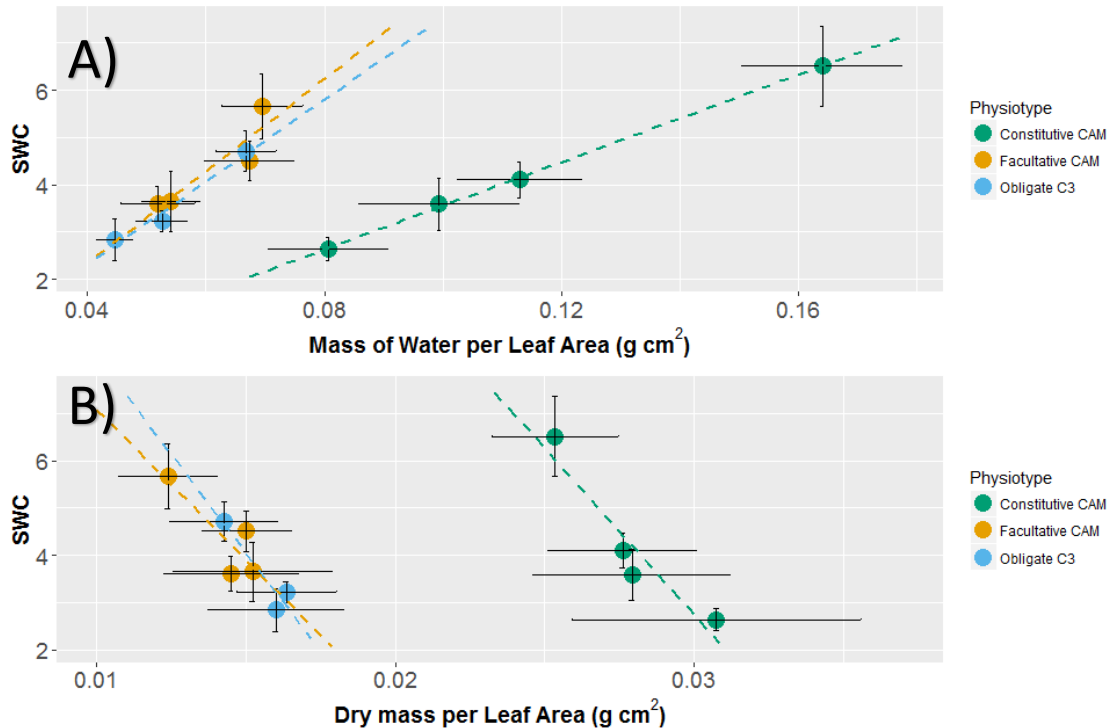


Fig. 2.1) Strong CAM plants have more water in their leaves, but do not have higher saturated water content (SWC). (A) Relationship between water mass per area (WMA) and saturated water content (SWC), used as a physiological metric for succulence, from plants grown in a glass-house in Cockle Park University Farm, Newcastle, UK. To show, statistically, that constitutive CAM plants do not have higher SWC, a nested linear model was built, with WMA, nested within the categorical variable 'physiotype' as fixed terms to describe SWC. This model found no significant difference between the SWC of constitutive CAM and facultative CAM species ($p = 0.055$) or between the SWC of constitutive CAM and obligate C₃ species ($p = 0.538$). There was a significant interaction term between WMA and each physiotype; for C₃ and facultative CAM species (blue and orange dots, respectively), higher WMA correlates with a higher SWC ($p < 0.001$ for both interaction terms). In addition, within the strong CAM species (green dots) a higher WMA correlates with higher SWC ($p < 0.001$ for the interaction term). Within-physiotype correlations are depicted by dashed lines. The reason that the higher WMA associated with constitutive CAM physiology does not cause higher SWC values is explained by investigating the leaf dry mass per area (B), as constitutive CAM plants have higher LMA as well as WMA. As with WMA, a nested linear model was built, with LMA nested within the categorical variable 'physiotype' as fixed terms to describe SWC. Again, this model shows no significant difference between the SWC of constitutive CAM species and facultative CAM species ($p = 0.091$) or between the SWC of constitutive CAM and obligate C₃ species ($p = 0.074$). Significant interaction terms exist between all physiotypes and LMA ($p < 0.001$ for all). Taken together, these statistical models show that changes to WMA and LMA *within* each physiotype effect SWC, but differences in these variables *between* physiotypes does not. Error bars represent ± 1 standard deviation, $n = 12$.

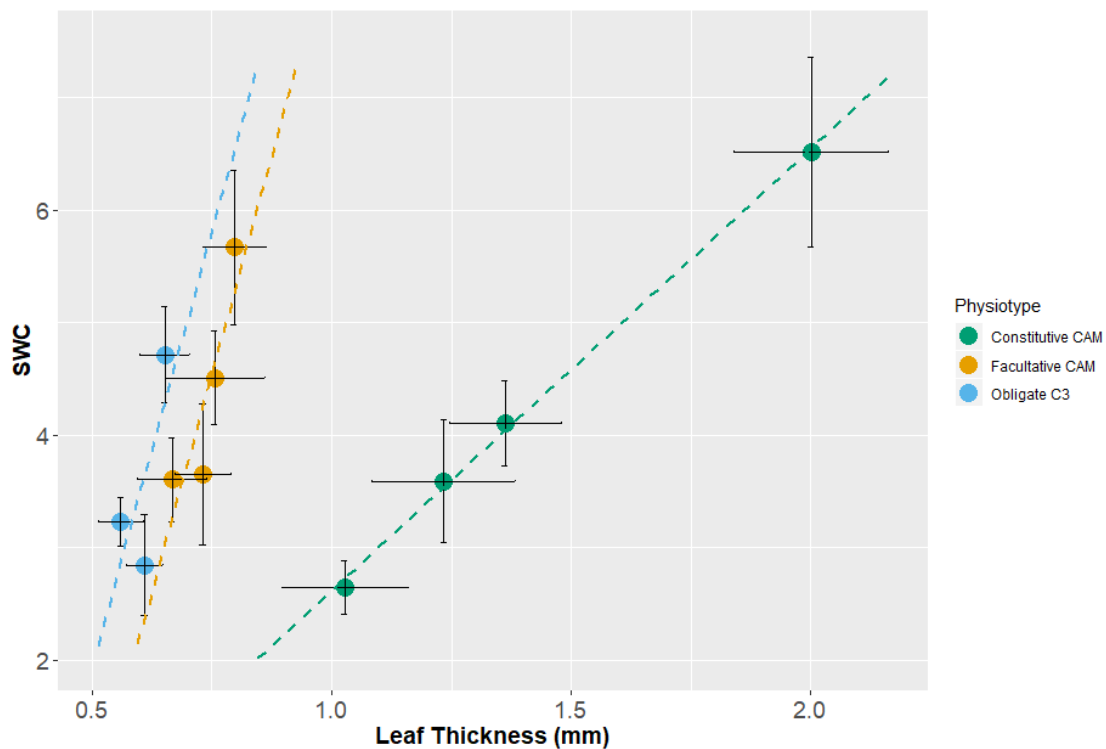


Fig. 2.2) Constitutive CAM species have thicker leaves, but do not have higher saturated water contents (SWC). Relationship between leaf thickness and saturated water content (SWC), used as a metric for succulence, from plants grown in a glass-house in Cockle Park University Farm, Newcastle, UK. A nested linear model was built with leaf thickness nested within the categorical variable 'physiotype'. This model demonstrated that no significant difference exists between the SWC of constitutive CAM species with facultative CAM species ($p = 0.065$) or between constitutive CAM species and obligate C_3 species ($p = 0.359$). There are significant interaction terms between all physiotypes and leaf thickness ($p < 0.001$, $p < 0.001$ & $p = 0.022$, for constitutive CAM, facultative CAM and obligate C_3 physiotypes, respectively). Taken together, this shows that differences in leaf thickness *between* physiotypes does not affect SWC but differences in leaf thickness *within* each physiotype significantly affects SWC.

The observation that WMA did not cause higher SWC, when it is associated with a constitutive CAM phenotype, led to the hypothesis that SWC was not determined by the large succulent chlorenchyma cells that host nocturnally accumulated malic acid (Fig. 2.1). In addition, when comparing species with the same photosynthetic physiology (dashed lines; Fig. 2.1), it was observed that WMA was associated with a higher SWC, and that this was true regardless of whether species were C₃, facultative or constitutive CAM (Fig. 2.1). Therefore, it was hypothesised that another form of succulent anatomy, that is independent of CAM (Barrera Zambrano et al., 2014), determines SWC. As hydrenchyma depth is known to vary considerably in *Clusia*, and is independent of CAM, it was predicted that this tissue was determining SWC. Put simply, it was hypothesised that succulent anatomy in the hydrenchyma but not the chlorenchyma determined SWC. Initial investigations confirmed that these two tissue layers were anatomically independent, as hydrenchyma and palisade layers showed no correlation in tissue depth or cell size with each other (Fig. 2.3). Having determined that succulent anatomy in the hydrenchyma and palisade are independent, it was possible to build models to describe the separate effects each form of succulent anatomy is having on SWC. A linear mixed effect model was built, using hydrenchyma, palisade and spongy mesophyll depth as fixed effect and species as a random effect. The initial model demonstrated that only hydrenchyma depth was acting as a significant explanatory variable for SWC (hydrenchyma, $p = 0.0028$; palisade, $p = 0.3286$; spongy mesophyll, $p = 0.9291$). This model was refined by removing the spongy mesophyll term; as this fixed effect was not shown to significantly influence SWC and as it is known that this tissue has not evolved large succulent cells in *Clusia* (Barrera Zambrano et al., 2014). A likelihood ratio test showed no significant difference between models (LR = 3.269785 and $p = 0.6585$), so spongy mesophyll depth was removed from the model. The subsequent model showed that hydrenchyma, and not palisade depth act as significant explanatory variables for SWC (Fig. 2.4). If palisade depth is removed as a fixed effect from this model, a likelihood ratio test showed no significant difference (Fig. 2.5). Therefore, it is possible to conclude that hydrenchyma depth, not palisade depth is contributing to SWC. In addition to analysing the depth of each tissue, it was shown that hydrenchyma cell size correlates with SWC, whereas palisade and spongy mesophyll cell size do not (Fig. 2.6). Taken together, these data show that succulent anatomy in the hydrenchyma, and not the palisade contributes to SWC.

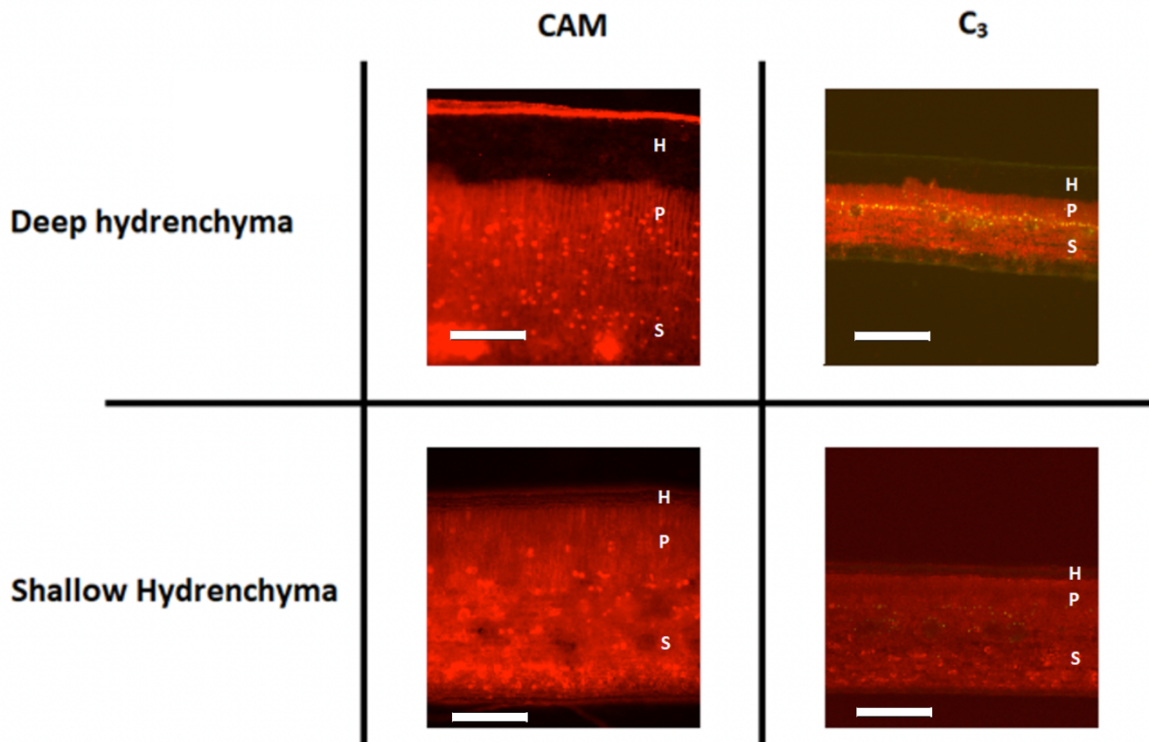


Fig. 2.3) There are two forms of succulent anatomy in *Clusia*. The development of CAM is associated with deeper palisade tissue, whereas increased hydrenchyma depth is independent of CAM. Hydrenchyma tissue appears transparent under fluorescent microscopy, due to the lack of chlorophyll in this tissue. Species shown are *top left*) *C. alata*; *bottom left*) *C. rosea*; *top right*) *C. multiflora*; *bottom right*) *C. grandiflora*. Tissue layers are labelled: H = hydrenchyma, P = palisade and S = spongy mesophyll. All scale bars = 300 μ m.

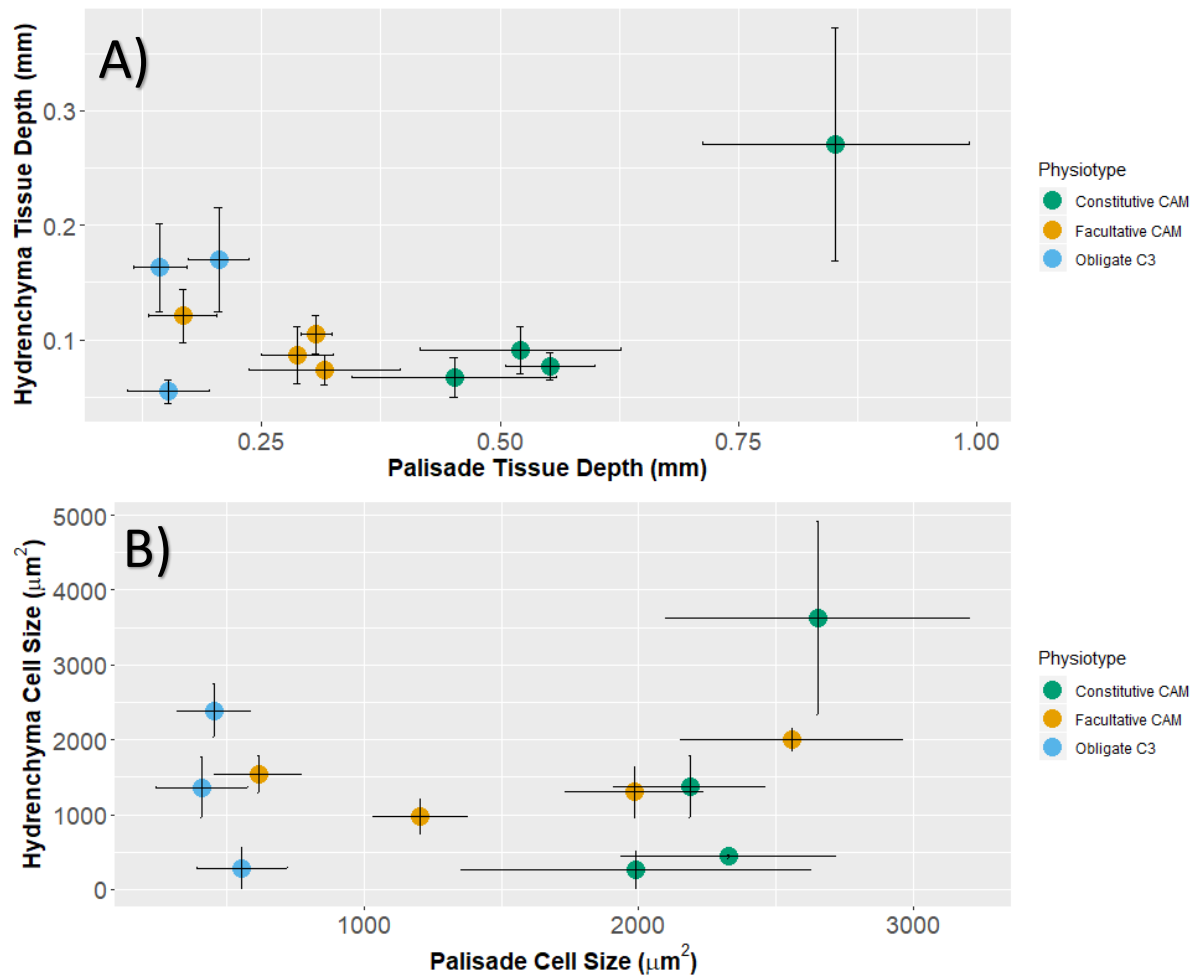


Fig. 2.4) All-cell and water-storage succulence are anatomically independent. (A) No significant relationship exists between palisade and hydrenchyma tissue depth ($p = 0.199$, Spearman's rank correlation). (B) No significant relationship exists between palisade and hydrenchyma cell size ($p = 0.546$, Spearman's rank correlation). All error bars represent ± 1 standard deviation, $n = 3$, data abstracted from Barrera Zambrano et al., (2014).

SWC is a meaningful metric for succulence as it is known to act as a proxy for capacitance, the ability of a leaf to buffer its water potential against water loss. This held true in *Clusia* as a linear mixed effect model demonstrated that SWC was a good predictor of hydraulic capacitance (Fig. 2.7). Therefore, as hydrenchyma, and not palisade depth had been shown to drive changes in SWC, it was predicted that a similar trend would exist to describe capacitance; that succulent anatomy in the hydrenchyma and not the chlorenchyma would provide capacitance. Another linear mixed effect model was built, with absolute capacitance as a response variable. This model was initially built with hydrenchyma, palisade and spongy mesophyll depth as fixed effects and species as a random effect. Capacitance values were calculated using the aforementioned model relating SWC to capacitance, in order to maximise the number of replicates, as high throughput determination of SWC allows a large number of replicate leaves to be measured ($n = 12$). Only hydrenchyma was found to be a significant explanatory variable (hydrenchyma, $p = 0.0176$; palisade, $p = 0.5111$; spongy mesophyll, $p = 0.5019$), and following the removal of spongy mesophyll depth as a fixed effect, a likelihood ratio test found no significant change to the model (LR = 7.637333, $p = 0.1774$). The final model found that hydrenchyma and not palisade depth significantly explained capacitance (Fig. 2.8), and removing palisade depth from this model had no significant difference when investigated using a likelihood ratio test (Fig. 2.8). In addition, previously published data from Barrera Zambrano et al., (2014) was also used to explore the relationship between hydrenchyma, palisade and spongy mesophyll cell size and bulk capacitance. These analyses found that hydrenchyma cell size correlates with capacitance, whereas palisade and spongy mesophyll cell size do not (Fig. 2.9). A possible functional explanation as to how hydrenchyma provides capacitance is via elasticity in the cell walls, allowing hydrenchyma cells to readily inflate and deflate in response to the water status of a leaf. To test this hypothesis, the bulk modulus of cell wall elasticity, ϵ , was estimated from pressure volume curves. The data indicate that species which invested a greater proportion of their leaf tissue into hydrenchyma have lower ϵ (Fig. 2.10), and that species with lower ϵ had a greater capacitance (Fig. 2.10).

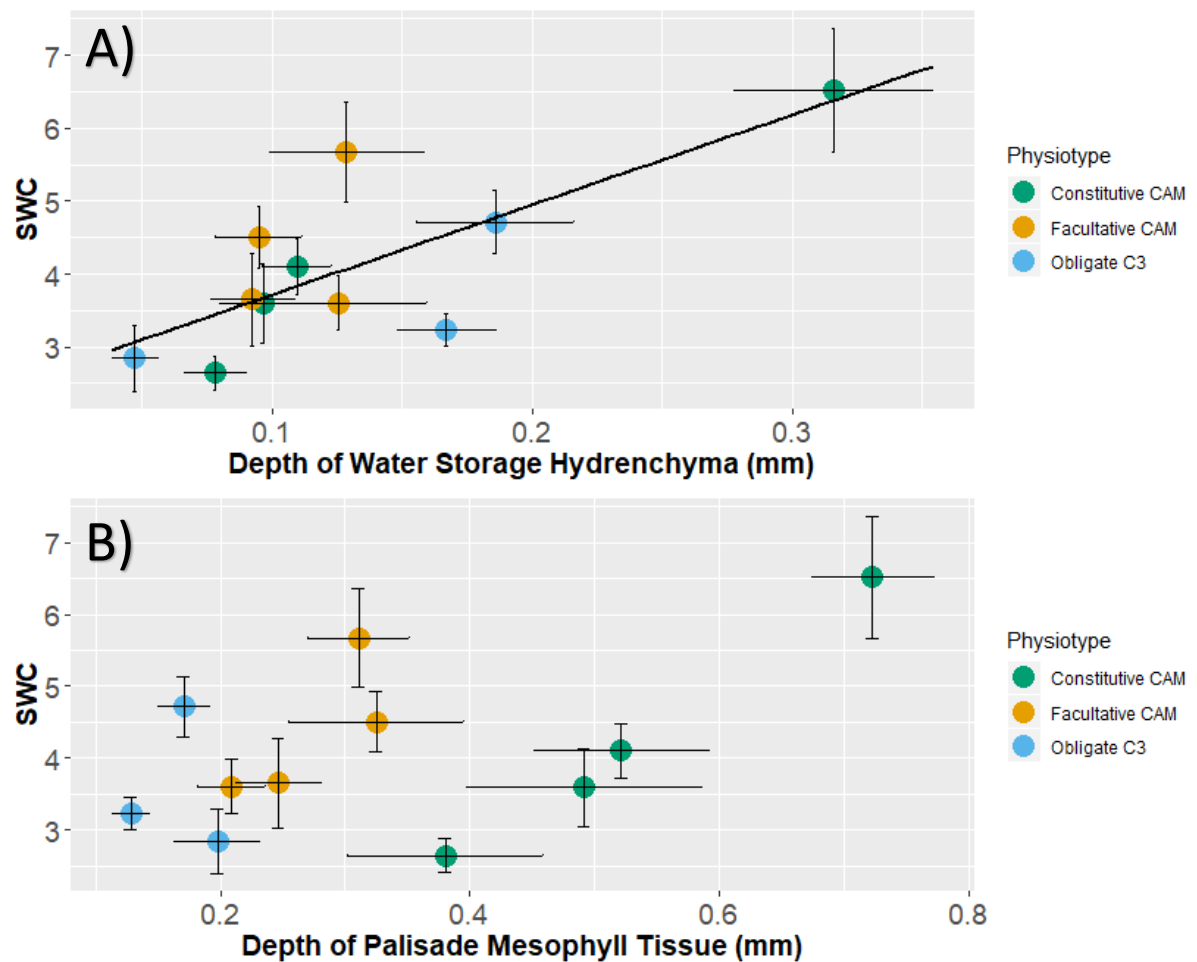


Fig. 2.5) Hydrenchyma tissue depth, not palisade depth contributes to saturated water content (SWC). (A) Depth of hydrenchyma tissue significantly predicts SWC ($p = 0.0081$) whereas (B) the depth of the palisade mesophyll tissue does not ($p = 0.2442$), in the linear mixed effect model. Furthermore, a likelihood ratio test determined that removing the palisade depth as an explanatory variable from the model did not have a significant effect (Likelihood ratio = 3.001439, $p = 0.5576$). Error bars represent ± 1 standard deviation, $n = 12$.

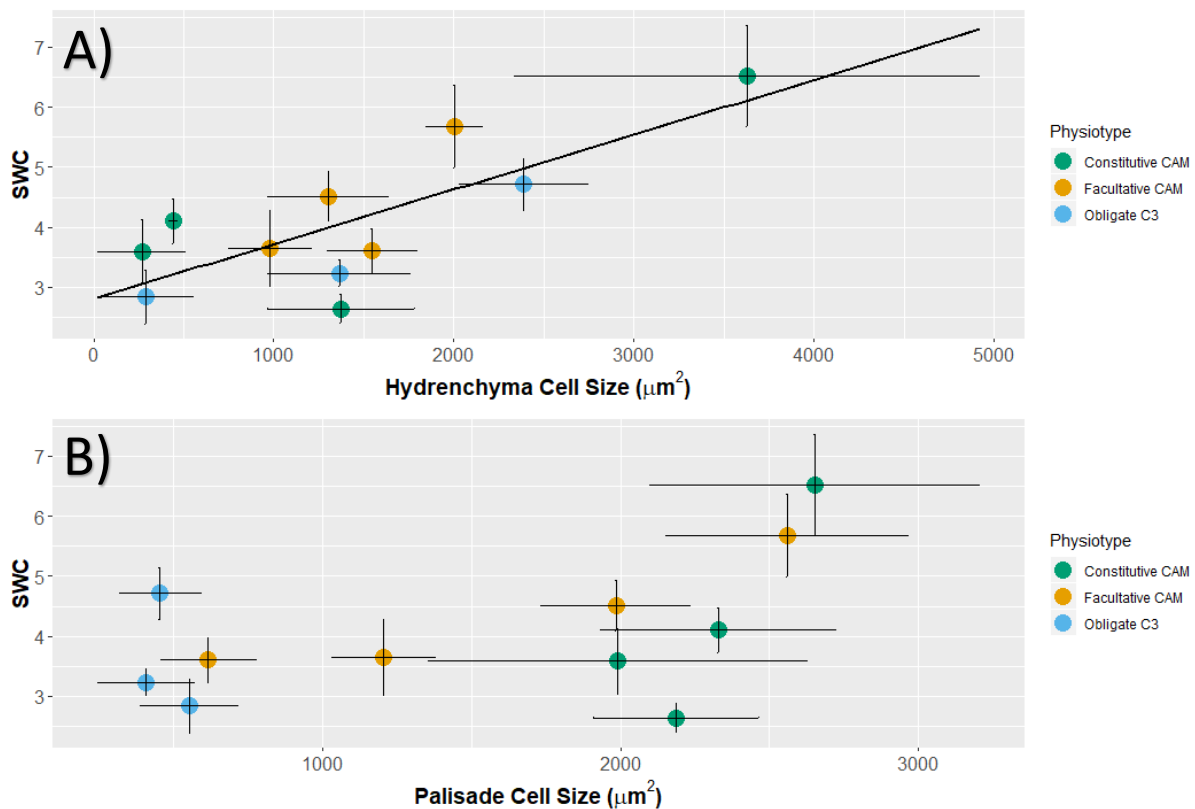


Fig. 2.6) Hydrrenchyma cell size, not palisade cell size contributes to saturated water content (SWC). (A) Size of hydrrenchyma cells significantly predicts SWC using a linear regression ($r^2 = 0.543$, $p = 0.005848$). (B) The size of palisade cells does not significantly predict SWC using a linear regression ($r^2 = 0.0222$, $p = 0.2967$). Error bars represent ± 1 standard deviation. Anatomical data is the mean of 3 replicates, from Barrera Zambrano et al., (2014), whereas SWC is the mean of 12 replicates sampled in this study.

In order to explore the relative contribution of each photosynthetic pathway and leaf hydraulic capacitance on drought tolerance in *Clusia*, the PHOTO3 model was adjusted to include leaf hydraulic capacitance (Hartzell et al., 2018). This model can able to predict the daily rate of transpiration and photosynthetic assimilation, and can be adjusted to simulate a C₃ or a CAM plant. The model was run using parameterisations for four hypothetical scenarios: C₃ with low hydraulic capacitance, C₃ with high hydraulic capacitance, CAM with low hydraulic capacitance, and CAM with high hydraulic capacitance. From the model outputs it was shown that both CAM and capacitance curtail drops in water potential (Fig. 2.11). High capacitance in either the C₃ or the CAM scenarios increase (makes them less negative) the minimum daily water potential. Comparison of the different photosynthetic scenarios using the PHOTO3 model showed that CAM also prevents water potentials from dropping to low values, and that this effect is far greater than that conferred by capacitance (Fig. 2.11). Whilst both adaptations (CAM and capacitance) act to prevent low leaf water potentials, the model showed that the effect of CAM on transpiration was the opposite of that attributed to capacitance (Fig. 2.11). CAM substantially minimised water loss from the onset of the dry down, as both CAM scenarios lost substantially less water than both C₃ scenarios. In contrast, capacitance appeared to cause a slight increase in transpiration in C₃ plants, after about 8 days of drought. Capacitance did not have any substantial effect on transpiration in CAM plants. Taken together, this model shows that both adaptations prevent plants from experiencing low water potentials, but CAM prevents water loss whilst capacitance does not.

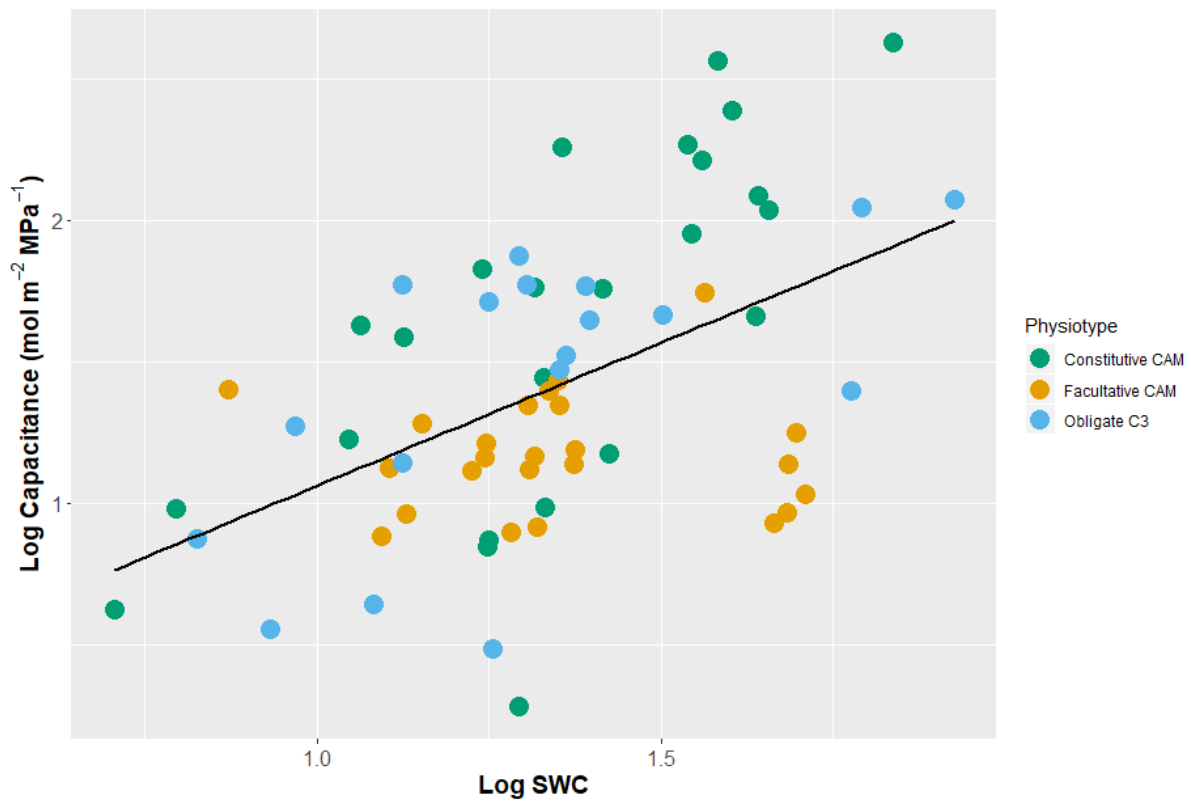


Fig. 2.7) Saturated water content (SWC) predicts capacitance, with a linear mixed effect model. The relationship between SWC and capacitance, for all leaves was measured with PV-curves. A random slope and random integer model was built, which showed SWC to be a significant predictor of capacitance ($p = 0.0032$). This was then refined to a random integer model, which also found SWC to be a significant predictor of capacitance ($p = 0.0015$). A likelihood ratio test found no significant difference between these models (Likelihood Ratio = 3.212141, $p = 0.2007$) so the simpler model was selected. Data was log transformed before models were built to ensure that the Q-Q plot fell along a straight line (data not shown).

2.4 Discussion

The data presented in this chapter demonstrate that the succulent syndrome is made up of two discrete, non-overlapping adaptations in *Clusia*, and provide the first dissection of these traits within a single genus. The hydrenchyma contributes significantly to SWC (Fig. 2.5 and Fig. 2.6) and hydraulic capacitance (Fig. 2.8 and Fig. 2.9) of the leaf, thereby buffering it against water loss. In contrast, the enlarged palisade cells do not provide capacitance (Fig. 2.8 and Fig. 2.9), instead acting primarily to host the CAM cycle, which in turn minimises transpiration (Fig. 2.11). Interestingly, WMA or leaf thickness alone is not a good predictor of capacitance, as these traits are themselves predominantly affected by enlarged palisade cells (Barrera Zambrano et al., 2014), which do not perform this function (Fig. 2.8 and Fig. 2.9). Hydrenchyma tissue, which is < 0.35 mm thick and makes up a minority of total leaf depth (Fig. 2.4), is able to buffer the leaf against water loss. This highlights the importance of thinking about succulence as a syndrome, rather than as a single trait, with pronounced tissue specialisation.

In *Clusia*, constitutive CAM species have distinctly different hydraulic physiology to C_3 and facultative CAM species, as they have both a higher WMA *and* a higher LMA (Fig. 2.1). Two possible explanations exist for this observation; either constitutive CAM plants have more cells, or they have larger cells with thicker cell walls. Each of these scenarios would generate leaves with both a higher mass of water and a greater dry mass, per leaf area. Since constitutive CAM species in *Clusia* are known to have evolved succulence via larger, rather than more numerous cells (Barrera Zambrano et al., 2014), it is likely that this high LMA is the consequence of increased cell wall thickness. Thick cell walls are found in the chlorenchyma of other CAM taxa, such as *Agave deserti* (Agavaceae) and *Kalanchoë daigremontiana* (Crassulaceae). The chlorenchyma cell walls of these constitutive CAM species are 1.6 μm and 0.92 μm , respectively; values far higher than the range observed in a study of 15 C_3 species (approx. 0.15-0.55 μm), or the range in a study of *Arabidopsis thaliana* (approx. 0.2-0.35 μm) (Tomás et al., 2013; Mizokami et al., 2019). Thick cell walls may provide a putative explanation for why enlarged palisade cells do not provide capacitance to the leaf, as thicker cell walls would presumably exhibit higher rigidity. As capacitance relies heavily on elastic cell walls (Fig. 2.10, but also see Males and Griffiths, 2018; Ogburn and Edwards 2010), which allow tissue to readily inflate and deflate to match the hydraulic needs of the leaf (Schmidt and Kaiser, 1987),

any situation where cell wall rigidity increases will prevent that tissue from acting as a hydraulic buffer. Therefore, it is predicted that in *Clusia*, whilst the palisade cells of constitutive CAM species have a greater water content than C₃ or facultative CAM relatives, the physical properties of these cells prevent them from acting as an effective, functional water store that can provide capacitance to the leaf.

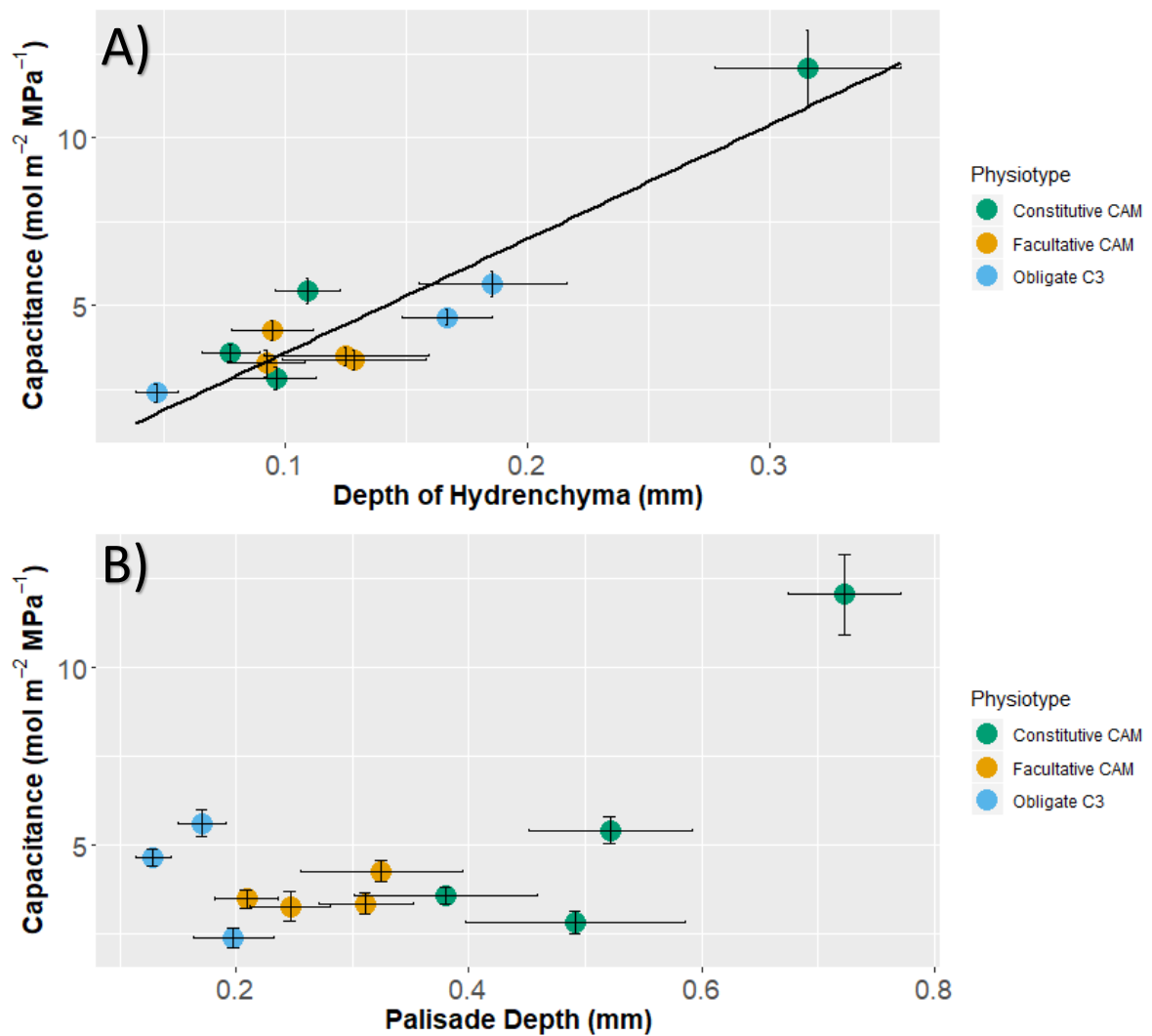


Fig. 2.8) Hydrenchyma tissue depth, not palisade depth contributes to capacitance. (A) Depth of hydrenchyma tissue significantly predicts capacitance ($p = 0.0162$) whereas (B) the depth of the palisade mesophyll tissue does not ($p = 0.3358$), in the linear mixed effect model. Furthermore, a likelihood ratio test determined that removing the palisade depth as an explanatory variable from the model did not have a significant effect (Likelihood ratio = 6.273135, $p = 0.1797$). Error bars represent ± 1 standard deviation, $n = 12$.

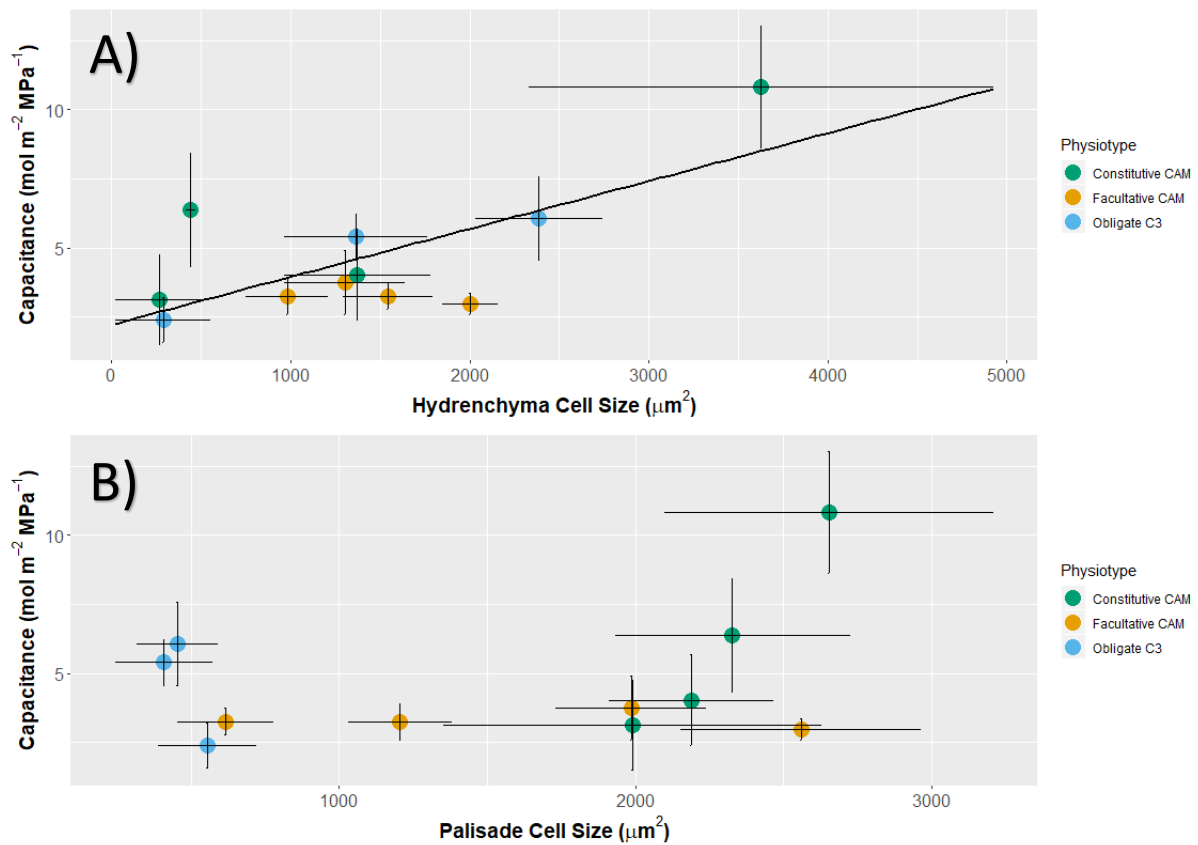


Fig. 2.9) Hydrrenchyma cell size, not palisade cell size contributes to capacitance. (A) Size of hydrrenchyma cells significantly predicts capacitance using a linear regression ($r^2 = 0.4502$, $p = 0.01421$). (B) The size of palisade cells does not significantly predict capacitance using a linear regression ($r^2 = -0.009582$, $p = 0.3663$). Error bars represent ± 1 standard deviation. Anatomical data is the mean of 3 replicates, abstracted from Barrera Zambrano et al., (2014), whereas SWC is the mean of 12 replicates sampled in this study.

This physiological framework for thinking about the succulent syndrome has implications for plant evolution. Much work still needs to be done to understand the evolution of CAM, despite it being one of the most remarkable cases of convergent evolution of a complex trait. Phylogenetic analyses have revealed that the evolution of constitutive CAM physiology, from a C₃-CAM intermediate phenotype (i.e. facultative CAM) is far rarer than the evolution of a C₃-CAM intermediate phenotype from an obligate C₃ ancestor (Edwards, 2019). Consequently the evolution of constitutive CAM occurs infrequently in nature (Edwards, 2019). However, the precise barriers preventing this evolutionary change are not fully understood. It has been suggested that the changes required for plants to overcome this evolutionary ‘rate determining step’ are mostly anatomical, as species with facultative or other C₃-CAM intermediate physiology have already acquired the necessary metabolic changes required for the CAM cycle (Nelson et al., 2005; Nelson et al., 2008). However, some succulent traits such as increased chlorenchyma cell size and reduced IAS, which are known to be physiologically important for CAM, may exist without the advent of a constitutive CAM phenotype (Nelson et al., 2008; Barrera Zambrano et al., 2014; Earles et al., 2018). This is seen in *C. minor* and *C. pratensis*, (the two facultative CAM species in Fig. 2.6, which have similar palisade cell size to the constitutive CAM species) and in other taxa, such as the Agavoideae (Heyduk et al., 2016). It seems unlikely that large cells or low IAS, alone, are the traits preventing the evolutionary transition from facultative to constitutive CAM, as these anatomical features can readily evolve in species that do not constitutively express CAM (Slaton and Smith 2002; Heyduk et al., 2016). Therefore, whilst the evolution of succulent tissue is thought to limit the transition into a constitutive CAM phenotype, it is still uncertain precisely what succulent anatomical adaptation is required for this evolutionary transition to occur (Edwards 2019). By combining both comparative anatomy with physiology, it might be possible to better elucidate what traits are limiting the evolutionary transition from facultative to constitutive CAM phenotypes. The data in this chapter demonstrate that, in *Clusia*, the increased water content associated with a constitutive CAM phenotype does not effectively buffer the leaf by providing increased hydraulic capacitance, which may be due to changes in the physical properties of cell walls in the constitutive CAM species. If CAM requires the evolution of large succulent cells in the photosynthetic tissue, but also requires a higher LMA to reinforce chlorenchyma cell walls, it is possible that a trade-off exists whereby the evolution of larger palisade cells for CAM is accompanied by these cells losing their ability to provide

capacitance. Put simply, the evolution of CAM might require plants to give up the capacitance derived from the chlorenchyma, despite CAM species evolving higher water contents in their photosynthetic tissue. If this trade-off between capacitance and CAM exists in the chlorenchyma it would act as a considerable barrier to the evolution of a strong CAM phenotype; if plants are already on a trajectory to evolving succulent physiology to provide greater effective water stores, then it may be difficult to evolve an anatomy that minimises the potential for increased capacitance.

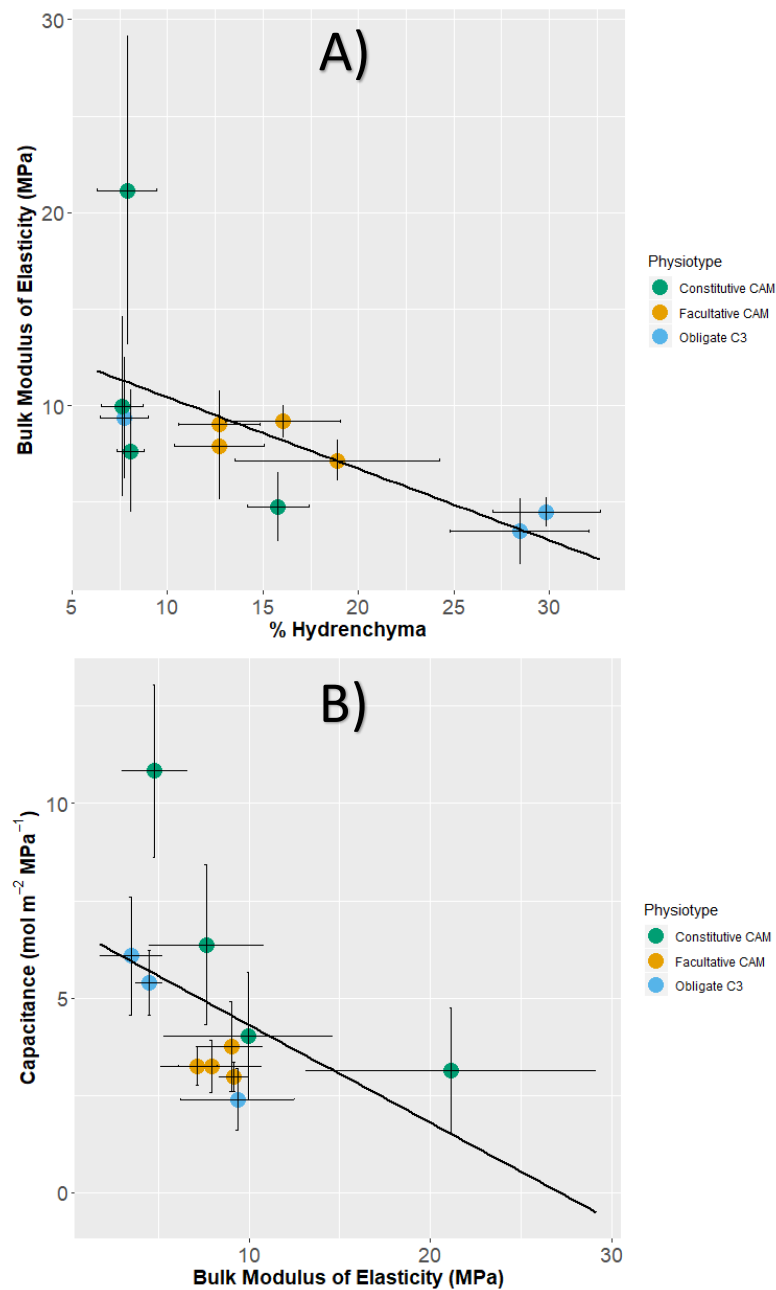


Fig. 2.10) Elasticity in the cell walls of hydrenchyma confers hydraulic capacitance. (A) Relationship between the percentage of total leaf depth made up by hydrenchyma and the bulk modulus of cell wall elasticity. Species that invest a greater proportion of leaf depth into hydrenchyma have lower bulk modulus of elasticity (i.e. more elastic cell walls) (Spearman's rank correlation, $p = 0.003$, $\rho = -0.827$, $n = 6$). (B) Species with lower bulk modulus of elasticity (i.e. more elastic cell walls) have higher capacitance (Spearman's rank correlation, $p = 0.028$, $\rho = -0.673$, $n = 6$). Error bars represent ± 1 standard deviation.

The aforementioned considerations rely on the idea that the large palisade cells in constitutive CAM species constrain capacitance due to some physical changes to these cells. To this end, it has been suggested that constitutive CAM species have thicker cell walls compared to C₃ and facultative CAM relatives, which can be inferred from the data presented in this study. However, this begs the question – if this is true, why would CAM plants require thicker cell walls? One explanation for this could come from the fact that CAM is a carbon concentrating mechanism, and as such requires that leaves have low mesophyll conductance to prevent CO₂ from escaping cells during the day, so that it can be used as an internal source to drive the Calvin cycle (Maxwell et al., 1997; Gillon et al., 1998; Earles et al., 2018). It has been known for some time that CAM plants have low internal air space to minimise mesophyll conductance (Nelson et al., 2005; Nelson et al., 2008; Earles et al., 2018; Males 2018). Despite *Clusia* species having relatively high IAS, compared to other CAM species, interspecific comparisons across this genus have found that greater employment of CAM is associated with lower mesophyll conductance (Gillon et al., 1998). Beyond IAS, cell wall thickness is increasingly being recognised as a strong determinant of mesophyll conductance in C₃ plants, as thick cell walls are able to limit the diffusion of CO₂ to a far greater extent than differences in IAS (Tomás et al., 2013). Furthermore, *Arabidopsis thaliana* plants grown in elevated atmospheric CO₂ concentrations are known to develop thicker cell walls, which limit mesophyll conductance (Mizokami et al., 2019). The elevated CO₂ concentrations in developing leaves of constitutive CAM species in *Clusia* could potentially be having this effect. This would explain why the leaves of facultative CAM species, which do the majority of their growth using C₃ photosynthesis (Winter et al., 2015), appear to have hydraulic physiology more closely related to obligate C₃ species (Fig. 2.1). Therefore, whilst highly speculative, it is interesting to consider that the evolution of CAM in *Clusia* may have been accompanied by increased cell wall thickness to limit mesophyll conductance and curtail CO₂ leakage but with the consequence of curtailed capacitance. This hypothesis could explain why CAM seems to be associated with a higher LMA, despite it acting antagonistically with hydraulic capacitance. Unfortunately, an exploration into mesophyll conductance and cell walls is outside of the scope of this chapter, or even this thesis, but it would be an interesting concept to explore further.

Table 2.1) Hydraulic capacitance values for high and low capacitance scenarios, used in PHOTO3 model

Parameter	Low Capacitance scenario	High Capacitance scenario	Units	Description
Capacitance	2.7	6.5	mol m ⁻² MPa ⁻¹	Absolute leaf hydraulic capacitance

Table 2.2) Photosynthetic parameters used in PHOTO3 model. Asterisk denotes parameters used for CAM scenario only.

Parameter	Value	Units	Description
LAI	2	-	Leaf area index
V _{c,max0}	3.15	μmol/m ² /s	Max carboxylation capacity
J _{max0}	6.3	μmol/m ² /s	Max. electron transport rate
Ψ _{l0}	-1.5	MPa	Point of maximum plant water stress
Ψ _{l1}	-0.5	MPa	Onset of plant water stress
M _{max} *	92	mol/m ³	Max malic acid storage
A _{max} *	1.1	μmol/m ² /sec	Max rate of malic acid storage flux

Table 2.3) Shared hydraulic values used for parameterising the PHOTO3 model.

Parameter	Value	Units	Description
TLP	-1.5	MPa	Turgor loss point
Z _r	0.4	m	Rooting depth
g _{min}	0	mm/s	Cuticular conductance, per unit leaf area
g _a	95	mm/s	Atmospheric conductance, per unit ground area
g _{leaf}	0.1	μm/MPa/s	Leaf hydraulic conductance, per unit leaf area
g _{p,max}	2	μm/MPa/s	Xylem hydraulic conductance, per unit leaf area
g _{w,max}	0.01	μm/MPa/s	Stem storage hydraulic conductance, per unit leaf area
vwt	0.58	mm	Stem water storage, per unit leaf area

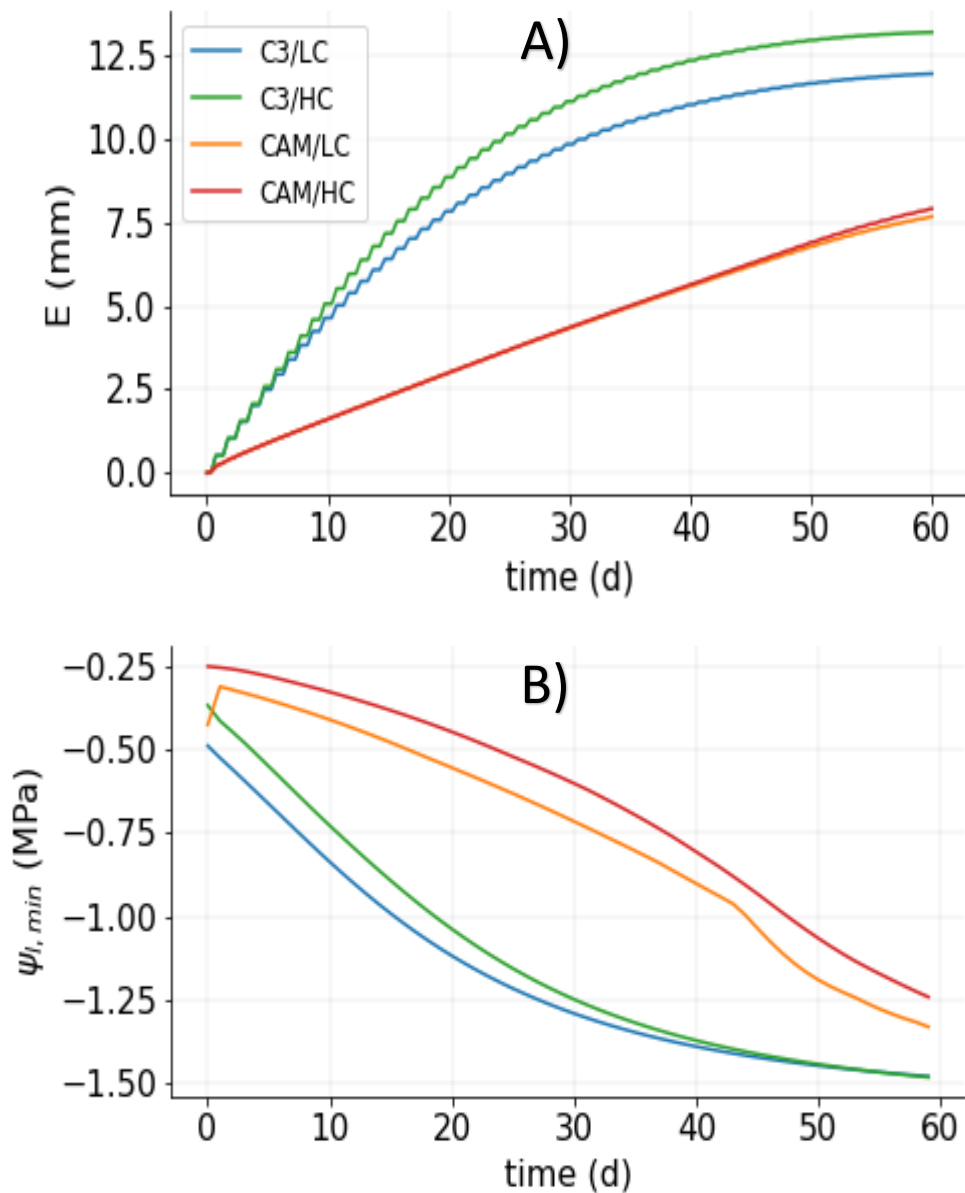


Fig. 2.11) Crassulacean acid metabolism prevents water loss, hydrenchyma does not. (A) Cumulative transpiration in over a 60 day dry-down simulation, using the PHOTO3 model (Hartzell et al., 2018). The model predicts that CAM plants, with either high or low capacitance, have lower transpiration rates than C₃ plants. Capacitance has little effect on transpiration in the setting of a CAM plant. In contrast, in the C₃ plants, high capacitance causes plants to exhibit a higher cumulative transpiration, which becomes more severe after approx. 10 days. (B) CAM causes plants to experience less negative water potentials than plant doing C₃ photosynthesis. This affect is greater than any effect of capacitance. Within both the CAM and the C₃ backgrounds, high capacitance causes the daily minimal water potential to be slightly less negative. No statistics were performed on these data as they are the output from an ecological model.

2.5 Conclusions and Future Considerations

This study has exploited the unusual anatomical and physiological diversity in *Clusia*, to construct a physiological framework for describing and analysing hydraulic capacitance and CAM. The data indicate that the different anatomical traits that contribute to leaf succulence in *Clusia* are independent of each other. Whilst this study has demonstrated that hydrenchyma and not chlorenchyma provide capacitance to the leaf, it does not address the role that these anatomical traits, or even capacitance itself, plays in species ability to tolerate negative water potentials. Further analysis is needed to assess how each of the succulent traits affects the turgor loss point (Chapter 3) and to identify any vascular reinforcements (Chapter 5) that are associated with succulence and CAM. Furthermore, whilst information about the hydrenchyma and chlorenchyma have been inferred from correlative analyses in this study, no physiological measurements has been made directly on these tissue layers. To confirm the findings and hypotheses outlined here, and develop them further, it is necessary to develop a method to dissect hydrenchyma from the abaxial chlorenchyma to study these tissues separately (Chapter 4). Finally, whilst it is interesting to explore the physiology of hydrenchyma and CAM, a deeper understanding of these adaptations can be acquired by exploring the role these traits play in the ecology and biogeography of *Clusia* (Chapter 4). Together, these considerations will provide a more comprehensive understanding of how the different components of the succulent syndrome each affect the biology of drought resistance in *Clusia*.

2.6 References

- Ahl, L. I., Mravec, J., Jørgensen, B., Rudall, P. J., Rønsted, N., & Grace, O. M. (2019). Dynamics of intracellular mannan and cell wall folding in the drought responses of succulent Aloe species. *Plant Cell and Environment*, (March), 1–14. <https://doi.org/10.1111/pce.13560>
- Arakaki, M., Christin, P.-A., Nyffeler, R., Lendel, A., Eggli, U., Ogburn, R. M., ... Edwards, E. J. (2011). Contemporaneous and recent radiations of the world's major succulent plant lineages. *Proceedings of the National Academy of Sciences*, *108*(20), 8379–8384. <https://doi.org/10.1073/pnas.1100628108>
- Barrera Zambrano, V. A., Lawson, T., Olmos, E., Fernández-García, N., & Borland, A. M. (2014). Leaf anatomical traits which accommodate the facultative engagement of crassulacean acid metabolism in tropical trees of the genus *Clusia*. *Journal of Experimental Botany*, *65*(13), 3513–3523. <https://doi.org/10.1093/jxb/eru022>
- Bartlett, M. S., Vico, G., & Porporato, A. (2014). Coupled carbon and water fluxes in CAM photosynthesis: modelling quantification of water use efficiency and productivity. *Plant and Soil*, *383*(1–2), 111–138. <https://doi.org/10.1007/s11104-014-2064-2>
- Blackman, C. J., & Brodribb, T. J. (2011). Two measures of leaf capacitance: Insights into the water transport pathway and hydraulic conductance in leaves. *Functional Plant Biology*, *38*(2), 118–126. <https://doi.org/10.1071/FP10183>
- Borland, A. M., Hartwell, J., Weston, D. J., Schlauch, K. a., Tschaplinski, T. J., Tuskan, G. a., ... Cushman, J. C. (2014). Engineering crassulacean acid metabolism to improve water-use efficiency. *Trends in Plant Science*, *19*(5), 327–338. <https://doi.org/10.1016/j.tplants.2014.01.006>
- Borland, A. M., Leverett, A., Hurtado-Castano, N., Hu, R., & Yang, X. (2018). Functional Anatomical Traits of the Photosynthetic Organs of Plants with Crassulacean Acid Metabolism. In W. W. Adams III & I. Terashima (Eds.), *The Leaf: A Platform for Performing Photosynthesis* (1st ed., pp. 281–305). https://doi.org/10.1007/978-3-319-93594-2_10

- Earles, J. M., Theroux-Rancourt, G., Roddy, A. B., Gilbert, M. E., McElrone, A. J., & Brodersen, C. R. (2018). Beyond Porosity: 3D Leaf Intercellular Airspace Traits That Impact Mesophyll Conductance. *Plant Physiology*, *178*(1), 148–162.
<https://doi.org/10.1104/pp.18.00550>
- Edwards, E. J. (2019). Evolutionary trajectories, accessibility, and other metaphors: the case of C4 and CAM photosynthesis. *New Phytologist*, *223*(4), 1742–1755.
<https://doi.org/10.1111/nph.15851>
- Grace, O. M., Buerki, S., Symonds, M. R. E., Forest, F., Van Wyk, A. E., Smith, G. F., ... Rønsted, N. (2015). Evolutionary history and leaf succulence as explanations for medicinal use in aloes and the global popularity of *Aloe vera*. *BMC Evolutionary Biology*, *15*(1), 1–12. <https://doi.org/10.1186/s12862-015-0291-7>
- Gustafsson, M., Winter, K., & Bittrich, V. (2007). Diversity, Phylogeny and Classification of *Clusia*. In U. Lüttge (Ed.), *Clusia A Woody Neotropical Genus of Remarkable Plasticity and Diversity* (pp. 95–116). Retrieved from
http://link.springer.com/chapter/10.1007/978-3-540-37243-1_7
- Hartzell, S., Bartlett, M. S., & Porporato, A. (2018). Unified representation of the C3, C4, and CAM photosynthetic pathways with the Photo3 model. *Ecological Modelling*, *384*(June), 173–187. <https://doi.org/10.1016/j.ecolmodel.2018.06.012>
- Heyduk, K., McKain, M. R., Lalani, F., & Leebens-Mack, J. (2016). Evolution of a CAM anatomy predates the origins of Crassulacean acid metabolism in the Agavoideae (Asparagaceae). *Molecular Phylogenetics and Evolution*, *105*, 102–113.
<https://doi.org/10.1016/j.ympev.2016.08.018>
- Males, J. (2018). Concerted anatomical change associated with crassulacean acid metabolism in the Bromeliaceae. *Functional Plant Biology*, *45*(7), 681–695.
<https://doi.org/10.1071/fp17071>
- Males, J. (2017). Secrets of succulence. *Journal of Experimental Botany*, *68*(9), 2121–2134.
<https://doi.org/10.1093/jxb/erx096>

- Males, J., & Griffiths, H. (2017). Functional types in the Bromeliaceae: relationships with drought-resistance traits and bioclimatic distributions. *Functional Ecology*, *31*(10), 1868–1880. <https://doi.org/10.1111/1365-2435.12900>
- Males, J., & Griffiths, H. (2018). Economic and hydraulic divergences underpin ecological differentiation in the Bromeliaceae. *Plant Cell and Environment*, *41*(1), 64–78. <https://doi.org/10.1111/pce.12954>
- Maxwell, K., Von Caemmerer, S., & Evans, J. R. (1997). Is a low internal conductance to CO₂ diffusion a consequence of succulence in plants with crassulacean acid metabolism? *Australian Journal of Plant Physiology*, *24*(6), 777–786. <https://doi.org/10.1071/PP97088>
- Mizokami, Y., Sugiura, D., Watanabe, C. K. A., Betsuyaku, E., Inada, N., & Terashima, I. (2019). Elevated CO₂-induced changes in mesophyll conductance and anatomical traits in wild type and carbohydrate metabolism mutants of *Arabidopsis thaliana*. *Journal of Experimental Botany*, *In press* XXXXX. <https://doi.org/10.1093/jxb/erz208>
- Nelson, E. a., & Sage, R. F. (2008). Functional constraints of CAM leaf anatomy: Tight cell packing is associated with increased CAM function across a gradient of CAM expression. *Journal of Experimental Botany*, *59*(7), 1841–1850. <https://doi.org/10.1093/jxb/erm346>
- Nelson, E. a., Sage, T. L., & Sage, R. F. (2005). Functional leaf anatomy of plants with crassulacean acid metabolism. *Functional Plant Biology*, *32*(5), 409–419. <https://doi.org/10.1071/FP04195>
- Ogburn, R. M., & Edwards, E. J. (2010). The ecological water-use strategies of succulent plants. In *Advances in Botanical Research* (1st ed., Vol. 55). <https://doi.org/10.1016/B978-0-12-380868-4.00004-1>
- Ogburn, R. M., & Edwards, E. J. (2012). Quantifying succulence: A rapid, physiologically meaningful metric of plant water storage. *Plant, Cell and Environment*, *35*(9), 1533–1542. <https://doi.org/10.1111/j.1365-3040.2012.02503.x>

- Ogburn, R. M., & Edwards, E. J. (2013). Repeated origin of three-dimensional leaf venation releases constraints on the evolution of succulence in plants. *Current Biology*, *23*(8), 722–726. <https://doi.org/10.1016/j.cub.2013.03.029>
- Richards, H. M. (1915). *Acidity and gas interchange in cacti*. Retrieved from <https://www.biodiversitylibrary.org/item/68027>
- Ripley, B. S., Abraham, T., Klak, C., & Cramer, M. D. (2013). How succulent leaves of Aizoaceae avoid mesophyll conductance limitations of photosynthesis and survive drought. *Journal of Experimental Botany*, *64*(18), 5485–5496. <https://doi.org/10.1093/jxb/ert314>
- Roberts, A., Griffiths, H., Borland, A. M., & Reinert, F. (1996). Is crassulacean acid metabolism activity in sympatric species of hemi-epiphytic stranglers such as *Clusia* related to carbon cycling as a photoprotective process? *Oecologia*, *106*(1), 28–38. <https://doi.org/10.1007/BF00334404>
- Schmidt, J., & Kaiser, W. (1987). Response of the Succulent Leaves of *Peperomia magnoliaefolia* to dehydration. *Plant Physiology*, *83*, 190–194.
- Schmidt, J. E., & Kaiser, W. M. (1987). Response of the Succulent Leaves of *Peperomia magnoliaefolia* to Dehydration . *Plant Physiology*, *83*(1), 190–194. <https://doi.org/10.1104/pp.83.1.190>
- Scholander, A. P. F., Hammel, H. T., Bradstreet, E. D., & Hemmingsen, E. A. (1965). Sap Pressure in Vascular Plants. *Science*, *148*(3668), 339–346.
- Scoffoni, C., Chatelet, D. S., Pasquet-Kok, J., Rawls, M., Donoghue, M. J., Edwards, E. J., & Sack, L. (2016). Hydraulic basis for the evolution of photosynthetic productivity. *Nature Plants*, *2*(6), 1–8. <https://doi.org/10.1038/nplants.2016.72>
- Tomás, M., Flexas, J., Copolovici, L., Galmés, J., Hallik, L., Medrano, H., ... Niinemets, Ü. (2013). Importance of leaf anatomy in determining mesophyll diffusion conductance to CO₂ across species: Quantitative limitations and scaling up by models. *Journal of Experimental Botany*, *64*(8), 2269–2281. <https://doi.org/10.1093/jxb/ert086>

- Tyree, M. T., & Hammel, H. T. (1972). The Measurement of the Turgor Pressure and the Water Relations of Plants by the Pressure-bomb Technique. *Journal of Experimental Botany*, 23(February), 267–282. <https://doi.org/10.1093/jxb/23.1.267>
- Winter, K., Garcia, M., & Holtum, J. a. M. (2008). On the nature of facultative and constitutive CAM: environmental and developmental control of CAM expression during early growth of *Clusia*, *Kalanchoë*, and *Opuntia*. *Journal of Experimental Botany*, 59(7), 1829–1840. <https://doi.org/10.1093/jxb/ern080>
- Winter, K. (2019). Ecophysiology of constitutive and facultative CAM photosynthesis. *Journal of Experimental Botany*, *In pr.* <https://doi.org/10.1093/jxb/erz002>
- Winter, K., Holtum, J. A. M., & Smith, J. A. C. (2015). Crassulacean acid metabolism: a continuous or discrete trait? *The New Phytologist*, 208(1), 73–78. <https://doi.org/10.1111/nph.13446>
- Winter, K., & Holtum, J. A. M. (2014). Facultative crassulacean acid metabolism (CAM) plants: powerful tools for unravelling the functional elements of CAM photosynthesis. *Journal of Experimental Botany*, 65(13), 3425–3441. <https://doi.org/10.1093/jxb/eru063>
- Yang, X., Cushman, J. C., Borland, A. M., Edwards, E. J., Wulfschleger, S. D., Tuskan, G. A., ... Holtum, J. A. M. (2015). A roadmap for research on crassulacean acid metabolism (CAM) to enhance sustainable food and bioenergy production in a hotter, drier world. *New Phytologist*, 207(3), 491–504. <https://doi.org/10.1111/nph.13393>

Chapter 3. The Role of Hydrenchyma and Crassulacean Acid Metabolism in Determining the Turgor Loss Point in *Clusia*

3.1 Introduction

The hydraulic drought response strategies of plants are often categorised as being either drought-tolerance or drought avoidance (Ogburn and Edwards, 2010; Bartlett et al., 2012b; Borland et al., 2015; Males 2017). Drought tolerance is typically considered the ability to maintain essential biological processes, such as stomatal and hydraulic conductance and net photosynthetic assimilation, despite the existence of low water potentials in the plant. For example, an extreme drought tolerance strategy is found in *Larrea tridentata* (Zygophyllaceae) in the Sonoran desert, which can tolerate water potentials as low as -3.5 MPa (Monson et al., 1982; Meinzer et al., 1986). In contrast, drought avoidance describes any adaptation that prevents a plant from experiencing low water potentials, thereby circumventing the need to tolerate this stress. Drought avoidance strategies can take many forms, for example drought-deciduousness, a greater investment in roots to access deep water sources or 'tanks' that hold pools of water at the base of the leaves (Lange and Zuber, 1977; Hasselquist et al., 2010; Males 2016; Males and Griffiths, 2017). An interesting example of a drought avoider, which is found sympatrically with *L. tridentata*, is *Prosopis velutina* (Fabaceae). This tree is believed to engage in 'hydraulic descent', a process by which water is transported away from the stems in lateral roots during monsoon season in the Sonoran desert, in order to increase soil moisture content for later use (Hultine et al., 2004). Thus, even within the same semi-arid ecosystem both drought-tolerance and drought-avoidance strategies can coexist.

Many different metrics have been used to assess the degree to which species are drought-avoiders or drought-tolerators. One such metric that was used for some time is the concept of isohydry/anisohydry (Borland et al., 2015; Farrell et al., 2016; Meinzer et al., 2016; Martínez-Vilalta et al., 2017). Isohydric plants were thought to maintain stable daily minimal water potentials in their tissues (Ψ_{\min}) even when soil water potential falls, by decreasing stomatal conductance, hence *avoiding* damaging low water potentials. Anisohydric species, on the other hand, were believed to experience more severe drops in Ψ_{\min} in response to decreased soil water availability, as they maintain stomatal conductance and *tolerate*

transpiration and the subsequent drops in water potential. These concepts were made more complex by the fact that a number of different methods were used to describe the iso/anisohdry of a species, including simply measuring the lowest Ψ_{\min} value in a season or seasonal ranges in Ψ_{\min} (Martínez-Vilalta et al., 2017). Other studies used more laborious methods, such as finding the slope of daily $\Psi_{\min} \sim \Psi_{\max} (\delta)$, or finding the area between δ and the slope where $\Psi_{\min} = \Psi_{\max}$ (the plants 'hydroscape') (Meinzer et al., 2016; Martínez-Vilalta et al., 2017). These latter two methods have the advantage of integrating both the water potential conferred by the environment (estimated to be equal to Ψ_{\max}) with the water potential caused by transpirational water loss (i.e. the difference between Ψ_{\min} and Ψ_{\max}), and consequently attempt to approximate the how a plant responds to the drought that has been imposed. However, these parameters are actually highly dependent on the environmental conditions of the plant, as they are all affected by the soil hydraulic conductance and the effect of the vapour pressure deficit on transpiration (Hochberg et al., 2018). Therefore, methods for measuring the relative iso/anisohdry of different species are becoming less popular as they are now considered to describe a plant-environment interaction rather than the ability of a plant to tolerate or avoid drought, in and of itself.

To characterise species hydraulic drought tolerance/avoidance, in a way that relates more to the plant itself rather than the environmental conditions it experiences, other physiological parameters have been used. To this end, a great deal of focus has been directed towards the turgor loss point (TLP) (Bartlett et al. 2012a; Bartlett et al., 2012b; Bartlett et al., 2014). The TLP describes a critical point at which plant tissue loses structural integrity (i.e. because the tissue or cells are 'wilting') and thus cannot sustain basic hydraulic functions (Tyree and Hammel 1972, Beadle et al., 1985; Trueba et al., 2019). To understand how the TLP occurs, it is necessary to consider a plant at full hydration: when water is available in the apoplast of a plant tissue, it will move into the cells by osmosis due to the presence of osmolytes in the cytoplasm and vacuole (Beadle et al., 1985). The consequence of this is that cells swell as they fill with water, causing the plasma membrane to push against the cell walls, which creates a positive pressure, called turgor pressure. Turgor pressure is able to keep leaves and herbaceous stems erect. When apoplastic water availability drops due to drought, less water is able to move into the cells by osmosis, despite the osmotic potential generated by osmolytes, and consequently the positive turgor pressure drops. The TLP describes the point at which lowering the water content of a plant tissue no longer causes a drop in turgor

pressure; thus if a plant can sustain turgor at lower water potentials, it will experience less damage from drought stress and hence it can be considered a drought tolerater (Hochberg et al., 2018).

The TLP is not a new parameter to plant physiologists; in fact botanists have been measuring this for almost half a century (Tyree and Hammel, 1972). However, recent work has highlighted the ecological importance of the TLP, specifically the water potential at which turgor is lost (which is used interchangeably with the acronym 'TLP' in this chapter) as a functional trait that is important in plant ecology and evolution (Hochberg et al., 2018). Global meta-analyses have shown that species inhabiting more water-limited ecosystems typically have lower TLP, meaning they can withstand lower water potentials before suffering the damaging effects of wilting (Bartlett et al., 2012b). In addition, the TLP is not a particularly plastic trait; on average the change that occurs due to drought stress makes up only 16% of the TLP, and the extent to which the TLP drops is lowest for evergreen tropical trees (Bartlett et al., 2014; Maréchaux et al., 2017). Furthermore, measuring the iso/anisohdry of 8 species under controlled conditions (to minimise the effect of environmental conditions on this parameter) found that it correlates strongly with the TLP (Meinzer et al., 2016). More anisohydric species had lower TLP; i.e. they were able to maintain stomatal conductance and turgor pressure at low water potentials as they are drought toleraters. The study by Meinzer et al., (2016) required a 40 day dry-down treatment under carefully regulated conditions to measure iso/anisohdry, however the TLP is preferred as a quicker yet meaningful metric for measuring the extent to which a species is tolerating or avoiding drought.

Both succulence and Crassulacean acid metabolism (CAM) are often considered examples of drought avoidance (Borland et al., 2015). This may seem somewhat paradoxical at first as both of these adaptations are typically found in annually or seasonally arid ecosystems (Ogburn and Edwards, 2010). However, the water stores available to succulent species are thought to keep the plant hydrated long after external water availability has ceased, thus providing capacitance which minimises damage occurring from low water potentials. In *Clusia* capacitance is provided by the hydrenchyma, an achlorophyllous water storage tissue layer in the leaf. As well as capacitance, CAM is also thought to help plants avoid drought, by minimising the transpirational water loss from stomata, hence slowing the rate that soils dry. Therefore, despite capacitance and CAM being adaptations to arid and semi-

arid environments, they are thought to be strategies to prevent plants from experiencing drought and the potential damage that accompanying low water potentials can cause. However, data presented in Barrera Zambrano et al., (2014) and Chapter 2 demonstrated that CAM is independent of capacitance, as the former occurs in the chlorenchyma and the latter is the consequence of the hydrenchyma. Since hydrenchyma and CAM can be considered distinct, functionally independent adaptations in the drought response of *Clusia* (Chapter 2), it is possible to determine which trait, if any, contributes more to the TLP. This will demonstrate the relative contribution each of these adaptations, which are traditionally both considered drought avoidance strategies, makes to species' ability to tolerate negative water potentials.

One trait that was shown to be important for the capacitance of succulent plants is the bulk modulus of elasticity (ϵ); a biophysical parameter that describes how readily leaf cell walls are able to stretch in response to the physical force imposed by cell turgor (Stiles and Martin, 1996; Ogburn and Edwards, 2010; Chapter 2). The hydrenchyma cell walls in leaves are believed to be highly elastic (i.e. have a low ϵ), which allows these cells to readily deform during drought stress to release their water into the photosynthetic cells (Chapter 2). However, elasticity might have a separate role in the plant drought response of succulent plants, as stretchy cell walls could potentially affect to the TLP. For example, in *Aloe* the hydrenchyma cell walls are able to fold into contorted shapes when the plant is left without any external water source, thus allowing the leaf to maintain its gross morphological structure despite experiencing extremely low relative water contents (Ahl et al., 2019). This folding presumably prevents the plasma membrane from separating from the cell wall when much of the water has been lost. Therefore, the hydrenchyma plasma membrane can keep pushing against the cell walls during drought; thereby maintaining cell turgor as water is lost. Whilst it is likely that this is the case in *Aloe*, directly demonstrating it would be very difficult, because pressure volume curves to measure ϵ and the TLP are technically challenging for extremely succulent, slow drying species. *Clusia*, on the other hand, exhibits diversity in its hydrenchyma which in turn affects ϵ (Chapter 2), making it an ideal model to test the role that elasticity is having on the TLP.

To understand how ϵ could be contributing to the TLP, it is important to consider the equation:

Equation 3.1

$$TLP = \frac{\pi_o \times \epsilon}{\pi_o + \epsilon}$$

Where π_o is the osmotic potential at full turgor (Bartlett et al., 2012b). Therefore, plants can theoretically evolve a lower TLP by decreasing π_o (making it more negative) or increasing the stretchiness of cell walls (lowering ϵ). In reality, studies on tropical and temperate trees as well as herbaceous grassland species found no evidence for ϵ contributing to the TLP (Bartlett et al., 2012b; Griffin-Nolan et al., 2019). The reason for this is that most species have cell walls so rigid that even considerable changes to ϵ are completely inconsequential compared to changes to π_o . Put differently, most plants do not have cell walls elastic enough to have any influence on the TLP. However, these studies did not include succulent species, which are known to have some of the lowest ϵ values (Stiles and Martin, 1996; Ogburn and Edwards, 2012). Therefore, it is interesting to address if the low ϵ values conferred by hydrenchyma (Chapter 2) are driving the TLP down.

This chapter tests three hypotheses to understand how succulence and CAM affect the TLP:

H₁ – Greater investment in hydrenchyma should drive the TLP up

H₂ – Greater use of CAM photosynthesis should drive the TLP up

H₃ – Low values of ϵ , due to greater investment in hydrenchyma, should drive the TLP up

3.2 Materials and Methods

3.2.1 Species Studied

This comparative study investigated all of the 11 *Clusia* species studied in Chapter 2. In addition, field measurements were carried out on 9 species grown in Gamboa Panama. These species were the C₃ species, *C. quadralanga*, *C. valeroi*, *C. cupulata*, and *C. peninsulae*, *C. fructinogusta*; the C₃-CAM intermediate species, *C. pratensis*, *C. minor*, *C. uvitana*; and the constitutive CAM species *C. rosea*. The photosynthetic phenotype of these species was determined according to Holtum et al., (2004), and confirmed in this study by measuring titratable acidity (see below). For field grown species, n = 2-4 except for *C. fructinogusta* where only one individual was available.

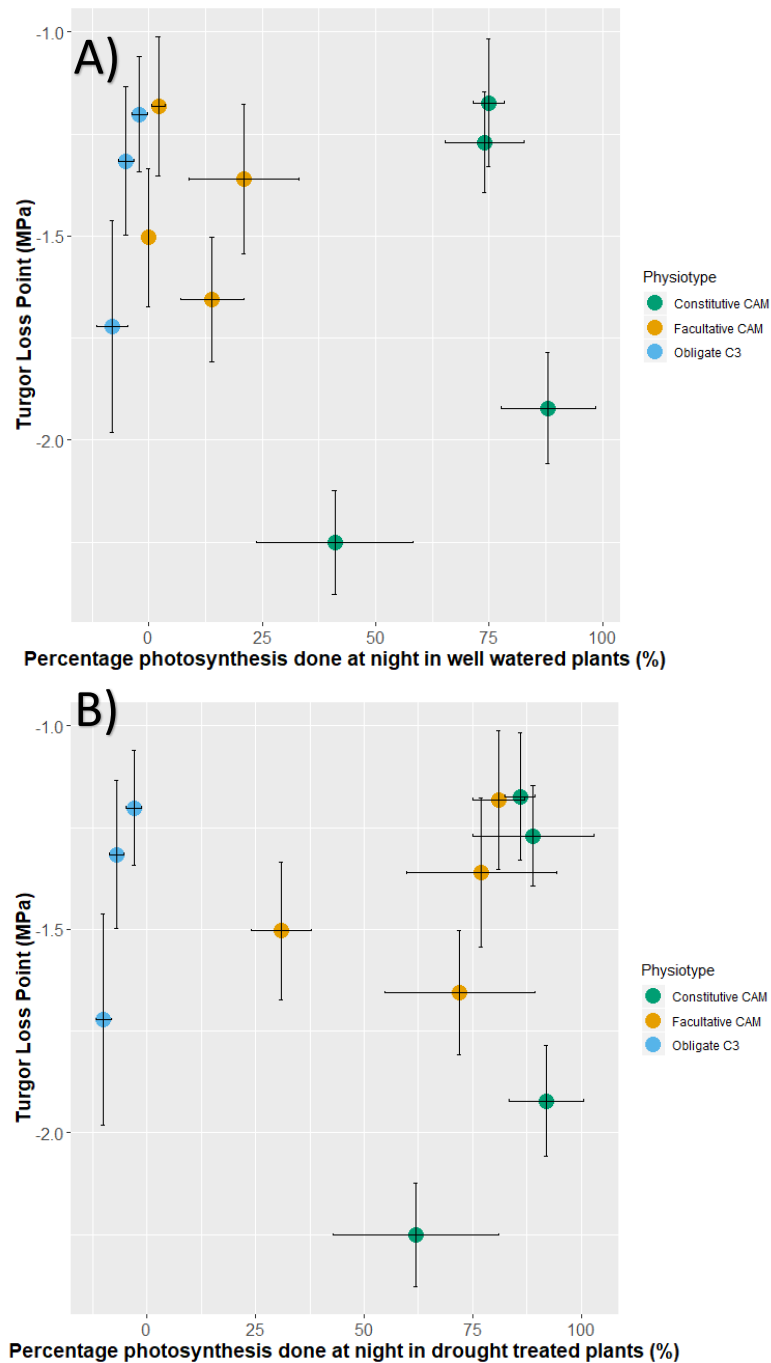


Fig. 3.1) Species that employ Crassulacean acid metabolism do not have different Turgor loss point to C₃ relatives, in *Clusia*. (A) No correlation exists between the percentage of photosynthesis done at night in well-watered plants (i.e. the degree to which a species exhibits a constitutive CAM phenotype), and the water potential at which turgor is lost ($p = 0.924$, $\rho = -0.036$, Spearman's Rank Correlation Test). (B) No correlation exists between the percentage of photosynthesis done at night in drought-treated plants (i.e. the degree to which a species exhibits a constitutive or facultative CAM phenotype), and the water potential at which turgor is lost ($p = 0.595$, $\rho = 0.182$, Spearman's Rank Correlation Test). Error bars represent \pm one standard deviation.

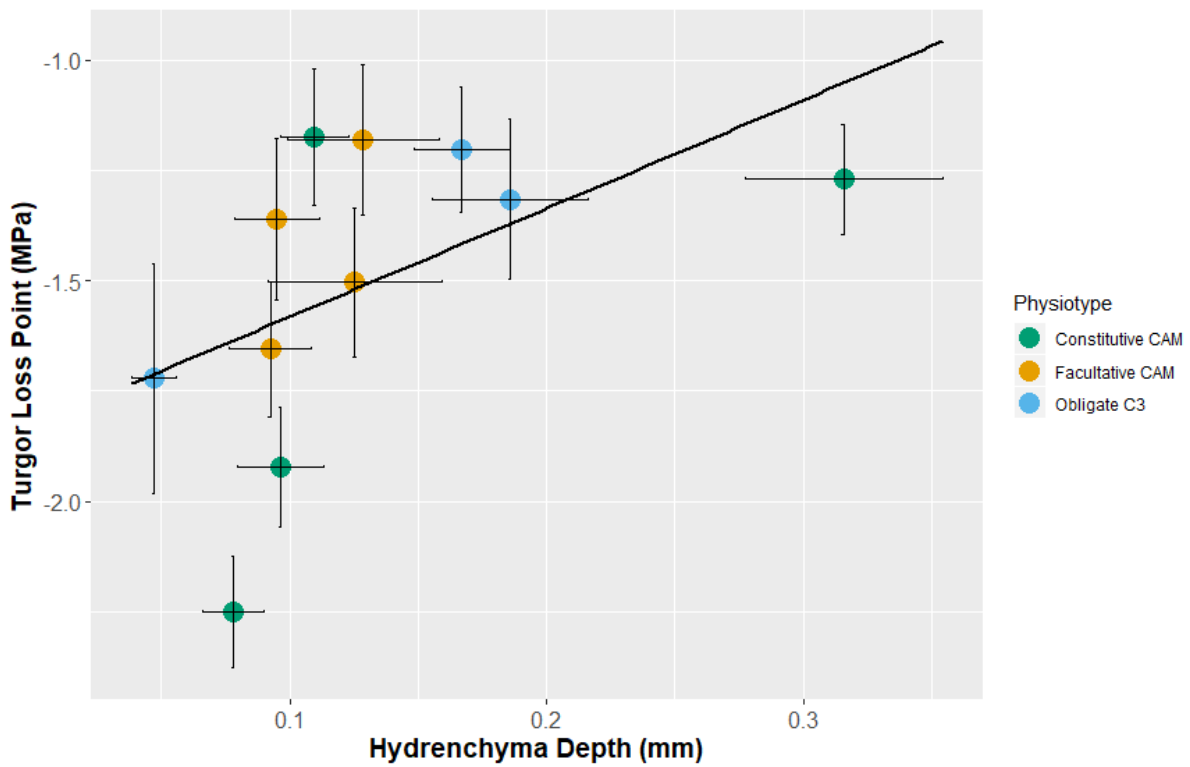


Fig. 3.2) Deeper hydrenchyma tissue raises the turgor loss point in *Clusia*. A positive correlation exists between hydrenchyma depth and TLP, such that species with deeper hydrenchyma lose turgor at less negative water potentials ($p = 0.025$, $\rho = 0.682$, Spearman's Rank Correlation Test). Error bars represent \pm one standard deviation.

3.2.2 Plant Growth Conditions

Plants sampled from Cockle Park Farm, Newcastle were grown in a glasshouse, as described in Chapter 2. Plants sampled for field measurements were grown outdoors at the Smithsonian Tropical Research Institute, Santa Cruz Experimental Research Facility, Gamboa, Republic of Panama (9.120085N, 79.701894W). The mature *Clusia* plants in this common garden were 2 to 7 meters tall, and were all over 4 years old. Plants received full sunlight and natural rainfall.

3.2.3 Pressure-Volume Curves

Values for capacitance, bulk modulus of elasticity and SWC were taken from Chapter 2. In addition to this, the water potential at which turgor is lost (TLP) was calculated from the same pressure volume curves. This was done by plotting the reciprocal of the leaf water potential against the relative water content (RWC) of the leaf, and identifying the inflection point where the line changed from a curve to a straight line (Sack and Pasquet-Kok, 2011). If there was ever any ambiguity between two points being the TLP, a linear regression was built twice for the straight portion of the line (i.e. the points including and after the TLP), with or without the ambiguous point, and the model that yielded the highest r^2 value was selected.

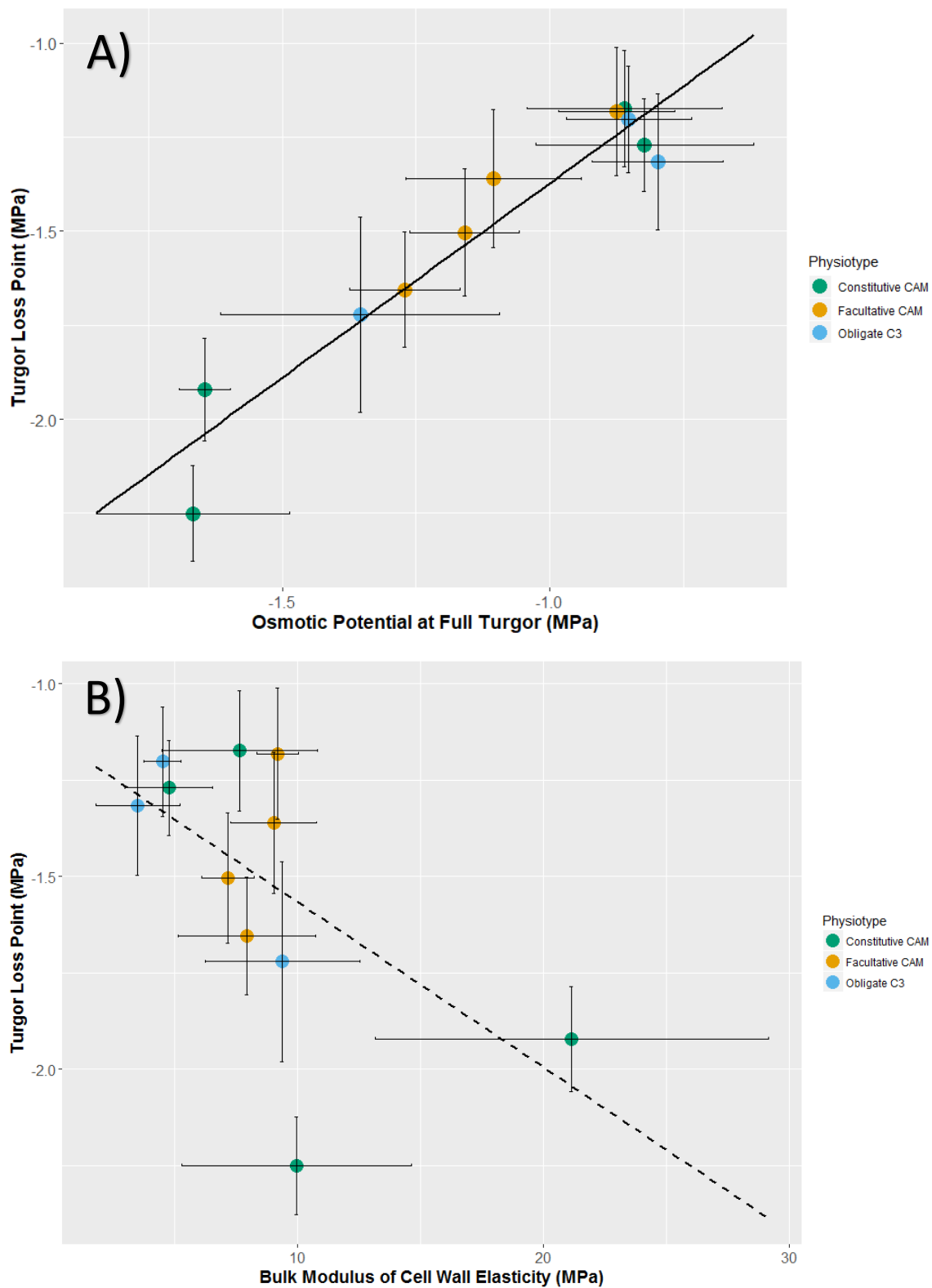


Fig. 3.3) The osmotic potential at full turgor, alone, is a strong determinant of the turgor loss point in *Clusia*. (A) A strong, positive correlation ($p = 0.003$, $\rho = 0.827$) exists between π_0 and TLP in *Clusia*. (B) A weak, negative correlation ($p = 0.0519$, $\rho = -0.609$) exists between ϵ and the TLP. Dashed line represents a p -value > 0.05 .

3.2.4 Anatomical Measurements

Anatomical measurements for the plants grown in Cockle Park Farm, Newcastle, UK were taken from Chapter 2. Additional anatomical measurements were made on plants grown in Gamboa, Panama. For these a similar protocol was carried out as in Chapter 2. Namely, between January and March, 2019, stems were harvested at least 6 nodes from the apex, and sealed in moist plastic bags to limit transpirational water loss. The stems were then taken to the laboratory in the Earl S. Tupper Centre, Smithsonian Tropical Research Institute, Panama City, where leaves were cut underwater, so that the cut petiole remained underwater whilst the rest of the leaf blade was not submerged. These leaves were then placed, like this, inside transparent plastic boxes, filled with wet tissues to maximise humidity. These boxes were then placed in plant growth chambers (12 hour light period, day/night temp 30/28 °C) and left to rehydrate for approx. 18h. The following day, rehydrated leaves were hand-sectioned, using a razor blade, and these sections were imaged using a fluorescent microscope (Nikon Eclipse 600 Microscope with a Nikon Dri-1 camera). Measurements of hydrenchyma depth were made using ImageJ (NIH).

3.2.5 Determining Osmotic Potential at Full Turgor (π_0) for Field-Grown Plants

Branches were sampled and leaves incubated as described for the anatomical measurements, above. Once incubated leaves had rehydrated, they were sampled at dawn (6:00 – 6:45 am) by punching a small (8 mm diameter) disk from the leaf lamina, taking care to avoid the midrib or leaf margins. This leaf disk was quickly punctured with metal tweezers approx. 10 times and frozen in liquid nitrogen. In total, punching and puncturing each leaf disk before they were frozen took less than 30 seconds. The osmotic potential was measured by transferring leaf disks into a C-52 thermocouple psychrometer chamber (Wescor) attached to a PSYPRO control box (Wescor). The disk was transferred from liquid nitrogen using forceps and allowed to thaw in the chamber. The psychrometer was used in a room regulated to 23 °C, and the value of π_0 was only accepted once 5 technical replicates yielded values with a range less than 0.1 MPa. The mean of these measurements was used as the final value.

3.2.6 Titratable Acidity

To determine the extent to which each of the field grown species does CAM, the dry-season dawn/dusk H^+ concentration (ΔH^+) were measured. All sampling was performed at 6:00 - 7:00 pm, 12th January, and 6:00 – 7:00 am 13th January. For each plant, 2 leaf disks (21 mm diameter) were cut from a sun-exposed leaf, and immediately frozen in liquid nitrogen. These were weighed, freeze-dried for 72 hours (Labonco, Freezeone 4.5, Kansas City, MO) and subsequently boiled in 50 % ethanol to extract acid contents. This extract was titrated against 25 mMol KOH, until it reached pH 7 (measured with a pH meter), to determine the H^+ content.

3.2.7 Determining the Impact of Osmotic Potential (π_0) at Full Turgor and Bulk Modulus of Elasticity (ϵ) on the Turgor Loss Point

The bulk modulus of cell wall elasticity and the osmotic potential at full turgor for the species grown at Cockle Park Farm, Newcastle were estimated using pressure-volume curve data from Chapter 2. In addition, published data for two leaf succulent species, *Deuterocohnia brevifolia* (Bromeliaceae) and *Anacampseros lanceolata* (Anacampserotaceae) were taken from the literature for comparison (Males and Griffiths, 2018; Ogburn and Edwards, 2012, respectively). The water potential at which turgor is lost (TLP) can be calculated from equation 3.1. For each species, a range of values for the theoretical TLP was calculated by holding π_0 constant, at its true value for a given species, and changing ϵ from 0 to 30 MPa. This generated graphs that display the theoretical effect of changing ϵ on the TLP (i.e. Fig. 3.4) at the true value of π_0 . On to these graphs, a vertical line was drawn, intersecting the curve at the true value of ϵ , with a grey error bar representing ± 1 SD of ϵ . Inspection of these graphs allowed qualitative assessment of the potential effect changing ϵ could have on the TLP, by assessing whether the true value of ϵ lies on the steep or flat portion of the curve. This analysis was repeated, holding ϵ constant and changing π_0 from 0 to -3 MPa, to assess the potential effect changes to π_0 would have on the TLP. To get a quantitative measure of the ‘phenotypic space’ of each species, the derivative of each curve (i.e. the tangent to the curve), at the point where the true value of ϵ or π_0 for a given species intersects with the simulated data [$f'(\epsilon)$ and $f'(\pi_0)$, respectively], was calculated.

3.2.8 Statistics

All statistics were performed using R version 3.4.1. Because data was being compiled from different sampling efforts, no linear mixed effect models could be built. Instead Spearman's rank correlations were used.

3.3 Results

3.3.1 *Crassulacean Acid Metabolism Does not Affect the Turgor Loss Point in Clusia*

As CAM is typically considered a drought-avoidance strategy, it was predicted that the deployment of CAM would drive the TLP up; as species that could engage in this photosynthetic mode would lose less water and therefore likely experience less negative water potentials. The percentage of total diel net CO₂ uptake performed at night in well-watered plants was used to assess the degree to which each of the 11 species constitutively exhibited a CAM phenotype (Barrera Zambrano et al., 2014). This measure of CAM did not significantly correlate with the TLP (Fig. 3.1). In addition, as many *Clusia* species are able to facultatively express a CAM phenotype in response to drought, the percentage of total diel photosynthesis done at night in drought treated plants was also tested for correlations with the TLP, but no significant correlations were found (Fig. 3.1). Taken together, these data show neither constitutive nor facultative CAM affect the TLP in *Clusia*.

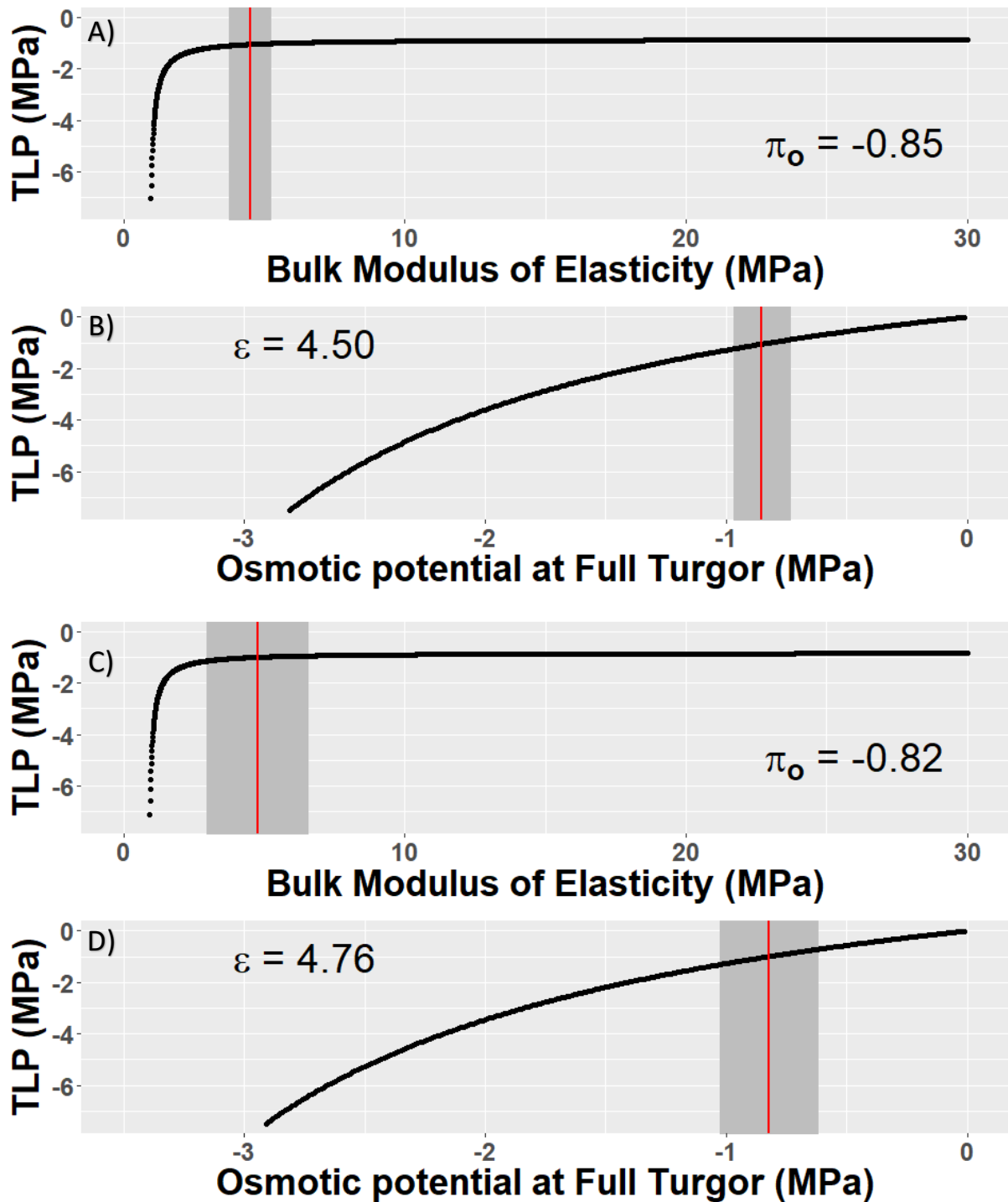


Fig. 3.4) Osmotic potential at full turgor, not the bulk modulus of elasticity has the potential to affect the turgor loss point in *C. tocuchensis* and *C. alata*. Data for *C. tocuchensis* is presented in A and B and data for *C. alata* is presented in C and D. (A and C) Simulating the TLP, holding π_0 constant, and changing ε shows a plateau effect of increasing ε . The true value of ε , represented by the red line, lies in this plateau. (B and D) Simulating the TLP, holding ε constant, and changing π_0 shows little plateau effect of increasing ε . The true value of π_0 , represented by the red line, lies on a sloped line. Grey bars represent \pm one standard deviation.

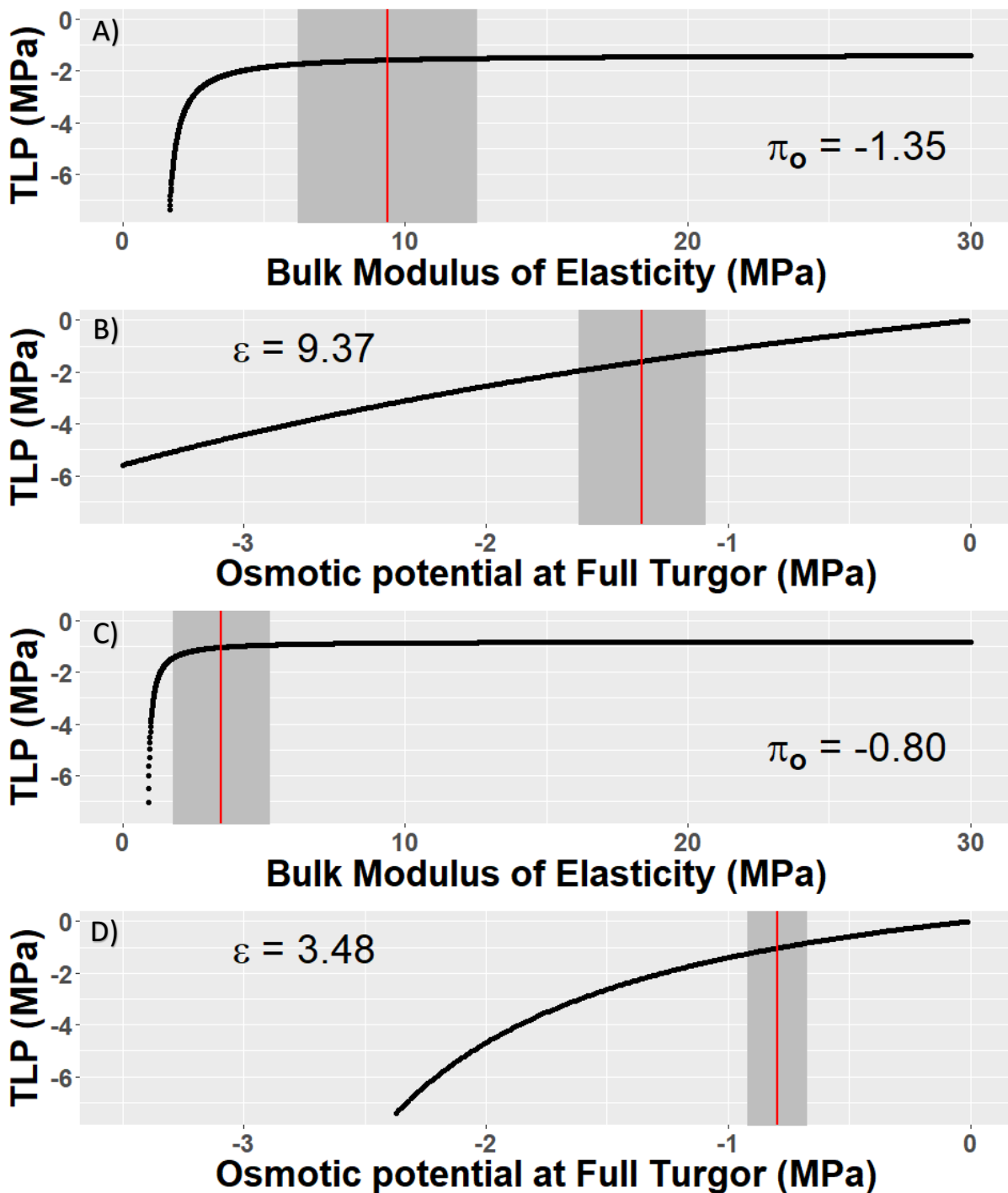


Fig. 3.5) Osmotic potential at full turgor, not the bulk modulus of elasticity has the potential to affect the turgor loss point in *C. grandiflora* and *C. multiflora*. Data for *C. grandiflora* is presented in A and B and data for *C. multiflora* is presented in C and D. (A and C) Simulating the TLP, holding π_0 constant, and changing ϵ shows a plateau effect of increasing ϵ . The true value of ϵ , represented by the red line, lies in this plateau. (B and D) Simulating the TLP, holding ϵ constant, and changing π_0 shows little plateau effect of increasing ϵ . The true value of π_0 , represented by the red line, lies on a sloped line. Grey bars represent \pm one standard deviation.

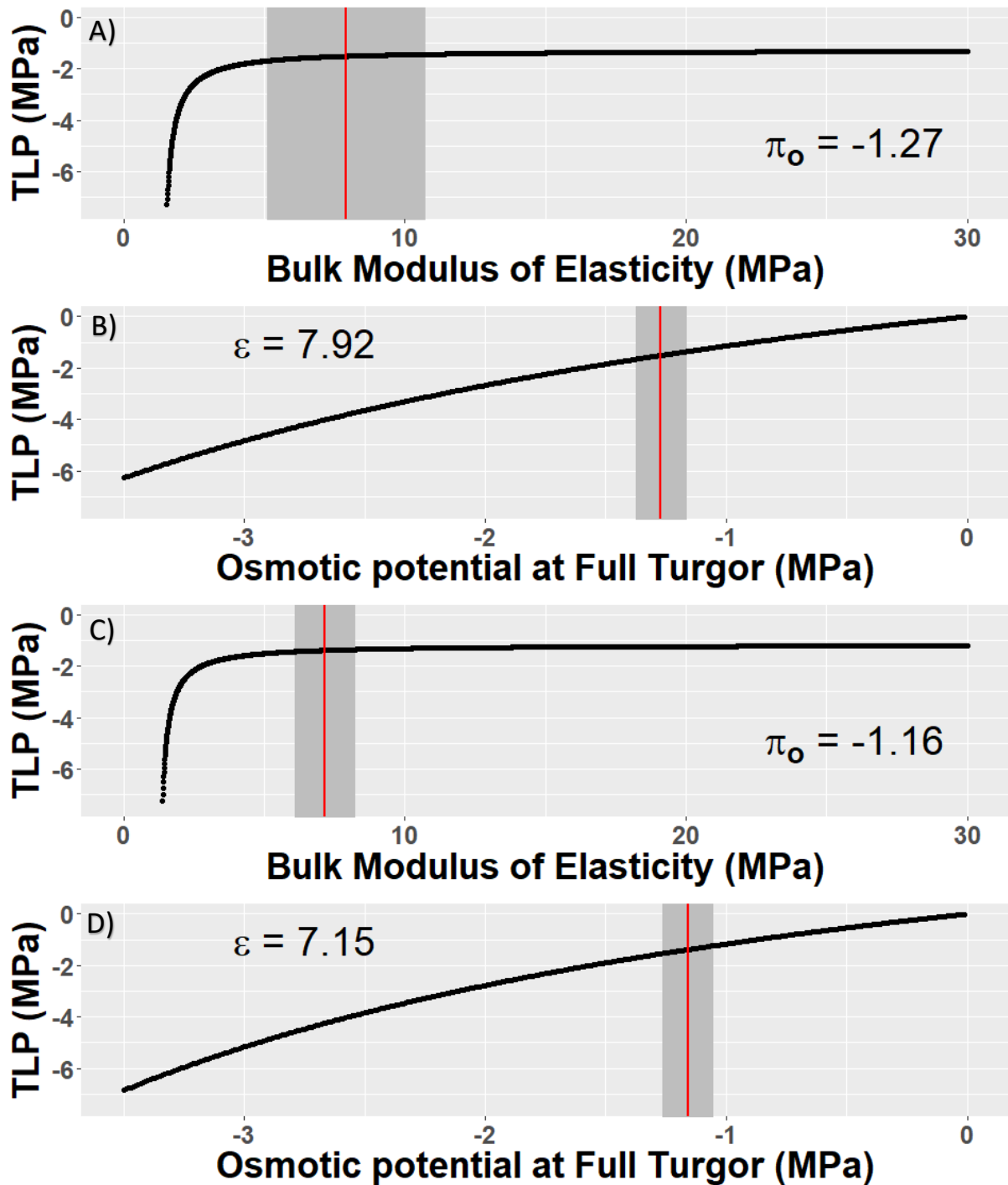


Fig. 3.6) Osmotic potential at full turgor, not the bulk modulus of elasticity has the potential to affect the turgor loss point in *C. lanceolata* and *C. aripoensis*. Data for *C. lanceolata* is presented in A and B and data for *C. aripoensis* is presented in C and D. (A and C) Simulating the TLP, holding π_o constant, and changing ϵ shows a plateau effect of increasing ϵ . The true value of ϵ , represented by the red line, lies in this plateau. (B and D) Simulating the TLP, holding ϵ constant, and changing π_o shows little plateau effect of increasing ϵ . The true value of π_o , represented by the red line, lies on a sloped line. Grey bars represent \pm one standard deviation.

3.3.2 Hydrenchyma Depth Affects the Turgor Loss Point in *Clusia*

As hydrenchyma is known to contribute significantly to saturated water content (SWC) and capacitance in *Clusia* (Chapter 2), it was predicted that hydrenchyma depth would also correlate with the TLP across species. Analysis of these parameters found that interspecific variation in hydrenchyma depth significantly correlates with the TLP, meaning species with deeper hydrenchyma have less negative TLP values (Fig. 3.2). These data show that increased investment into hydrenchyma tissue causes species to be less able to tolerate low water potentials in *Clusia*.

3.3.3 Contribution of Osmotic Potential at Full Turgor (π_0) and Bulk Modulus of Elasticity (ϵ) to the Turgor Loss Point in *Clusia*

To understand, mechanistically, how the TLP is controlled in *Clusia*, the extent to which π_0 and ϵ contribute to the TLP was assessed. As these variables are known to relate to the TLP according to equation 3.1, π_0 and ϵ were expected to positively correlate with the TLP. There was a tight positive correlation between π_0 and the TLP (Fig. 3.3). Therefore, it is likely that π_0 is a strong determinant of the TLP in *Clusia*. Analysis of the relationship between ϵ and the TLP, on the other hand, found a weak, non-significant *negative* correlation (Fig. 3.3).

To better understand if ϵ is determining the TLP in *Clusia*, simulations were constructed, to understand the 'phenotypic space' for each species (Fig 3.4 to 3.9). The TLP was calculated according to equation 3.1, holding π_0 constant (at its true value) and changing ϵ . The true value for ϵ was then plotted on to these simulated data (e.g. the straight vertical line on Fig. 3.4A). Qualitative assessment of these graphs for every *Clusia* species (Figs 3.4 to 3.9) demonstrated that the true value of ϵ lay on the plateau of the line, meaning changes to ϵ would have little to no effect on the TLP. In contrast, when ϵ was held constant and π_0 changed to simulate the TLP, the true value of π_0 lay on the curved portion of the graph for every *Clusia* species (Figs 3.4 to 3.9). This means that changing π_0 would affect the TLP for these species. These analyses confirm that the correlation between π_0 and TLP in Fig. 3.3 reflects a mechanistic control of the TLP, whereas the negative correlation between ϵ and the TLP is likely due to a confounding variable, and does not reflect a mechanistic control of the TLP.

3.3.4 Changes to Bulk Modulus of Elasticity (ϵ) can Affect the Turgor Loss Point in Highly Succulent Species

To test if highly succulent taxa can ever inhabit a 'phenotypic space' in which ϵ contributes to the TLP, the aforementioned approach (simulating the TLP based on π_0 and ϵ) was repeated for two species, *Deuterocohnia brevifolia* (Bromeliaceae) and *Anacampseros lanceolata* (Anacampserotaceae). The former is a water storage succulent with, 52% of its cross-sectional leaf area made up by hydrenchyma (Males 2018), whilst the latter is an all-cell succulent, without hydrenchyma (Fig. 3.10). When π_0 was changed to simulate the TLP, the true value of π_0 fell on a curved portion of the line for both species (Fig. 3.11). In addition, when ϵ was changed to simulate the TLP, the true value of ϵ fell on a curved portion of the line for both species (Fig. 3.11). To assess this quantitatively, the derivative of all curves, at the point the true value intersects the simulated data, [$f'(\epsilon)$ and $f'(\pi_0)$] was calculated (Table 3.1). The value of $f'(\pi_0)$, was much higher for these highly succulent species than the *Clusia* species studied. Likewise, $f'(\epsilon)$ was much higher for these species than for the *Clusia* species studied. Taken together, these analyses show that the TLP of highly succulent taxa is influenced by both π_0 and ϵ .

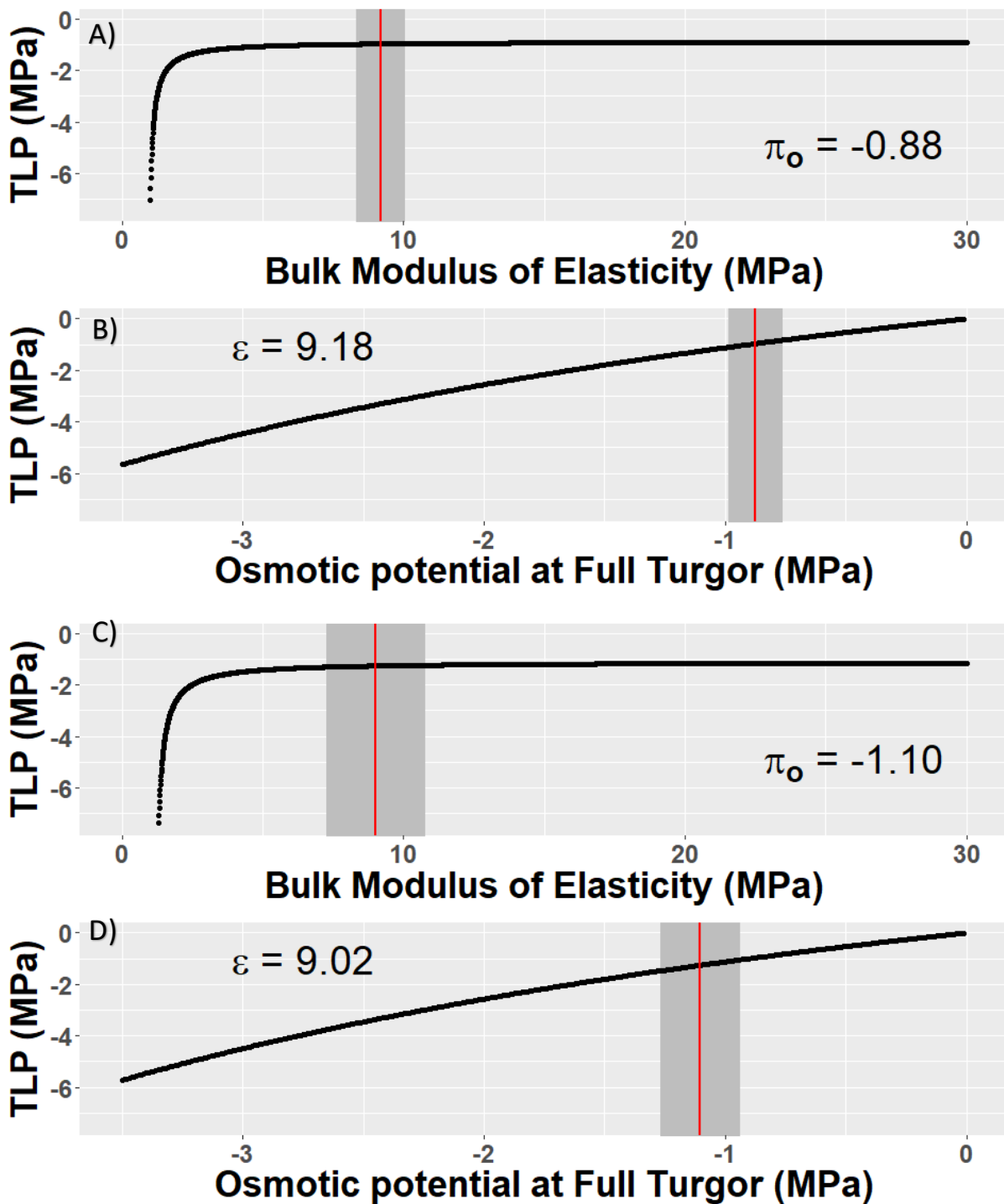


Fig. 3.7) Osmotic potential at full turgor, not the bulk modulus of elasticity has the potential to affect the turgor loss point in *C. pratensis* and *C. minor*. Data for *C. pratensis* is presented in A and B and data for *C. minor* is presented in C and D. (A and C) Simulating the TLP, holding π_o constant, and changing ϵ shows a plateau effect of increasing ϵ . The true value of ϵ , represented by the red line, lies in this plateau. (B and D) Simulating the TLP, holding ϵ constant, and changing π_o shows little plateau effect of increasing ϵ . The true value of π_o , represented by the red line, lies on a sloped line. Grey bars represent \pm one standard deviation.

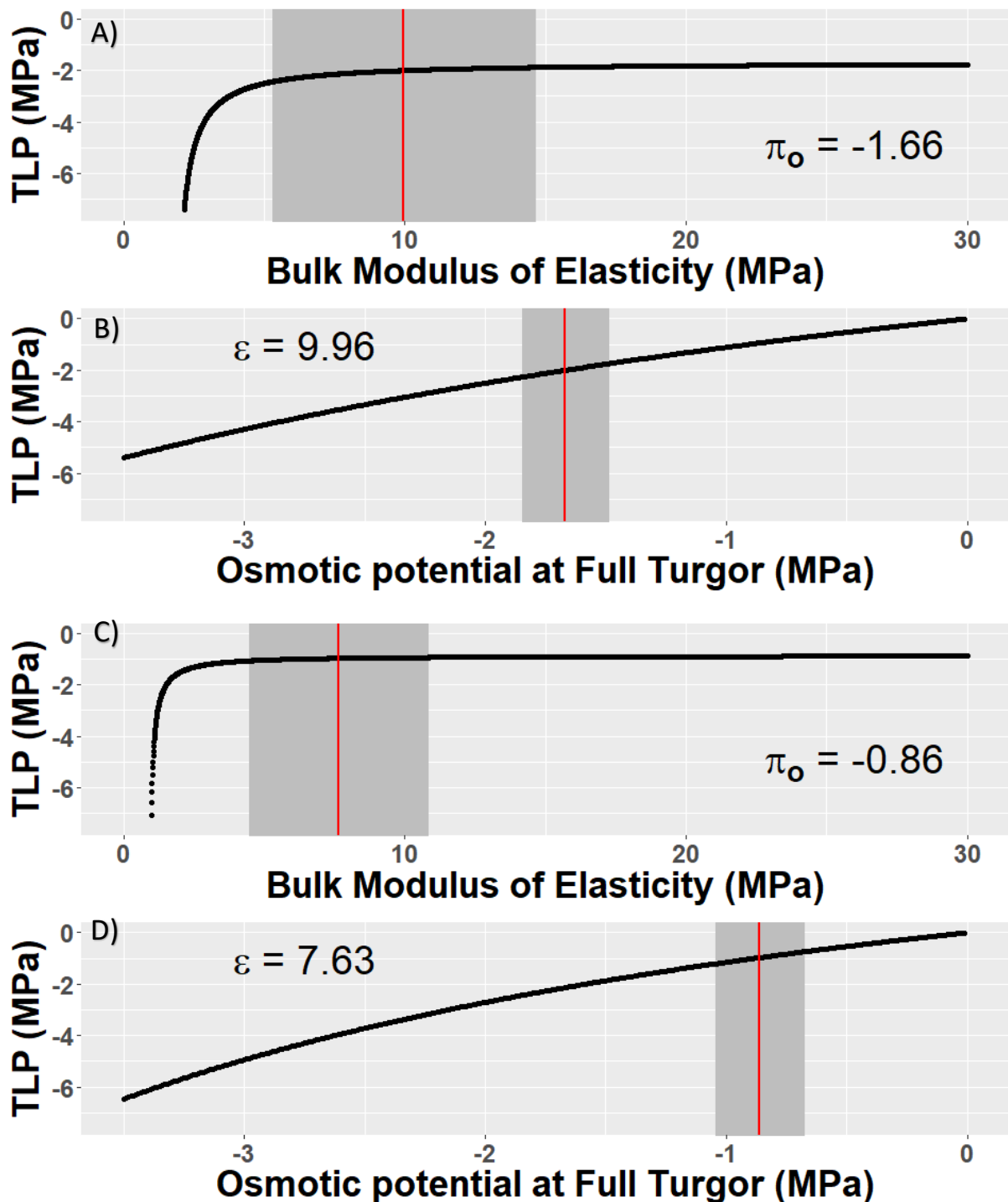


Fig. 3.8) Osmotic potential at full turgor, not the bulk modulus of elasticity has the potential to affect the turgor loss point in *C. rosea* and *C. fluminensis*. Data for *C. rosea* is presented in A and B and data for *C. fluminensis* is presented in C and D. (A and C) Simulating the TLP, holding π_0 constant, and changing ϵ shows a plateau effect of increasing ϵ . The true value of ϵ , represented by the red line, lies in this plateau. (B and D) Simulating the TLP, holding ϵ constant, and changing π_0 shows little plateau effect of increasing ϵ . The true value of π_0 , represented by the red line, lies on a sloped line. Grey bars represent \pm one standard deviation.

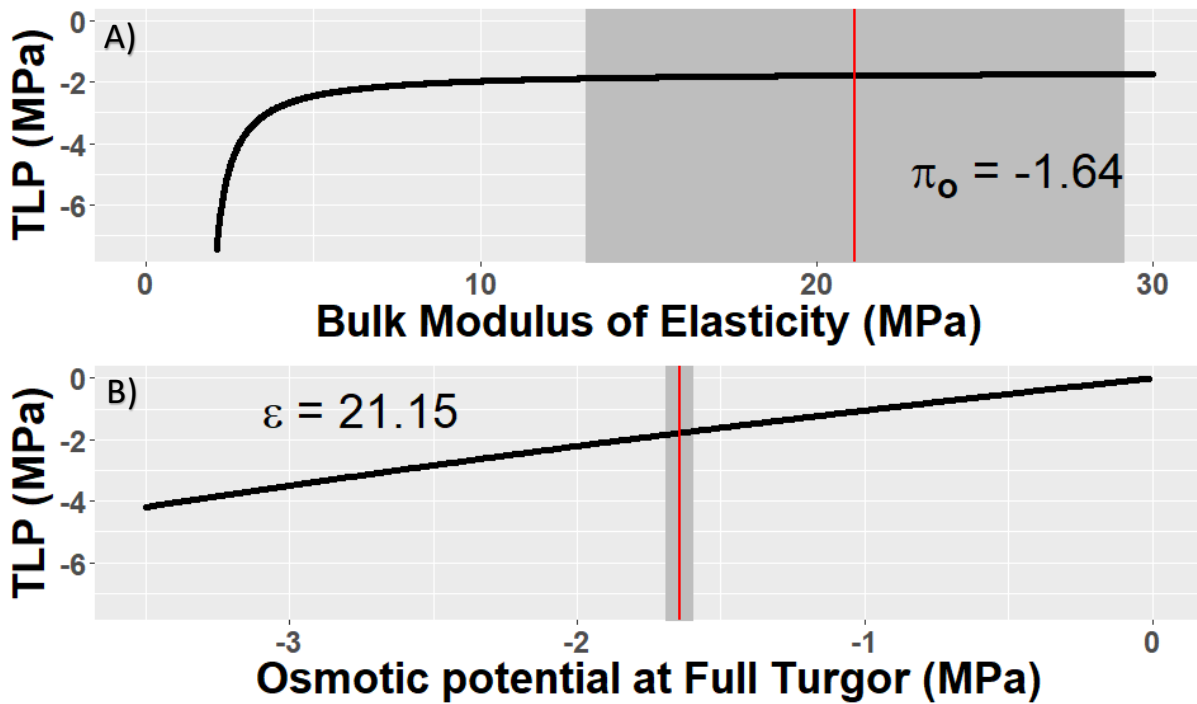


Fig. 3.9) Osmotic potential at full turgor, not the bulk modulus of elasticity has the potential to affect the turgor loss point in *C. hilariana*. (A) Simulating the TLP, holding π_o constant, and changing ε shows a plateau effect of increasing ε . The true value of ε , represented by the red line, lies in this plateau. (B) Simulating the TLP, holding ε constant, and changing π_o shows little plateau effect of increasing ε . The true value of π_o , represented by the red line, lies on a sloped line. Grey bars represent \pm one standard deviation.

3.3.5 Field Measurements

Field measurements of π_0 were used as a proxy for the TLP, as these two parameters correlate tightly in *Clusia* (Fig. 3.3). This meant drought tolerance could be determined using a thermocouple psychrometer, allowing very quick, high-throughput measurements on field-grown plants. To this end, π_0 was measured for 9 species of *Clusia* grown in the field in Gamboa, Panama. Analysis of π_0 , as a proxy for the TLP, found that hydrenchyma depth correlated positively with the TLP, meaning species with deeper hydrenchyma have less negative TLP values (Fig. 3.12). In addition, no correlation was found between the dry-season dawn/dusk difference in acid content (ΔH^+) and the TLP (Fig. 3.12). Taken together, these data show that, like lab-grown plants, the TLP is determined by hydrenchyma, and not by CAM in *Clusia*.



Fig. 3.10) *Anacampseros lanceolata* is an all-cell succulent. As evidenced by the presence of chlorophyllous cells throughout the entire leaf. Photo kindly provided by twitter user, @LithopsStories, on 05/07/2019; link available at: https://twitter.com/Ali_P_Leverett/status/1147057669225754629

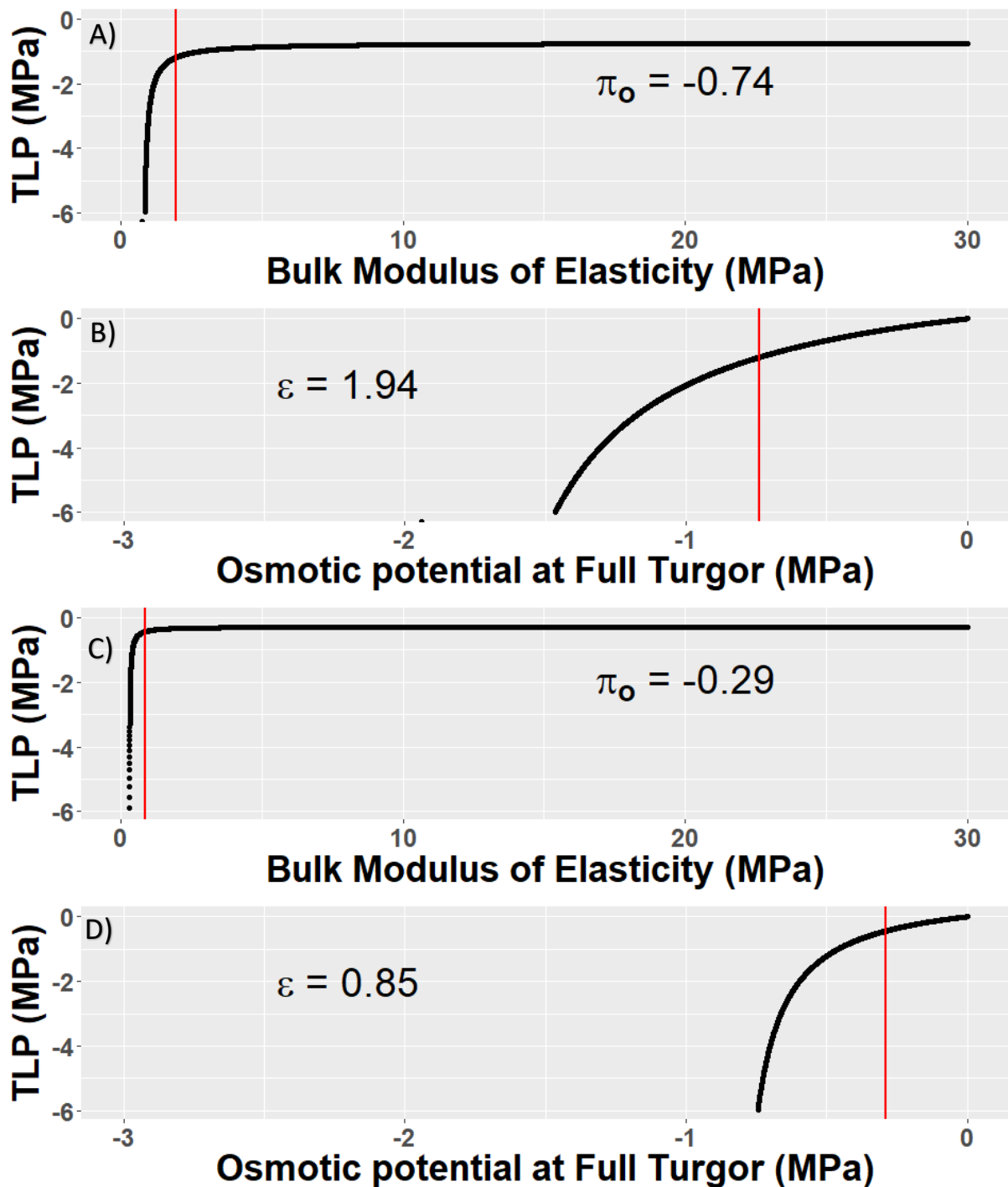


Fig. 3.11) Elasticity does contribute to the turgor loss point in other succulent species. Osmotic potential at full turgor and the bulk modulus of elasticity has the potential to affect the TLP in (A and B) *Deuterocohnia brevifolia* (Bromeliaceae) and (C and D) *Anacampseros lanceolata* (Anacampserotaceae). Simulating the TLP, holding π_o constant, and changing ϵ shows a plateau effect of increasing ϵ . The true value of ϵ , represented by the red line, lies in the curved portion of the line, not the plateau. (A and C) Simulating the TLP, holding ϵ constant, and changing π_o shows little plateau effect of increasing ϵ (B and D). The true value of π_o , represented by the red line, lies on a sloped portion of the line. For all graphs, the true value, represented by the vertical red line falls on a curved portion of the simulated data, meaning any theoretical change to π_o or ϵ would affect the TLP.

Table 3.1) Derivative of the slope at the point where the true value for π_0 or ϵ intersects the simulated data

Species	Turgor Loss Point (MPa)	Effect of changing π_0 $f'(\pi_0)$	Effect of changing ϵ $f'(\epsilon)$
<i>Clusia grandiflora</i>	-1.72	1.365	0.028
<i>Clusia tocuchensis</i>	-1.20	1.520	0.054
<i>Clusia multiflora</i>	-1.32	1.686	0.089
<i>Clusia lanceolata</i>	-1.66	1.418	0.036
<i>Clusia aripoensis</i>	-1.50	1.425	0.038
<i>Clusia pratensis</i>	-1.18	1.223	0.011
<i>Clusia minor</i>	-1.36	1.297	0.019
<i>Clusia rosea</i>	-2.25	1.440	0.040
<i>Clusia fluminensis</i>	-1.17	1.270	0.016
<i>Clusia hilariana</i>	-1.92	1.175	0.007
<i>Clusia alata</i>	-1.27	1.460	0.043
<i>Deuterocohnia brevifolia</i>	-0.92	2.612	0.380
<i>Anacampseros lanceolata</i>	-0.47	2.301	0.268

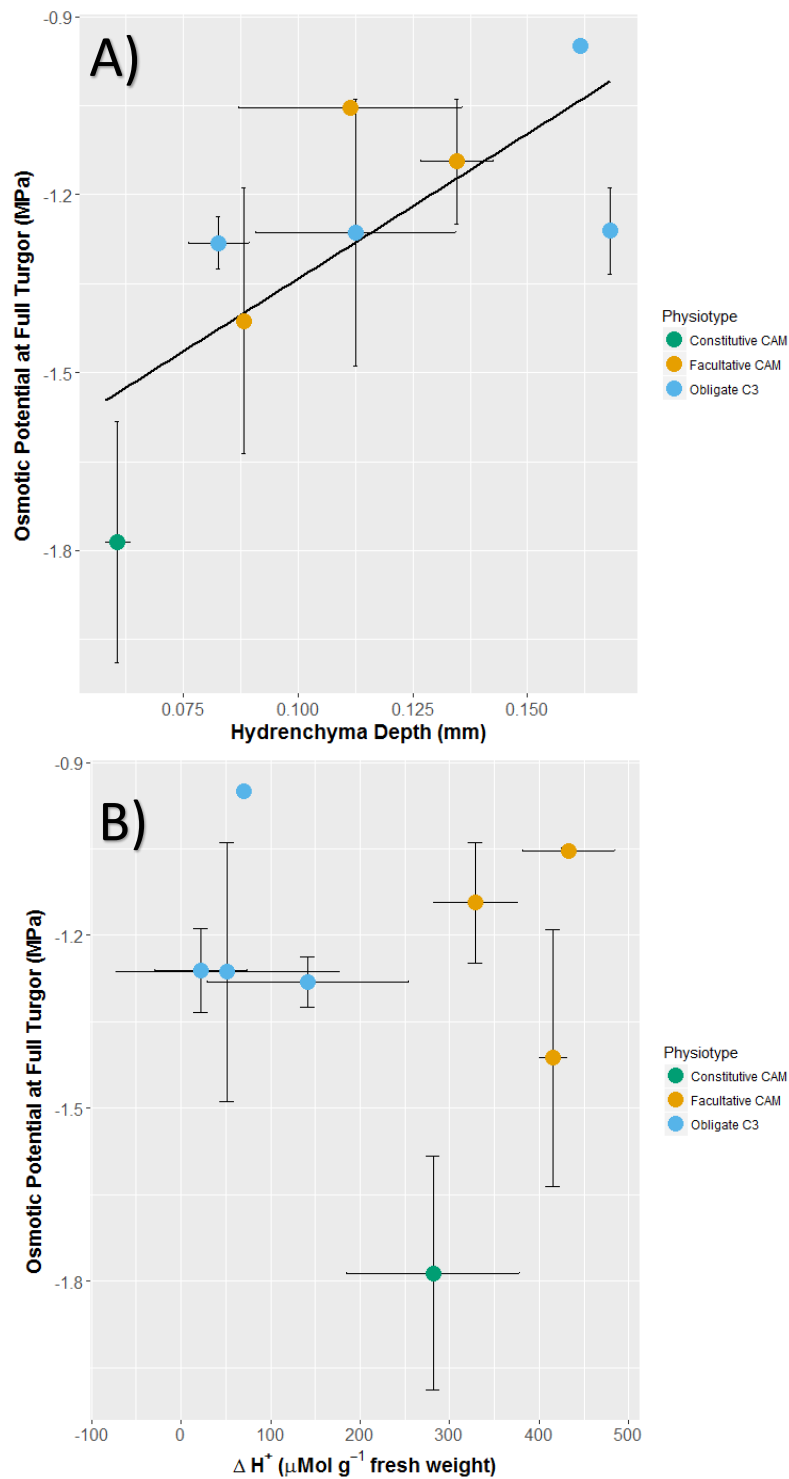


Fig. 3.12) Hydrenchyma, but not Crassulacean acid metabolism influences the osmotic potential at full turgor (π_o), in field grown trees in Gamboa, Panama. (A) A significant positive correlation exists between hydrenchyma depth and the osmotic potential at full turgor, which was used as a proxy for the TLP ($p = 0.046$, $\rho = 0.738$, Spearman's rank correlation). (B) No significant relationship exists between the dawn-dusk difference in acid content during the dry season in Panama and the osmotic potential at full turgor ($p = 0.9345$, $\rho = -0.0476$, Spearman's rank correlation). Error bars represent \pm one standard deviation, $n = 2-4$.

3.4 Discussion

3.4.1 Summary of Findings

A body of research (Borland et al., 1998; Barrera Zambrano et al; and Chapter 2; also see Chapter 4) has demonstrated that CAM and hydrenchyma are independent adaptations in *Clusia*. Consequently, this genus is an ideal model for testing how these different traits associated with the succulent syndrome each independently contribute to drought tolerance. As CAM and hydrenchyma are independent adaptations in *Clusia*, hypotheses 1 and 2 in the introduction to this chapter are incompatible; since it is highly unlikely that both adaptations are driving the TLP up in a statistically significant manner. In fact, the data presented in this chapter found that hydrenchyma has a significant influence on the TLP, and that this is likely due to changes in π_0 rather than ϵ . In contrast, the extent to which species are able to employ CAM photosynthesis does not appear to affect the TLP. These data provide evidence that hydrenchyma causes species to be considered 'drought avoiders' in the typical sense; species with this tissue are less able to tolerate negative water potentials associated with drought. CAM, on the other hand, does not appear to be an adaptation that affects species ability to tolerate low water potentials.

3.4.2 Crassulacean Acid Metabolism (CAM) Does not Affect the Turgor Loss Point

One notable conclusion drawn from the data presented in this study is that the extent to which species engage in CAM photosynthesis, either constitutively or facultatively, does not correlate with the TLP (Fig. 3.1). This analysis made use of pre-existing data from the *Clusia* collection at Newcastle (Barrera Zambrano et al., 2014), in which the percentage of photosynthesis done at night in both well-watered and drought-treated plants was measured, to determine the degree to which CAM is used in both optimal and water-limited conditions. These data are a particularly robust way of phenotyping the physiology of CAM plants, as they capture weak CAM photosynthesis and account for the phenotypic plasticity seen in facultative CAM plants. Therefore, use of these data for the analyses in this chapter represent strong evidence that CAM does not affect the TLP in *Clusia* (Edwards 2019; Winter 2019). This finding is somewhat puzzling as CAM is typically believed to prevent water loss, so it was

predicted that species exhibiting this photosynthetic physiology would not experience and thus have to tolerate low water potentials to the same extent as C₃ relatives. However, these data are congruous with findings from the Bromeliaceae, in which CAM terrestrial species are no better at tolerating low water potentials than their C₃-terrestrial relatives (Males and Griffiths 2017). More work needs to be done to determine if this observation holds true across all instances of CAM.

3.4.3 Investment in Hydrenchyma Raises the Turgor Loss Point

The effect that hydrenchyma depth has on the TLP is not trivial; in Fig. 3.2, approx. 0.1 mm deeper hydrenchyma appeared to cause a 1 MPa rise in TLP (although additional hydrenchyma depth after this appeared to have little effect). To put this into perspective, the TLP of most species are in the range of -3 to -0.5 MPa (Bartlett et al., 2012b), and a study of 50 Bromeliad species, including the C₃ and CAM terrestrial and epiphytic species, found that the TLP ranged from 0.6 to 1.6 MPa (Males and Griffiths, 2016). Therefore, in *Clusia* the hydrenchyma has a considerable impact on species' ability to tolerate negative water potentials. The ranges in hydrenchyma depth observed in this experiment are very small compared to several other succulent genera with hydrenchyma, such as *Peperomia* and *Tillandsia* (Kaul 1977; Loeschen et al., 1993). Therefore, species' ability to tolerate low water potentials in *Clusia* appears to be highly sensitive to subtle differences in hydrenchyma depth.

3.4.4 Osmotic Potential at Full Turgor (π_0), not Bulk Modulus of Cell Elasticity (ϵ) is the Mechanism by Which Hydrenchyma Affects the Turgor Loss Point

To generate a more mechanistic understanding of how hydrenchyma drives the TLP up, the effect of ϵ and π_0 were explored, as these parameters are known to mathematically relate to the TLP according to equation 3.1, and are suspected to be lower in species that invest more in hydrenchyma depth (Chapter 2). Initial tests demonstrated that a strong, positive correlation exists between π_0 and the TLP; a trend known to hold true across diverse tree species (Bartlett et al., 2012b). As discussed above, the TLP appears to be determined by the depth of hydrenchyma (Fig. 3.2), and these data offer a possible explanation for how this may occur; it is likely that hydrenchyma drives the TLP up by increasing the value of π_0 (i.e. making π_0 less negative). Further work needs to be done to confirm that hydrenchyma has a

higher π_0 (see Chapter 4) but if this is the case, it would mean that a greater investment in this tissue would cause the total leaf osmolality to be lower, hence making the TLP less negative.

As succulent species are known to have very elastic cell walls (Stiles and Martin, 1996; Ogburn and Edwards, 2010), it was hypothesised that the low values of ϵ conferred by hydrenchyma (Chapter 2) could be driving the TLP down. Initial analysis found the opposite effect, as a weak negative correlation exists between ϵ and the TLP. It was predicted that this finding was a mathematical artefact, and was in fact the consequence of hydrenchyma causing leaves to have higher (less negative) π_0 at the same time as having low ϵ . To demonstrate this, an analysis to assess the 'phenotypic space' of each species was performed. The phenotype (i.e. the true value of π_0 or ϵ) for each species was plotted onto simulated data, to show how changes to this parameter would affect the TLP. This approach demonstrated that changes to π_0 would have a large effect on the TLP (Fig 3.4B to 3.9B). In contrast, changes to ϵ would have no effect on the TLP (Fig 3.4A to 3.9A), for all species of *Clusia* studied. This revealed that the weak correlation observed in Fig. 3.3 was not the consequence of ϵ mechanistically controlling the TLP, thus confirming that this trend was an artefact. Taken together, these data show that π_0 and not ϵ is the mechanistic basis through which hydrenchyma depth determines the TLP.

3.4.5 Quantifying the 'Phenotypic Space'; How Best to Interpret This Analysis?

The aforementioned analysis, to assess the 'phenotypic space' of each species was quantified by finding the derivative of each curve at the point at which the true value of π_0 or ϵ intersected the simulated data (Table 3.1). By doing this, it is possible to quantitatively judge the degree to which a change to either π_0 or ϵ would affect the TLP. This type of analysis, which was developed specifically for this chapter, needs to be interpreted with caution. The units for both π_0 and ϵ are MPa, so it might seem appropriate to compare the derivative for the line generated by altering π_0 ($f'(\pi_0)$) with that of the line generated by altering ϵ ($f'(\epsilon)$). However, the range of π_0 in nature is typically about 3 MPa, whereas for ϵ it is 30 MPa. Therefore, any comparison of these derivatives will be biased, as the value for $f'(\pi_0)$ will nearly always be higher than for $f'(\epsilon)$. More meaningful interpretations can be obtained from comparing $f'(\pi_0)$ or $f'(\epsilon)$ between species. To this end, comparing the *Clusia* species to the highly succulent species, *Deuterocohnia brevifolia* and *Anacampseros lanceolata* (Ogburn and Edwards, 2012; Males 2018; Males and Griffiths 2018) shows that species outside of *Clusia*

with greater leaf succulence have higher values of $f'(\pi_0)$ and $f'(\epsilon)$. This reconfirms that π_0 has a substantial mechanistic control on the TLP in highly succulent taxa, and also provides a proof-of-principle demonstration that in highly succulent taxa, cell wall elasticity can have some mechanistic control on the TLP (Stiles and Martin, 1996). This is true for species with and without hydrenchyma tissue (Males 2018; Fig. 3.10). This might explain the observation that structural polysaccharide composition of two highly succulent *Aloe* species changes in response to drought (Ahl et al., 2019); extremely succulent species might be able to adjust their TLP by changing the physical properties of their cell walls. It is important to note that this comparison; i.e. comparing two highly succulent taxa selected from the literature with data on *Clusia*, is by no means comprehensive. To explore this further, it would be interesting to undertake a meta-analysis to understand which succulent traits, beyond ϵ itself, affect $f'(\epsilon)$.

3.4.6 Osmotic Potential at Full Turgor (π_0) Can Be Used as a Proxy for the Turgor Loss Point, for Field Measurements

The simple conclusion to be drawn from these analyses is that, in *Clusia*, interspecific variance in the TLP is controlled predominantly by π_0 . This observation means that π_0 can be used as a meaningful and reliable proxy for the TLP in *Clusia*. As π_0 can be calculated in a fraction of the time, using an osmometer or psychrometer, this method has become very popular for ecologists who wish to understand the drought tolerance of species grown in the field (Maréchaux et al., 2015; Griffin-Nolan et al., 2019; Medeiros et al., 2019; Méndez-Alonzo et al., 2019). Thus, to confirm the findings outlined so far; i.e. that hydrenchyma and not CAM is the adaptation determining the TLP, field measurements were taken, on mature trees grown in Gamboa, Panama.

To analyse the extent to which each species does CAM, the dawn/dusk difference in titratable acidity (ΔH^+) was used to phenotype the 9 species available. Sampling was done in the dry season, and therefore both facultative and constitutive expression of CAM was detected. These data were all congruous with the findings of Holtum et al., (2004), except for *C. quadralanga*, which showed some evidence of weak CAM (Fig. 3.12). However, only two individuals of this species were available for sampling, and it is likely that this inconsistency is the result of an outlier. As such, this species is still phenotyped as obligate C_3 in Fig. 3.12. Comparison of ΔH^+ with π_0 found no correlation (Fig. 3.12), which is congruous with the

findings from plants grown in glasshouses at Cockle Park Farm, Newcastle (Fig. 3.12). Furthermore, hydrenchyma depth correlated positively with the TLP (Fig. 3.12). Approximately a 0.075 mm increase in hydrenchyma depth conferred a 0.5 MPa increase in π_0 meaning that, like glasshouse-grown plants, the TLP is highly sensitive to subtle changes in this tissue depth. Taken together, these data provide evidence that the TLP in *Clusia* in the field is determined by hydrenchyma and not CAM.

3.5 Conclusions and Future Considerations

The data presented in this study provide evidence that hydrenchyma depth has a strong effect on the TLP in *Clusia*, whereas CAM does not. Hydrenchyma is a drought avoidance strategy; greater investment in the development of this tissue causes species to be less tolerant of low leaf water potentials. CAM, on the other hand appears to have no effect on species ability to tolerate negative water potentials. However, whilst these data describe species' ability to tolerate low water potentials, further work is required to understand how hydrenchyma and CAM affect species distributions (see Chapter 4). Beyond this, since CAM in *Clusia* does not affect the ability of species to tolerate low water potential, it cannot be considered a drought avoidance strategy in the classical sense. It is intriguing to consider if the primary role of CAM might not be to prevent the plant from experiencing low water potentials, but instead to maintain metabolic rates during drought (see Chapter 6). One other finding of this study is that the TLP is mechanistically controlled by changes to π_0 . The effect that hydrenchyma has on the TLP is therefore likely due to this tissue affecting the π_0 of the leaf. Whilst this can be inferred from the data presented here, direct comparison of π_0 in the hydrenchyma to the rest of the leaf is needed to confirm this prediction (see Chapter 4).

3.6 References

- Ahl, L. I., Mravec, J., Jørgensen, B., Rudall, P. J., Rønsted, N., & Grace, O. M. (2019). Dynamics of intracellular mannan and cell wall folding in the drought responses of succulent Aloe species. *Plant Cell and Environment*, (March), 1–14. <https://doi.org/10.1111/pce.13560>
- Barrera Zambrano, V. A., Lawson, T., Olmos, E., Fernández-García, N., & Borland, A. M. (2014). Leaf anatomical traits which accommodate the facultative engagement of crassulacean acid metabolism in tropical trees of the genus *Clusia*. *Journal of Experimental Botany*, 65(13), 3513–3523. <https://doi.org/10.1093/jxb/eru022>
- Bartlett, M. K., Scoffoni, C., Ardy, R., Zhang, Y., Sun, S., Cao, K., & Sack, L. (2012). Rapid determination of comparative drought tolerance traits: Using an osmometer to predict turgor loss point. *Methods in Ecology and Evolution*, 3(5), 880–888. <https://doi.org/10.1111/j.2041-210X.2012.00230.x>
- Bartlett, M. K., Scoffoni, C., & Sack, L. (2012). The determinants of leaf turgor loss point and prediction of drought tolerance of species and biomes: A global meta-analysis. *Ecology Letters*, 15(5), 393–405. <https://doi.org/10.1111/j.1461-0248.2012.01751.x>
- Bartlett, M. K., Zhang, Y., Kreidler, N., Sun, S., Ardy, R., Cao, K., & Sack, L. (2014). Global analysis of plasticity in turgor loss point, a key drought tolerance trait. *Ecology Letters*, 17(12), 1580–1590. <https://doi.org/10.1111/ele.12374>
- Beadle, C. L., Ludlow, M. M., & Honeysett, J. L. (1985). Water Relations. In J. Coombs, D. O. Hall, S. P. Long, & J. M. O. Scurlock (Eds.), *Techniques in Bioproductivity and Photosynthesis* (2nd ed., pp. 50–61). Pergamon.
- Borland, A. M., Técsi, L. I., Leegood, R. C., & Walker, R. P. (1998). Inducibility of crassulacean acid metabolism (CAM) in *Clusia* species; physiological/biochemical characterisation and intercellular localization of carboxylation and decarboxylation processes in three species which exhibit different degrees of CAM. *Planta*, 205(3), 342–351. <https://doi.org/10.1007/s004250050329>

- Borland, A. M., Wulschleger, S. D., Weston, D. J., Hartwell, J., Tuskan, G. a., Yang, X., & Cushman, J. C. (2015). Climate-resilient agroforestry: physiological responses to climate change and engineering of crassulacean acid metabolism (CAM) as a mitigation strategy. *Plant, Cell & Environment*, *38*, 1833–1849. <https://doi.org/10.1111/pce.12479>
- Edwards, E. J. (2019). Evolutionary trajectories, accessibility, and other metaphors: the case of C4 and CAM photosynthesis. *New Phytologist*, *223*(4), 1742–1755. <https://doi.org/10.1111/nph.15851>
- Farrell, C., Szota, C., & Arndt, S. K. (2017). Does the turgor loss point characterize drought response in dryland plants? *Plant Cell and Environment*, *40*(8), 1500–1511. <https://doi.org/10.1111/pce.12948>
- Griffin-Nolan, R. J., Ocheltree, T. W., Mueller, K. E., Blumenthal, D. M., Kray, J. A., & Knapp, A. K. (2019). Extending the osmometer method for assessing drought tolerance in herbaceous species. *Oecologia*, *189*(2), 353–363. <https://doi.org/10.1007/s00442-019-04336-w>
- Hasselquist, N. J., Allen, M. F., & Santiago, L. S. (2010). Water relations of evergreen and drought-deciduous trees along a seasonally dry tropical forest chronosequence. *Oecologia*, *164*(4), 881–890. <https://doi.org/10.1007/s00442-010-1725-y>
- Hochberg, U., Rockwell, F. E., Holbrook, N. M., & Cochard, H. (2018). Iso/Anisohdry: A Plant–Environment Interaction Rather Than a Simple Hydraulic Trait. *Trends in Plant Science*, *23*(2), 112–120. <https://doi.org/10.1016/j.tplants.2017.11.002>
- Holtum, J. A. M., Aranda, J., Virgo, A., Gehrig, H. H., & Winter, K. (2004). $\delta^{13}\text{C}$ values and crassulacean acid metabolism in *Clusia* species from Panama. *Trees*, *18*, 658–668. <https://doi.org/10.1007/s00468-004-0342-y>
- Hultine, K. R., Scott, R. L., Cable, W. L., Goodrich, D. C., & Williams, D. G. (2004). Hydraulic redistribution by a dominant, warm-desert phreatophyte: Seasonal patterns and response to precipitation pulses. *Functional Ecology*, *18*(4), 530–538. <https://doi.org/10.1111/j.0269-8463.2004.00867.x>

- Kaul, R. B. (1977). The Role of the Multiple Epidermis in Foliar Succulence of Peperomia (Piperaceae). *Botanical Gazette*, 138(2), 213–218.
- Lange, O. L., & Zuber, M. (1977). Frerea indica, a stem succulent CAM plant with deciduous C3 leaves. *Oecologia*, 31, 67–72. <https://doi.org/10.1007/BF00348709>
- Loeschen, V. S., Martin, C. E., Smith, M., & Eder, S. L. (1993). Leaf Anatomy and CO₂ Recycling during Crassulacean Acid Metabolism in Twelve Epiphytic Species of Tillandsia (Bromeliaceae). *International Journal of Plant Sciences*, 154(1), 100–106.
- Males, J. (2016). Think tank: water relations of Bromeliaceae in their evolutionary context. *Botanical Journal of the Linnean Society*, 181(3), 415–440. <https://doi.org/10.1111/boj.12423>
- Males, J. (2018). Concerted anatomical change associated with crassulacean acid metabolism in the Bromeliaceae. *Functional Plant Biology*, 45(7), 681–695. <https://doi.org/10.1071/fp17071>
- Males, J. (2017). Secrets of succulence. *Journal of Experimental Botany*, 68(9), 2121–2134. <https://doi.org/10.1093/jxb/erx096>
- Males, J., & Griffiths, H. (2017). Functional types in the Bromeliaceae: relationships with drought-resistance traits and bioclimatic distributions. *Functional Ecology*, 31(10), 1868–1880. <https://doi.org/10.1111/1365-2435.12900>
- Males, J., & Griffiths, H. (2018). Economic and hydraulic divergences underpin ecological differentiation in the Bromeliaceae. *Plant Cell and Environment*, 41(1), 64–78. <https://doi.org/10.1111/pce.12954>
- Maréchaux, I., Bartlett, M. K., Iribar, A., Sack, L., & Chave, J. (2017). Stronger seasonal adjustment in leaf turgor loss point in lianas than trees in an Amazonian forest. *Biology Letters*, 13(1). <https://doi.org/10.1098/rsbl.2016.0819>
- Maréchaux, I., Bartlett, M. K., Sack, L., Baraloto, C., Engel, J., Joetzjer, E., & Chave, J. (2015). Drought tolerance as predicted by leaf water potential at turgor loss point varies

- strongly across species within an Amazonian forest. *Functional Ecology*, 29(10), 1268–1277. <https://doi.org/10.1111/1365-2435.12452>
- Martínez-Vilalta, J., & Garcia-Forner, N. (2017). Water potential regulation, stomatal behaviour and hydraulic transport under drought: deconstructing the iso/anisohydric concept. *Plant Cell and Environment*, 40(6), 962–976. <https://doi.org/10.1111/pce.12846>
- Medeiros, C. D., Scoffoni, C., John, G. P., Bartlett, M. K., Inman-Narahari, F., Ostertag, R., ... Sack, L. (2019). An extensive suite of functional traits distinguishes Hawaiian wet and dry forests and enables prediction of species vital rates. *Functional Ecology*, 33(4), 712–734. <https://doi.org/10.1111/1365-2435.13229>
- Meinzer, F. C., Rundel, P. W., Sharifi, M. R., & Nilsen, E. T. (1986). Turgor and osmotic relations of Sonoran desert plant *Larrea tridentata*. *Plant, Cell & Environment*, 9, 467–475.
- Meinzer, F. C., Woodruff, D. R., Marias, D. E., Smith, D. D., McCulloh, K. A., Howard, A. R., & Magedman, A. L. (2016). Mapping ‘hydroscares’ along the iso- to anisohydric continuum of stomatal regulation of plant water status. *Ecology Letters*, 19(11), 1343–1352. <https://doi.org/10.1111/ele.12670>
- Méndez-Alonzo, R., Ewers, F. W., Jacobsen, A. L., Pratt, R. B., Scoffoni, C., Bartlett, M. K., & Sack, L. (2019). Covariation between leaf hydraulics and biomechanics is driven by leaf density in Mediterranean shrubs. *Trees*, 33(2), 507–519. <https://doi.org/10.1007/s00468-018-1796-7>
- Monson, R. K., & Smith, S. D. (1982). Seasonal Water Potential Components of Sonoran Desert Plants. *Ecology*, 63(1), 113–123.
- Ogburn, R. M., & Edwards, E. J. (2012). Quantifying succulence: A rapid, physiologically meaningful metric of plant water storage. *Plant, Cell and Environment*, 35(9), 1533–1542. <https://doi.org/10.1111/j.1365-3040.2012.02503.x>

- Ogburn, R. M., & Edwards, E. J. (2010). The ecological water-use strategies of succulent plants. In *Advances in Botanical Research* (1st ed., Vol. 55).
<https://doi.org/10.1016/B978-0-12-380868-4.00004-1>
- Sack, L., Pasquet-Kok, J. & Nicotra, A. (2011) Leaf pressure–volume curve parameters [WWW document] URL <http://prometheuswiki.publish.csiro.au/tiki-index.php?page=Leaf+pressure-volume+curve+parameters> [accessed 11 August 2017]
- Stiles, K. C., & Martin, C. E. (1996). Effects of drought stress on CO₂ exchange and water relations in the CAM epiphyte *Tillandsia utriculata* (Bromeliaceae). *Journal of Plant Physiology*, 149(6), 721–728. [https://doi.org/10.1016/S0176-1617\(96\)80098-8](https://doi.org/10.1016/S0176-1617(96)80098-8)
- Trueba, S., Pan, R., Scoffoni, C., John, G. P., Davis, S. D., & Sack, L. (2019). Thresholds for leaf damage due to dehydration: declines of hydraulic function, stomatal conductance and cellular integrity
- Tyree, M. T., & Hammel, H. T. (1972). The Measurement of the Turgor Pressure and the Water Relations of Plants by the Pressure-bomb Technique. *Journal of Experimental Botany*, 23(February), 267–282. <https://doi.org/10.1093/jxb/23.1.267>
- Winter, K. (2019). Ecophysiology of constitutive and facultative CAM photosynthesis. *Journal of Experimental Botany*, In pr. <https://doi.org/10.1093/jxb/erz002>

Chapter 4. Functional Ecology and Physiology of Hydrenchyma in *Clusia*

4.1 Introduction

The above-ground organs of plants often exhibit several adaptations to arid and semi-arid conditions. These include, but are not limited to, Crassulacean acid metabolism (CAM), a waxy impermeable cuticle as well as hairy and/or pale leaves and cladodes (Mooney et al., 1977; Boom et al., 2005). In addition, many species have specialised achlorophyllous water storage tissue called hydrenchyma, which acts as a water store (Barcikowski and Nobel, 1984; Smith et al., 1987; Schmidt and Kaiser, 1987; Gibeaut and Thomson 1989; Schulte and Nobel, 1989; Goldstein et al., 1991; Nowak and Martin, 1997; Nobel, 2006). Hydrenchyma tissue is an adaptation found across the tracheophytes; this tissue type is present in Eudicots, Monocots and even Ferns (Herrera et al., 2000; Chiang et al., 2013; Males 2018). In leaves, hydrenchyma typically exists either as a central tissue, for example the clear ‘gel’ in an *Aloe* leaf (Grace et al., 2015) or the storage tissue at the centre of massive *Agave* leaves (Smith et al., 1987), or as an adaxial, epidermal layer, as found in *Peperomia reflexa* (Piperaceae), *Pitcairnia paniculata* (Bromeliaceae) and in many *Clusia* species (Clusiaceae) (Kaul 1977; Males 2018; Barrera Zambrano et al., 2014; respectively). Both sub-mesophyllous and epidermal hydrenchyma tissue in leaves, as well as the central hydrenchyma in stem-succulents provides capacitance to the plant (Chapter 1; Smith et al., 1987; Goldstein et al., 1991). Thus, hydrenchyma acts to buffer the water potential of photosynthetic tissue during dehydration.

Despite the importance of hydrenchyma for the drought response of many succulent taxa, relatively few studies have investigated this adaptation (a google scholar search for the term “Crassulacean acid metabolism” anywhere in the text yields 18500 results, whereas a search for any of “water storage parenchyma”, “hydrenchyma” or “multiple epidermis” gets only 939 hits, 07/07/2019). Investigations into the ecological significance of hydrenchyma are particularly scarce and much of our understanding is anecdotal; based on papers reporting laboratory experiments into the physiology of hydrenchyma (Virzo et al., 1983; Schmidt and Kaiser, 1987; Nowak and Martin, 1997), and the observation that this tissue layer is often found in drought adapted taxa (Ogburn and Edwards, 2010). One study investigated the intraspecific variation in leaf hydrenchyma in the fern *Pyrrhosia lanceolata*, across a 1.8 fold precipitation gradient in Taiwan (Chiang et al., 2013). These authors reported that plants

invest more in hydrenchyma when they experience more days without rainfall per month, during the dry season. However, no work has investigated the ecological importance of interspecific variation in hydrenchyma, and the impact it has on species distribution and climatic niches. Many authors have suggested that hydrenchyma might be an important adaptation for epiphytism, allowing plants to survive the water limited environment of the canopy (Freschi et al., 2010; Silvera and Lasso, 2016). However, unlike the association of CAM with epiphytism, which has been robustly tested for both the Bromeliaceae and Orchidaceae (Crayn et al., 2004; Silvera et al., 2009), the association of hydrenchyma with an epiphytic lifestyle is based on observations of individual species (Katia Silvera, personal communication). Likewise, in clades made up of predominantly terrestrial species, strong evidence exists to show that the evolution of CAM accompanied radiations into drier, hotter environments (Bone et al., 2015). No such studies have been made for hydrenchyma.

The genus *Clusia* exhibits high interspecific variation in hydrenchyma depth (Barrera Zambrano et al., 2014; Chapter 2). As mentioned above, this tissue provides hydraulic capacitance to leaves; a highly specialised role that the large chlorenchyma cells associated with the CAM cycle do not perform (Chapter 2). In addition, the evolution of deeper hydrenchyma tissue in *Clusia* appears to have caused species to be less able to tolerate negative water potentials; meaning species that invest more in this tissue have higher turgor loss points (Chapter 3). Therefore, the hydrenchyma tissue in *Clusia* prevents leaves from experiencing, but also makes them more vulnerable to, low water potentials. Thus, the development of hydrenchyma in *Clusia* can be considered a typical drought avoidance strategy, insofar as it prevents the leaf from experiencing low water potentials. It is important to stress that strategies to avoid and tolerate low water potentials are known to coexist in different species in the same ecosystem (for example *Agave deserti* and *Atriplex polycarpa* in the Sonoran Desert (Smith et al., 1987; Monson and Smith, 1982)), so an adaptation that prevents limits the extent to which leaf water potentials fall will not *a priori* exist more often in arid environments. Nevertheless, the avoidance of negative water potentials conferred by hydrenchyma is typical of semi-arid ecosystems (Ogburn and Edwards, 2010), leading to the hypothesis that, in *Clusia*, hydrenchyma will allow plants to inhabit environments or niches in which water availability is limited.

It is important to consider that plants can experience limited water availability at different temporal scales; i.e. long-term seasonal drought, day-to-day drought and even more acute water limitations within the diel cycle. For example, two locations may receive the same amount of rain over the course of a month, but if this rain falls in small amounts each day it will have a drastically different effect on plants than if it all falls at once in the first few days of the month. This consideration was important for the study of *Pyrrosia lanceolata*, as it was the mean days without water, and not the overall precipitation that determined interspecific variation in hydrenchyma investment in this fern (Chiang et al., 2013). At an even shorter scale, the transpiration from a leaf can sometimes occur at substantially higher rates than the hydraulic conductance, meaning that tissues can momentarily experience water deficits at points in the diel cycle of gas exchange. Even under well-watered conditions, the CAM species *Agave deserti* and *Kalanchoë daigremontiana* can experience very low or even a complete loss of chlorenchyma cell turgor at night due to transpirational water loss (Smith et al., 1987; Smith and Lüttge, 1985). A similar effect was recorded in the C₃ tropical tree species *Pentaclethra macroloba* (Fabaceae) which can momentarily approach zero turgor in the middle of the day (Oberbauer et al., 1987). Therefore, the water deficits that leaves experience can be the consequence of transient changes over the diel cycle as well as long term water shortage associated with aridity.

To explore the ecological significance of hydrenchyma within the genus *Clusia*, species distributions were used in conjunction with remote access climatic data (Hijmans et al., 2005) to acquire information on the climatic niche for the 11 species that have previously been thoroughly phenotyped (Barrera Zambrano et al., 2014; Chapter 2, Chapter 3). These data were used to test if aridity predicted interspecific variation in hydrenchyma depth. These data only resolve broad scale climatic niches (i.e. annual precipitation / precipitation of the driest month) and cannot address the extent to which species experience acute drought at the scale of days or hours. However, this research provides the first attempt to characterise the relevance of interspecific hydrenchyma to species distributions. In addition, CAM, which does not affect a species ability to tolerate low water potentials (Chapter 3; also see Males and Griffiths, 2017), was also investigated to see if this trait is impacted by species climatic niche distribution. Furthermore, field measurements were made for species inhabiting a high-elevation cloud forest in Cerro Jefe (Pierce et al., 2002) and plants living in lowland tropical dry forest in Panama (Slot and Winter, 2017), to compare the hydrenchyma depth of species

in these two environments. By comparing the anatomy of *Clusia* species inhabiting ecosystems with differing water availability, it was possible to test the hypothesis that hydrenchyma is an important functional trait for tolerating severe long-term seasonal drought in the lowland ecosystems.

To complement these analyses, and to develop a better understanding of whether hydrenchyma is important for drought at shorter time scales, a method was developed to dissect the hydrenchyma from the chlorenchyma in *C. alata* (constitutive CAM) and *C. tocuchensis* (obligate C₃). Using this technique, a pilot study was carried out which could move beyond the correlative analyses employed in Chapters 2 and 3, and directly assess the properties of hydrenchyma tissue. Physiological measurements of acid contents, osmolality, and relative water contents (RWC) were made at different points in the day and night. These were compared with 24 hour gas exchange profiles to understand if dynamic changes to stomatal conductance, over the day/night cycle, affect the water relations of hydrenchyma tissue. These data provided the first evidence that hydrenchyma water contents fluctuates with changing stomatal conductance, which suggests that hydrenchyma is able to provide capacitance over short time periods. Alongside the ecological analyses, these data suggest that the predominant ecophysiological role of hydrenchyma, in *Clusia*, might not be tolerance of long-term drought, but rather the maintenance of high water potentials over the diel cycle.

4.2 Materials and Methods

4.2.1 Climatic Niche Determination

Remote-access climatic data was obtained for the 11 well characterised species described in Barrera Zambrano et al., (2014) and in Chapters 2 and 3. Species distributions were acquired from the Global Biodiversity Information Facility (<https://www.gbif.org/en/>), except for *C. tocuchensis* for which no record existed. The distribution of *C. tocuchensis*, which is endemic to Trinidad (Borland et al., 1992), was obtained from geographical records from the ICUN redlist (Johnson et al., 2017). Spatial distributions were used to acquire climatic variables from the WorldClim database, Version 1.4 (<https://www.worldclim.org/>). This work was done by both Alistair Leverett and Kate Ferguson.

4.2.2 Field Collections and Anatomical Measurements

Comparisons were made between species living in a montane cloud forest at Cerro Jefe (1007m above sea level; 0913794N, 07922995W), and lowland tropical dry forest at Gamboa (38m above sea level; 9.120085N, 79.701894W). Species sampled in Cerro Jefe were *C. coclensis*, *C. cretosa*, *C. liesneri*, *C. multiflora* and *C. osseocarpa*. For species sampled from Cerro Jefe, n = 4-5. Species sampled in Gamboa were the C₃ species, *C. quadralanga*, *C. valeroi*, *C. cupulata*, and *C. peninsulae*, *C. fructinogusta*; the C₃-CAM intermediate species, *C. pratensis*, *C. minor*, *C. uvitana*; and the constitutive CAM species *C. rosea*. For species sampled from Gamboa, n = 2-4, except for *C. fructinogusta*, for which only one individual was available. The photosynthetic phenotype of these species was determined according to Holtum et al., (2004), and confirmed in this study by measuring titratable acidity (see below). Both environments experience a dry season between the months of January and March, which is when all sampling was done. The dry season in the cloud forest is characterised by higher mist, humidity and precipitation as well as lower temperatures (Pierce et al., 2002), as compared to Gamboa. In contrast, the dry season in the lowland tropical dry forest experiences very high temperatures, of around 35 °C, and strong winds.

To assess the depth of hydrenchyma in species living in the two sites, branches were cut and placed in plastic bags and returned to the laboratory at the Earl S. Tupper centre,

Panama City, Panama. The third leaf from the apex of each branch was then cut, underwater, and the cut petiole remained submerged in water to incubate. Rehydrating leaves were then placed in a box overnight, which was filled with damp tissues to increase humidity. The following day, leaves were hand sectioned, with a razor blade, and sections were imaged with a fluorescent microscope (Nikon Eclipse 600 Microscope with a Nikon Dri-1 camera). Hydrenchyma depth was measured using ImageJ (NIH).

The photosynthetic physiology of each species was characterised using the dawn/dusk titratable acidity presented in Chapter 3. In addition to this, the dawn/dusk acid titratable acidity was measured for 5 species only found in the cloud forest in Cerro Jefe, using the same methodology as described in Chapter 3.

4.2.3 Laboratory Plant Growth Conditions

Clusia tocuchensis and *C. alata* plants, used for dissections, were grown in 3-5 litre pots, containing a mix of loam-based compost (John Innes No. 2, Sinclair Horticulture Ltd, Lincoln, UK) and sand (3:1 v/v). At least three weeks prior to experiments, potted plants were placed inside a plant growth chamber (SANYO Fitotron) for 24 hours (12 hour light period, day/night temp 25/19 °C) to allow plants to acclimate. Plants received approx. 500 $\mu\text{M m}^{-2} \text{s}^{-1}$ PFD at leaf height. 2 days prior to any experiment, pots were heavily watered and left in trays containing a thin layer of water, to prevent any soil dehydration.

4.2.4 Dissections and Anatomical Images

To dissect the hydrenchyma from the chlorenchyma, a rectangle of leaf lamina, approx. 5 mm by 50 mm, was cut half way along the proximal-distal axis of the leaf, taking care to avoid leaf margins or midribs. A razor blade was used to make a small incision between the hydrenchyma and chlorenchyma, which can be recognised as the former is white and the latter green. Following this, the flat side of the razor was inserted into the incision and the two tissue layers were separated. To ensure that the dissection method worked, each tissue layer was hand-sectioned and imaged under a Leitz Diaplan microscope, using a GXCAM HiChrome-S camera (GT Vision Ltd).

4.2.5 Titratable Acidity and Osmolality

Leaves were harvested 15 minutes before dawn and dusk for each species. A 2-3 cm² rectangle of leaf lamina was cut, midway along the proximal-distal axis of the leaf. The margin of this leaf rectangle used was traced on to a piece of paper, which was then scanned using a flatbed scanner, to determine area using ImageJ (NIH). Following this, the hydrenchyma and chlorenchyma layers were dissected using a flat razor blade, and these tissue layers were immediately frozen in liquid nitrogen. Leaf tissue was then flash frozen in liquid nitrogen and crushed using a tissue lyser (Quiagen). Samples were then incubated in 80 % methanol (Fisher) for 45 minutes and centrifuged at 142 G for 10 minutes. Following this, the supernatant was titrated against 0.5 Mol NaOH (Sigma), using phenolphthalein (Sigma) as an indicator, to determine the concentration of H⁺ ions.

Osmolality was measured for the same dawn-dusk samples using an Osmomat 030 cryoscopic osmometer (Gonotec). Lysed leaf tissue was vortexed in 200 µL deionised water, and 20 µL of this extract was placed into the osmometer to determine osmolality (Osmol kg⁻¹). The osmotic potential was calculated according to the van't Hoff equation.

4.2.6 Gas Exchange

CO₂ assimilation and stomatal conductance to H₂O were measured over a 24 hour period using a LI-6400XT infrared gas analyser (LiCOR, Lincoln, NE, USA). Leaves were sealed into a leaf chamber fluorometer cuvette, set to track external light conditions and humidity conditions, and data was logged every 15 minutes. Three biological replicates were made for each species, and one representative graph is included to show photosynthesis and stomatal conductance for each species.

4.2.7 Diel Changes in Relative Water Content

To measure diel changes to relative water constant in each species, leaves were harvested every 4 hours over a 24 hour period. Leaves were cut and tissue layers dissected immediately. Each tissue layer was weighed to the nearest milligram and then placed to soak in deionised water for 8 hours to rehydrate. Following this incubation period, the tissue was

weighed again and finally the tissue was dried for 2 days at 75 °C and weighed to calculate the DM. The RWC was calculated according to the equation:

Equation 4.1

$$RWC = \frac{FM_t - DM}{FM_{FT} - DM} \times 100$$

Where FM_t is the fresh mass at time, t . Unfortunately, the chlorenchyma tissue often sunk during rehydration, which is likely due to water infiltrating internal air spaces (Arndt et al., 2015). Consequently, it was deemed that there was no objective way to assess the true FM_{FT} value for chlorenchyma tissue, so this data was not reported.

4.2.8 Measurement of Saturated Water Content

Leaves were rehydrated prior to weighing, in the same way as in Chapters 2 and 3. Briefly, leaves were cut underwater from branches, still attached to potted plants, to prevent embolisms. Leaves were incubated in deionised water, so that the cut petiole was fully submerged, and the lamina was not. Incubating leaves were sealed inside clear plastic bags, into which water was sprayed to maximise the humidity. Bagged leaves were then placed inside a plant growth chamber (SANYO Fitotron) for 24 hour (12 hour light period, day/night temp 25/19 °C) to allow leaves to rehydrate. Once leaves were rehydrated, leaf lamina was dissected, using the method outlined above, and each tissue layer was weighed to the nearest milligram. Dissected material was then dried in an oven at 75 °C for two days and weighed to determine dry mass. Saturated water content (SWC) was calculated using the equation:

Equation 4.2

$$SWC = \frac{FM_{FT} - DM}{DM}$$

Where FM_{FT} is the fresh mass at full turgor, and DM is the dry mass of the tissue.

4.2.9 Statistics and Graphs

All statistics were done using R version 3.5.2 (R core team, 2008) and graphs were made using the package “ggplot2”.

4.3 Results

4.3.1 Aridity Predicts the Occurrence of Crassulacean Acid Metabolism (CAM) but not of Hydrenchyma in *Clusia*

Species distributions were cross referenced with remote access climatic data for the 11 well characterised species from the *Clusia* collection in Newcastle. This approach estimated the climatic niche of each species. No correlation was found between the hydrenchyma depths found in the different *Clusia* species and the mean annual precipitation or the precipitation of the driest month (Fig. 4.1a, 4.1b). Taken together, these data show that long-term aridity, over the course of a year or month, does not predict the existence of hydrenchyma depth in *Clusia*.

A significant correlation was found between the mean annual precipitation and the percentage of photosynthesis done at night in well-watered conditions in the different *Clusia* species (i.e. the extent to which species can constitutively engage in CAM) (Fig. 4.1c). Furthermore, a significant correlation was found between the precipitation of the driest month and the percentage of photosynthesis done in drought-treated plants of the different species (i.e. the extent to which CAM can be employed as a drought-response strategy) (Fig. 4.1d). Taken together these data show that, in *Clusia*, constitutive CAM is an adaptation to low annual precipitation and both facultative and constitutive CAM are adaptations to seasonal aridity.

4.3.2 Species in the Cloud Forests in Panama are Characterised by Deep Hydrenchyma

The effect of variation in hydrenchyma depth on species distributions was also investigated by measuring the depth of this water storage tissue in different environments in Panama. As different species were present in each location (Table 4.1), this approach did not have sufficient resolution to distinguish inter- and intraspecific variation in hydrenchyma depth. Leaf material was collected from plants living in either a seasonally dry lowland ecosystem in Gamboa, or from a more humid, high elevation cloud forest ecosystem in Cerro Jefe. Comparing the mean hydrenchyma depth of all species in the cloud forest with those living in lowland forest found that species in the cloud forest had deeper hydrenchyma (Fig.

4.2, Fig. 4.3). The dry season dawn-dusk titratable acidity values were $< 8 \mu\text{mol g}^{-1}$ fresh weight, for all species living in the cloud forest, indicating that they are not able to engage in CAM photosynthesis (Table 4.1), whereas dawn-dusk titratable acidity measurements recorded for species living in the lowland ecosystem (from Chapter 3) showed a variety of photosynthetic physiologies (Table 4.1). Therefore, the presence of CAM is more common to the lowland ecosystem, whereas the presence of deep hydrenchyma tissue is not. Taken together, this provides further suggestive evidence that, unlike CAM, hydrenchyma might not be primarily acting as an adaptation to annual or seasonal aridity.

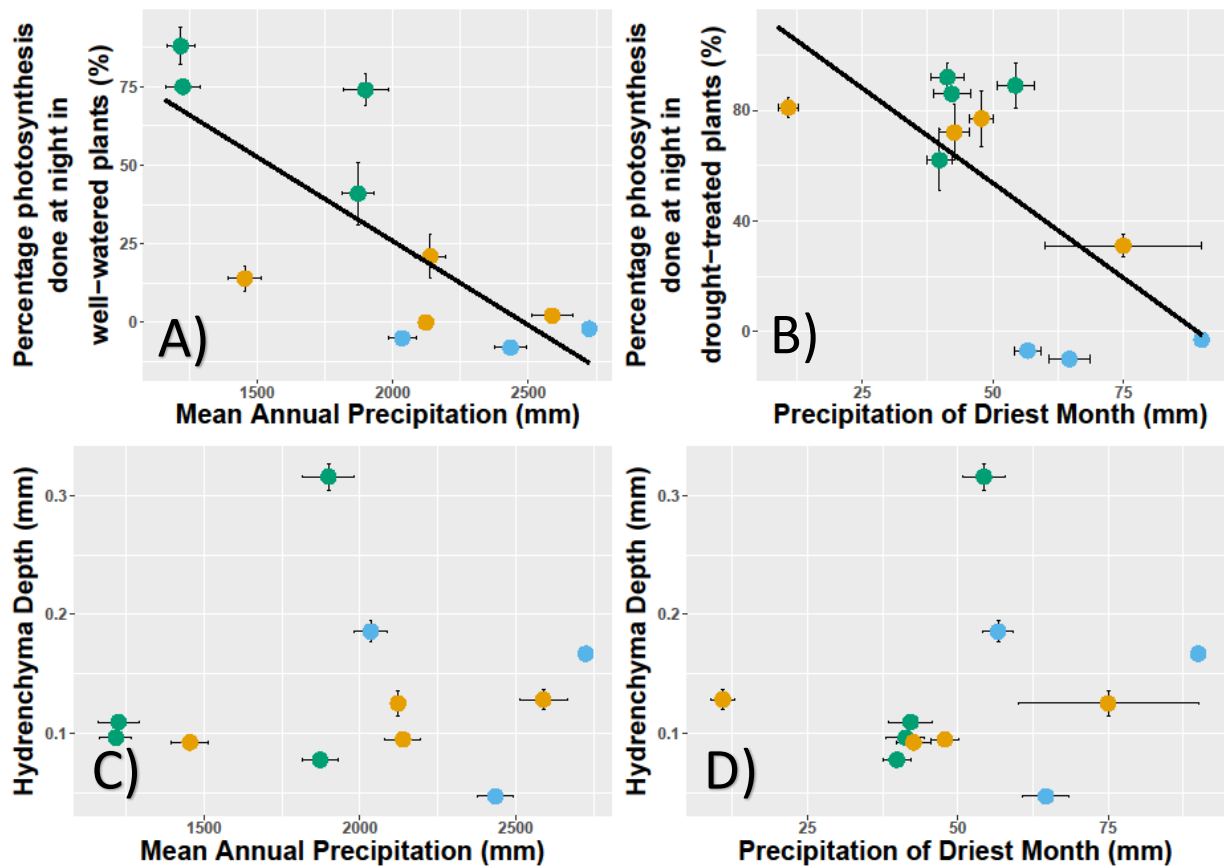


Fig. 4.1) Aridity does not predict the occurrence of hydrenchyma, but it does predict the occurrence of CAM in *Clusia*. Interspecific variation in hydrenchyma depth across 11 species with different photosynthetic physiotypes did not correlate with either (C) the mean annual precipitation (Spearman's rank correlation; $\rho = 0.200$, $p = 0.558$), nor with (D) the precipitation of the driest month (Spearman's rank correlation; $\rho = 0.264$, $p = 0.435$). However, (A) the percentage of total photosynthesis done at night, under well-watered conditions, in these 11 *Clusia* species, showed a significant negative correlation with the mean annual precipitation (Spearman's rank correlation; $\rho = -0.745$, $p = 0.012$). In addition, (B) interspecific variation in the percentage of photosynthesis done at night, under drought-treated conditions, showed a significant negative correlation with the precipitation of the driest month (Spearman's rank correlation; $\rho = -0.627$, $p = 0.044$). Taken together, these data show that investment in hydrenchyma does not predict species climatic niche, but both constitutive and facultative CAM predict species ability to tolerate long-term aridity. Error bars represent \pm one SD.

Table 4.1) Dawn – Dusk ΔH^+ values for 5 species sampled in the montane cloud forest, Cerro Jefe, and 9 species sampled in lowland tropical dry forest, Gamboa, Panama.

Species	ΔH^+ ($\mu\text{mol g}^{-1}$ Fresh weight)	Standard Deviation of ΔH^+	Number of replicates	Photosynthetic Physiology	Location
<i>C. coclensis</i>	7.48	34.92	5	Obligate C ₃	Cerro Jefe
<i>C. cretosa</i>	-16.45	17.05	5	Obligate C ₃	Cerro Jefe
<i>C. liesneri</i>	-27.41	63.81	4	Obligate C ₃	Cerro Jefe
<i>C. multiflora</i>	-11.93	109.89	5	Obligate C ₃	Cerro Jefe
<i>C. osseocarpa</i>	-33.06	121.87	5	Obligate C ₃	Cerro Jefe
<i>C. cupulata</i>	22.08	51.05	2	Obligate C ₃	Gamboa
<i>C. valeroi</i>	-20.99	112.96	2	Obligate C ₃	Gamboa
<i>C. quadralanga</i>	141.41	112.49	2	Obligate C ₃	Gamboa
<i>C. peninsulae</i>	51.45	124.66	2	Obligate C ₃	Gamboa
<i>C. fructinogusta</i>	69.70	na	1	Obligate C ₃	Gamboa
<i>C. pratensis</i>	329.08	46.73	4	Facultative CAM	Gamboa
<i>C. minor</i>	414.93	15.12	3	Facultative CAM	Gamboa
<i>C. uvitana</i>	432.98	51.64	3	Facultative CAM	Gamboa
<i>C. rosea</i>	281.41	96.73	4	Constitutive CAM	Gamboa

4.3.3 Validation of Dissection Method

A method was developed for dissecting the adaxial hydrenchyma from the abaxial chlorenchyma in *Clusia* leaves. To develop this method, the 11 well characterised species from the Newcastle *Clusia* collection were ranked, based on the depth of their hydrenchyma tissue (Fig. 4.4). The constitutive CAM species, *C. alata* has the deepest hydrenchyma tissue, and was therefore chosen for downstream, analyses. The C₃ species with the deepest hydrenchyma was *C. multiflora*, however leaves of this species frequently have curves and kinks in the lamina, which make dissections more difficult. For this reason, the C₃ species with similarly deep hydrenchyma, *C. tocuchensis*, was chosen for further analysis.

To validate the dissection method, hydrenchyma tissue was imaged, after dissection, to ensure that no material from the palisade was attached. Post-dissection, the hydrenchyma was hand-sectioned, and the images showed no sign of palisade tissue (Fig. 4.5a). In addition, the abaxial surface of the hydrenchyma layer was imaged. This showed many large, round cells of the hydrenchyma, but no palisade cells were present (Fig. 4.5b). Together, these results confirmed that the dissection method was separating the two tissue layers and was a valid way to experimentally analyse the physiology of hydrenchyma tissue.

4.3.4 Titratable Acidity

To test for the existence of CAM in each tissue layer, titratable acidity was measured at dawn and dusk in both the hydrenchyma and the chlorenchyma. In the constitutive CAM species, *C. alata*, a significantly higher acid content was present in the chlorenchyma at dawn compared to dusk (Fig. 4.6). This was not true in the hydrenchyma, which did not exhibit a significant change in acid content between dawn and dusk. In the obligate C₃ species, *C. tocuchensis*, there was no significant difference in the acid content of the chlorenchyma between dawn and dusk, nor was there a significant difference between the acid content in the hydrenchyma at dawn and dusk (Fig. 4.7). The same conclusions could be made from statistical analyses when acid content is standardised on the basis of fresh weight, dry weight or per cm² leaf area basis (Fig. 4.6, Fig. 4.7). Taken together, these data show that CAM occurs only in the chlorenchyma tissue of *Clusia*.

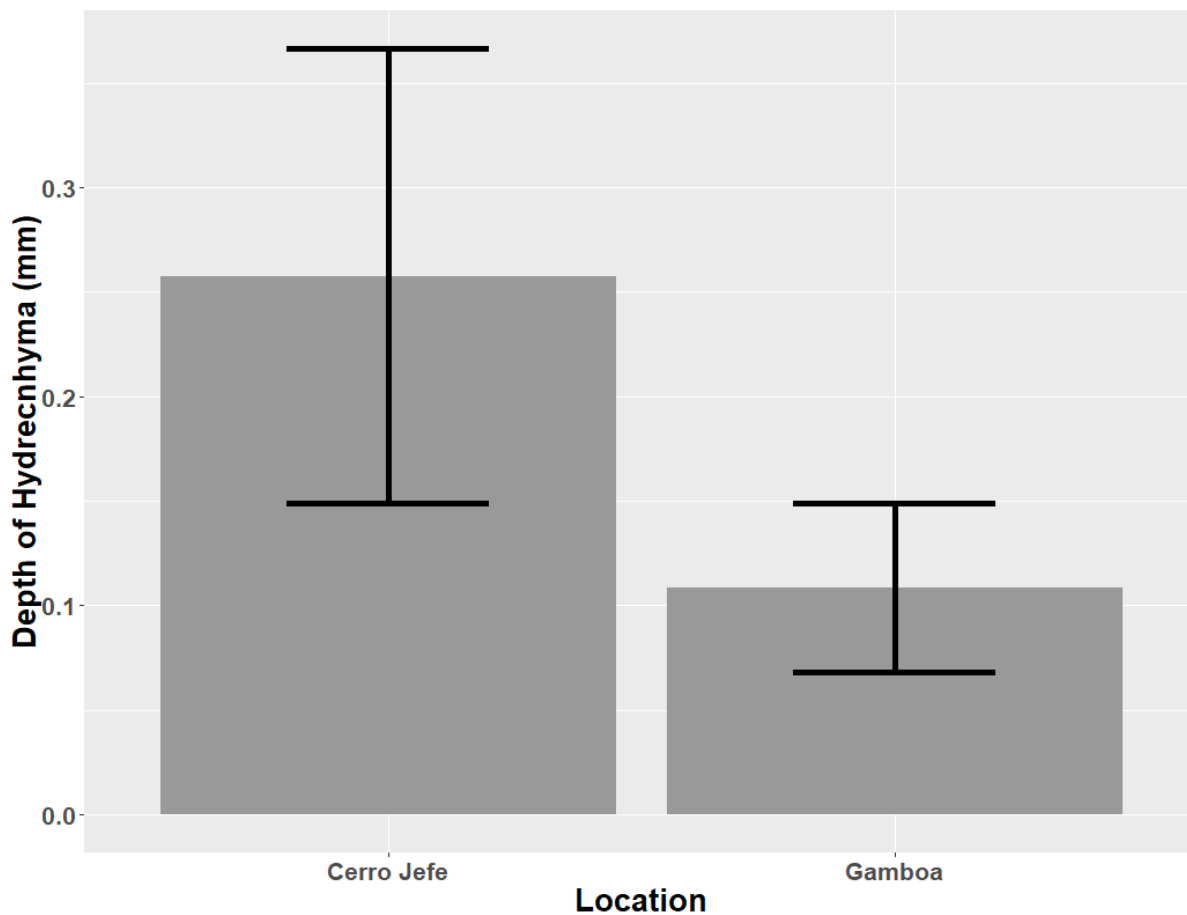


Fig. 4.2) *Clusia* Species in cloud forest ecosystem have significantly deeper hydrenchyma tissue to those living in lowland seasonally dry forest in Panama ($p = 0.035$, Welch's t-test). Bars represent the mean hydrenchyma depth for species at each location, and error bars represent \pm one SD of mean hydrenchyma depth for each site.

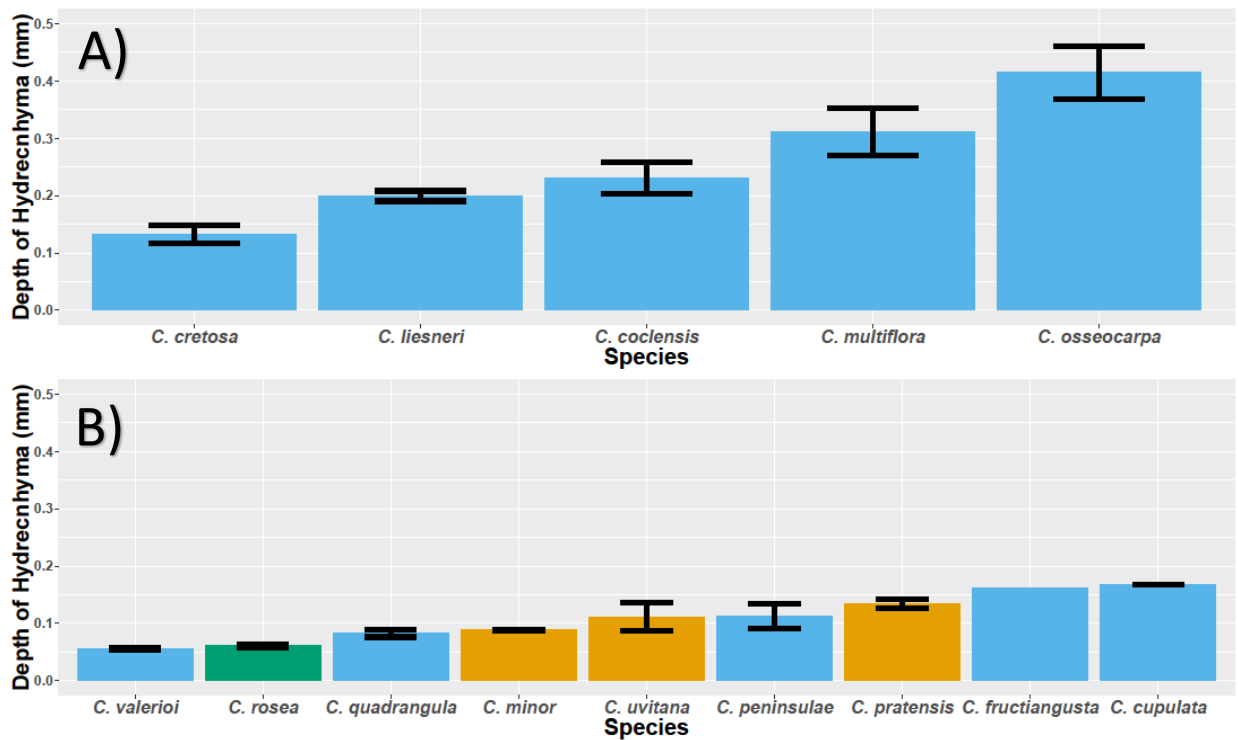


Fig. 4.3) Species in cloud forest ecosystem have deeper hydrenchyma tissue than those living in lowland seasonally dry forest in Panama. The 5 C_3 species found in (A) Cerro Jefe montane ecosystem all had deeper hydrenchyma tissue than any of the 9 species growing in (B) the lowland tropical dry forest environment in Gamboa. Error bars represent \pm one SD of the mean for each species. No error bar is present for *C. fructiangusta* because only one individual was available for sampling.

4.3.5 The Osmotic Potential Remains Stable and Low in Hydrenchyma Tissue

The osmotic potential was measured at dawn and dusk on the same leaves that were analysed for titratable acidity analysis. In *C. alata*, the chlorenchyma tissue showed a significantly higher osmotic potential at dawn than at dusk (Fig. 4.8). In *C. alata* there was no significant difference between the osmotic potential of the hydrenchyma at dawn and dusk. However, the osmotic potential of the hydrenchyma was significantly lower than that of the chlorenchyma at both times of the day (Fig. 4.8). In *C. tocuchensis*, there was no significant difference between the osmotic potential of the chlorenchyma at dawn and at dusk or of the hydrenchyma at dawn and at dusk (Fig. 4.9). However, in this C₃ species there was a significant difference between the osmotic potential of the hydrenchyma and the chlorenchyma (Fig. 4.9). Taken together, these data indicate that the hydrenchyma can maintain a stable osmotic potential, which is lower than that observed in the chlorenchyma and is independent of the photosynthetic mode of the plant.

4.3.6 The Water Content of the Hydrenchyma Mirrors Gas Exchange of a C₃ and CAM Species

The diel gas exchange profiles of *C. tocuchensis* and *C. alata* confirmed that they are C₃ and CAM, respectively, under well-watered conditions. *Clusia tocuchensis* maintains a net positive CO₂ assimilation during the day and a slight net CO₂ efflux at night. In contrast, *C. alata* maintains a very slight net CO₂ efflux in the day and a net positive CO₂ assimilation rate at night (Fig. 4.10). No existence of phases 2 and 4 of the CAM cycle were found in the photosynthetic gas exchange profiles of *C. alata*. The diel stomatal conductance of *C. tocuchensis* and *C. alata* were qualitatively very similar to those for photosynthetic assimilation (Fig. 4.11). In *C. tocuchensis*, stomata were open during the day but closed towards the end of the light period and remained closed over the night. In contrast, stomatal conductance in *C. alata* momentarily increased at the start of the photoperiod but fell to zero during the day. In the night stomata opened in *C. alata*, indicative of CAM photosynthesis.

To investigate if changes in hydrenchyma water stores occurred over the diel cycle and to establish if this reflected stomatal conductance of these species, the RWC was measured

for this tissue every 4 hours, over a 24-hour period, in well-watered plants. In *C. tocuchensis* the hydrenchyma was least hydrated throughout the day, while stomatal conductance was highest (Fig. 4.11, Fig. 4.12). RWC, then increased between the pre-dusk measurement and the first measurement at night, coinciding with stomatal closure. After this, the RWC remained high for the rest of the night, as stomata remained closed. In *C. alata*, the hydrenchyma RWC was low in the morning, just after the momentary morning increase in stomatal conductance (Fig. 4.11, Fig. 4.12). The RWC then increased by the afternoon and remained high into the evening, coinciding with a period of stomatal closure. RWC then fell in the first 4 hours of the night and remained low for the remainder of the night period, during which this CAM species opened stomata. Taken together, these data show that the hydrenchyma mirrored the stomatal conductance in the leaf for both C₃ and CAM species of *Clusia*, such that periods of high stomatal conductance were accompanied by water loss from the hydrenchyma.

Unfortunately, it was not possible to confidently measure the RWC of the chlorenchyma tissue in *Clusia*. Chlorenchyma tissue has high internal air space (IAS) in *Clusia*, compared to other CAM plants and it was believed that this space was filling with water when tissue was incubated in distilled water to rehydrate (Smith and Heuer, 1981; Barrera Zambrano et al., 2014; Arndt et al., 2015). This was suggested by sinking of the chlorenchyma tissue during the rehydration process. As there was no way to objectively determine the time at which the tissue had reached the true value of 'full hydration', these data were not collected. In contrast, the hydrenchyma tissue would sink at the beginning of the rehydration process, as this tissue has very little IAS. Consequently, data on the RWC of hydrenchyma tissue could be measured.

4.3.7 Saturated Water Content (SWC) is Higher in the Hydrenchyma Than the Chlorenchyma

Based on correlative investigations (Chapter 2), it was predicted that SWC would be higher in the hydrenchyma than the chlorenchyma. To directly test this, the hydrenchyma of *C. alata* and *C. tocuchensis* was dissected from the chlorenchyma and SWC was measured in each layer. In both species the hydrenchyma tissue had a significantly higher SWC than the chlorenchyma (Fig. 3.13). Taken together, these data confirm that hydrenchyma provide higher SWC to the leaf.

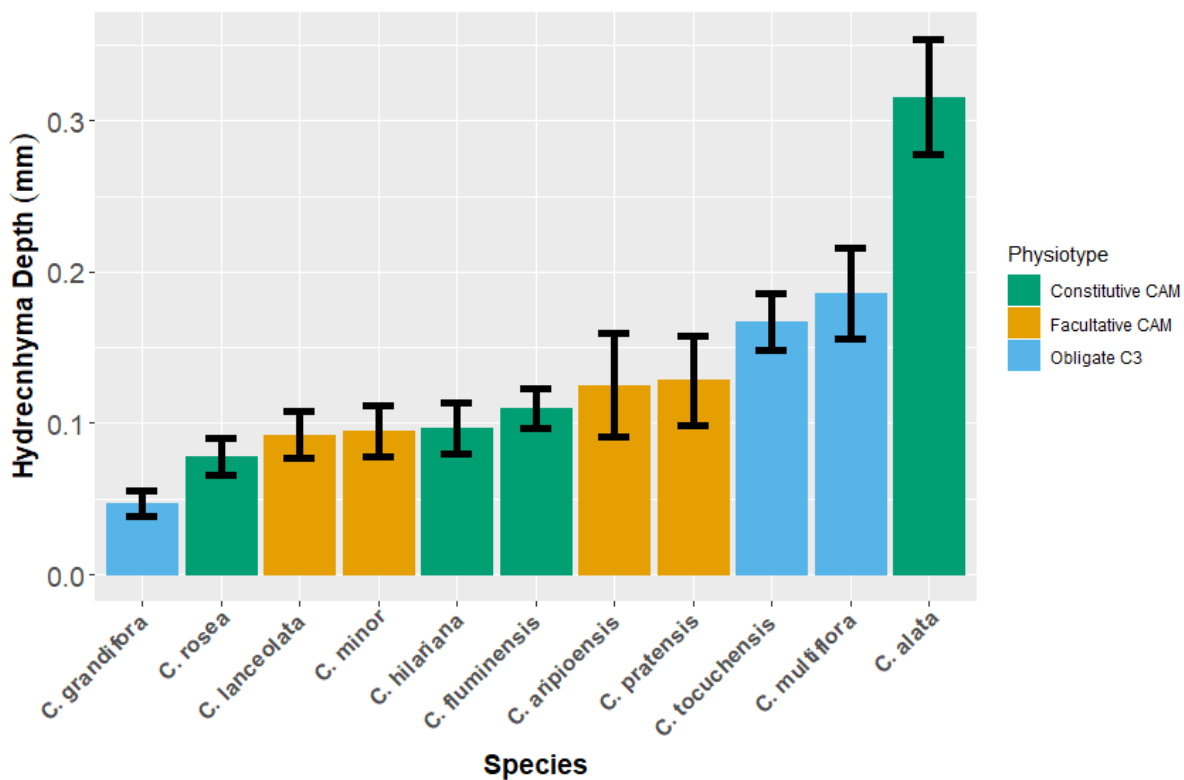


Fig. 4.4) *Clusia alata* and *C. tocuchensis* have deep hydrenchyma tissue. Of the 11, well-characterised species from chapter 2, *C. alata* has the deepest hydrenchyma tissue. *Clusia tocuchensis* has the third deepest hydrenchyma tissue, slightly lower than *C. multiflora*. *Clusia tocuchensis* was chosen for physiological analysis because it has flatter, smoother leaves, making dissections of the adaxial hydrenchyma from the abaxial chlorenchyma possible. Error bars represent \pm one standard deviation.

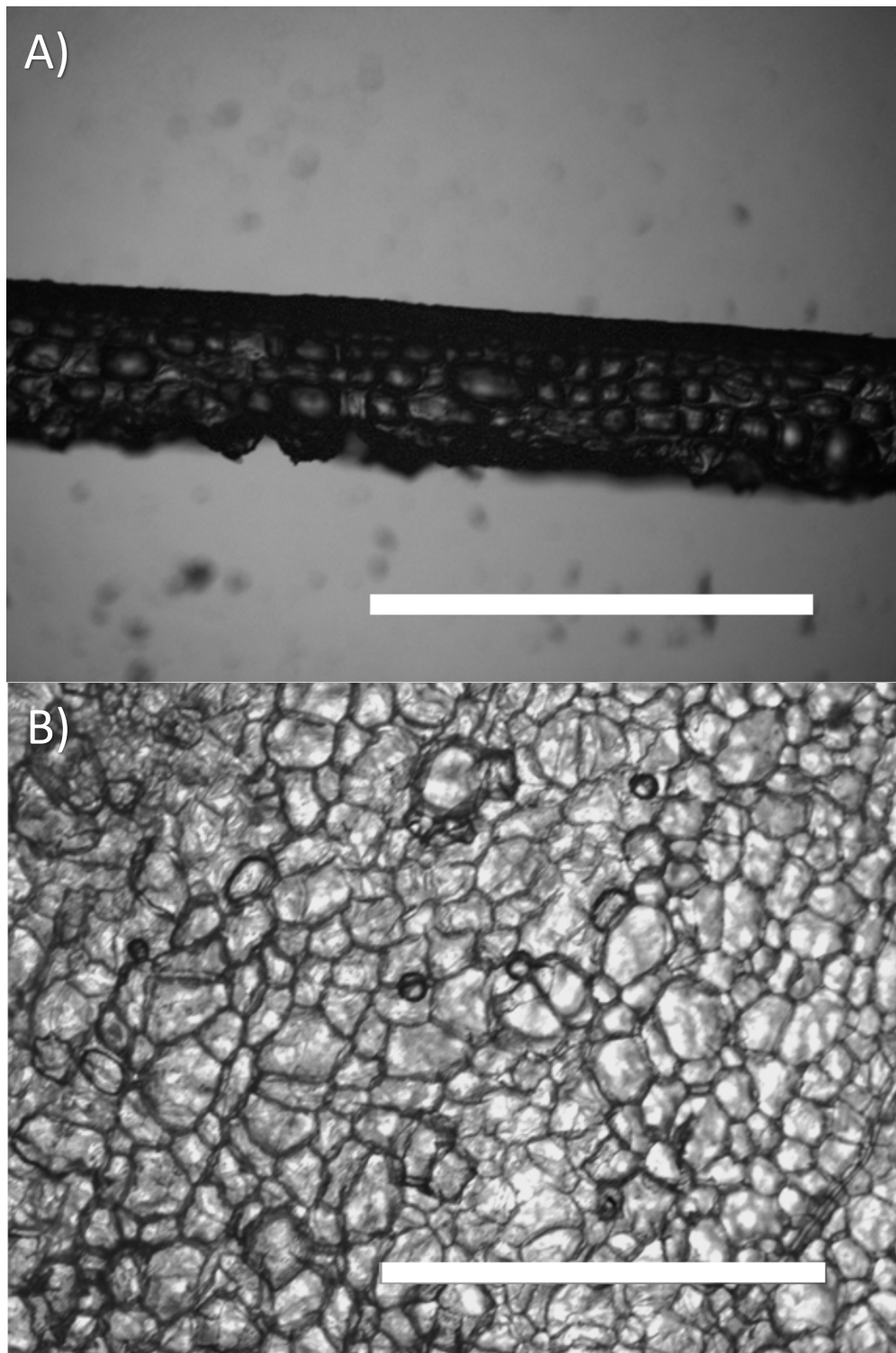


Fig. 4.5) The method for dissecting the hydrenchyma successfully separates this tissue from the palisade. (A) Sections of *C. alata* hydrenchyma were hand-cut, after the dissection of this tissue from the chlorenchyma, and imaged under a light microscope. (B) In addition the abaxial view of the hydrenchyma tissue, post-dissection, was imaged, displaying the bulbous cells. Both images are free of palisade mesophyll cells. Scale bars = 1 mm.

4.4 Discussion

4.4.1 Aridity does not Determine Interspecific Variability in Hydrenchyma Depth in *Clusia*

The data presented in this study call into question the importance of hydrenchyma as an adaptation to long-term aridity. Remote access data, used to estimate species climatic niches, found no relationship between the mean annual precipitation or precipitation of the driest month with the depth of hydrenchyma in the *Clusia* species examined (Fig. 4.1a, 4.1b). It is worth noting that the use of remote access data in this study does not have enough resolution to detect short term drought events or fluctuations in VPD that occur over the time scale of days or even hours. Shorter term drought events were important for the study of *Pyrrosia lanceolata*, as it was the mean days without water, and not the overall precipitation that determined interspecific variation in hydrenchyma depth in this fern (Chiang et al., 2013). Therefore, it is important not to overstate the findings from these analyses; interspecies variation in hydrenchyma depth does not appear to be driven by long-term drought at the scale of a year or a month, but shorter-term drought events might contribute more.

In addition to remote access distribution data, field measurements in Panama found that *Clusia* species inhabiting the high elevation cloud forest in Cerro Jefe all had deeper hydrenchyma than those living in the lowland dry tropical forest environment in Gamboa. The sampling effort from Gamboa is somewhat artificial, as free-living trees have been taken from different sites and planted at the Santa Cruz Experimental Research Facility, Gamboa. However, the species from this site are naturally found in lowland seasonally dry forests (Holtum et al., 2004), and species from the cloud forests cannot survive the extensive dry season in Gamboa (Klaus Winter, personal communication). Therefore, the decision to compare species in the lowland tropical dry forest in Gamboa to those in the cloud forests at Cerro Jefe is justified as these two environments were populated by species that naturally occur in ecosystems with contrasting environmental conditions.

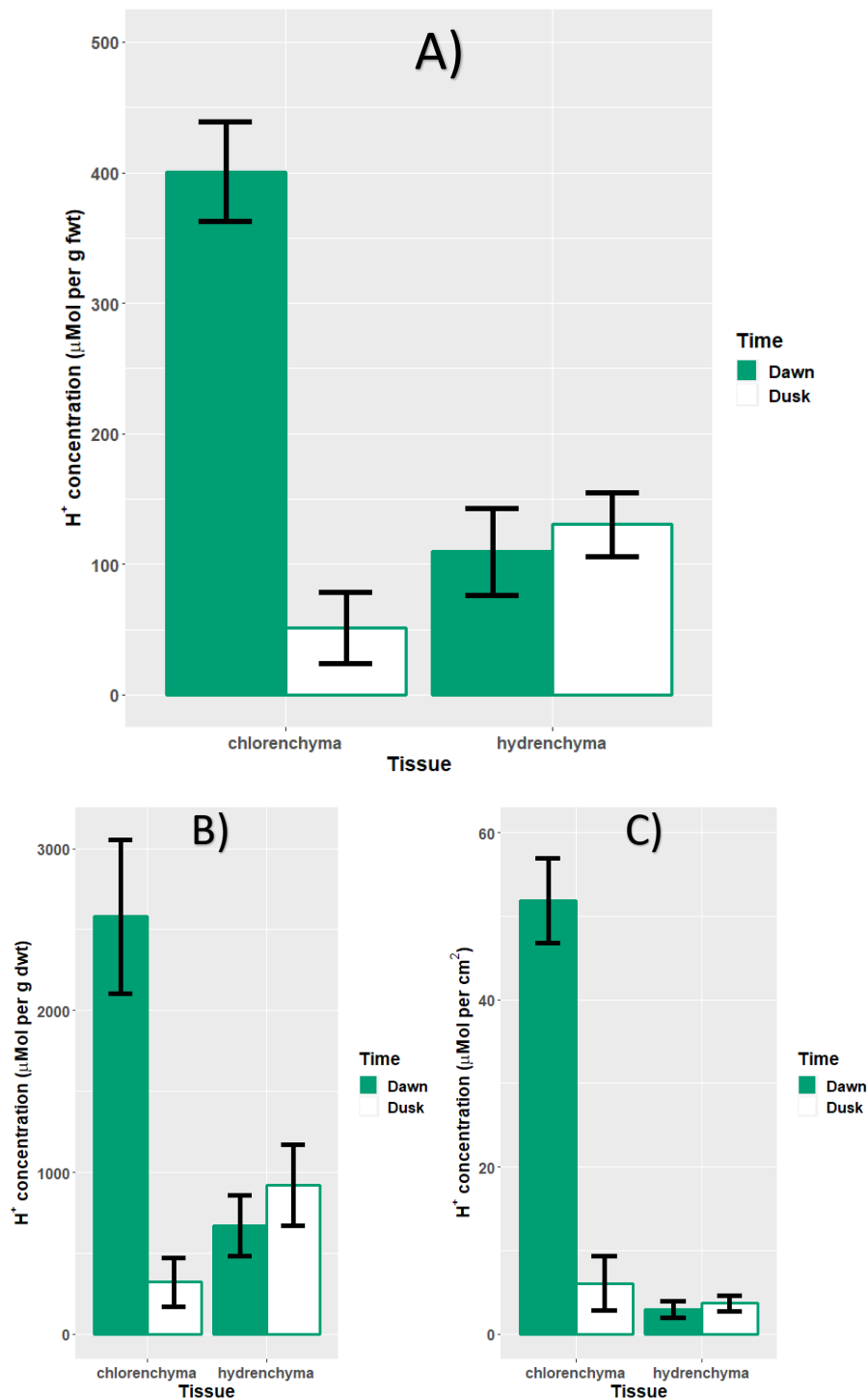


Fig. 4.6) Crassulacean acid metabolism occurs in the chlorenchyma and not the hydrenchyma in *C. alata*. Measurements of titratable acidity shows that the chlorenchyma of *C. alata* has significantly higher H⁺ concentration at dawn than at dusk, and that this is not true for the hydrenchyma. This is true when H⁺ concentration is expressed per g fresh weight (A: $p < 0.001$ for chlorenchyma, $p = 0.917$ for hydrenchyma), as well as H⁺ concentration per g dry weight (B: $p = 0.002$ for chlorenchyma, $p = 0.996$ for hydrenchyma) and H⁺ concentration per cm² leaf area (C: $p < 0.001$ for chlorenchyma, $p = 0.941$ for hydrenchyma). All statistics are the result of one tailed, paired t-tests, and all error bars represent \pm one standard deviation.

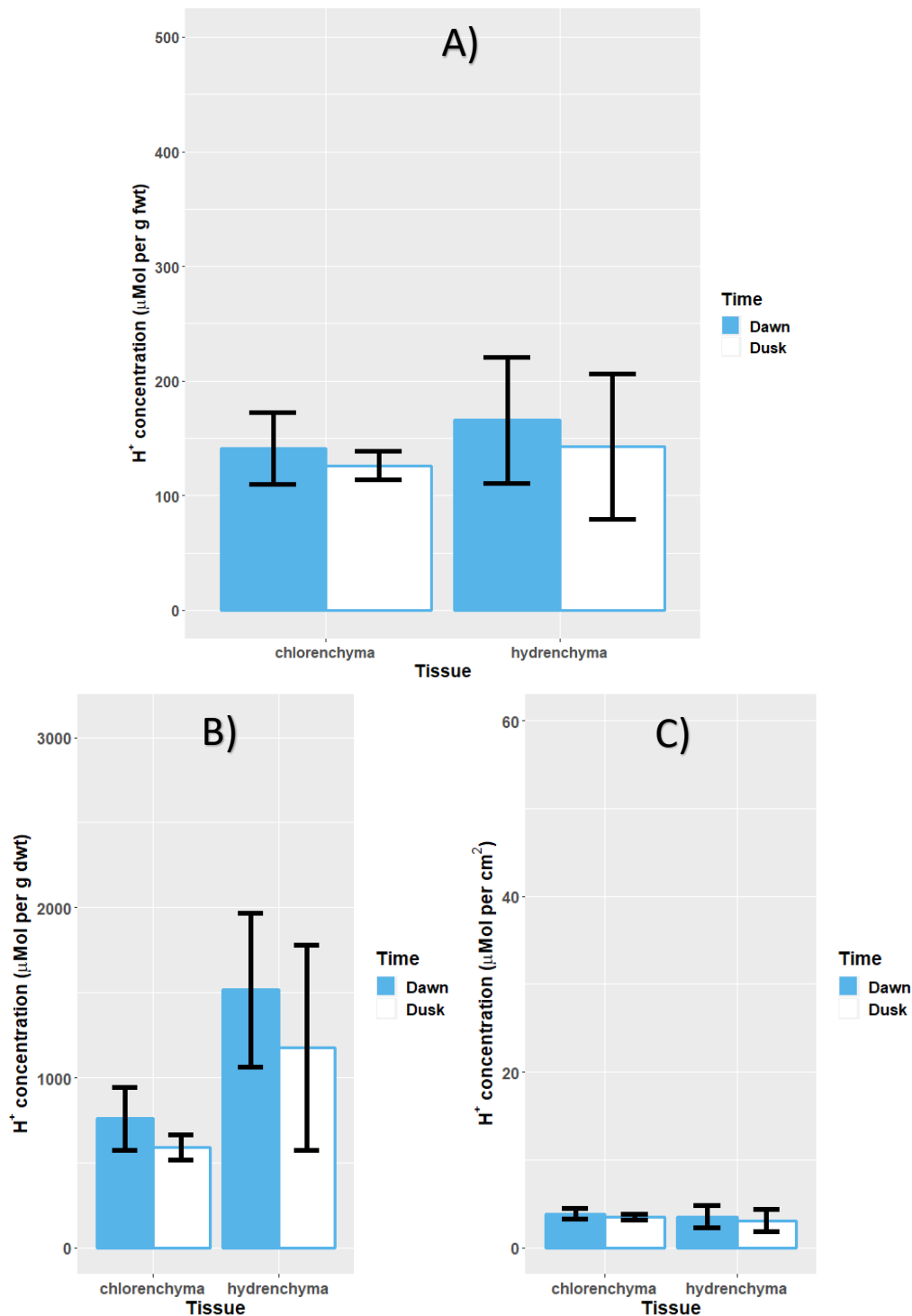


Fig. 4.7) Crassulacean acid metabolism does not occur in the chlorenchyma or the hydrenchyma in *C. tocuchensis*. Measurements of titratable acidity shows that the chlorenchyma of *C. tocuchensis* does not have significantly higher H⁺ concentration at dawn than at dusk, and that this is also true for the hydrenchyma. This is true when H⁺ concentration is expressed per g fresh weight (A: p = 0.136 for chlorenchyma, p = 0.142 for hydrenchyma), as well as H⁺ concentration per g dry weight (B: p = 0.097 for chlorenchyma, p = 0.1881 for hydrenchyma) and H⁺ concentration per cm² leaf area (C: p = 0.118 for chlorenchyma, p = 0.251 for hydrenchyma). All statistics are the result of one tailed, paired t-tests, and all error bars represent ± one standard deviation.

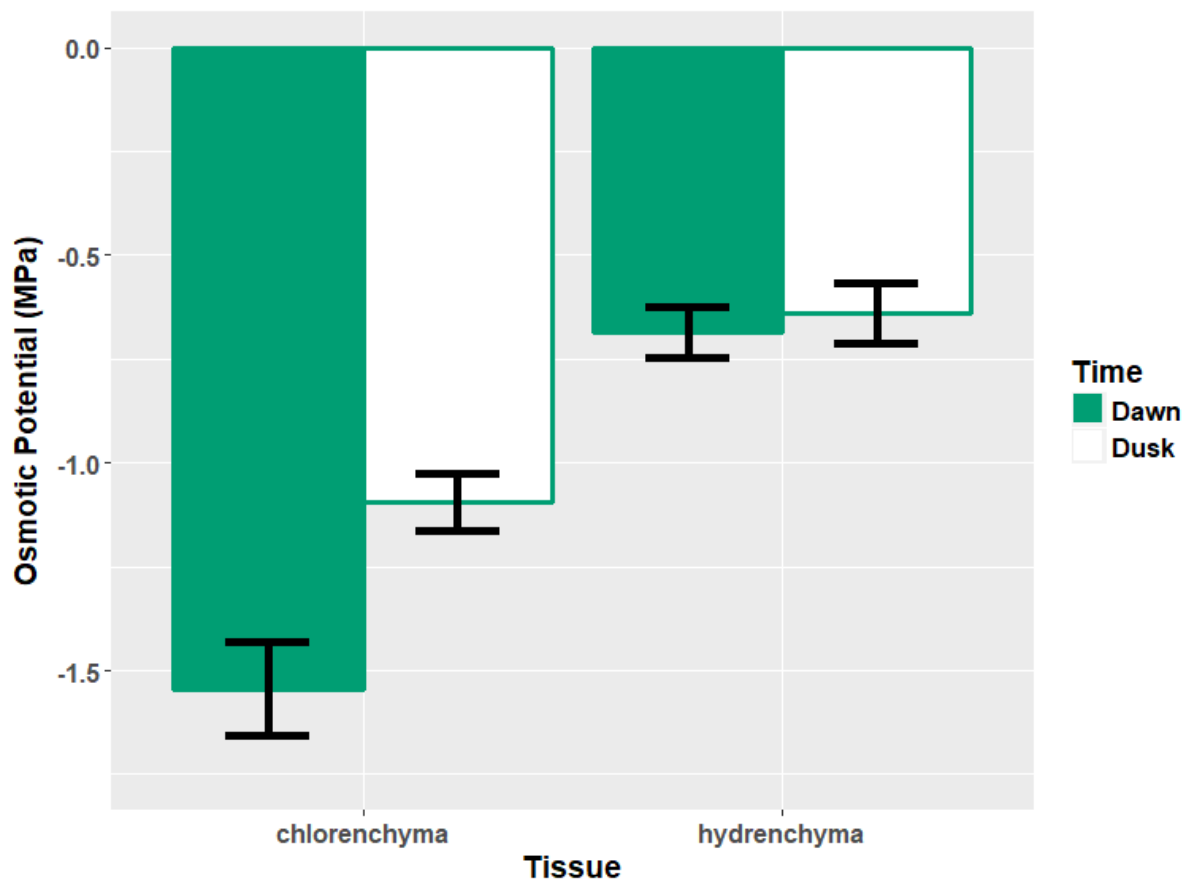


Fig. 4.8) *Clusia alata* hydrenchyma maintains a stable osmotic potential which is higher than chlorenchyma. Osmotic potential is lower at dawn than at dusk in the chlorenchyma tissue, but this is not true for the hydrenchyma tissue. An ANOVA showed that there is a significant difference between each measurement of osmotic potential ($p < 0.001$) and Post-Hoc Tukey-Kramer analysis found 3 significantly different groups, one represented by the chlorenchyma at dawn, another represented by the chlorenchyma at dusk and a third represented by the hydrenchyma at both dawn and dusk. Error bars represent \pm one standard deviation

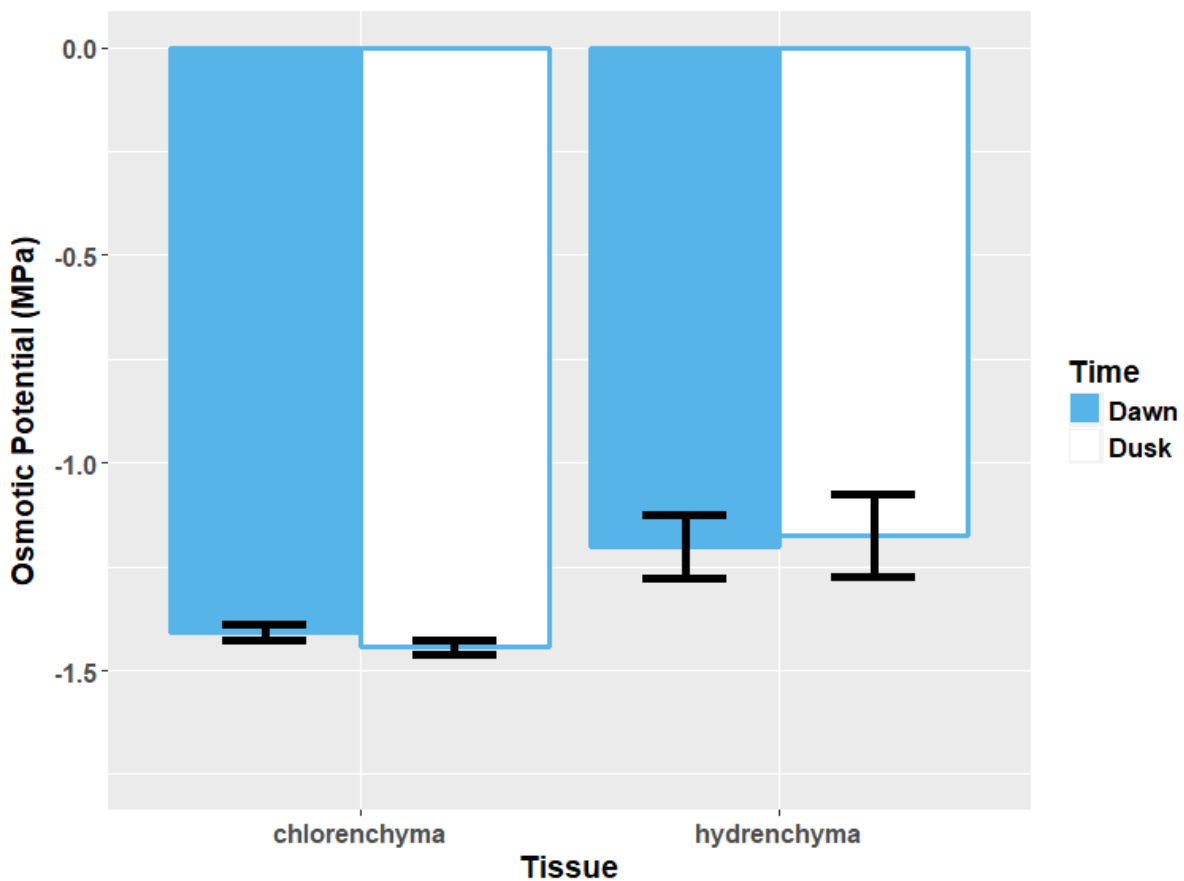


Fig. 4.9) *Clusia tocuchensis* hydrenchyma maintains a stable osmotic potential which is higher than chlorenchyma. Osmotic potential is not lower at dawn than at dusk in the chlorenchyma tissue, nor is it higher at dusk than at dawn in the hydrenchyma tissue. An ANOVA showed that there is a significant difference between each measurement of osmotic potential ($p < 0.001$) and Post-Hoc Tukey-Kramer analysis found 2 significantly different groups, one represented by the chlorenchyma at both dawn and dusk, and another represented by the hydrenchyma at both dawn and dusk. Error bars represent \pm one standard deviation.

The dry season in Central American montane cloud forests are characterised by higher rainfall and humidity and lower temperatures than those experienced in lowland tropical dry forests (Pierce et al., 2002; Goldsmith et al., 2013). The environmental conditions of the montane forests all contribute to a lower vapour pressure deficit (VPD) which minimises water loss from plants. Therefore, it was surprising that species in the tropical montane cloud forest had deeper hydrenchyma tissue than those in the lowland tropical dry forest (Fig. 4.2, Fig. 4.3). However, the daily variance in VPD is known to be higher on cloudy days than sunny days in montane forests, which leads to higher daily fluctuations in transpiration rates (Cavelier 1990). Thus, it is possible that the capacitance provided by hydrenchyma has adapted to fluctuating conditions in this high elevation ecosystem, rather than to more stable, long-term drought. When leaves experience a sudden and dynamic increase in VPD, over the time scale of minutes, they typically respond by closing stomata to prevent gas exchange (McAdam and Brodribb, 2016). Plants detect higher VPD by recognising a drop in the RWC of the leaf; reduced water content causes cells to shrink and this triggers ABA production which in turn leads to stomatal closure (McAdam and Brodribb, 2016; Sack et al., 2018). It is conceivable that the hydrenchyma in species living in Cerro Jefe cloud forest is acting to circumvent this process; water from the hydrenchyma might prevent the RWC from dropping in the chlorenchyma mesophyll, thus stomata will be less likely to shut in response to sudden increases in VPD (McAdam and Brodribb, 2018). This would be beneficial in an ecosystem where clouds are likely to return, and light is limited (Pierce et al., 2002), as plants would be able to make use of high gas exchange rates to facilitate photosynthetic assimilation when momentary periods of sunshine occur. A comparable situation is seen in the tolerance of sun flecks in shade leaves. Shade leaves benefit from high water contents as it allows them to maintain cell turgor and lose water to achieve evaporative cooling when sunlight hits the leaf. It is important that shade leaves can make use of momentary light availability, even at the expense of water loss, as this radiation is likely to be infrequently available low down in the canopy (Schymanski et al., 2013). Analogous to this, hydrenchyma allows *increased* rates of transpiration when drought occurs (Chapter 2), which may maintain high rates of stomatal gas exchange when cloud cover momentarily disappears, and sunlight becomes more available. More work is required to test this hypothesis but research into this question would benefit from studying the many genera in Cerro Jefe, besides *Clusia*, that have hydrenchyma tissue, such as *Freziera*, *Hilia*, and *Schlegelia* (A. Leverett, unpublished observation).

Another possible explanation for the prevalence of deeper hydrenchyma in species inhabiting the cloud forest is that this tissue is playing a role in 'foliar uptake', a process by which wet leaves absorb the condensation from clouds and mist to help maintain turgor (Eller et al., 2016). A comparison of a montane and lower pre-montane forest near Monteverde, Costa-Rica found that the former had higher incidence of clouds, and leaves in this environment were wet for a greater proportion of the day (Goldstein et al., 2013). These authors also report that the species in the montane forest can absorb water through their leaf lamina at higher rates than species in the pre-montane forest, but they do not report any possible anatomical adaptations that may facilitate this difference in foliar uptake. In more succulent species, the low bulk modulus of elasticity in hydrenchyma tissue likely facilitates movement of water into the tissue, as cells can rapidly inflate to absorb water quickly (Schulte and Nobel, 1989; Nobel 2006; Ogburn and Edwards, 2010). If water from mist can travel freely from the abaxial to adaxial surface of leaves via the apoplast (Eller et al., 2016), it is possible that in the high elevation species of *Clusia*, hydrenchyma acts as a 'sponge' that can fill rapidly, thereby facilitating the dynamic uptake of water from clouds. If hydrenchyma is facilitating foliar uptake, this would be another example of this tissue maintaining the water relations of leaves in response to dynamic changes in water availability, over the course of a day.

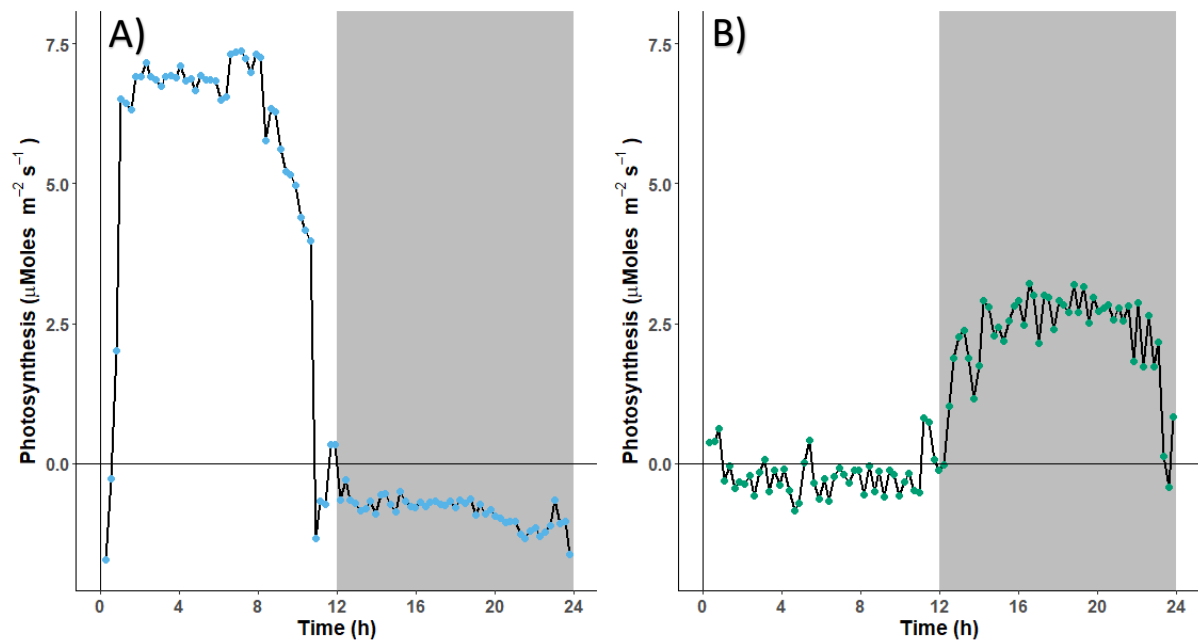


Fig. 4.10) *Clusia alata* and *C. tocuchensis* have distinct photosynthetic physiologies.

Twenty-four hour photosynthetic rates were measured using a LI-COR for each species. (A) *Clusia tocuchensis* exhibits a net efflux of CO_2 during the night, and a net influx of CO_2 at night, indicative of C_3 photosynthesis. (B) *Clusia alata* exhibits a net influx of CO_2 during the night and a very small net efflux of CO_2 during the day, indicative of CAM. Gas exchange was performed on well-watered plants and figures presented here are representative of 3 biological replicates.

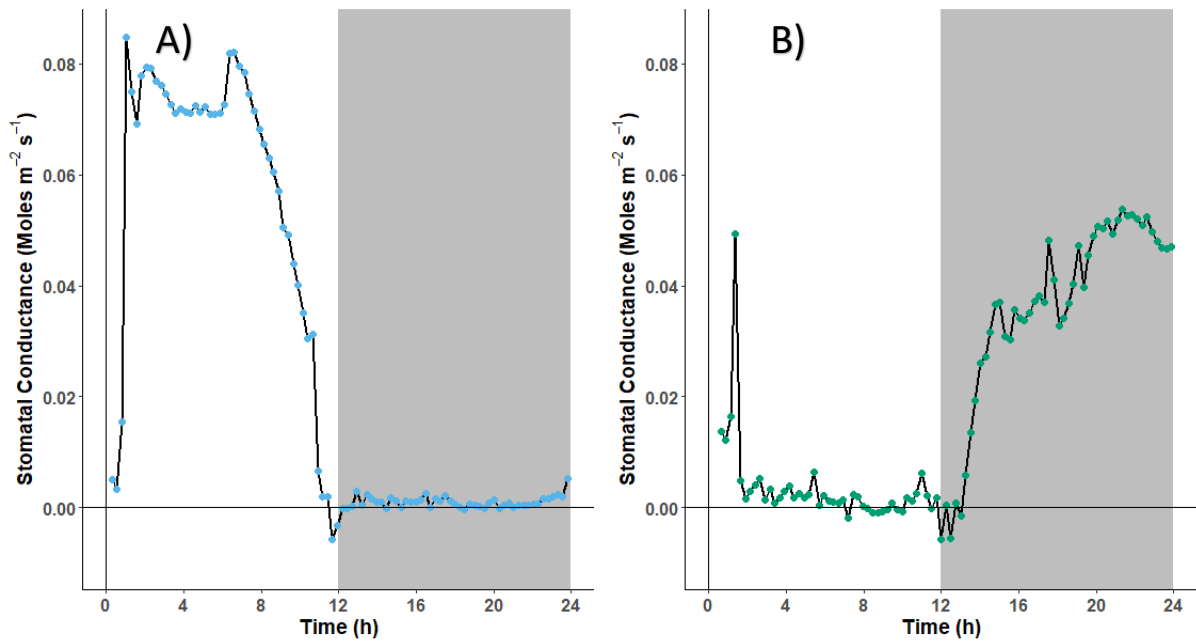


Fig. 4.11) *Clusia alata* and *C. tocuchensis* have distinct stomatal conductance profiles. 24 hour change in stomatal conductance were measured using a LI-COR for each species. (A) *Clusia tocuchensis* exhibits no positive stomatal conductance during the night (stomata remain closed), and a positive stomatal conductance (stomata are open) during the day, indicative of C₃ photosynthesis. (B) *Clusia alata* exhibits a positive stomatal conductance during the night, and another peak in the morning, with very little to no positive stomatal conductance (stomata are closed) later in the day, indicative of CAM. Gas exchange was performed on well-watered plants and figures presented here are representative of 3 biological replicates.

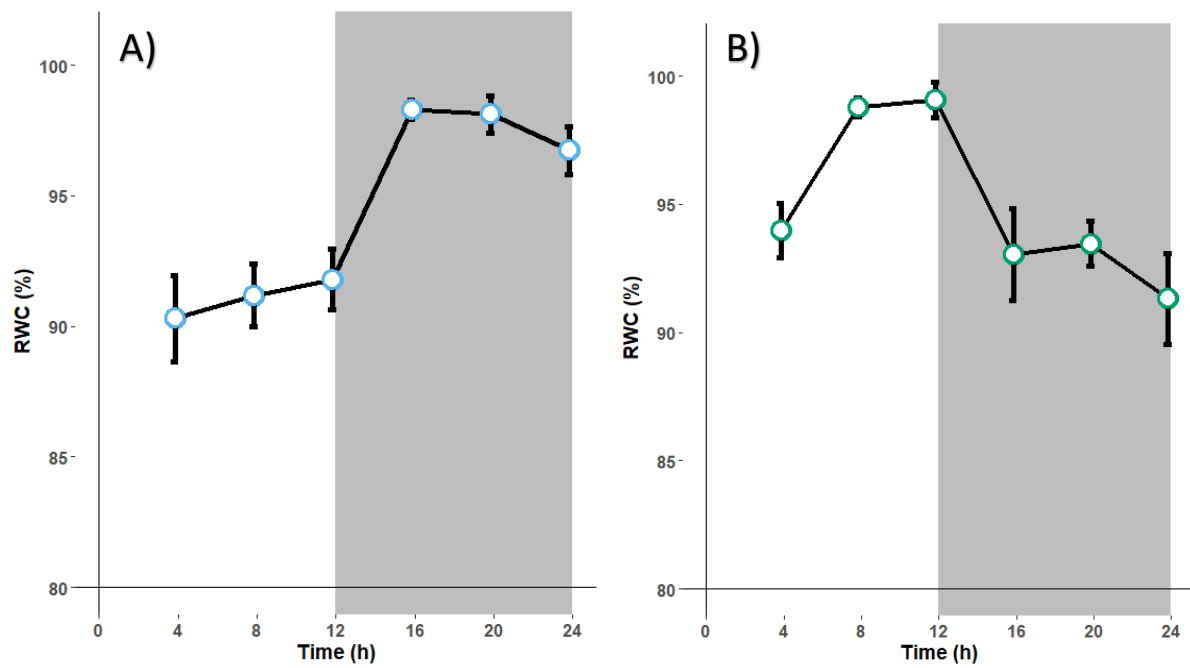


Fig. 4.12) Diel fluctuations in hydrenchyma relative water content (RWC) are different in C₃ and CAM species. The relative water content of hydrenchyma is lower in the day for (A) the obligate C₃ species *C. tocutensis* and lower in the night for (B) the constitutive CAM species, *C. alata*. Graphs show the RWC for each species sampled every four hours. Error bars represent \pm one standard error.

4.4.2 The Physiology of Hydrenchyma: Validation of Method

To better understand if hydrenchyma functions to meet the changing requirements of the leaf over the course of a day, a method was developed to dissect this tissue from the abaxial chlorenchyma in *C. alata* and *C. tocuchensis*, which exhibit constitutive CAM and obligate C₃ physiology, respectively. These species were chosen because they have the deepest hydrenchyma, alongside flat lamina, meaning they were the most amenable to dissection (Fig. 4.4). Similar dissections have been performed in the massive leaves of *Agave deserti* and a number of stem succulents (Barcikowski and Nobel 1984; Goldstein et al., 1991; Nobel 2006). In addition, several studies have investigated the role of adaxial hydrenchyma in the leaf by dissecting this layer from the abaxial chlorenchyma layers in different species of *Peperomia* (Schmidt and Kaiser, 1987; Nishio and Ting, 1987). However, unlike dissections in *Peperomia*, which require the use of 70x magnification to carefully separate tissue layers (Nishio and Ting, 1987), dissection in *Clusia* can be done extremely quickly (approx. 2 seconds) with the naked eye, by separating tissue at a weak point directly between the chlorenchyma and the hydrenchyma. This means that hydrenchyma tissue can instantly be weighed or placed in water or liquid nitrogen (depending on the experiment). This allows accurate determination of the properties of this tissue and reduces the possibility that dehydration during the dissection process is affecting the data.

4.4.3 The Physiology of Hydrenchyma: Maintenance of a Stable Osmotic Potential and Absence of Crassulacean Acid Metabolism

Initial investigations found no difference between dawn and dusk H⁺ concentration in the hydrenchyma of either *C. tocuchensis* or *C. alata* (Fig. 4.6, Fig. 4.7), demonstrating that CAM is not occurring in this tissue, irrespective of the photosynthetic physiology of the species. A lack of acid accumulation in the hydrenchyma is congruent with immunostaining experiments that found enzymes integral to CAM were absent from this tissue in a number of *Clusia* species (Borland et al., 1998). This result in *Clusia* is in contrast to the findings from *Peperomia camptotricha* which is reported to accumulate malate in the adaxial hydrenchyma (Nishio and Ting, 1987; Ting et al., 1994). *Clusia* seems to behave more like *Agave deserti*, which does not

accumulate acid overnight in the hydrenchyma, as CAM occurs only in the outer green tissue layers of the leaf (Smith et al., 1987). As a consequence of CAM being absent in the hydrenchyma in *A. deserti*, this species is able to maintain a stable osmotic potential over 24 hours, which is always substantially lower than that of the chlorenchyma tissue. Congruous with this, no difference in osmotic potential was observed between dawn and dusk in the hydrenchyma tissue of either *Clusia* species, and osmotic potentials of the hydrenchyma were always lower than those observed in the chlorenchyma (Fig. 4.8, Fig. 4.9). A stable osmotic potential was achieved despite there being substantial differences in the RWC of hydrenchyma at dawn and dusk, for both species (Fig. 4.12). Since the hydrenchyma tissue in *Clusia* can maintain a stable osmotic potential despite losing water, the hydrenchyma tissue must be losing osmolytes in conjunction with water loss throughout the day. This phenomenon has been documented in several species, as osmolytes are believed to either move into the chlorenchyma (Barcikowski and Nobel, 1984; Schmidt and Kaiser, 1987; Shulte and Nobel, 1989) or precipitate into starch (Goldstein et al., 1991), which maintains an osmotic gradient between the hydrenchyma and chlorenchyma. This osmotic gradient causes water to flow from the hydrenchyma into the chlorenchyma, thus buffering the photosynthetic tissue against water loss.

In addition, the RWC of the hydrenchyma mirrored the stomatal conductance of both *C. tocuchensis* and *C. alata*; drops in RWC coincided with higher stomatal conductance (Fig. 4.11, Fig. 4.12). These data are preliminary, and more work needs to be done to determine if diel changes to transpiration or osmotic potential of the chlorenchyma (due to CAM) are driving water loss from the hydrenchyma. However, the data presented are strongly suggestive that the capacitance that the hydrenchyma provides is likely acting to buffer leaves over the 24-hour diel cycle, meaning this tissue plays a relevant role in short term drought. If hydrenchyma tissue predominantly evolved to protect leaves against short-term drought, this might explain why this adaptation does not appear to correlate with the long-term aridity that some species experience in the field.

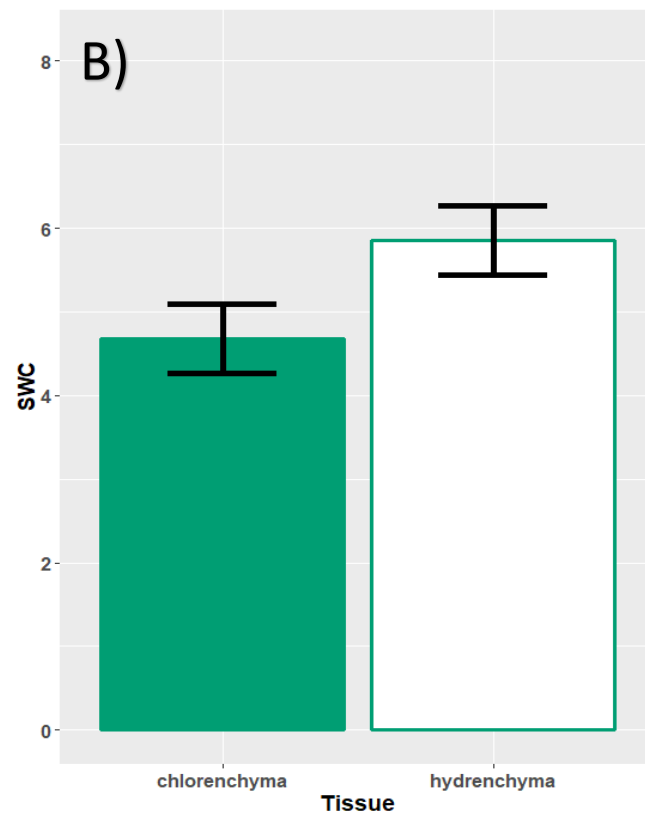
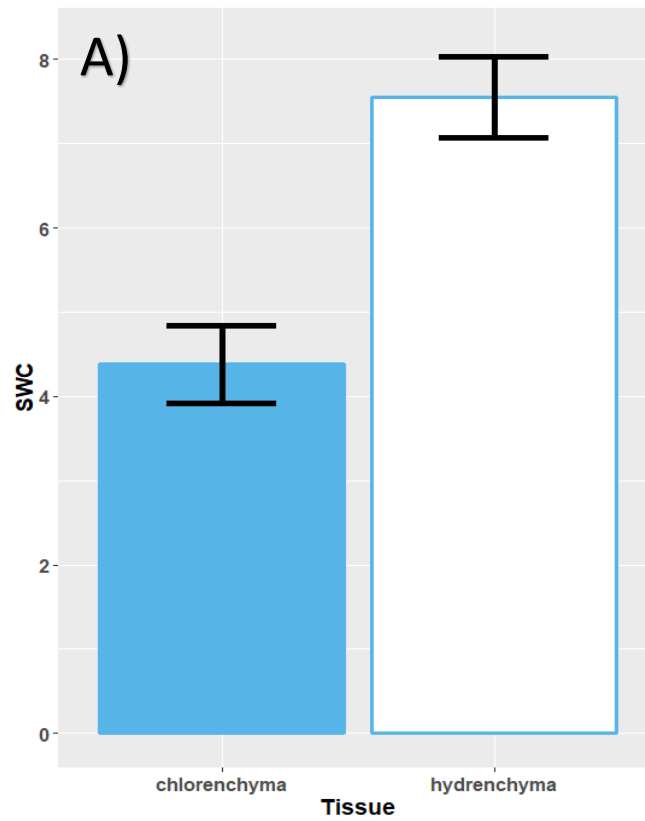


Fig. 4.13) Saturated water content (SWC) is higher in the hydrenchyma than the chlorenchyma. A significantly higher SWC was found in the hydrenchyma than the chlorenchyma in (A) *C. tocuchensis* (two tailed, paired t-test, $p < 0.001$) and (B) *C. alata* (two tailed, paired t-test, $p < 0.001$). Error bars represent \pm one standard deviation.

4.4.4 Long Term Aridity Does Affect Interspecific Variation in Crassulacean Acid Metabolism

Chapters 2 and 3 highlighted the relevance of hydrenchyma in the drought response of *Clusia*, as this tissue provides capacitance and increases the turgor loss point. Therefore, the main aims of this chapter were to investigate the ecological and physiological significance of hydrenchyma tissue. However, it was also possible to investigate the role of long-term aridity in the occurrence of CAM photosynthesis, using the remote-access climatic data presented here. Even though CAM does not affect species ability to tolerate low water potentials (Chapter 3) and the large chlorenchyma cells that host this metabolic cycle do not provide capacitance to the leaf (Chapter 2), the data presented in this study demonstrate that CAM is an adaptation to long term drought. The percentage of photosynthesis done in well-watered plants (i.e. the degree to which species can constitutively engage in CAM) correlated negatively with the mean annual precipitation (Fig. 4.1c). These data show that species that constitutively employ CAM are better suited to ecosystems that experience greater aridity, over the course of a year. In addition to this, the percentage of diel photosynthesis done at night under droughted conditions (which represents the extent to which species can constitutively *or* facultatively engage in CAM) correlated negatively with the precipitation of the driest month (Fig. 4.1d). Thus, if seasonal drought occurs, it confers an advantage to species that constitutively express CAM or can switch into this photosynthetic mode in response to low water availability. This is congruous with findings from the Eulophiinae subtribe (Orchidaceae), in which terrestrial CAM species are found in an ecological niche characterised by hotter, drier forests (Bone et al., 2015).

4.5 Conclusions

The climatic data analysed in this chapter found that, in *Clusia*, low water availability at the time scale of years or months does not predict interspecific differences in hydrenchyma depth. This finding suggests that hydrenchyma may instead be more important for shorter-term drought experienced over the diel cycle. This possibility was reinforced by physiological data demonstrating that the osmotic potential of this tissue remains high and stable, despite the RWC fluctuating over 24 hours. The ecology of CAM, on the other hand, does appear to be influenced by long-term drought; both yearly and monthly aridity significantly correlates with the occurrence of strong and intermediate CAM phenotypes, respectively. It has already been shown (Chapter 2) that hydrenchyma and CAM play distinctly different roles in the hydraulic physiology of *Clusia*; hydrenchyma protects the leaves when experiencing water loss, whereas CAM prevents water loss. Therefore, it appears that the prevention of water loss associated with CAM, rather than the prevention of low water potentials associated with hydrenchyma, contributes more to species distributions into more arid ecosystems.

Chapter 3 showed that CAM cannot not be considered a typical 'drought avoidance' adaptation, as species with this photosynthetic physiology do not have higher turgor loss points. However, the observation made in this chapter, namely that CAM species are more commonly distributed in drier ecosystems, demonstrates that CAM is an ecologically important adaptation for tolerating long term drought. Therefore, CAM appears to be an adaptation that facilitates species' ability to inhabit dry environments without affecting their ability to tolerate low water potentials. This might provide an explanation for why CAM, and not hydrenchyma, contributes significantly to the distribution of species; hydrenchyma buffers leaves against water loss, but makes them more vulnerable to negative water potentials (Chapter 2; Chapter 3), whereas CAM prevents water loss with no such trade-off.

4.6 References

- Arndt, S. K., Irawan, A., & Sanders, G. J. (2015). Apoplastic water fraction and rehydration techniques introduce significant errors in measurements of relative water content and osmotic potential in plant leaves. *Physiologia Plantarum*, *155*(4), 355–368.
<https://doi.org/10.1111/ppl.12380>
- Barcikowski, W., & Nobel, P. S. (1984). Water Relations of Cacti During Desiccation : Distribution of Water in Tissues. *Botanical Gazette*, *145*(1), 110–115.
- Barrera Zambrano, V. A., Lawson, T., Olmos, E., Fernández-García, N., & Borland, A. M. (2014). Leaf anatomical traits which accommodate the facultative engagement of crassulacean acid metabolism in tropical trees of the genus *Clusia*. *Journal of Experimental Botany*, *65*(13), 3513–3523. <https://doi.org/10.1093/jxb/eru022>
- Bone, R. E., Smith, J. A. C., Arrigo, N., & Buerki, S. (2015). A macro-ecological perspective on crassulacean acid metabolism (CAM) photosynthesis evolution in Afro-Madagascan drylands: Eulophiinae orchids as a case study. *New Phytologist*, *208*(2), 469–481.
<https://doi.org/10.1111/nph.13572>
- Boom, A., Sinnige Damsté, J. S., & De Leeuw, J. W. (2005). Cutan, a common aliphatic biopolymer in cuticles of drought-adapted plants. *Organic Geochemistry*, *36*(4), 595–601. <https://doi.org/10.1016/j.orggeochem.2004.10.017>
- Borland, A. M., Griffiths, H., Maxwell, C., Broadmeadow, M. S. J., Griffiths, N. M., & Barnes, J. D. (1992). On the ecophysiology of the Clusiaceae in Trinidad: expression of CAM in *Clusia minor* L. during the transition from wet to dry season and characterization of three endemic species. *New Phytologist*, *122*(2), 349–357.
<https://doi.org/10.1111/j.1469-8137.1992.tb04240.x>
- Borland, A. M., Técsi, L. I., Leegood, R. C., & Walker, R. P. (1998). Inducibility of crassulacean acid metabolism (CAM) in *Clusia* species; physiological/biochemical characterisation and intercellular localization of carboxylation and decarboxylation processes in three species which exhibit different degrees of CAM. *Planta*, *205*(3), 342–351.
<https://doi.org/10.1007/s004250050329>

- Cavelier, J. (1990). Tissue water relations in elfin cloud forest tree species of Serrania de Macuira, Guajira, Colombia. *Trees*, 4(3), 155–163. <https://doi.org/10.1007/BF00225780>
- Chiang, J. M., Lin, T. C., Luo, Y. C., Chang, C. Te, Cheng, J. Y., & Martin, C. E. (2013). Relationships among rainfall, leaf hydrenchyma, and Crassulacean acid metabolism in *Pyrrosia lanceolata* (L.) Fraw. (Polypodiaceae) in central Taiwan. *Flora*, 208(5–6), 343–350. <https://doi.org/10.1016/j.flora.2013.04.007>
- Crayn, D. M., Winter, K., & Smith, J. A. C. (2004). Multiple origins of crassulacean acid metabolism and the epiphytic habit in the Neotropical family Bromeliaceae. *Proceedings of the National Academy of Sciences of the United States of America*, 101(10), 3703–3708. <https://doi.org/10.1190/segam2015-5905882.1>
- Eller, C. B., Lima, A. L., & Oliveira, R. S. (2016). Cloud forest trees with higher foliar water uptake capacity and anisohydric behavior are more vulnerable to drought and climate change. *The New Phytologist*, 211(2), 489–501. <https://doi.org/10.1111/nph.13952>
- Freschi, L., Takahashi, C. A., Cambui, C. A., Semprebom, T. R., Cruz, A. B., Mioto, P. T., ... Mercier, H. (2010). Specific leaf areas of the tank bromeliad *Guzmania monostachia* perform distinct functions in response to water shortage. *Journal of Plant Physiology*, 167(7), 526–533. <https://doi.org/10.1016/j.jplph.2009.10.011>
- Gibeaut, D. M., & Thomson, W. W. (1989). Leaf Ultrastructure of *Peperomia obtusifolia*, *P. camptotricha*, and *P. scandens*. *Botanical Gazette*, 150(2), 108–114.
- Goldsmith, G. R., Matzke, N. J., & Dawson, T. E. (2013). The incidence and implications of clouds for cloud forest plant water relations. *Ecology Letters*, 16(3), 307–314. <https://doi.org/10.1111/ele.12039>
- Goldstein, G., Andrade, J., & Nobel, P. (1991). Differences in Water Relations Parameters for the Chlorenchyma and the Parenchyma of *Opuntia ficus-indica* Under Wet Versus Dry Conditions. *Functional Plant Biology*, 18(2), 95. <https://doi.org/10.1071/pp9910095>
- Grace, O. M., Buerki, S., Symonds, M. R. E., Forest, F., Van Wyk, A. E., Smith, G. F., ... Rønsted, N. (2015). Evolutionary history and leaf succulence as explanations for medicinal use in

- aloes and the global popularity of Aloe vera. *BMC Evolutionary Biology*, 15(1), 1–12.
<https://doi.org/10.1186/s12862-015-0291-7>
- Herrera, A., Fernández, M. D., & Taisma, M. A. (2000). Effects of drought on CAM and water relations in plants of *Peperomia carnevalii*. *Annals of Botany*, 86(3), 511–517.
<https://doi.org/10.1006/anbo.2000.1210>
- Hijmans, R. J., Cameron, S. E., Parra, J. L., Jones, P. G., & Jarvis, A. (2005). Very high resolution interpolated climate surfaces for global land areas. *International Journal of Climatology*, 25(15), 1965–1978. <https://doi.org/10.1002/joc.1276>
- Holtum, J. A. M., Aranda, J., Virgo, A., Gehrig, H. H., & Winter, K. (2004). $\delta^{13}\text{C}$ values and crassulacean acid metabolism in *Clusia* species from Panama. *Trees*, 18, 658–668.
<https://doi.org/10.1007/s00468-004-0342-y>
- Johnson W, Van den Eynden V, Oatham M. 2017. *The IUCN red list of threatened species. Clusia tocuchensis*. [WWW document] URL <http://www.iucnredlist.org/details/115943201/0>. [accessed 30 January 2018].
- Kaul, R. B. (1977). The Role of the Multiple Epidermis in Foliar Succulence of *Peperomia* (Piperaceae). *Botanical Gazette*, 138(2), 213–218.
- Males, J. (2018). Concerted anatomical change associated with crassulacean acid metabolism in the Bromeliaceae. *Functional Plant Biology*, 45(7), 681–695.
<https://doi.org/10.1071/fp17071>
- Males, J., & Griffiths, H. (2017). Functional types in the Bromeliaceae: relationships with drought-resistance traits and bioclimatic distributions. *Functional Ecology*, 31(10), 1868–1880. <https://doi.org/10.1111/1365-2435.12900>
- McAdam, S. A. M., & Brodribb, T. J. (2018). Mesophyll Cells Are the Main Site of Abscisic Acid Biosynthesis in Water-Stressed Leaves. *Plant Physiology*, 177(3), 911–917.
<https://doi.org/10.1104/pp.17.01829>

- McAdam, S. A. M., & Brodribb, T. J. (2016). Linking Turgor with ABA Biosynthesis: Implications for Stomatal Responses to Vapor Pressure Deficit across Land Plants. *Plant Physiology*, 171(3), 2008–2016. <https://doi.org/10.1104/pp.16.00380>
- Nishio, J. N., & Ting, I. P. (1987). Carbon Flow and Metabolic Specialization in the Tissue Layers of the Crassulacean Acid Metabolism Plant, *Peperomia camptotricha*. *Plant Physiology*, 84(3), 600–604. <https://doi.org/10.1104/pp.84.3.600>
- Nobel, P. S. (2006). Parenchyma-chlorenchyma water movement during drought for the hemiepiphytic cactus *Hylocereus undatus*. *Annals of Botany*, 97(3), 469–474. <https://doi.org/10.1093/aob/mcj054>
- Nowak, E. J., & Martin, C. E. (1997). Physiological and Anatomical Responses to Water Deficits in the CAM Epiphyte *Tillandsia ionantha* (Bromeliaceae). *International Journal of Plant Sciences*, 158(6), 818–826.
- Oberbauer, S. F., Strain, B. R., & Riechers, G. H. (1987). Field water relations of a wet-tropical forest tree species, *Pentaclethra macroloba* (Mimosaceae). *Oecologia*, 71(3), 369–374. <https://doi.org/10.1007/BF00378709>
- Ogburn, R. M., & Edwards, E. J. (2010). The ecological water-use strategies of succulent plants. In J.-C. Kader & M. Delseny (Eds.), *Advances in Botanical Research* (1st ed., Vol. 55, pp. 179–225). <https://doi.org/10.1016/B978-0-12-380868-4.00004-1>
- Pierce, S., Winter, K., & Griffiths, H. (2002). The role of CAM in high rainfall cloud forests: an in situ comparison of photosynthetic pathways in Bromeliaceae. *Plant, Cell and Environment*, 25(2), 1181–1189. Retrieved from <http://onlinelibrary.wiley.com/doi/10.1046/j.1365-3040.2002.00900.x/pdf>
- Sack, L., John, G. P., & Buckley, T. N. (2018). ABA accumulation in dehydrating leaves is associated with decline in cell volume not turgor pressure. *Plant Physiology*, 176(January), pp.01097.2017. <https://doi.org/10.1104/pp.17.01097>
- Schmidt, J. E., & Kaiser, W. M. (1987). Response of the Succulent Leaves of *Peperomia magnoliaefolia* to Dehydration. *Plant Physiology*, 83(1), 190–194. <https://doi.org/10.1104/pp.83.1.190>

- Schulte, P. J., & Nobel, P. S. (1989). Responses of a CAM Plant to Drought and Rainfall : Capacitance and Osmotic Pressure Influences on Water Movement. *Journal of Experimental Botany*, 40(210), 61–70. Retrieved from <http://jxb.oxfordjournals.org/lookup/doi/10.1093/jxb/40.1.61>
- Schymanski, S. J., Or, D., & Zwieniecki, M. (2013). Stomatal Control and Leaf Thermal and Hydraulic Capacitances under Rapid Environmental Fluctuations. *PLoS ONE*, 8(1). <https://doi.org/10.1371/journal.pone.0054231>
- Silvera, K., & Lasso, E. (2016). Ecophysiology and Crassulacean Acid Metabolism of Tropical Epiphytes. In G. Goldstein & L. S. Santiago (Eds.), *Tropical Tree Physiology* (6th ed., pp. 25–43). Springer.
- Silvera, K., Santiago, L. S., Cushman, J. C., & Winter, K. (2009). Crassulacean acid metabolism and epiphytism linked to adaptive radiations in the Orchidaceae. *Plant Physiology*, 149(4), 1838–1847. <https://doi.org/10.1104/pp.108.132555>
- Slot, M., & Winter, K. (2017). High tolerance of tropical sapling growth and gas exchange to moderate warming. *Functional Ecology*, 32(3), 599–611. <https://doi.org/10.1111/1365-2435.13001>
- Smith, J. A. C., & Lüttge, U. (1985). Day-night changes in leaf water relations associated with the rhythm of crassulacean acid metabolism in *Kalanchoë daigremontiana*. *Planta*, 163(2), 272–282. <https://doi.org/10.1007/BF00393518>
- Smith, J. A. C., Schulte, P. J., & Nobel, P. S. (1987). Water flow and water storage in *Agave deserti*: osmotic implications of crassulacean acid metabolism. *Plant, Cell & Environment*, 10, 639–648.
- Smith, J. A. C., & Heuer, S. (1981). Determination of the volume of intercellular spaces in leaves and some values for CAM plants. *Annals of Botany*, 48(6), 915–917. <https://doi.org/10.1093/oxfordjournals.aob.a086200>

Ting, I. P., Patel, A., Sipes, D. L., Reid, P. D., & Walling, L. L. (1994). Differential expression of photosynthesis genes in leaf tissue layers of *Peperomia* as revealed by tissue printing. *American Journal of Botany*, *81*(4), 414–422. <https://doi.org/10.2307/2445490>

Virzo de Santo, A., Alfani, A., Russo, G., & Fioretto, A. (1983). Relationship between CAM and Succulence in Some Species of Vitaceae and Piperaceae. *Botanical Gazette*, *144*(3), 342–346.

Chapter 5. Leaf Vascular Adaptations Associated with Crassulacean Acid Metabolism and Succulence in *Clusia*

5.1 Introduction

5.1.1 Leaves: the Site of Water Loss From Trees

The field of leaf hydraulics has grown in the last 15 years, following the discovery that leaves act as a hydraulic bottleneck in trees, accounting for more than 30 % of the hydraulic resistance in the soil to atmosphere continuum (Sack et al., 2003; Sack and Holbrook 2006; Sack and Tyree 2006; Scoffoni et al., 2011). As more than 40 trillion tonnes of water traverse plants each year (Chahine 1992; Sack and Tyree 2006), and with the growing threat of global warming (Sheffield and Wood 2008), it is essential to establish a good understanding of the relationships between physiological traits and hydraulic adaptations in leaves. Crassulacean acid metabolism (CAM), which causes reorganised stomatal dynamics, so that stomata are open in the night and closed during the middle of the day (Borland et al., 2014; Yang et al., 2015), is a physiological adaptation that minimises water loss (Chapter 2) and thus seems likely to affect the vascular anatomy and hydraulics of a leaf.

To understand the impact that vascular anatomy has on the hydraulic physiology of leaves, comparative analyses of closely related species can be very informative (Scoffoni et al., 2011; Scoffoni et al., 2016b; Scoffoni et al., 2017). By comparing C₃, facultative CAM, and constitutive CAM species it is possible to identify vascular traits that correlate with a species' photosynthetic physiotype (Males 2017, Males and Griffiths, 2018). Recently, an emphasis has been put on comparing hydraulic traits at the taxonomic level of the genus, as comparisons made at higher taxonomic levels can give opposing results, due to the greater phylogenetic distance between species (Liu et al., 2015; Scoffoni et al., 2016b). This has led scientists to focus on phenotypically diverse genera, such as *Viburnum* to understand fundamental ways in which anatomy drives the physiology of plants (Chatelet et al., 2013; Edwards et al., 2014; Scoffoni et al., 2016). There are some model genera emerging for the comparative study of CAM, such as Australian *Calandrinia* (Winter and Holtum, 2011; Holtum et al., 2017), and *Yucca* (Heyduk et al., 2016a). However, these genera have not been extensively phenotypically screened, and thus it is not certain if they contain the entire spectrum of C₃, weak and/or

facultative CAM and constitutive CAM species. *Clusia*, on the other hand, is an ideal model genus for comparative analyses; it contains a full range of photosynthetic physiotypes, which co-inhabit the same ecosystems (Popp et al., 1987; Borland et al., 1993; Franco et al., 1994; Roberts et al., 1996; Grams et al., 1998; Lüttge 1999; Holtum et al., 2004; Winter et al., 2005; Winter et al., 2009; Barrera Zambrano et al., 2014). Moreover, even under well-watered conditions, *Clusia* contains a complete spectrum of photosynthetic physiotypes; there are C₃ species that assimilate all their CO₂ during the day, as well those expressing weak and strong forms of CAM photosynthesis, which assimilate a small or large proportion of their diel CO₂ during the night, respectively. Therefore, *Clusia* is an ideal model for testing how CAM affects the vascular anatomy of leaves across closely related species.

Measurements of transpirational water loss in well-watered *Clusia* species found that *C. uvitana* and *C. rosea* (which were expressing weak and strong forms of CAM, respectively) lost less water than C₃ relatives (Winter et al., 2005). In addition, *C. rosea* lost substantially less water than *C. uvitana*, indicating that the strength of CAM has a considerable effect on transpiration. Furthermore, parameterisation of the PHOTO3 model with data from *Clusia* found that CAM causes plants to lose water more slowly than C₃ plants (Chapter 2). The low diel transpiration rates associated with CAM are likely the result of diurnal stomatal closure (i.e. phase III), which prevents water loss during the hottest, driest portion of the day. In addition, the maximal stomatal conductance each species achieves over the diel cycle correlates negatively with CAM (Barrera Zambrano et al., 2014). *Clusia* species that do a greater proportion of their photosynthesis during the night, in well-watered conditions have lower maximal stomatal conductance, measured in the morning (Barrera Zambrano et al., 2014). Therefore, not only does CAM decrease the diel water loss from leaves, it also minimises any short-term spikes in water loss that could cause momentary dehydration to the leaf at certain points of the day.

5.1.2 Veins are Important for Conducting Water

Water that is lost from transpiration across stomata needs to be replaced, in order to prevent the leaf from dehydrating, as this would cause a loss of cell turgor, a drop in photosynthetic efficiency and could damage the leaf. Whilst some species can absorb water from the atmosphere to rehydrate (Mooney et al., 1977; Eller et al., 2016; Males 2016), most

leaves gain water from their stem to replace that which is lost by transpiration. To facilitate the flow of water from the petiole into the leaf, efficient hydraulic conductance (the movement of water through a leaf across a given water potential gradient) is required to replace water lost through the stomata. To achieve this, tracheophytes have evolved xylem conduits; hollow tubular cells that conduct water into the distal portions of the leaf (Esau 1965; Scoffoni et al., 2016a). In angiosperm leaves, xylem conduits consist of small tracheids and wider vessels, which both conduct water. The vasculature is typically arranged in a single plane in a leaf, such that larger veins furcate into smaller, finer veins that radiate into the leaf lamina (Esau 1965). The midrib and the two orders of veins that branch off from this are typically described as the major veins, and are characterised by thick, structurally reinforced xylem tissue. The finer, branched veins that furcate off the third order veins (i.e. the fourth order and above) are described as minor veins; these typically radiate into the lamina tissue until they eventually end at vein termini (Sack and Scoffoni, 2013). This vascular architecture allows leaves to efficiently conduct water across the leaf, thereby minimising dehydration when transpiration is occurring.

5.1.3 Vein Length per Leaf Area (VLA) Determines Hydraulic Conductance

Whilst some highly succulent species have veins in multiple planes in a leaf (Balsamo and Uribe 1988; Ogburn and Edwards, 2013; Heyduk et al., 2016; Borland et al., 2018), most species have veins arranged in a single, flat plane. If the vasculature is arranged in a single plane, it becomes possible to quantify the density of veins in a given area of leaf, by clearing the lamina of pigment and staining the lignified vascular tissue (Sack and Frole 2006). This measurement of vein density, known as the vein length per unit area (VLA), determines a species' ability to conduct water across the leaf (Scoffoni et al., 2011; Sack and Scoffoni; 2013). A higher VLA has two complementary effects: it facilitates the flow of water into the lamina tissue, and it minimises the distance water needs to travel outside of the xylem (Scoffoni et al., 2017). As a result, VLA has been shown to correlate strongly with the hydraulic conductance of a leaf, as species with higher VLA can more easily conduct water (Scoffoni et al., 2016b; Scoffoni et al., 2017). Measurements of hydraulic conductance in species doing CAM are rare, but one study found that the maximal leaf hydraulic conductance and vein density were both lower in constitutive CAM species than C₃ species, in the Bromeliaceae (Males and Griffiths, 2018). This finding is intuitive, as CAM minimises water loss, so leaves

that exhibit this metabolic adaptation would not require water to be replaced as fast as C_3 species. However, studies on the Bromeliaceae have not built a complete picture of the relationship between CAM and vascular architecture, because they measured vein density as the intervein distance ($IVD = 1/VLA$) from sectioned leaf material in this family (Males 2017; Males and Griffiths, 2018). Therefore, these studies did not have the resolution to compare major and minor veins, nor the ability to measure vein endings. In *Clusia*, leaf venation exists in one plane for all species, just below the palisade tissue (Popp et al., 1987; Borland et al., 1998; Fig. 5.1, this study), thus VLA is a meaningful parameter for estimating vein density traits. Furthermore, by studying *Clusia*, it is possible to investigate vascular adaptations associated with CAM within a single genus, which increases the confidence that any findings are not due to the phylogenetic distance between species. Therefore, *Clusia* is an ideal model to understand how the reduced transpirational water loss conferred by CAM affects VLA and the density of vein termini, and whether interspecific differences in VLA are the result of changes to major or minor veins.

5.1.4 Measuring Vein Density in Three Dimensions

Measurements of VLA are valuable to understand how leaf vascular architecture has adapted to match the alternate rates of water loss between species. However, it is important to consider that veins are distributed in the leaf in three dimensions; whilst VLA describes the abundance of veins in a two-dimensional plane, the density of veins is also determined by the depth of the mesophyll tissue in which they are found (Zwieniecki and Boyce, 2014). For example, if VLA is kept constant, but the leaf thickness increases, the three-dimensional density of veins in the leaf will be lower, and as a result water will need to travel further after leaving the xylem, in order to fully infiltrate the mesophyll tissue. Based on this consideration, Noblin et al., (2008) used both model and real leaves to investigate if there was an optimal placement of veins in three-dimensional leaf tissue. This study found that the optimal vascular architecture is one where IVD roughly equals the vein to lower epidermal distance ($IVD \approx VED$). An IVD:VED ratio > 1 meant that insufficient veins were available to efficiently replace the water that was lost from stomata (Fig. 5.2). Conversely, an IVD:VED ratio < 1 would mean that the leaves have 'overinvested' in veins; veins are present without any increase to the efficiency with which water lost from the stomata is replaced (Fig. 5.2). It is important to note that overinvestment in veins is defined here as an IVD:VED ratio < 1 , rather than simply a

higher VLA. Investigations of diverse tracheophyte species found the existence of IVD:VED ratios > 1 in some ferns, flat-leaved gymnosperms and basal angiosperms, but found that derived angiosperms were predominantly characterised by leaves where IVD:VED ratio = 1 (Zwieniecki and Boyce, 2014). The authors of this paper argued that the convergent evolution of optimal vein placement confers efficient leaf hydraulic conductance to derived angiosperms. This efficient hydraulic conductance might have freed angiosperms to evolve into hotter, drier environments and is therefore a putative explanation for the rapid radiation of this clade into every niche across the world (Darwin, 1903). Furthermore, no derived angiosperm species were found with IVD:VED ratios < 1 , which was taken as additional evidence that there was no benefit from overinvesting in veins.

Whilst research into diverse species demonstrated that for most angiosperm species, $IVD \approx VED$, investigations of more closely related species, within the Eucalypts and the Bromeliaceae, found that some species do have IVD:VED ratios < 1 (de Boer et al., 2016; Males, 2017). In the Eucalypts, leaf thickness correlates negatively with the IVD:VED ratio, as species with thicker leaves overinvest in veins (de Boer et al., 2016). The authors of this study provided modelling evidence to suggest that greater leaf thickness causes higher hydraulic resistance in the mesophyll apoplast, meaning that leaves need overinvestment in vein placement in order to maintain efficient hydraulic conductance across the whole leaf. A contrasting explanation for vascular overinvestment was made by Males (2018), who suggested that the high hydraulic capacitance of thick leaves could require greater vascular conductance in order to quickly refill water reserves following rainfall. According to this hypothesis, high capacitance allows leaves to lose greater volumes of water during transpiration (Chapter 2), and these reserves must be replaced rapidly when water becomes available (Males 2018, Chapter 2). Therefore, the overinvestment in veins may be an adaptation to quickly refill capacitance pools. The genus *Clusia* is an ideal model to test these two alternative hypotheses. In *Clusia*, leaf thickness is determined predominantly by large chlorenchyma cells, associated with CAM, whereas capacitance is independent of leaf thickness and instead controlled by specialised hydrenchyma tissue (Chapter 2). Therefore, if any species are found with vascular overinvestment in *Clusia*, it would be possible to investigate if this vascular anatomical trait is determined more by hydrenchyma depth/capacitance or CAM/leaf thickness. If CAM and leaf thickness result in IVD:VED ratios < 1 , then it is likely that vascular overinvestment has evolved to overcome high apoplastic resistance associated with this anatomical adaptation. In

contrast, if hydrenchyma depth is affecting vascular overinvestment, it is likely that IVD:VED ratios < 1 are needed to provide high hydraulic conductance to rapidly refill stored water for capacitance pools.

5.1.5 Conduit Dimensions Effect Embolism Formation

Finally, to complete the characterisation of vascular traits associated with CAM, it is necessary to explore xylem anatomy inside the veins, by measuring the dimensions of the water-conducting conduits. Water travels across the xylem conduits under tension, due to the pulling force from transpirational water loss (Sack and Holbrook, 2006; Brodribb et al., 2016). Under tension, water exists at a metastable state and can spontaneously change phase from liquid to gas, which breaks the contiguity of the transpiration stream and causes a loss of hydraulic conductance. What causes the phase change, from liquid to gas within the vasculature is not entirely understood, but it is known that wider xylem conduits are more vulnerable to the formation of emboli (Lens et al., 2013; Scoffoni et al., 2016a). Wider vessels are believed to be more vulnerable to cracks and imperfections in their pit-membranes (the membrane-bound pores that connect neighbouring conduits), which can 'seed' the formation of gaseous bubbles. As a result, eudicot species with wide conduits often exhibit a 50 % loss of hydraulic conductance (P50) at higher water potentials (Scoffoni et al., 2016a). Therefore, this study sought to measure the cross-sectional area of vessels in *Clusia* as a proxy for each species' P50. By exploring the interspecific variation in leaf vessel sizes, it is possible to ask if the water-conservation conferred by CAM frees species to evolve wider vessels. Vessels in the petiole and central midrib were measured since the first order major veins are known to be the predominant site at which emboli originate (Brodribb et al., 2016; Klepsch et al., 2018).

5.2 Materials and Methods

5.2.1 Species Studied

This comparative study investigated the 11 species of *Clusia* described previously in this thesis (see Chapter 2, 3 and 4). Nine of these species were used by Barrera Zambrano et al., (2014). These are: the C₃ species – *Clusia multiflora*, *C. tocuchensis* and *C. grandiflora*; the intermediate/facultative CAM species – *C. lanceolata*, *C. aripoensis* and *C. minor*; and the constitutive CAM – *C. rosea*, *C. alata* and *C. hilariana*. These represent a phylogenetically diverse spread of species (Gustafsson et al., 2007, Barrera Zambrano et al., 2014 – and references therein). As in Chapters 2, 3 and 4, two new species were included. These are the facultative CAM species, *C. pratensis* (Winter et al., 2008; Winter and Holtum, 2014) and the constitutive CAM species, *C. fluminensis* (Roberts et al., 1996).

5.2.2 Plant Growth Conditions

Plants that were sampled for anatomical or water relations measurements (below), were grown in a glass house in Cockle Park farm, as a part of the Newcastle *Clusia* collection. The glass house has fitted photosynthetic LED lights allowing plants to receive a minimum 12 hour light day. The glass house was kept at 25 °C during the day and 23 °C during the night. Plants were watered every 2 days.

5.2.3 Photosynthetic Gas Exchange

The gas exchange data used in these comparative analyses was from Barrera Zambrano et al., (2014) plus data on *Clusia pratensis* and *C. fluminensis* from Chapter 2.

5.2.4 Vein Length per Leaf Area (VLA) and Vein to Epidermal Surface (VED)

Vein length per unit area was measured with the protocol outlined by Scoffoni and Sack (<http://prometheuswiki.publish.csiro.au/tiki-index.php?page=Quantifying+leaf+vein+traits>), which was optimised for working with *Clusia* leaves. From each plant, the third or fourth leaf from the apex was sampled from the Newcastle *Clusia*

collection in glass houses in Cockle Park Farm and brought into the lab in Newcastle, during the summer months of June, July and August, 2017. Each leaf was imaged in a flatbed scanner (hp Scanjet 5530 Photosmart Scanner, Hp, UK) and, using ImageJ (NIH) leaf area was measured. Primary VLA (i.e. VLA of the midrib) was then measured by dividing the length of the midrib, from the most proximal to most distal end of the leaf blade, by the leaf area. VLA and VED was measured by both A. Leverett alongside Kate Ferguson.

Due the thick, waxy leaves of *Clusia* it was not possible to clear whole leaves to measure VLA, so instead, for each leaf, a 2 by 3 cm (or 1 by 2 cm rectangle for smaller leaves of *C. lanceolata* and *C. minor*) rectangle was cut half way along the proximal-distal axis of the leaf blade. This rectangle did not include the leaf margin or the midrib. Both abaxial and adaxial surfaces were gently rubbed with a nail file to remove some wax and make fine perforations in this external layer. Following this, the leaf rectangles were soaked for 45 minutes in 3:1 95 % ethanol (Fisher Chemical): glacial acetic acid (Fisher Chemical) to further remove wax. These leaf rectangles were then transferred to 5 % NaOH (w/v) (BDH Chemicals Ltd) and soaked for 45 minutes to clear green pigments. Leaf material was then transferred to 50 % (v/v) bleach in aqueous solution for 15 minutes to remove blackened phenolics. Leaf material was washed in water 4 times, each for 15 minutes and then dehydrated, by transferal to solutions containing increasing concentrations of ethanol (dehydration series was 30 %, 50 %, 70 % and 100 % ethanol, each lasting 20 minutes). Once the leaf tissue was fully dehydrated, it was transferred to a staining solution containing 1 % (w/v) Safranin-O (Sigma-Aldrich) in 100 % ethanol for 2 minutes. Leaf tissue was then washed in 100 % ethanol 3 times, and rehydrated, by repeating the dehydration series in the opposite order. Finally, leaf tissue was transferred to 5 % ethanol for storage overnight. Leaf rectangles were imaged using a flatbed scanner (CanoScan 9000F, Cannon LTD, UK) at 4800 x 4800 dpi resolution (Fig. 5.3). As this could not capture the highest orders of minor veins, images were also generated using a light microscope (Leitz Diaplan). For each leaf, 3 technical replicates were imaged (GXCAM HiChrome-S, GT Vision Ltd), under the microscope (Fig. 5.4). ImageJ (NIH) was used to measure VLA on images; namely, major VLA was measured by adding the VLA of the primary vein to major VLA from scanned images of leaf rectangles and minor VLA was measured using images taken under the microscope. Total leaf VLA was calculated as the sum of major and minor VLA. The total VLA was used to calculate intervein distance using the equation:

Equation 5.1

$$IVD = \frac{1}{VLA}$$

For each leaf, the average distance from vein to lower epidermal surface was also measured. Adjacent to the position at which VLA was measured, the leaf lamina was sectioned by hand, using a fresh razor blade and stored in 5 % phosphate buffered saline (Sigma-Aldrich). Sections were imaged using a camera (Q-IMAGING, QICAM, fast 1394) attached to a fluorescence microscope (Leica DMRB) under blue light. As veins are in one plane in *Clusia* leaves (Fig. 5.1), VED was calculated as the distance from the middle of a vein to the lower epidermal surface, averaged for 3 technical replicates, per leaf. For each species, 7-9 replicate leaves were used. It was not possible to generate clear images for *C. rosea* leaves, so this species was omitted from this analysis.

5.2.5 Cross-Sectional Vessel Area

Leaves were sampled from the Newcastle *Clusia* collection between March and April 2017 and brought into the lab. Leaf area was measured using a flatbed scanner (hp Scanjet 5530 Photosmart Scanner, Hp, UK), as described above. Midribs were sectioned, by hand, half way along the proximal-distal axis of the leaf blade. Petioles, were sectioned using a vibrating microtome (Ci LTD, UK) which was set to cut 100 μ m sections at 80 Hz. Sections were then transferred to 5 % phosphate buffered saline (Sigma-Aldrich) and stored overnight. Sections were imaged using a camera (Q-IMAGING, QICAM, fast 1394) attached to a fluorescence microscope (Leica DMRB) under blue light, which illuminates lignified veins. For each image, the cross-sectional vessel area was measured using ImageJ (NIH). For each species, n = 4, for both petiole and midribs.

5.2.6 Statistics

All statistics were performed using R version 3.4.1.

5.3 Results

5.3.1 Crassulacean Acid Metabolism is Associated with Lower Vein Length per Leaf Area (VLA)

To explore the effect of CAM on vein density, the vein length per leaf area was measured for multiple species of *Clusia*. Since *C. rosea* was omitted from this study, the final data set was comprised of 10 species; 3 constitutive CAM, 4 facultative CAM and 3 obligate C₃. Interspecific comparisons found that species that do a greater proportion of their CO₂ assimilation at night, under well-watered conditions, had significantly lower total VLA (Fig. 5.5a). Separate analysis of the major and minor VLA found that only the latter significantly correlated with CAM (Fig. 5.5c, Fig. 5.4). No correlation was found between the proportion of CO₂ assimilation done at night and the major VLA (Fig. 5.5b, Fig. 5.3). As minor VLA, and not major VLA, is lower in species that do CAM, the ratio of major to minor veins showed a significant positive correlation with the proportion of CO₂ assimilation at night in each species (Fig. 5.6). Taken together, these data suggest that species that do CAM require lower VLA, which is the consequence of lower minor VLA.

5.3.2 Crassulacean Acid Metabolism is Associated with Fewer Vein Endings

Minor veins often end at vein termini (Fig. 5.4), at which point all water moves through out of the xylem and into the mesophyll tissue. As vein termini are found in the minor veins, it was suspected that minor VLA and vein termini density would positively correlate with each other. Analysis of 10 *Clusia* species confirmed this hypothesis, as minor VLA correlated significantly with vein termini density (Fig. 5.7a). In addition, because CAM was correlated with minor vein density, it was suspected that species engaged in CAM would have fewer vein termini in a given leaf area. A linear regression found that the percentage of CO₂ assimilation done at night, under well-watered conditions correlated with the density of vein termini (Fig. 5.7b). Thus, the low minor VLA associated with CAM results in leaves with fewer vein termini.

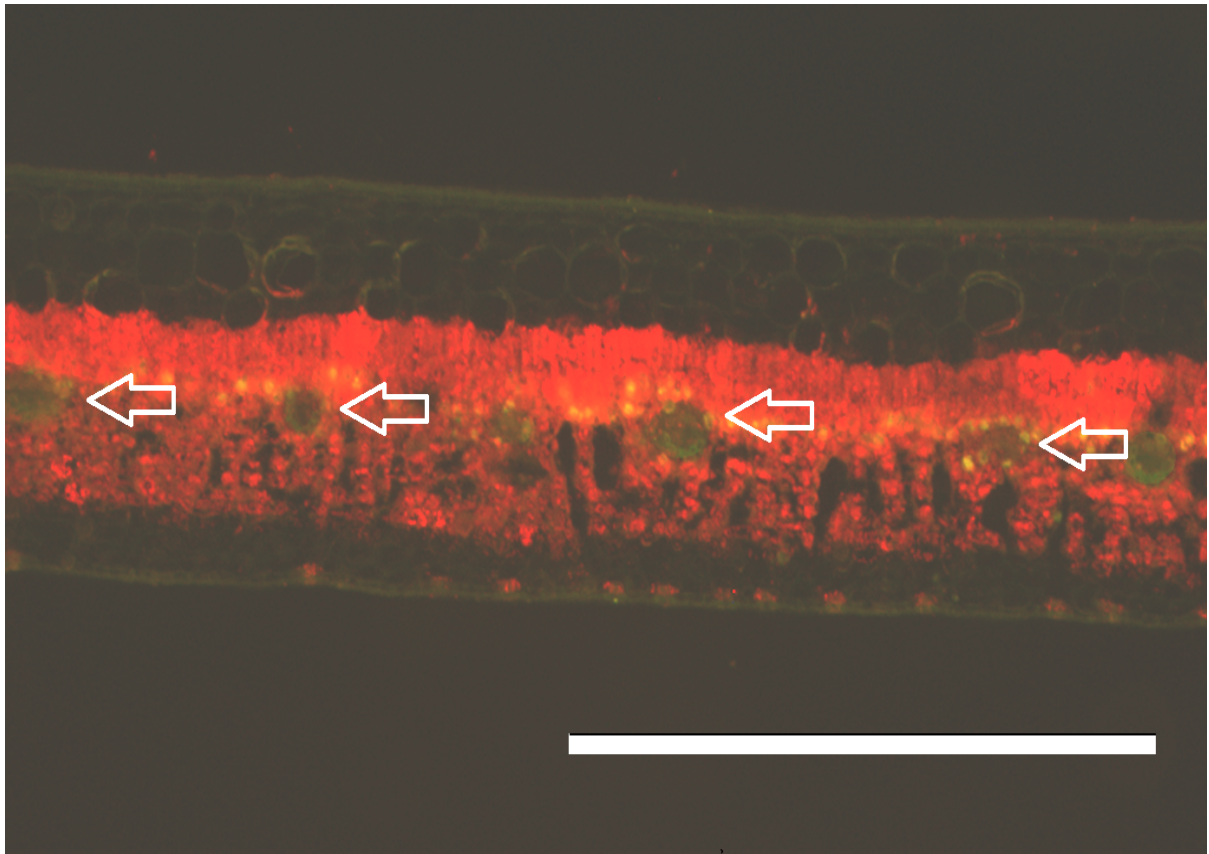
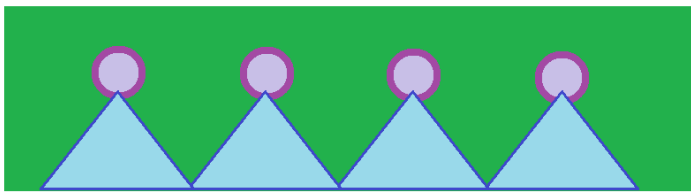
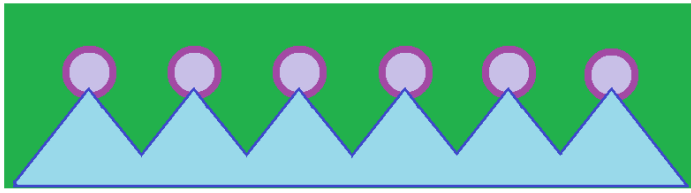


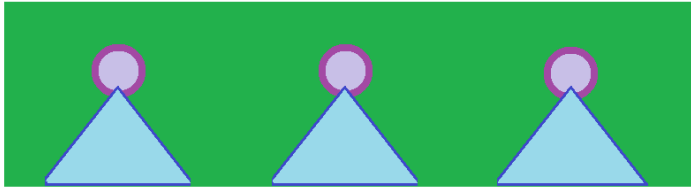
Fig. 5.1) Veins develop in one plane in *Clusia* leaves. Image shows the mesophyll of *C. tocuchensis*, with arrows pointing to the veins, which all fall in one flat plane in the leaf. All species had veins in one, flat plane between the palisade and spongy mesophyll tissue layers. Scale bar = 1 mm.



$$\text{IVD:VED} = 1$$



$$\text{IVD:VED} < 1$$



$$\text{IVD:VED} > 1$$

Fig. 5.2) Schematic diagram depicting the effect of IVD:VED ratio on water movement into the mesophyll. Each image represents the cross sectional tissue within a leaf. After leaving the veins (purple) water (blue) will move into the mesophyll tissue. In reality water will move in all directions but for simplicity only abaxial flow is depicted here. When IVD:VED = 1, sufficient vasculature is available to efficiently replace lost water in the mesophyll. This is represented by water reaching all portions of the abaxial face of the leaf after leaving the xylem. However, when IVD:VED is < 1, the leaf is 'overinvesting' in veins, meaning more veins are present without any increase to the efficiency of hydraulic flow into the mesophyll. Finally, if the IVD:VED ratio is > 1, insufficient veins are available to efficiently replace lost water in the mesophyll.

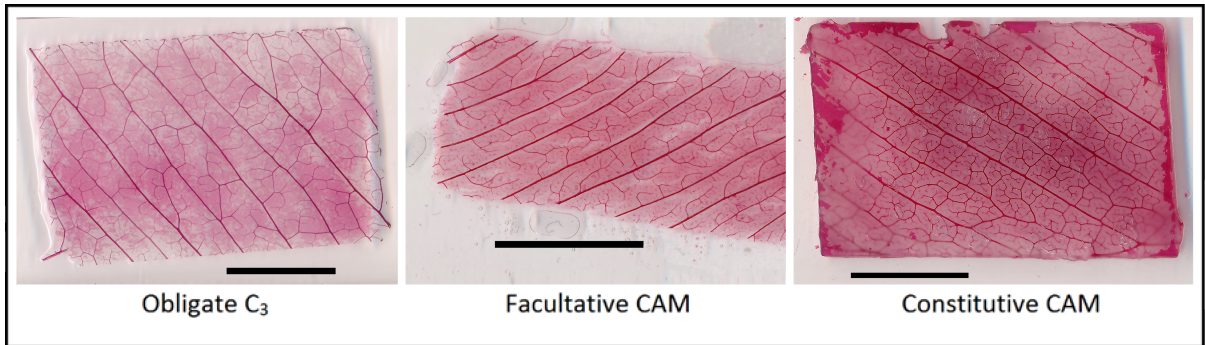


Fig. 5.3) Leaf tissue used for determining major VLA. Scale bar = 10 mm.

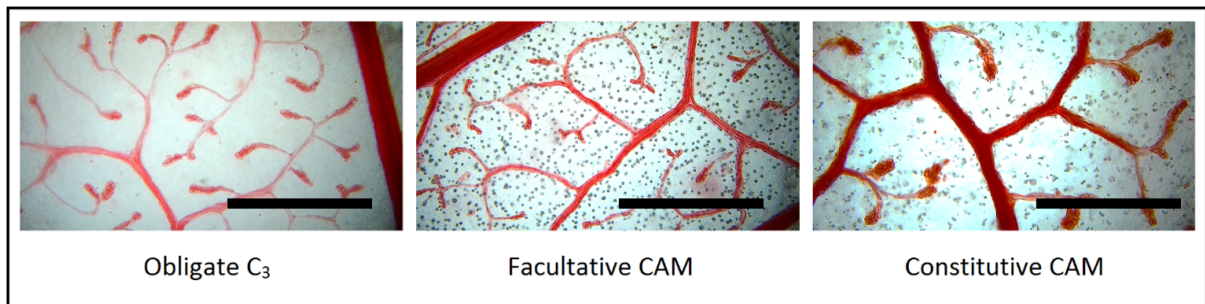


Fig. 5.4) Images used to measure minor VLA. Scale bar = 1 mm.

5.3.3 Thicker Leaves, Associated With Crassulacean Acid Metabolism, Require Vascular Overinvestment

Most derived angiosperm species have evolved an optimal vein placement, where IVD \approx VED (Zwieniecki and Boyce, 2014). However, some species with thicker leaves are known to overinvest in veins, meaning their IVD:VED ratios are < 1 (de Boer et al., 2016; Males 2017). IVD was calculated for 10 species of *Clusia* using equation 5.1. Plotting IVD against VED found that facultative CAM species diverged slightly from the line where IVD = VED (Fig. 5.8). In addition, the constitutive CAM species diverged considerably from the line where IVD = VED (Fig. 5.8). Both the facultative and constitutive CAM plants have higher VED values without corresponding changes to IVD. Put simply, the evolution of CAM has resulted in deeper mesophyll tissue, but IVD does not decrease by the same extent. To confirm that IVD:VED ratios differed between each physiotype, an ANOVA model was built with (photosynthetic) physiotype as a categorical variable and IVD:VED ratio the dependent variable. The mean IVD:VED ratio was 1.027, 0.825 and 0.476 for obligate C₃, facultative CAM and constitutive CAM species, respectively. A post-hoc Tukey-Kramer analysis found that these means were all unique; meaning the IVD:VED ratio for each physiotype was significantly different from all others. However, this ANOVA analysis treated CAM as a categorical variable. Therefore, to further confirm this finding, a linear regression was built between the proportion of CO₂ assimilation done at night, under, well-watered conditions (which is a continuous variable to describe CAM) and the IVD:VED ratio. This analysis found that the proportion of CO₂ assimilation done at night, under well-watered conditions, significantly correlated with the IVD:VED ratio (Fig. 5.9). Taken together these data show that the presence of CAM is accompanied by overinvestment in veins, in *Clusia*.

Two hypotheses exist in the literature to explain the existence of vascular overinvestment in leaves. The explanation from de Boer et al., (2016) is that high leaf thickness increases hydraulic resistance in the apoplast, and vascular overinvestment is required to overcome this. An alternative hypothesis, by Males (2018) is that some leaves require vascular overinvestment to increase the speed with which they can replace water lost due from large capacitance pools. The IVD:VED ratio correlated with CAM (and therefore also with leaf thickness) in *Clusia*. As CAM is independent of capacitance in *Clusia* (Chapter 2), it was predicted that IVD:VED ratios < 1 are an adaptation to increased leaf thickness in CAM species,

and not an adaptation to allow rapid refilling of capacitance pools in the hydrenchyma. Accordingly, it was also shown that hydrenchyma depth, which confers capacitance by inflating/deflating to buffer leaf water potential, did not affect the IVD:VED ratio (Fig. 5.10). In short, the data thus far appeared to reinforce the hypothesis from de Boer et al., (2016) over that of Males (2018). To confirm this, a multiple linear regression was built, with leaf thickness and hydrenchyma depth as explanatory variables and the IVD:VED ratio as a dependent variable. This analysis found that the IVD:VED ratio correlated significantly with leaf thickness, but not with hydrenchyma depth (Fig. 5.10). Thus, the thick leaves associated with CAM, rather than the increased capacitance from hydrenchyma, is likely the reason for vascular overinvestment in *Clusia*.

5.3.4 Crassulacean Acid Metabolism Does Not Impact Vessel Sizes

In eudicots, large vessels are more vulnerable to the formation of gaseous emboli, which occur during drought, when water potentials drop (Scoffoni et al., 2016a). Therefore, it was hypothesised that the ability to do CAM under droughted conditions would minimise these negative water potentials and allow species to evolve larger vessels to conduct water. To test this hypothesis, petioles and midribs were sectioned and imaged (Fig. 5.11), to measure the cross-sectional area of vessels. A multiple linear regression found that the percentage of CO₂ assimilation done at night, in drought-treated plants, did not correlate with midrib vessel cross-sectional area. However, this model did find that leaf area correlated significantly with midrib vessel cross-sectional area (Fig. 5.12). A similar multiple linear regression also found that the percentage of CO₂ assimilation done at night, in drought-treated plants, did not correlate with petiole vessel cross-sectional area, but that leaf area did correlate with petiole vessel cross-sectional area (Fig. 5.13). Taken together, these data show that the extent to which species can employ CAM during drought does not affect the vessel sizes in the leaf.

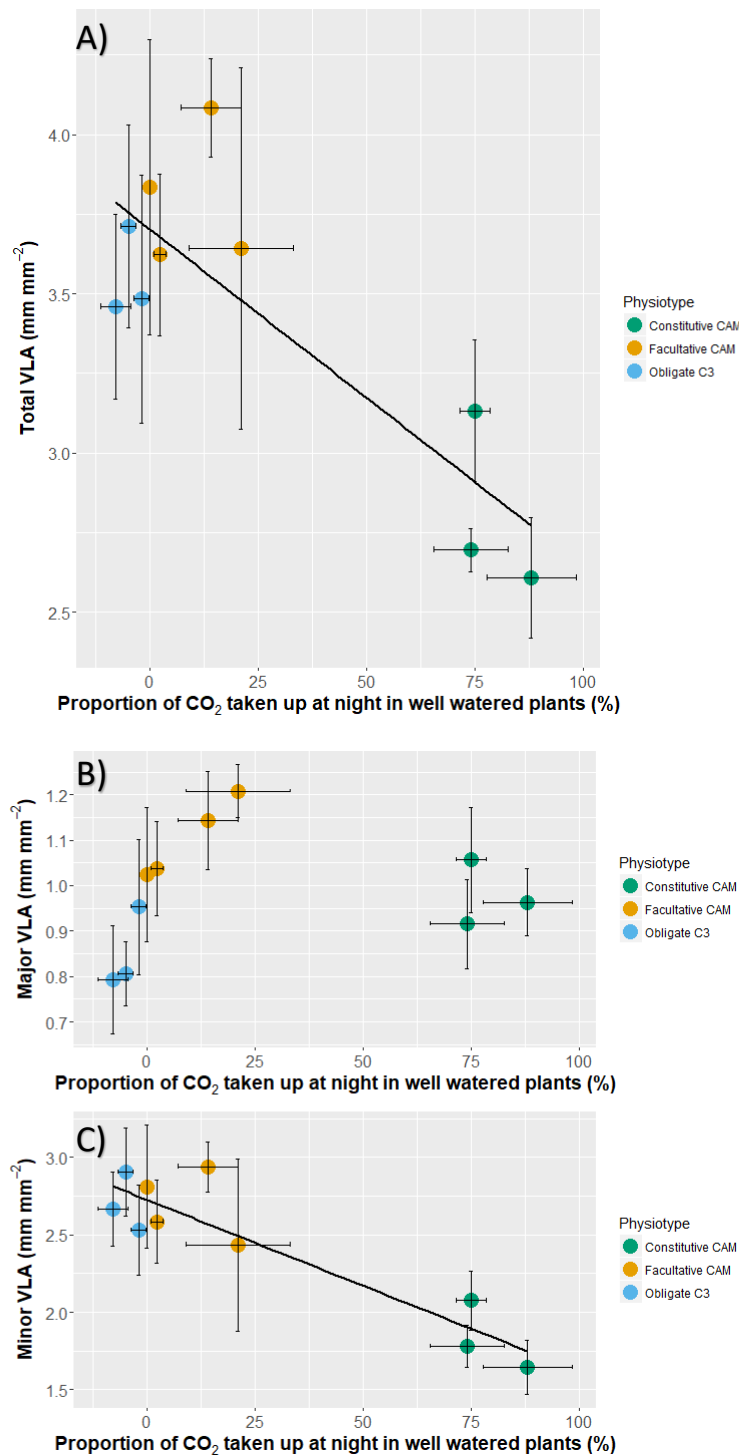


Fig. 5.5) Constitutive CAM species have lower vein densities. (A) Species that do a greater proportion of photosynthetic assimilation at night have lower vein densities (Linear regression; $r^2 = 0.661$ $p = 0.002$). The major veins are not contributing to the relationship between CAM and vein density, as (B) shows no significant relationship exists between species that do a greater proportion of photosynthetic assimilation at night and major VLA (Linear regression; $r^2 = -0.101$, $p = 0.693$). The relationship between CAM and vein density is best explained by the significant correlation between species that do a greater proportion of photosynthetic assimilation at night and minor VLA (Linear regression; $r^2 = 0.818$, $p < 0.001$). 7-9 replicate leaves were used per species, error bars represent error bars represent ± 1 SD.

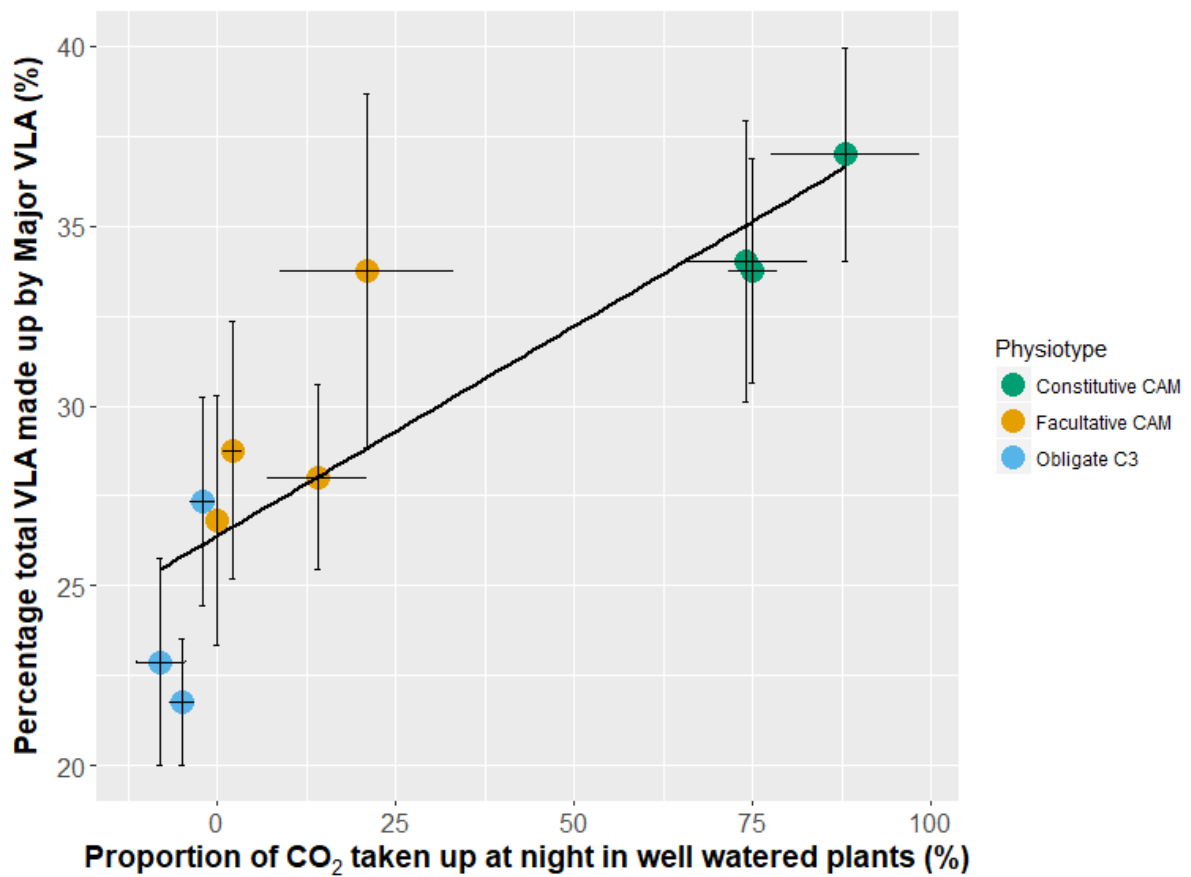


Fig. 5.6) Species that do Crassulacean acid metabolism have a greater major : minor VLA ratio. A significant correlation was found between the percentage of CO₂ taken up at night, in well-watered plants, and the percentage of total VLA made up by major VLA (linear regression; $r^2 = 0.726$, $p = 0.001$). 7-9 replicate leaves were used per species, error bars represent error bars represent ± 1 SD.

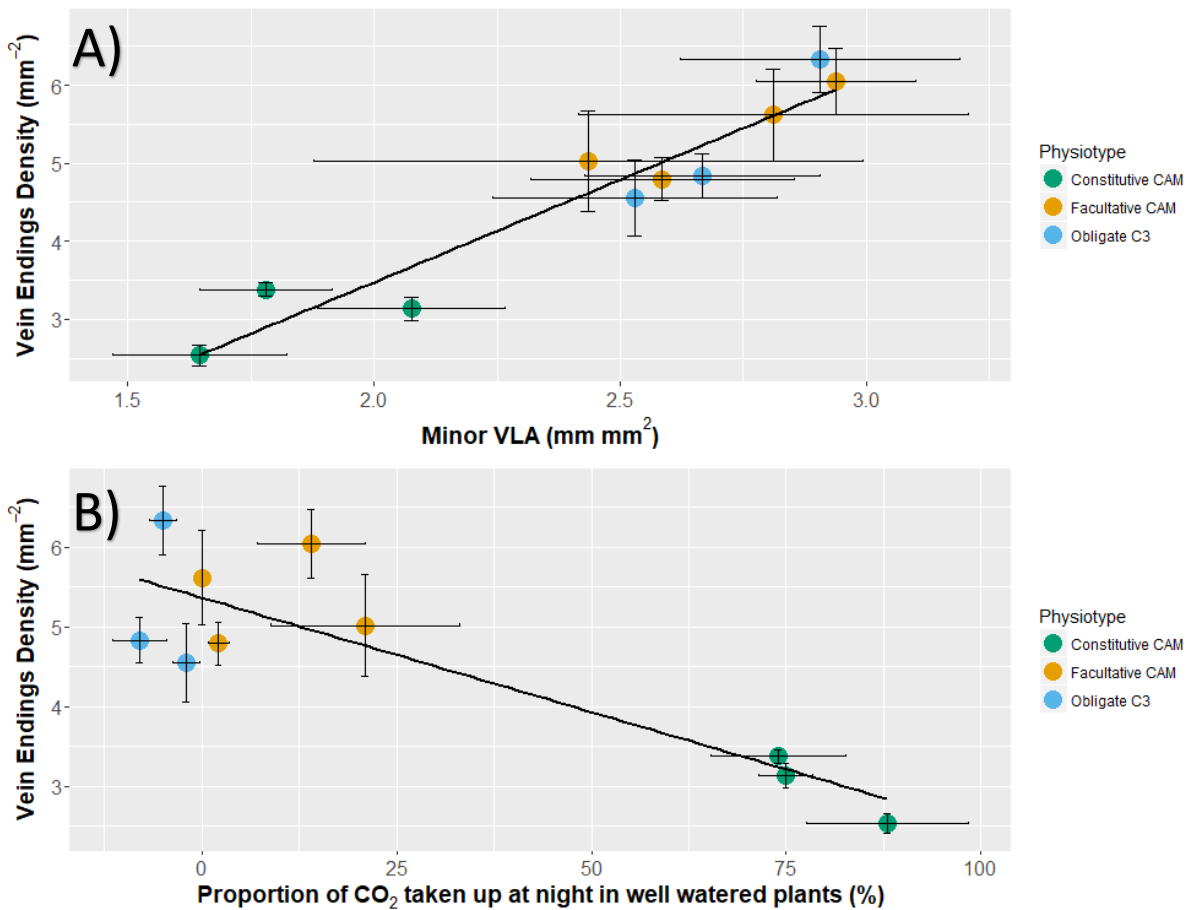


Fig. 5.7) Crassulacean acid metabolism species have fewer vein termini. (A) Species that do a greater proportion of photosynthetic assimilation at night have a lower density of vein termini per leaf area (linear regression; $r^2 = 0.709$, $p = 0.001$). This is likely due to the density of vein termini being lower in species with lower vein densities, as total VLA significantly correlated with the density of vein endings (linear regression; $r^2 = 0.833$, $p < 0.001$). 7-9 replicate leaves were used per species, error bars represent error bars represent ± 1 SD.

5.4 Discussion

5.4.1 Summary of Findings

One technical drawback to studying hydraulic traits in *Clusia* is the presence of secretory ducts that produce latex when the leaf is cut from the stem (Borland et al., 1998). The latex from these ducts clogs the veins, preventing measurements of the flow of water into the leaf, which is a prerequisite for the analysis of hydraulic conductance. Nevertheless, by measuring the vascular anatomy in *Clusia* leaves, it is possible to make informed predictions about how the water conservation conferred by CAM affects the hydraulic needs of the leaf. The data presented here demonstrate that species that constitutively express CAM had lower VLA, which is achieved by changes to the minor VLA (Fig. 5.4, Fig. 5.5). In addition, the thicker leaves associated with CAM have IVD:VED ratios are < 1 , meaning that they are overinvesting in veins (Fig. 5.8, Fig. 5.9). Vascular overinvestment appears to be an adaptation to greater leaf thickness associated with CAM, rather than for the refilling of large capacitance pools in the hydrenchyma (Fig. 5.10). In summary, the leaves that employ CAM have evolved a low VLA, presumably for low hydraulic flow rates, in combination with IVD:VED ratios < 1 to maintain efficient transfer of water across the mesophyll of thick leaves. These adaptations are likely to represent hydraulic solutions to the low transpiration rates and thick chlorenchyma that are integral to the functioning of CAM. In contrast, the vessel sizes in *Clusia* appear to primarily be an adaptation to leaf size, and not CAM, suggesting that CAM does not affect the predisposition of vessels to the formation of gaseous emboli.

5.4.2 Low Vein Length per Leaf Area (VLA) in Species Doing Crassulacean Acid Metabolism

Plants that employ CAM photosynthesis under well-watered conditions can minimise water loss in comparison to C_3 species (Winter et al., 2005, Chapter 2). Constitutive expression of CAM minimises water loss both over the time scale of days and hours (Winter et al., 2005; Barrera Zambrano et al., 2014). As a result, leaves engaged in CAM require lower VLA to replace the water that is lost from transpiration. This is congruent with findings from the Bromeliaceae, in which constitutive CAM species have higher IVD values than C_3 relatives (Males and Griffiths, 2018). In addition, the interspecific variation in VLA found in *Clusia* is a

consequence of changes to minor VLA, and not major VLA (Fig. 5.4, Fig. 5.5). Furthermore, the density of vein termini in the leaves are lower in species that constitutively engage in CAM (Fig. 5.7b). Minor veins facilitate the movement of water far into the leaf lamina, and vein termini result in all water inside conduits moving into the mesophyll tissue, as it can no longer traverse the xylem. Consequently, minor vein VLA and vein termini density are integral traits for keeping the mesophyll well hydrated when water is being lost from open stomata. Lower minor VLA and vein termini densities in *Clusia* are therefore highly suggestive that species doing CAM require lower hydraulic conductance, as water needs to be replaced at a slower rate than in C₃ leaves.

Facultative CAM species in *Clusia* have VLA values that are more like those of the obligate C₃ species than the constitutive CAM species (Fig. 5.5a, 5c). This suggests that the VLA values in *Clusia* are adapted to the strength of CAM under well-watered conditions, rather than the strength of CAM plants exhibit during drought events. Therefore, it is likely that low VLA in *Clusia* is not an adaptation to species ability to do CAM during drought, but rather a means to optimise hydraulic conductance under well-watered conditions. There are other traits in facultative CAM species, such as carbon isotope ratios, which resemble that of C₃ plants (Winter et al., 2015; Winter 2019). C₃-like phenotypic traits in the facultative CAM species of *Clusia* and other taxa are believed to be the consequence of CAM only being used for short periods of the year, during the dry season. VLA appears to also follow this trend; despite facultative CAM species being able to minimise their transpirational water loss during drought, the VLA is adapted to provide sufficient water during periods when the leaf is doing C₃ photosynthesis.

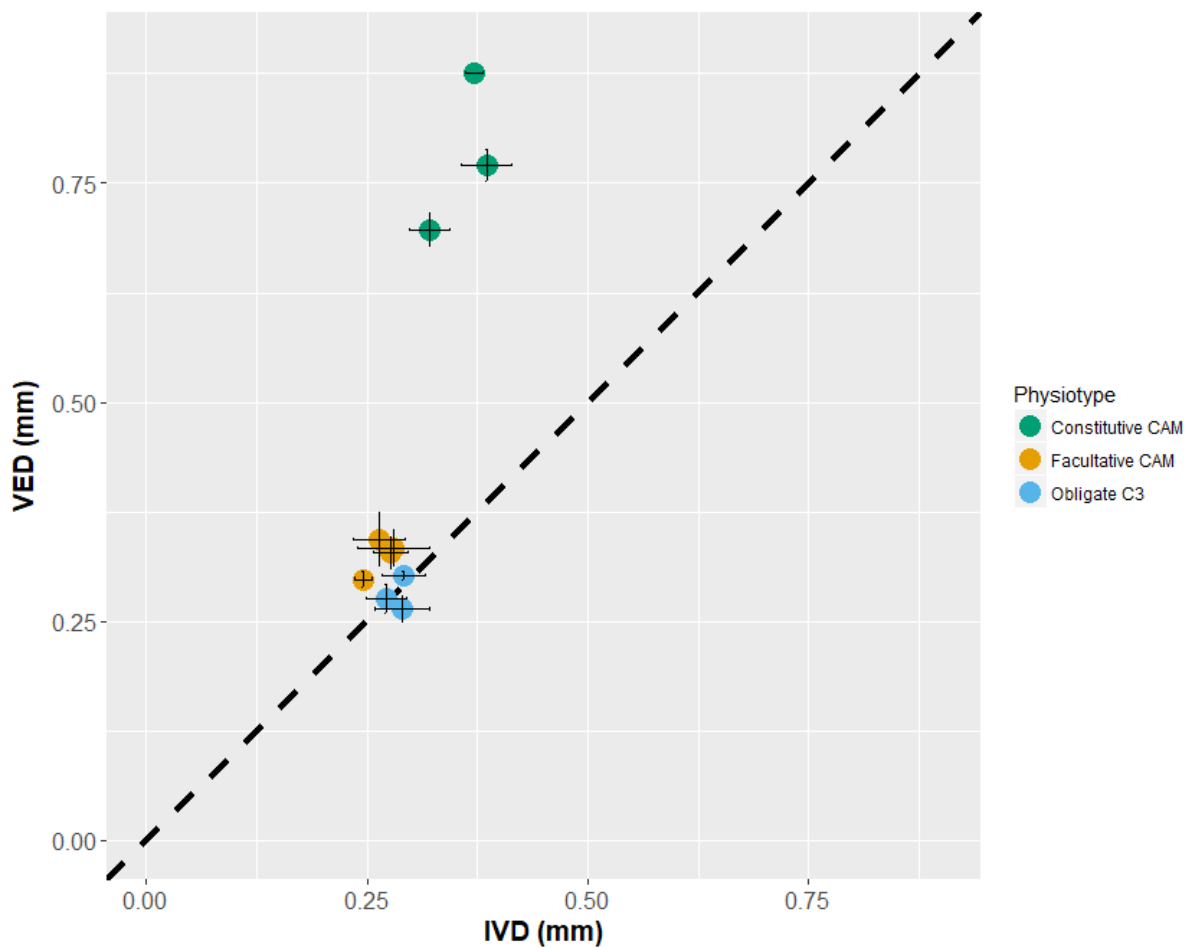


Fig. 5.8) CAM species overinvest in vasculature. The obligate C₃ species sit close to the line where IVD:VED = 1 (dashed line), whereas the facultative and constitutive CAM species diverge from this line. An ANOVA model was built, with the IVD:VED ratio as the dependent variable and physiotype as the categorical explanatory variable. A post-hoc Tukey Kramer analysis found that all physiotypes were significantly different from each other. C₃ species had an average IDV:VED ratio of 1.027, facultative CAM species had an average IVD:VED ratio of 0.825 and constitutive CAM species had an average IVD:VED ratio of 0.476. For each species, n = 7-9, error bars represent ± 1 SD.

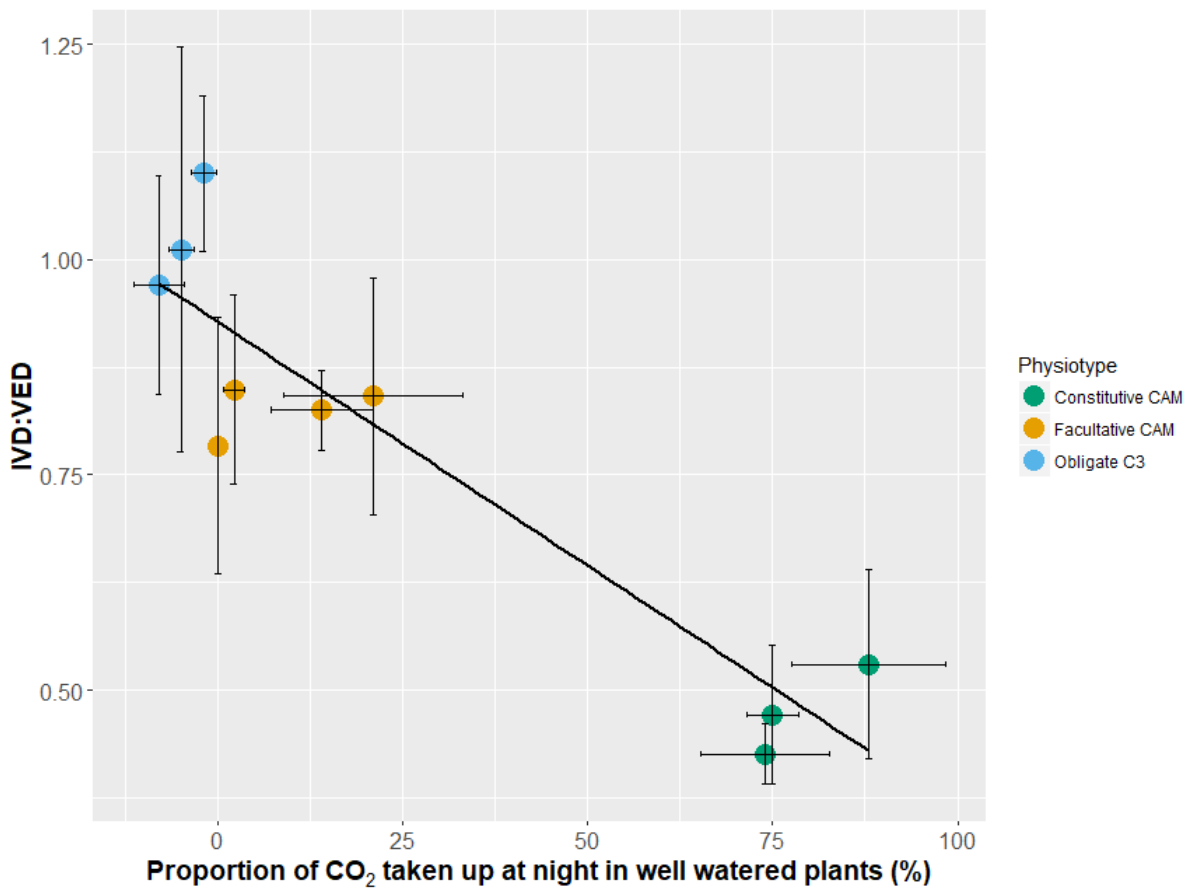


Fig. 5.9) CAM species overinvest in vasculature. The proportion of CO₂ taken up at night, under well watered conditions displayed a significant negative correlation with the IVD:VED ratio (linear regression; : $r^2 = 0.829$, $p < 0.001$). For each species, $n = 7-9$, error bars represent ± 1 SD.

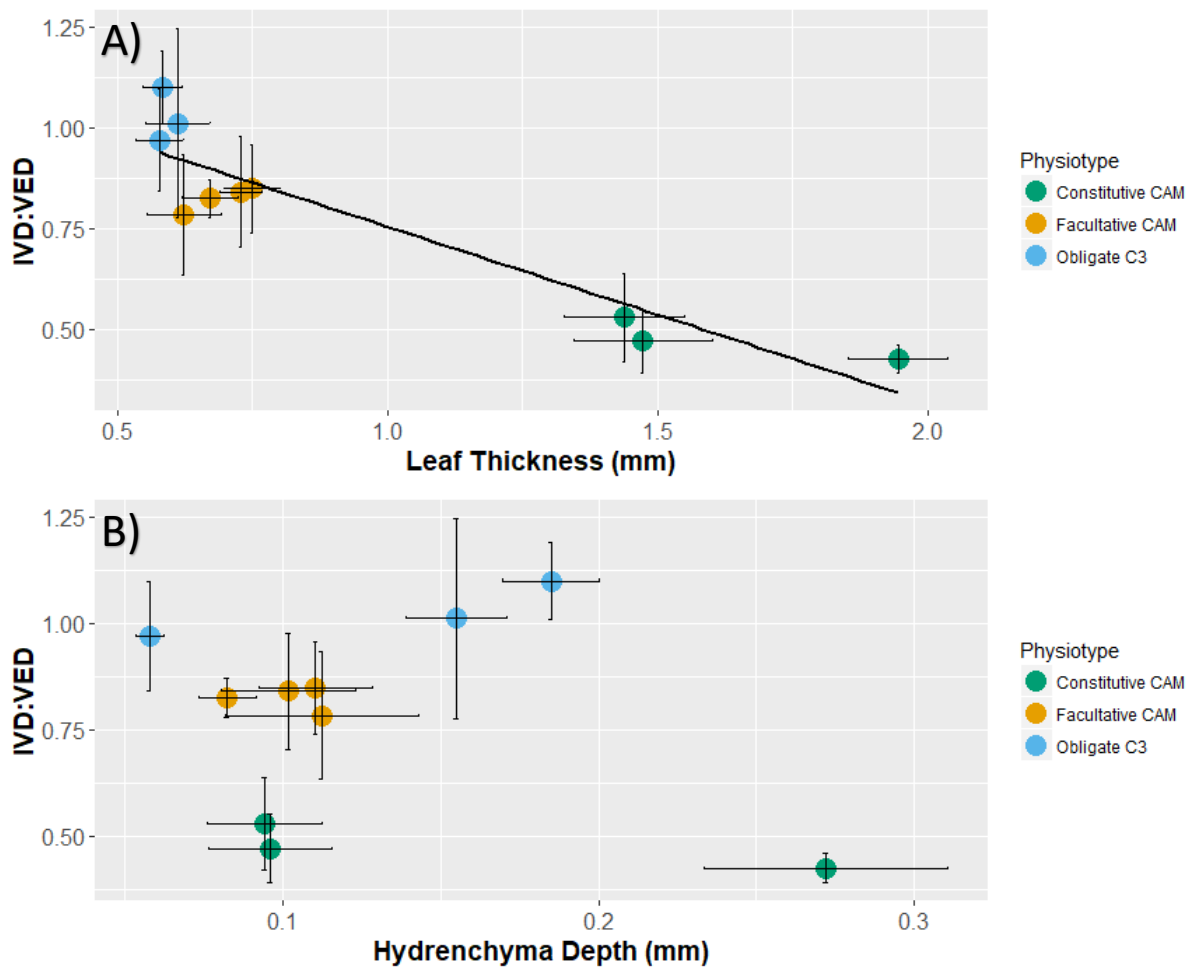


Fig. 5.10) Vascular overinvestment is an adaptation to leaf thickness, and not hydrrenchyma depth. A multiple linear regression model was built, with leaf thickness, hydrrenchyma depth and leaf area as explanatory variables and the IVD:VED ratio as a dependent variable. Leaf area had no significant effect or interaction terms, so it was removed from the model. The subsequent model, with leaf thickness and hydrrenchyma depth as explanatory variables, found that (A) species that do a greater proportion of photosynthetic assimilation at night have lower IVD:VED ratios ($p < 0.001$), whereas (B) hydrrenchyma depth is not a significant explanatory variable for IVD:VED ratios ($p = 0.107$). Data were log transformed before building the model, to meet the assumptions of this statistical test. For each species, $n = 7-9$, error bars represent ± 1 SD.

5.4.3 Overinvestment in Veins in Species Doing Crassulacean Acid Metabolism

It may seem paradoxical that the leaves of constitutive CAM plants can both have a low VLA and overinvest in veins. However, whilst VLA is lower in constitutive CAM species than C_3 relatives, it is not as low as would be expected based on leaf thickness. Put differently, when two-dimensional estimates of vein density (VLA or IVD) were standardised for a third dimension in the leaf (VED), the outcome was that constitutive CAM species had *higher* vein densities ($IVD:VED < 1$). The optimal vein placement in most leaves, to ensure water moves from the veins to the mesophyll most efficiently, is one where $IVD \approx VED$ (Noblin et al., 2008). In *Clusia* the IVD:VED ratios of obligate C_3 species are approximately 1, meaning that these species have 'optimal' vein placement for efficient movement of water into the mesophyll. Facultative and constitutive CAM species have IVD:VED ratios < 1 , meaning that these species are overinvesting in vasculature, according to the predictions of optimal vein placement made by Noblin et al., (2008) and Zwieniecki and Boyce (2014). Low IVD:VED ratios in *Clusia* appear to be an adaptation to leaf thickness, rather than to capacitance of the leaf, which is provided by hydrenchyma (Fig. 5.10). This suggests that vascular overinvestment is required to overcome increased apoplastic hydraulic resistance in thick leaves, rather than to allow rapid refilling of water pools required for capacitance. Models describing the movement of water outside of bundle sheath cells predict that species with increasing cell size and associated cell wall thickness conduct a greater proportion of their water through the apoplast, and a lower proportion through the gas phase (John et al., 2013; Buckley 2015). As the flow of water through the gas phase is faster, due to the free diffusion across the IAS, species that exhibit a greater proportion of flow through the apoplast will also be characterised by higher hydraulic resistance in the mesophyll. Therefore, it is likely that as *Clusia* species evolve larger cells (Barrera Zambrano et al., 2014), and possibly thicker cell walls (Chapter 2) for CAM, the apoplastic resistance increases. If this is the case, then low IVD:VED ratios could be a means to circumvent this problem; more veins will continue to allow leaves to efficiently transfer water to the mesophyll, even when chlorenchyma has developed pronounced tissue succulence.

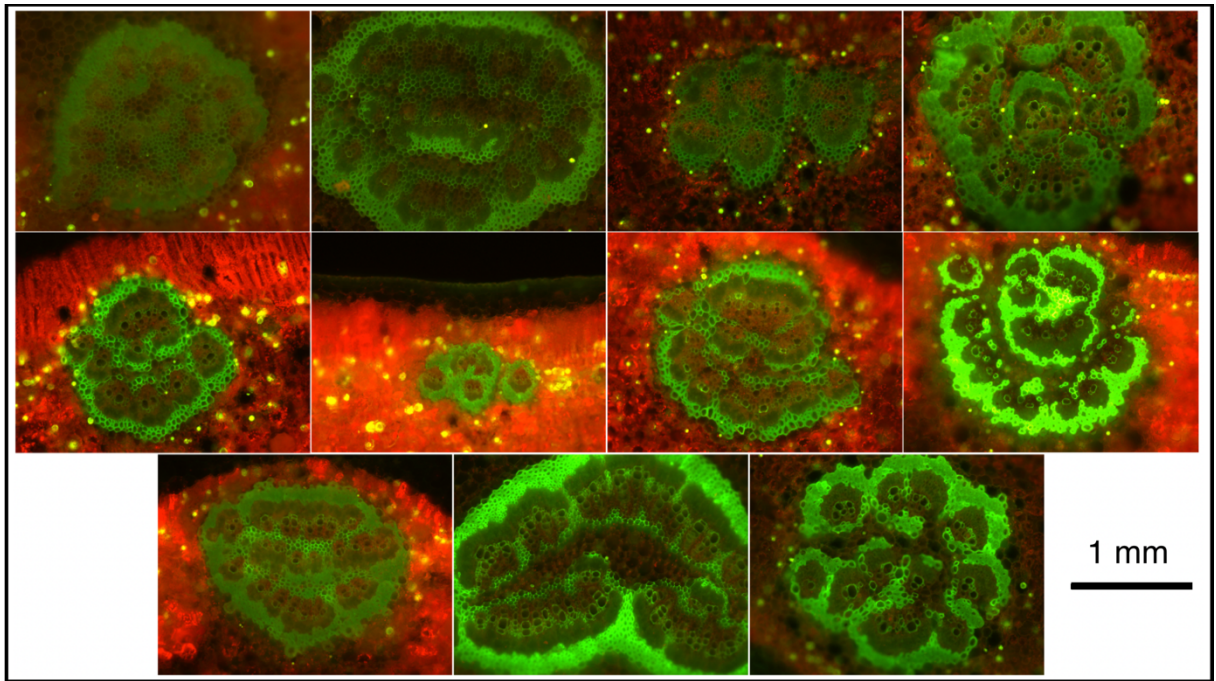


Fig. 5.11) Example images used to measure midrib xylem vessels. Top row, from left to right: *Clusia hilariana*, *C. fluminensis*, *C. alata*, *C. rosea*. Middle row: *C. minor*, *C. lanceolata*, *C. pratensis*, *C. aripioensis*. Bottom row: *C. tocuchensis*, *C. multiflora*, *C. grandiflora*.

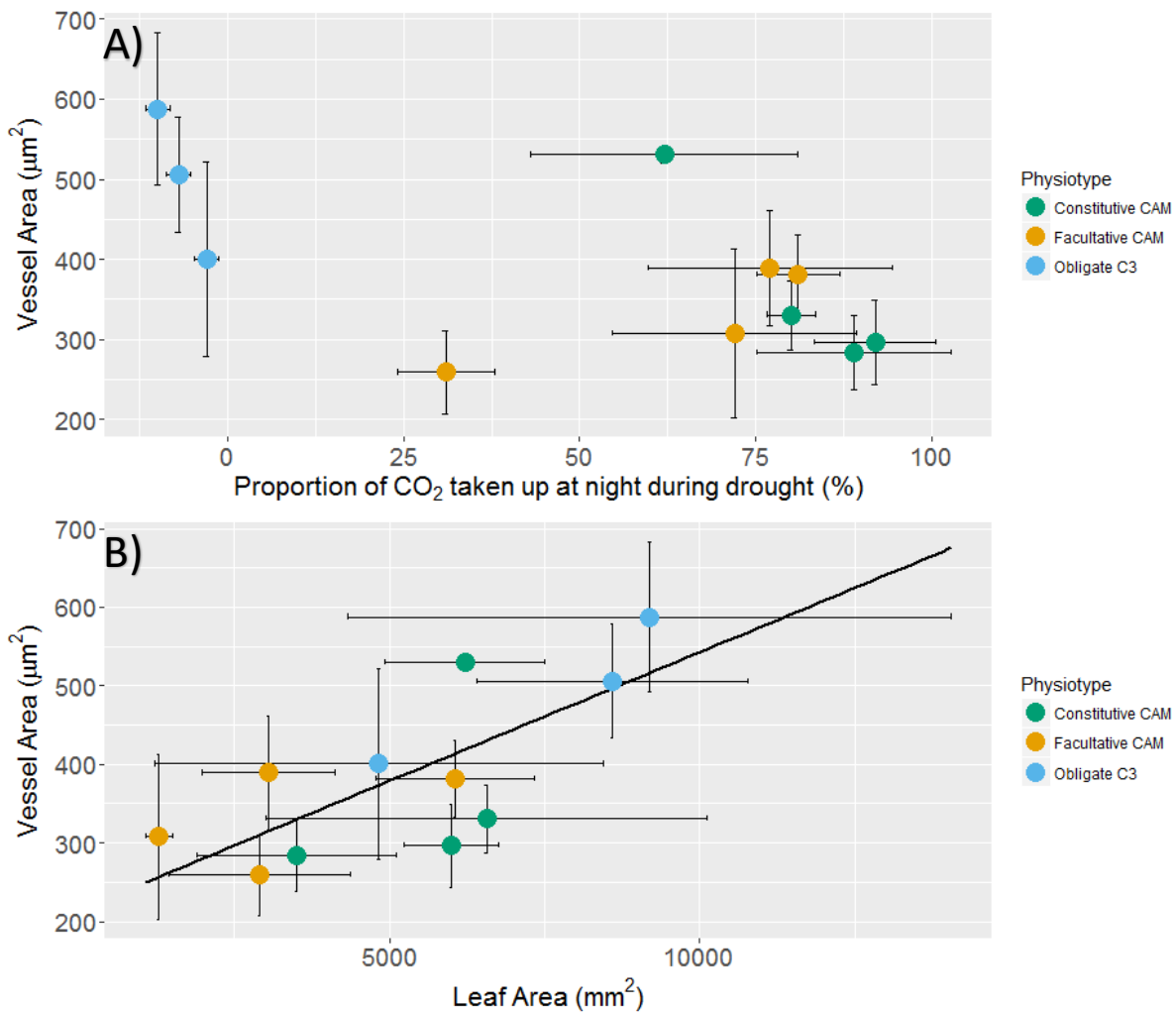


Fig. 5.12) Species that employ CAM photosynthesis during drought have not evolved narrower xylem vessels, in their midribs. (A) No significant relationship exists between the proportion of diel CO_2 assimilation that is taken up at night in drought treated plants and the average vessel cross-sectional area. (B) Species with larger leaves have wider vessels. A multiple linear regression found the proportion of photosynthesis, done at night did not correlate significantly with vessel cross-sectional area ($p = 0.89$), whereas leaf area showed a significant positive correlation with vessel cross-sectional area ($p < 0.001$). In addition, a significant interaction term exists between the aforementioned dependent variables ($p = 0.011$). For each species, $n = 4$, error bars represent ± 1 SD.

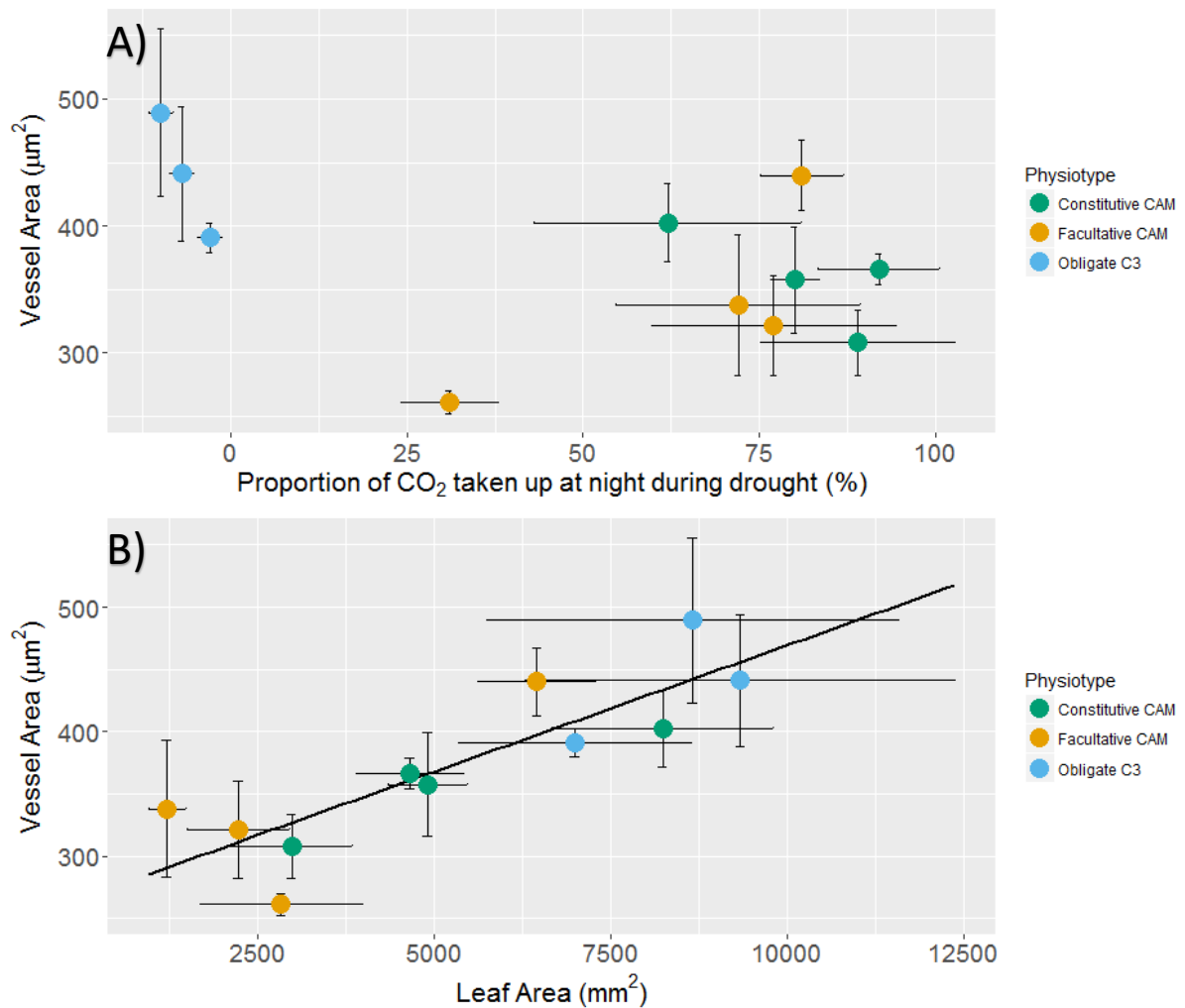


Fig. 5.13) Species that employ CAM photosynthesis during drought have not evolved narrower xylem vessels, in their petioles. (A) No relationship exists between the proportion of diel CO_2 assimilation that is taken up at night in drought treated plants and the average vessel cross-sectional area. (B) Species with larger leaves have wider vessels. A multiple linear regression found the proportion of photosynthesis, done at night did not correlate significantly with vessel cross-sectional area ($p = 0.87$), whereas leaf area showed a significant positive correlation with vessel cross-sectional area ($p < 0.001$). In addition, a significant interaction term exists between the aforementioned dependent variables ($p < 0.001$). For each species, $n = 4$, error bars represent ± 1 SD.

5.4.4 Crassulacean Acid Metabolism and Vessel Size; no Relationship Exists

The width of vessels was used as a proxy for leaf vulnerability to emboli, as wide vessels are known to be more vulnerable to the seeding of gaseous bubbles. However, no significant relationship was found between vessel diameter in either the petiole or the midrib and the strength of CAM under drought-treated conditions (Fig. 5.12, Fig. 5.13). This suggests that *Clusia* species doing CAM during drought events are no less likely than C₃ to experience negative water potentials that could cause emboli. However, this conclusion must be treated as preliminary, as without a direct estimation of xylem vulnerability, through the measurement of P50, it is not possible to precisely know how susceptible leaves are to emboli formation. Nevertheless, these data are in agreement with the conclusions of Chapter 3; namely that the presence of CAM does not result in a species becoming a 'drought avoider', in *Clusia*. CAM does not result in a species having a less negative turgor loss point (Chapter 3), nor does CAM appear to result in species conduit anatomy being less vulnerable to the formation of emboli. This calls into question the exact ecophysiological function that CAM is performing in *Clusia*. Whilst CAM will undoubtedly minimise water loss in this genus of tropical trees (Winter et al., 2005), it is not apparent that this reduced transpiration is for the prevention of damaging negative water potentials. It is possible that the purpose of CAM in *Clusia* is to prevent water loss in order to maintain metabolic rates and prevent carbon starvation during drought (Hartmann 2015; Choat et al., 2018). To understand if this is the case, a more thorough profiling of the metabolic physiology and molecular control of CAM in *Clusia* is needed (Chapter 6).

5.4.5 Towards a Complete Anatomical Characterisation of *Clusia*

This chapter builds on the characterisation of *Clusia* mesophyll tissue by Barrera Zambrano et al., (2014), which offers a uniquely comprehensive description of the anatomical traits associated with CAM (Edwards 2019) and has been cited as a paper 'of outstanding interest' by reviewers (Niechayev et al., 2019). The data presented here represent the first characterisation of vascular anatomy associated with CAM photosynthesis at the taxonomic level of the genus. The present study demonstrates that CAM not only affects the anatomy of photosynthetically active tissues, but also contributes to the vascular architecture; the low transpiration rate associated with CAM is associated with less VLA, and the succulent

photosynthetic tissue appears to require an overinvestment in veins to efficiently provide water to the mesophyll. These findings demonstrate that CAM requires a complex suite of anatomical changes, to optimise the photosynthetic and hydraulic needs of the leaf.

5.5 References

- Balsamo, R. A., & Uribe, E. G. (1988). Leaf anatomy and ultrastructure of the Crassulacean-acid-metabolism plant *Kalanchoe daigremontiana*. *Planta*, *173*(2), 183–189.
<https://doi.org/10.1007/BF00403009>
- Borland, A. M., Griffiths, H., Broadmeadow, M. S. J., Fordham, M. C., & Maxwell, C. (1993). Short-term changes in carbon-isotope discrimination in the C3-CAM intermediate *Clusia minor* L. growing in Trinidad. *Oecologia*, *95*(3), 444–453.
<https://doi.org/10.1007/BF00321001>
- Borland, A. M., Leverett, A., Hurtado-Castano, N., Hu, R., & Yang, X. (2018). Functional Anatomical Traits of the Photosynthetic Organs of Plants with Crassulacean Acid Metabolism. In W. W. Adams III & I. Terashima (Eds.), *The Leaf: A Platform for Performing Photosynthesis* (1st ed., pp. 281–305). https://doi.org/10.1007/978-3-319-93594-2_10
- Brodribb, T. J., Skelton, R. P., Mcadam, S. A. M., Bienaimé, D., Lucani, C. J., & Marmottant, P. (2016). Visual quantification of embolism reveals leaf vulnerability to hydraulic failure. *New Phytologist*, *209*(4), 1403–1409. <https://doi.org/10.1111/nph.13846>
- Buckley, T. N. (2015). The contributions of apoplastic, symplastic and gas phase pathways for water transport outside the bundle sheath in leaves. *Plant, Cell and Environment*, *38*(1), 7–22. <https://doi.org/10.1111/pce.12372>
- Chahine, M. T. (1992). The Hydrological Cycle and its Influence on Climate. *Nature*, *359*, 373–379. <https://doi.org/10.1038/359373a0>
- Chatelet, D. S., Clement, W. L., Sack, L., Donoghue, M. J., & Edwards, E. J. (2013). The evolution of photosynthetic anatomy in *Viburnum* (Adoxaceae). *International Journal of Plant Sciences*, *174*(9), 1277–1291. <https://doi.org/10.1086/673241>
- Choat, B., Brodribb, T. J., Brodersen, C. R., Duursma, R. A., López, R., & Medlyn, B. E. (2018). Triggers of tree mortality under drought. *Nature*, *558*(7711), 531–539.
<https://doi.org/10.1038/s41586-018-0240-x>

- Darwin, C. (1903). Letter 395. TO J.D. HOOKER. In *More Letters Of Charles Darwin Vol. II* (pp. 20–22). London: John Murray, Albemarle Street.
- de Boer, H. J., Drake, P. L., Wendt, E., Price, C. A., Schulze, E.-D., Turner, N. C., ... Veneklaas, E. J. (2016). Apparent Overinvestment in Leaf Venation Relaxes Leaf Morphological Constraints on Photosynthesis in Arid Habitats. *Plant Physiology*, *172*(4), 2286–2299. <https://doi.org/10.1104/pp.16.01313>
- Edwards, E. J. (2019). Evolutionary trajectories, accessibility, and other metaphors: the case of C4 and CAM photosynthesis. *New Phytologist*, *223*(4), 1742–1755. <https://doi.org/10.1111/nph.15851>
- Edwards, E. J., Chatelet, D. S., Sack, L., & Donoghue, M. J. (2014). Leaf life span and the leaf economic spectrum in the context of whole plant architecture. *Journal of Ecology*, *102*(2), 328–336. <https://doi.org/10.1111/1365-2745.12209>
- Eller, C. B., Lima, A. L., & Oliveira, R. S. (2016). Cloud forest trees with higher foliar water uptake capacity and anisohydric behavior are more vulnerable to drought and climate change. *New Phytologist*, *211*(2), 489–501. <https://doi.org/10.1111/nph.13952>
- Esau, K. (1965). *Anatomy of Seed Plants* (1st ed.). John Wiley & Sons.
- Franco, A. C., Olivares, E., Ball, E., Lüttge, U., & Haag-Kerwer, A. (1994). In situ studies of Crassulacean acid metabolism in several sympatric species of tropical trees of the genus *Clusia*. *New Phytologist*, *126*(2), 203–211. <https://doi.org/10.1111/j.1469-8137.1994.tb03938.x>
- Grams, T. E. E., Herzog, B., & Luttge, U. (1998). Are there species in the genus *Clusia* with obligate C3 photosynthesis? *Journal of Plant Physiology*, *152*(1), 1–9. [https://doi.org/10.1016/S0176-1617\(98\)80094-1](https://doi.org/10.1016/S0176-1617(98)80094-1)
- Gustafsson, M., Winter, K., & Bittrich, V. (2007). Diversity , Phylogeny and Classification of *Clusia*. In U. Lüttge (Ed.), *Clusia A Woody Neotropical Genus of Remarkable Plasticity and Diversity* (pp. 95–116). Retrieved from http://link.springer.com/chapter/10.1007/978-3-540-37243-1_7

- Heyduk, K., Burrell, N., Lalani, F., & Leebens-Mack, J. (2016). Gas exchange and leaf anatomy of a C3-CAM hybrid, *Yucca gloriosa* (Asparagaceae). *Journal of Experimental Botany*, 67(5), 1369–1379. <https://doi.org/10.1093/jxb/erv536>
- John, G. P., Scoffoni, C., & Sack, L. (2013). Allometry of cells and tissues within leaves. *American Journal of Botany*, 100(10), 1936–1948. <https://doi.org/10.3732/ajb.1200608>
- Klepsch, M., Zhang, Y., Kotowska, M. M., Lamarque, L. J., Nolf, M., Schuldt, B., ... Jansen, S. (2018). Is xylem of angiosperm leaves less resistant to embolism than branches? Insights from microCT, hydraulics, and anatomy. *Journal of Experimental Botany*, 69(22), 5611–5623. <https://doi.org/10.1093/jxb/ery321>
- Liu, H., Xu, Q., He, P., Santiago, L. S., Yang, K., & Ye, Q. (2015). Strong phylogenetic signals and phylogenetic niche conservatism in ecophysiological traits across divergent lineages of Magnoliaceae. *Scientific Reports*, 5(September 2014), 1–12. <https://doi.org/10.1038/srep12246>
- Lüttge, U. (1999). One morphotype, three physiotypes: Sympatric species of *Clusia* with obligate C3 photosynthesis, obligate CAM and C3-CAM intermediate behaviour. *Plant Biology*, 1(2), 138–148. <https://doi.org/10.1111/j.1438-8677.1999.tb00237.x>
- Males, J. (2017). Adaptive variation in vein placement underpins diversity in a major Neotropical plant radiation. *Oecologia*, 185(3), 375–386. <https://doi.org/10.1007/s00442-017-3956-7>
- Males, J. (2016). Think tank: water relations of Bromeliaceae in their evolutionary context. *Botanical Journal of the Linnean Society*, 181(3), 415–440. <https://doi.org/10.1111/boj.12423>
- Males, J., & Griffiths, H. (2018). Economic and hydraulic divergences underpin ecological differentiation in the Bromeliaceae. *Plant Cell and Environment*, 41(1), 64–78. <https://doi.org/10.1111/pce.12954>
- Mooney, H. A., Weisser, P. J., & Gulmon, S. L. (1977). Environmental Adaptations of the Atacaman Desert Cactus *Copiapoa haseltoniana*. *Flora*, 166(2), 117–124. [https://doi.org/10.1016/s0367-2530\(17\)32124-2](https://doi.org/10.1016/s0367-2530(17)32124-2)

- Niechayev, N. A., Pereira, P. N., & Cushman, J. C. (2019). Understanding trait diversity associated with crassulacean acid metabolism (CAM). *Current Opinion in Plant Biology*, *49*, 74–85. <https://doi.org/10.1016/j.pbi.2019.06.004>
- Noblin, X., Mahadevan, L., Coomaraswamy, I. A., Weitz, D. A., Holbrook, N. M., & Zwieniecki, M. A. (2008). Optimal vein density in artificial and real leaves. *Proceedings of the National Academy of Sciences of the United States of America*, *105*(27), 9140–9144. <https://doi.org/10.1073/pnas.0709194105>
- Ogburn, R. M., & Edwards, E. J. (2013). Repeated origin of three-dimensional leaf venation releases constraints on the evolution of succulence in plants. *Current Biology*, *23*(8), 722–726. <https://doi.org/10.1016/j.cub.2013.03.029>
- Popp, M., Kramer, D., Lee, H., Diaz, M., Ziegler, H., & Liittge, U. (1987). Crassulacean acid metabolism in tropical dicotyledonous trees of the genus *Clusia*. *Trees*, *1*, 238–247.
- Roberts, A., Griffiths, H., Borland, A. M., & Reinert, F. (1996). Is crassulacean acid metabolism activity in sympatric species of hemi-epiphytic stranglers such as *Clusia* related to carbon cycling as a photoprotective process? *Oecologia*, *106*(1), 28–38. <https://doi.org/10.1007/BF00334404>
- Sack, L., & Frole, K. (2006). Leaf structural diversity is related to hydraulic capacity in tropical rain forest trees. *Ecology*, *87*(2), 483–491. <https://doi.org/10.1890/05-0710>
- Sack, L., & Holbrook, N. M. (2006). Leaf Hydraulics. *Annual Review of Plant Biology*, *57*(1), 361–381. <https://doi.org/10.1146/annurev.arplant.56.032604.144141>
- Sack, L., & Scoffoni, C. (2013). Leaf venation : structure , function , development , evolution , ecology and applications in the past, present and future. *New Phytologist*, 983–1000. <https://doi.org/10.1111/nph.12253>
- Sack, L., & Tyree, M. T. (2005). Leaf Hydraulics and Its Implications in Plant Structure and Function. In *Vascular Transport in Plants* (pp. 93–114). <https://doi.org/10.1016/B978-0-12-088457-5.50007-1>

- Scoffoni, C., Rawls, M., McKown, A., Cochard, H., & Sack, L. (2011). Decline of Leaf Hydraulic Conductance with Dehydration: Relationship to Leaf Size and Venation Architecture. *Plant Physiology*, *156*(2), 832–843. <https://doi.org/10.1104/pp.111.173856>
- Scoffoni, C., Albuquerque, C., Brodersen, C. R., Townes, S. V., John, G. P., Bartlett, M. K., ... Sack, L. (2017). Outside-Xylem Vulnerability, Not Xylem Embolism, Controls Leaf Hydraulic Decline during Dehydration. *Plant Physiology*, *173*(2), 1197–1210. <https://doi.org/10.1104/pp.16.01643>
- Scoffoni, C., Albuquerque, C., Brodersen, C. R., Townes, S. V., John, G. P., Cochard, H., ... Sack, L. (2016a). Leaf vein xylem conduit diameter influences susceptibility to embolism and hydraulic decline. *New Phytologist*, *213*(3), 1076–1092. <https://doi.org/10.1111/nph.14256>
- Scoffoni, C., Chatelet, D. S., Pasquet-Kok, J., Rawls, M., Donoghue, M. J., Edwards, E. J., & Sack, L. (2016b). Hydraulic basis for the evolution of photosynthetic productivity. *Nature Plants*, *2*(6), 1–8. <https://doi.org/10.1038/nplants.2016.72>
- Sheffield, J., & Wood, E. F. (2008). Global trends and variability in soil moisture and drought characteristics, 1950-2000, from observation-driven simulations of the terrestrial hydrologic cycle. *Journal of Climate*, *21*(3), 432–458. <https://doi.org/10.1175/2007JCLI1822.1>
- Winter, K., Garcia, M., & Holtum, J. a. M. (2008). On the nature of facultative and constitutive CAM: environmental and developmental control of CAM expression during early growth of *Clusia*, *Kalanchoe*, and *Opuntia*. *Journal of Experimental Botany*, *59*(7), 1829–1840. <https://doi.org/10.1093/jxb/ern080>
- Winter, K. (2019). Ecophysiology of constitutive and facultative CAM photosynthesis. *Journal of Experimental Botany*, *In pr.* <https://doi.org/10.1093/jxb/erz002>
- Winter, K., Aranda, J., & Holtum, J. A. M. (2005). Carbon isotope composition and water-use efficiency in plants with crassulacean acid metabolism. *Functional Plant Biology*, *32*(5), 381–388. <https://doi.org/10.1071/FP04123>

Winter, K., Garcia, M., & Holtum, J. A. M. (2009). Canopy CO₂ exchange of two neotropical tree species exhibiting constitutive and facultative CAM photosynthesis, *Clusia rosea* and *Clusia cylindrica*. *Journal of Experimental Botany*, *60*(11), 3167–3177.
<https://doi.org/10.1093/jxb/erp149>

Winter, K., Holtum, J. A. M., & Smith, J. A. C. (2015). Crassulacean acid metabolism: a continuous or discrete trait? *The New Phytologist*, *208*(1), 73–78.
<https://doi.org/10.1111/nph.13446>

Winter, K., & Holtum, J. A. M. (2014). Facultative crassulacean acid metabolism (CAM) plants: powerful tools for unravelling the functional elements of CAM photosynthesis. *Journal of Experimental Botany*, *65*(13), 3425–3441.
<https://doi.org/10.1093/jxb/eru063>

Yang, X., Cushman, J. C., Borland, A. M., Edwards, E. J., Wullschleger, S. D., Tuskan, G. A., ... Holtum, J. A. M. (2015). A roadmap for research on crassulacean acid metabolism (CAM) to enhance sustainable food and bioenergy production in a hotter, drier world. *New Phytologist*, *207*(3), 491–504. <https://doi.org/10.1111/nph.13393>

Zwieniecki, M. A., & Boyce, C. K. (2014). Evolution of a unique anatomical precision in angiosperm leaf venation lifts constraints on vascular plant ecology. *Proceedings of the Royal Society B: Biological Sciences*, *281*(1779), 20132829–20132829.
<https://doi.org/10.1098/rspb.2013.2829>

Chapter 6. Crassulacean Acid Metabolism Allows Plants to Maintain Higher Core Metabolic Rates During Drought, in *Clusia*

6.1 Introduction

6.1.1 *Global Warming is Killing Trees*

With the growing recognition of increasing global temperatures, it has been predicted that the future will be characterised by more frequent and severe drought events (Sheffield and Wood 2008). The impact of droughts on forest ecosystems is already apparent across many temperate and tropical ecosystems (Choat et al., 2018). For example, in the tropics, during the 2005 drought in the Amazon rainforest, a 100 mm deficit in precipitation caused a 5.3 megagram ha⁻¹ drop in biomass; a loss which was caused by the death of trees (Phillips et al., 2009). Another example of tree mortality occurred during severe drought events in Northern Australia in late 2015, during which the die-off of 7400 ha of mangrove forests was documented (Duke et al., 2017). It is predicted that as drought continues to intensify across the globe, such die off events will intensify, and a greater area of landmass will become vulnerable to droughts (Choat et al., 2018). Therefore, it is integral that the physiological mechanisms that lead to tree death be fully understood, in order to understand how global warming is going to affect ecosystems and ecosystem services, worldwide.

6.1.2 *Tree Mortality: Hydraulic Failure vs Carbon Starvation*

The prevailing model for describing tree death in response to drought, outlines two events: hydraulic failure and carbon starvation (McDowell et al., 2008; Hartmann 2015; Choat et al., 2018; McDowell et al., 2019). Hydraulic failure is defined as an irreversible loss of stem hydraulic conductance, largely due to the formation of gaseous emboli in the xylem conduits. Emboli form during drought because water moving through the conduits exists at a negative pressure, and as a result can spontaneously change phase from a liquid to a gas (Milburn 1973; Brodersen et al., 2010; Williamson 2017; Klepsch et al., 2018). When a large number of embolism events occur, a tree will not be able to conduct water to distal tissue, which will consequently dehydrate and die (Choat et al., 2018). Whilst some species may be able to refill embolised conduits if water availability increases, if hydraulic refilling does not occur fast

enough, the tree will die (Brodersen et al., 2010; Brodersen and McElrone, 2013). In addition, dehydration during hydraulic failure is thought to cause turgor loss, which results in further decline in the hydraulic efficiency of water transport (Scoffoni et al., 2017; Trueba et al., 2019). In contrast, carbon starvation is defined as a partial loss of non-structural carbohydrate (NSC) reserves, which lead to energy deficits that slow metabolism and eventually cause mortality (Hartmann et al., 2015). Early work suggested that trees die of either hydraulic failure or carbon starvation; as researchers argued that these processes were mutually exclusive (McDowell et al., 2008). This framework proposed that if stomata remain open during drought, the plant would be able to continue assimilating atmospheric CO₂ but will experience greater water loss and consequently high xylem tension would cause drops in hydraulic conductance. In contrast, if stomata shut during drought, elevated xylem tensions were thought to be avoided, but CO₂ assimilation would no longer continue, and plants would experience carbon starvation. However, recently, it has become apparent that hydraulic failure and carbon starvation are not independent phenomena, but rather interlinked events that affect each other. For example, the refilling of embolised conduits is thought to rely on NSC reserves, which act as osmolytes, meaning that carbon starvation can amplify losses in hydraulic conductance (Brodersen et al., 2010; Nardini et al., 2011). In addition, leaf turgor pressure, which will drop if a plant is dehydrating due to hydraulic failure, is thought to be necessary for the mobilisation of NSC reserves via the phloem, meaning that hydraulic failure can facilitate carbon starvation during drought (Choat et al., 2018). Thus, hydraulic failure and carbon starvation interact in a complex and often overlapping manner, eventually combining to lead to tree death during drought. However, carbon starvation and hydraulic failure still provide a good overall framework for considering the variety of different events that occur in the lead up to the death of a tree, as these processes represent the interconnected processes that combine to contribute to plant mortality.

6.1.3 Avoiding Drought Induced Mortality: Crassulacean Acid Metabolism

One adaptation that is frequently found in taxa experiencing annual or seasonal drought is Crassulacean acid metabolism (CAM), a metabolic adaptation that allows plants to achieve remarkably high water use efficiencies (WUE is defined as the moles of carbon gained per mole of water lost) (Winter et al., 2005; Borland et al., 2014; Borland et al., 2015). CAM functions by assimilating CO₂ in the dark, into malic and sometimes citric acid, which is then

stored, overnight (Richards, 1915; Borland et al., 1993; Lüttge 1999; Niechayev et al., 2019). The following morning, these organic acids are decarboxylated to regenerate CO₂ within the leaf which is fed into the Calvin-Benson cycle behind closed stomata. As CAM allows plants to keep their stomata shut during the hottest, driest period of the day, it is most commonly thought to be an adaptation to reduce transpiration rates during drought events (Winter et al., 2005). Put simply, the high WUE conferred by CAM is often thought to be an adaptation to prevent hydraulic failure during drought events, as this metabolic adaptation slows the rate of transpirational water loss from plants (Winter et al., 2005).

If the ecophysiological role of CAM is to lower transpirational rates and prevent hydraulic failure, it is expected that species with this metabolic adaptation will not be as tolerant to low water potentials as C₃ species, as they will be able to avoid this stress in nature. In the Bromeliaceae, one study found that the hydraulic physiology of terrestrial species doing CAM is less tolerant to low water potentials; CAM species exhibit a turgor loss point (TLP) and a 50 % drop in leaf hydraulic conductance (P50) at less negative water potentials than C₃ relatives (Males and Griffiths, 2018). These differences in hydraulic physiology indicate that CAM acts to prevent hydraulic failure, as species with this metabolic adaptation have not evolved to be as tolerant to negative water potentials as C₃ relatives. However, another study, which analysed a greater number of species found no difference between the TLP of constitutive CAM and C₃ species (Males and Griffiths, 2017), suggesting that CAM does not prevent plants from needing to tolerate low water potentials during drought. It is possible that these contrasting results are the consequence of the large phylogenetic distance between species studied, as intergeneric comparisons may be introducing artefacts to this analysis, making it difficult to draw robust conclusions.

In order to minimise the effect of phylogenetic distance in comparative analyses, it is favourable to study phenotypically diverse, but closely related species (Scoffoni et al., 2016). The genus *Clusia* has an unparalleled level of photosynthetic diversity, as this genus contains a spectrum of C₃, C₃-CAM intermediate, facultative and constitutive CAM species (Popp et al., 1987; Grams et al., 1998; Holtum et al., 2004; Barrera Zambrano et al., 2014). Therefore, *Clusia* is an ideal system for studying the ecophysiology of CAM photosynthesis, as it is possible to undertake comparative analyses within a single genus. Research into the climatic niche of *Clusia* found that CAM is an adaptation to environmental aridity; constitutive CAM appears to

be an adaptation to low mean annual precipitation, and facultative CAM to low seasonal precipitation (Chapter 4). In addition, results from both experimental and modelling approaches have demonstrated that the ability to employ CAM slows the rate of water loss from plants, in *Clusia* (Winter et al., 2005; Chapter 2). However, the hydraulic physiology of *Clusia* does not show signs that CAM affects species' ability to tolerate low water potentials; CAM does not appear to affect species' TLP (Chapter 3), nor does succulent chlorenchyma tissue, which is needed to store organic acids at night for CAM, provide capacitance to the leaf (Chapter 2). Furthermore, investigations into vascular anatomy found no evidence that CAM affected vessel diameter; a characteristic known to affect vulnerability to embolism (Chapter 5). Taken together, these results suggest that the ecophysiological role of CAM during drought might not be completely explained as an adaptation to curtail hydraulic failure.

6.1.4 Does Crassulacean Acid Metabolism Curtail Carbon Starvation During Drought?

If the primary role of CAM is not to prevent hydraulic failure, it is possible that this carbon concentrating mechanism is instead acting to minimise carbon starvation during drought. As described above, carbon starvation occurs during drought due to the partial loss of NSC reserves and the slowing of metabolism. For example, one study found that in slow-dying *Pinus edulis* trees, the nocturnal respiratory rate declined as NSC reserves (defined as the starch + free low molecular weight sugars) were depleted (Sevanto et al., 2014). In addition, the same study found that during drought, an initial drop in photosynthetic assimilation was followed by a steady drop in the nocturnal respiratory rate. Therefore, these findings indicate that the process of carbon starvation involves the slowing down of metabolic rates, in association with the loss of NSC stores, prior to mortality events. Put differently, drops to photosynthesis and nocturnal respiration rates are symptoms of falling NSC reserves, during carbon starvation events that lead to plant mortality. Further evidence that carbon starvation affects core metabolic rates comes from work on *Eucalyptus saligna* trees. In *E. saligna*, drought treatment caused trees to exhibit lower nocturnal respiratory rates, but this effect was offset if plants were grown in elevated CO₂ environments; as high CO₂ allowed plants to assimilate more carbon and thereby minimised the effect of carbon starvation (Crous et al., 2011). Therefore, nocturnal respiratory rates represent a good diagnostic tool to analyse the effect of drought on core metabolism during carbon starvation.

Whilst CAM often causes a considerable reduction to productivity under well-watered conditions (Shameer et al., 2018), some evidence suggests that under droughted conditions CAM might cause plants to have higher carbon assimilation than C₃ species (Borland et al., 1998). By undertaking gas exchange during the night, when vapour pressure deficits are lower, plants doing CAM can maintain a greater diel CO₂ assimilation as drought progresses, as their stomata will not shut as much as C₃ species experiencing the same level of drought. For example, a comparison of diel CO₂ assimilation of *C. aripoensis* (weak inducible CAM), *C. minor* (strong inducible CAM) and *C. rosea* (constitutive CAM) found that species able to assimilate a greater amount of CO₂ at night experienced less severe drops in diel integrated net CO₂ uptake after 10 days of drought (Borland et al., 1998). In this study, *C. rosea* even experienced a slight *increase* in diel photosynthesis upon experiencing water-limited conditions (Borland et al., 1998). Therefore, it is possible that CAM is acting to maintain high metabolic rates during drought and preventing carbon starvation, in *Clusia*.

To test the hypothesis that CAM functions to maintain core metabolic processes under water stress, the drought response of *C. pratensis* (facultative CAM) was compared to that of *C. tocuchensis* (obligate C₃). By comparing two closely related species during a dry-down experiment, it was possible to identify physiological and/or genetic changes that occur exclusively in *C. pratensis*. If such changes are exclusively occurring in this facultative CAM species, they are likely to be associated with the 'CAM drought-response' rather than the C₃ drought response common to most plant species. By comparing diel patterns of net CO₂ exchange under well-watered and drought-treated conditions, this study assessed if CAM minimises the effect of drought-induced photosynthetic decline. Beyond this, measurements of nocturnal oxygen consumption were made to assess the degree to which CAM plants can maintain respiratory rates during drought, as nocturnal respiratory decline is symptomatic of carbon starvation (Crous et al., 2011; Sevanto et al., 2014). Even if plants are not sufficiently stressed to cause mortality, oxygen consumption rates still provide useful information about initial changes to respiration during drought. These initial changes to respiratory rates can be used to make strong inferences about which species is more likely to experience greater damage from metabolic declines should plants experience further dehydration. If the ecophysiological role of CAM is to minimise the symptoms of carbon starvation, it is expected

that *C. pratensis* should be able to maintain a higher nocturnal respiratory than *C. tocuchensis* under drought stress.

To complement these physiological approaches, the transcriptomes of each species were sequenced and analysed to explore the genetic regulation of the C₃ and CAM drought responses. After the assembly of a transcriptome, transcripts can be allocated categories, called gene ontology terms (GO terms) to describe the biological process or cellular compartment that is affected by a particular gene product. Through the use of GO enrichment analyses, it is possible to identify GO terms that occur more frequently in a set of differentially expressed genes than expected by their abundance in a transcriptome. Therefore, GO enrichment can identify biological processes or cellular compartments that are significantly affected when a species is subject to stress (Alexa et al., 2006). Previous work on tree species has demonstrated that metabolic declines are reflected in transcriptomic changes during drought events. For example, one study, which profiled the transcriptomic changes that occurred in *Populus trichocarpa* (Saliaceae), found that falling photosynthetic rates during drought are mirrored by declines in the transcript abundance of genes functioning in photosynthesis and starch synthesis (Tang et al., 2015). By performing GO enrichment on the genes that are upregulated in response to drought in *C. pratensis* and *C. tocuchensis*, this study explored metabolic changes that are controlled at the transcript level in *Clusia*. In addition, transcripts were identified that are upregulated exclusively in the CAM drought response. These are transcripts that exhibit increased steady-state abundance after drought in *C. pratensis*, but no upregulation of homologous genes in *C. tocuchensis*. These, so called 'core-CAM genes' were also analysed for GO enrichment to ask if the genetic CAM-drought response reflects changes to photosynthetic and/or respiratory processes. Together, the approaches used in this study attempt to characterise the effect of drought on core metabolism in *Clusia*, both at a physiological and genetic level, to understand if CAM is acting to minimise the symptoms of carbon starvation.

6.2 Materials and Methods

6.2.1 Plant Growth Conditions

Plants used for long-term gas exchange profiling (Fig. 6.1) were grown under the same conditions as for the gas exchange experiments described in Chapter 2. Namely, plants were propagated from cuttings taken from mature trees grown in a glass house in Cockle Park Farm, Newcastle. Cuttings were initially harvested 3 to 4 internodes below the stem apical meristem and were cut just below the node, to facilitate root growth. The species used were *C. toouchensis* (obligate C₃), *C. pratensis* (facultative CAM) and *C. fluminensis* (constitutive CAM). Cuttings were transferred to 200 ml pots containing 2:1:1 soil (John Innes No. 2, Sinclair Horticulture Ltd, Lincoln, UK), perlite (Sinclair, UK) and sand, to allow drainage. Pots were placed in a thermal incubator that warmed the soil to 23 °C. The incubator was lined with sand that was watered every 2 days to ensure the soil remained wet and the air remained humid. Individual pots were watered if, upon inspection they appeared too dry. Once plants had rooted, they were transferred to 3 litre pots containing a 3:1 mix of soil (John Innes No. 2, Sinclair Horticulture Ltd, Lincoln, UK) and sand. Plants were grown for 6 months following propagation under fluorescent lights (F100W/840, Polyflux cool white, Light Emission Technology, New York, USA), which provided approx. 300 $\mu\text{mol m}^{-2} \text{s}^{-1}$ PFD at plant height. Plants were kept at a relative humidity level of 65-75 % and a temperature of 27 °C during the day and 18 °C at night.

All other experiments were conducted in controlled growth rooms in Oak Ridge National Laboratory (ORNL), USA. Plants were propagated in 2013 from cuttings and grown in glass houses in ORNL. At least 3 weeks prior to sampling, plants were transferred to a controlled growth room and were subject to 12 hours light and 12 hours dark, with temperatures of 26 °C in the day and 19 °C at night. The day time light intensity was approx. 550 $\mu\text{mol m}^{-2} \text{s}^{-1}$ PFD at plant height. To study drought responses, watering was withheld, and pots weighed every day to determine the percentage of water lost. Intermediate drought was achieved at days 14 and 16 for *C. pratensis* and *C. toouchensis*, respectively. Full drought was achieved at days 20 and 22 for *C. pratensis* and *C. toouchensis*, respectively. Plants were sampled on different days to ensure that the same percentage of soil water content had been lost from the two species.

6.2.2 Gas Exchange

Long term drought gas exchange profiles (Fig. 6.1) were measured in controlled growth rooms in Newcastle University, for *C. tocuchensis*, *C. pratensis* and *C. fluminensis*. One week prior to starting a drought treatment plants were watered every day to ensure that soil was saturated with water. One day prior to drought, plants were watered heavily, so that the trays containing pots contained approx. 2 cm of water. The following day, plants were moved from the trays and a light-exposed leaf was inserted into a compact mini cuvette system, Central Unit CMS-400 linked to a BINOS-100 infra-red gas analyser (Heinz Walz GmbH, Effeltrich, Germany). The temperature of the cuvette tracked the temperature in the growth room and the gas flow through the cuvette was set to 400-500 ml min⁻¹. The rate of Photosynthetic assimilation was recorded every 20 minutes for 14 days. DIAGAS software (Heinz Walz GmbH, Effeltrich, Germany) was used to calculate the rates of photosynthetic assimilation on a leaf area basis.

Gas exchange measurements at ORNL were made on *C. tocuchensis* and *C. pratensis* using a LI-COR LI-6400XT Portable system. To avoid burn-out and failure of the cuvette fan under prolonged and continuous measurements of gas exchange during periods of extended drought, short term, diel measurements of leaf gas exchange were made at key stages of the dry-down experiment. Plants were measured under well-watered conditions, as well as those experiencing intermediate and full drought (outlined above). Leaf gas exchange was measured over 24 hours, using a leaf chamber fluorometer cuvette, set to track external light temperature conditions and data was logged every 15 minutes. These data were collected by Professor Anne Borland, prior to the start of this PhD project.

6.2.3 Nocturnal Oxygen Consumption

As the light reactions of photosynthesis produce O₂, all experiments to assess nocturnal O₂ consumption were performed in the dark or with a green light filter. Plants were sampled and measured under either well-watered or full drought conditions. Nocturnal O₂ consumption was measured using a Hansatech oxygen electrode and recorded with Hansatech oxygraph software (Hansatech Ltd, UK). The oxygen electrode was assembled according to the instruction manual, using cigarette rolling paper (Rizla Blue) as the connecting

membrane, and 50 % saturated KCl (Sigma) as the electrolyte. The chamber was kept at 19 °C, to replicate nocturnal growing conditions. Inside the chamber one foam disk was kept moist with deionised water and another with 1M KHCO₃ (Sigma). The oxygen electrode was calibrated by injecting 1 ml air and recording the signal change. From the proximal end of each leaf a 10 cm² leaf was cut and placed in the chamber. For each species/treatment combination, 3 leaves were measured. Leaves were given 4 minutes to acclimate and O₂ content measurements were then taken every 2.5 seconds for 20 minutes. This experiment ran overnight, starting from midnight and the experimental design was: the night was divided into 3 periods (early, mid and late), which were each 1.5 hours. Within each period, 1 measurement was taken for each species/treatment combination, in a random order. Lights did not turn on in the growth cabinet until 1.5 hours after the experiment had finished. Average night time O₂ consumption rate was calculated as the arithmetic mean across all periods for each species/treatment combination and was standardised by leaf fresh weight (Fig. 6.3), leaf dry weight (Fig. 6.4A) or per leaf area (Fig. 6.4B).

6.2.4 Malate and Citrate Assays

Leaves were sampled every 6 hours, over a 24-hour period, at 6 am, 12 pm, 6 pm and 12 am. A 30 mm diameter disk was cut from the leaf lamina, half way along the proximal-distal axis of the leaf, taking care to exclude the midrib. Leaf disks were immediately snap frozen in liquid N₂ before subsequent freeze-drying. Samples of freeze-dried tissue were crushed with a pestle and mortar into a fine powder and heated in 80 % methanol (Fisher) for 1 hour. Following this, samples were centrifuged for 15 minutes at 142 G, and the supernatant was aliquoted and 0.01 g of activated charcoal (BDH Ltd) was added. These samples were then re-centrifuged, and the supernatant was used for malate and citrate assays.

To analyse malate and citrate contents, the organic acid extracts were dried down and resuspended in 200 mMol Bicine buffer at pH 7.8. The concentration of malate and citrate was then measured using the biochemical assays of Hohorst (1970) and Möllering (1985), respectively. Malate and citrate contents were standardised on a fresh weight and dry weight basis, but as no qualitative difference existed between these, only the former is shown, for clarity (Fig. 6.5, Fig. 6.6).

6.2.5 Biological Sampling and RNA Sequencing

For each species, leaves were sampled from well-watered, intermediate drought-treated and strong drought-treated plants (outlined above). At each drought interval, leaves were sampled pre-dusk (6pm) and three biological replicates were used for each species/drought combination. RNA was extracted and paired-end short reads were sequenced using an Illumina HiSeq 2500 platform. Leaf sampling was conducted by Professor Anne Borland, RNA extractions and library preparation was conducted by Rebecca Albion in the laboratory of Prof John Cushman (University of Nevada, Reno) and sequencing was performed by Richard Tillett, University of Nevada, Reno.

6.2.6 De novo Transcriptome Assembly

Raw reads were trimmed and checked for quality using Trimmomatic. *De novo* transcriptome assemblies were constructed using three alignment programs (Soapdenovo trans, Bridger and Trinity) and assessed using BUSCO. As all BUSCO values were considered good, all individual assemblies were then combined using Evidentialgene, to generate a transcriptome. This work was carried out by Richard Tillett, University of Nevada, Reno.

6.2.7 Homolog Identification and Transcriptome Annotation

Open reading frames (ORFs) were identified in the transcriptome FASTA files using ORFfinder (NCBI). These ORFs were used as input into OrthoFinder (Emms and Kelly, 2015), to find homologs. OrthoFinder was configured to use the two *Clusia* translated transcriptomes, as well as the proteomes of *Arabidopsis thaliana* (Brassicaceae), *Kalanchoe laxiflora* (Crassulaceae) and *Poplar populus* (Salicaceae). In addition, another run of OrthoFinder was performed using 9 species: these were the five already mentioned, plus *Manihot esculenta* (Euphorbiaceae), *Ricinus communis* (Euphorbiaceae), *Linum usitatissimum* (Linaceae) and *Salix purpurea* (Salicaceae). Like *Clusia*, these additional species are all in the order Malpighiales. As OrthoFinder often identified many homologs for any one *Clusia* transcript, the top homolog from the most curated genome was allocated for descriptive purposes. For transcripts that could not be annotated using OrthoFinder, Conditional Orthology Assignment (Aubry et al., 2014) was used to find orthologs in the *Arabidopsis thaliana* genome (Fig. 6.7).

6.2.8 Transcript Quantification, Differential Expression and Comparison of Two *Clusia* Species

All reads were pseudoaligned using Kallisto version 0.42.5 (Bray et al., 2016), with 100 bootstrap samples, to quantify transcript abundance. The Sleuth R package (Pimentel et al., 2016) was then used to undertake differential expression analysis within one species. OrthoFinder was run, with only *Clusia* translated transcriptomes as input, to determine homologs between *C. pratensis* and *C. tocuchensis*. To determine which transcripts were differentially expressed in *C. pratensis* to a greater extent than in *C. tocuchensis*, an in-house R script was written. This script identified any transcript that showed a significant differential upregulation between well-watered and droughted conditions, that was also more highly upregulated (i.e. had a greater fold change) in *C. pratensis* than all homologs in *C. tocuchensis*. Homologs identified by OrthoFinder are a combination of orthologs and paralogs. It was also observed that the intermediate drought (day 14) in *C. pratensis* was another case of a C₃ drought response, as nocturnal CO₂ assimilation did not occur (Fig. 6.2). Therefore, to identify the 'core-CAM' genes, transcripts were only accepted if they also showed a higher rate of change between days 14 and 20 to that observed between days 0 and 14, in *C. pratensis* (Figs. 6.8 to 6.11). For all analyses a comparison was considered significant if $q < 0.01$.

6.2.9 Gene Ontology (GO) Enrichment Analysis

The GO terms were allocated for any one gene by extracting all unique GO terms from every homolog identified using OrthoFinder (see Homolog Identification and Transcriptome Annotation). GO terms were then used to construct a GO universe, separately for each species. GO enrichment analyses were performed using TopGO (Alexa et al., 2006) employing the 'weight01' algorithm, and Fishers exact test. GO enrichment was initially done on all genes that were upregulated between the well-watered and full drought treatment, for each species. A further GO enrichment was performed on the 'core-CAM genes', against the GO universe built from the *C. pratensis* transcriptome.

6.3 Results

6.3.1 Long Term Gas Exchange – Newcastle, UK

To assess the effect of CAM on drought induced CO₂ limitations, long-term gas exchange profiles were measured during a 12 day dry-down experiment. The obligate C₃ species, *C. tocuchensis*, showed a gradual decline in diurnal CO₂ assimilation, which resulted in a fall in the net diel CO₂ assimilation over the drought period (Fig. 6.1A). After 10 days of drought, *C. tocuchensis* exhibited no net diel CO₂ uptake, as diurnal assimilation was equal to nocturnal loss of CO₂ from respiration. After 12 days of drought, diurnal CO₂ assimilation completely stopped, and consequently *C. tocuchensis* exhibited a net CO₂ efflux of 12.85 Mol m⁻² day⁻¹. No initiation of CAM (i.e. net dark CO₂ uptake) was observed in this species. In contrast, diel CO₂ uptake in the facultative CAM species, *C. pratensis*, dropped by approximately 60 % after 5 days of drought, due to its changing photosynthetic physiology from C₃ to CAM (Fig. 6.1B). By the 5th night, nocturnal assimilation had reached approx. 1 μmol m⁻² s⁻¹, as *C. pratensis* had induced strong CAM. After this point, further drought did not cause any substantial drop in net diel CO₂ assimilation. The constitutive CAM species, *C. fluminensis*, did not exhibit any substantial drop in net diel CO₂ assimilation, and employed CAM photosynthesis throughout the entire dry-down treatment (Fig. 6.1C). Taken together, these data show that the use of CAM, either facultatively or constitutively, allows *Clusia* plants to maintain net CO₂ assimilation for longer during drought, compared to the C₃ species.

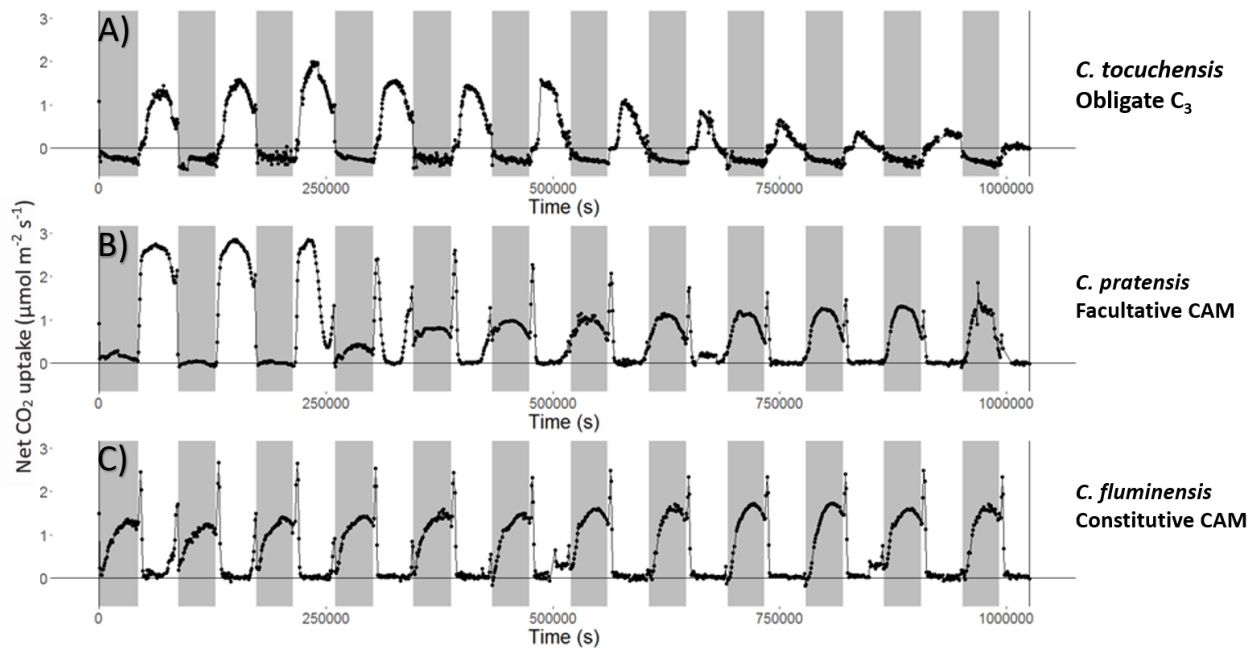


Fig. 6.1) Crassulacean acid metabolism prevents stomatal closure during drought and ensures a positive carbon balance. Net CO₂ assimilation was measured for a leaf of *C. tocuchensis* (obligate C₃), *C. pratensis* (facultative CAM), and *C. fluminensis* (constitutive CAM). White and grey bars represent day and night time, respectively. (A) Under well-watered conditions, during the first 2 diel cycles, *C. tocuchensis* exhibited a net positive diurnal CO₂ uptake and slight net nocturnal CO₂ efflux, indicative of C₃ photosynthesis. Upon experiencing drought, *C. tocuchensis* gradually reduced diurnal CO₂ assimilation. (B) Under well-watered conditions, during the first two days of drought, *C. pratensis* exhibited a positive diurnal CO₂ uptake indicative of C₃ photosynthesis. No nocturnal CO₂ efflux was detected, which may be indicative of very weak CAM. Upon experiencing drought, *C. pratensis* decreased net diurnal assimilation and increased net nocturnal CO₂ assimilation, by switching photosynthetic physiology from C₃ to CAM. At day four, all four phases of CAM gas exchange are present, but further drought caused a loss of phase IV and a reduction of phase II. (C) Under well-watered conditions, *C. fluminensis* exhibited all four phases of CAM gas exchange. There was a net positive diurnal CO₂ assimilation, due to phases II and IV of CAM, in the morning and evening, respectively. Midday rates of CO₂ assimilation were zero. In addition, a net positive nocturnal CO₂ assimilation was observed, due to phase I of CAM. Upon experiencing drought, *C. fluminensis* showed a loss of phase IV, but all other phases of CO₂ assimilation remained at an equivalent rate. These data represent representative graphs from three biological replicates per species.

6.3.2 Short Term Gas Exchange – Oak Ridge National Laboratory, USA

To measure the gas exchange profiles of the plants that were subsequently sampled for oxygen consumption and RNA-seq analysis, diel assimilation rates were recorded for *C. pratensis* and *C. tocuchensis*, grown in ORNL, USA. Gas exchange was measured using a LI-COR LI-6400XT IRGA platform. Under well-watered conditions, both species assimilated CO₂ during the day, and exhibited a low net CO₂ efflux at night (Fig. 6.2). Upon receiving an intermediate level of drought (14 – 16 days), both species exhibited a lower net positive diurnal gas exchange and a slight decrease in nocturnal CO₂ efflux. However, during intermediate drought, neither species exhibited any positive nocturnal CO₂ assimilation. Upon experiencing full drought (20 – 22 days), *C. pratensis* exhibited a further drop in diurnal CO₂ assimilation, such that photosynthesis only occurred in the morning, and to a lesser extent in the evening (Fig. 6.2A). Nocturnal CO₂ gas exchange became positive for *C. pratensis* plants under full drought conditions, indicative of an induction of CAM (Fig. 6.2A). In contrast, under full drought, *C. tocuchensis* exhibited a decrease in diurnal assimilation, but no positive nocturnal CO₂ gas exchange was seen, indicative of a C₃ drought response (Fig. 6.2B). Taken together, these data show that during the dry-down experiment, *C. pratensis* switched photosynthetic physiology from C₃ to CAM, whereas *C. tocuchensis* remained C₃. In addition, the induction of nocturnal CO₂ assimilation in *C. pratensis* shows that CAM allows plants to maintain higher rates of net CO₂ assimilation under extended drought than is possible with C₃ photosynthesis.

6.3.3 Nocturnal Oxygen Consumption

To explore the effect of CAM on respiratory metabolic rates during drought, an oxygen electrode was used to measure nocturnal O₂ consumption in *C. pratensis* and *C. tocuchensis*, under well-watered and full-drought conditions. *Clusia pratensis* plants under full drought in this experiment used CAM for net CO₂ assimilation. When O₂ consumption was standardised by leaf fresh weight (Fig. 6.3), no significant difference was found between nocturnal O₂ consumption in either species, under well-watered conditions. Upon receiving drought, *C. pratensis* exhibited a significant increase in nocturnal O₂ consumption, whereas no significant change was observed in *C. tocuchensis*. When O₂ consumption was standardised by leaf dry weight (Fig. 6.4A), no significant difference was found between nocturnal O₂ consumption in either species, under well-watered conditions. Drought induced a non-significant increase in

O₂ consumption in *C. pratensis* as well as a non-significant decrease in O₂ consumption in *C. toouchensis*. The consequence of these non-significant changes in each species was that under full drought, *C. pratensis* exhibited a significantly higher O₂ consumption rate than *C. toouchensis*. Finally, when O₂ consumption was standardised by leaf area (Fig. 6.4B), no significant difference was found between nocturnal O₂ consumption in either species, under well-watered conditions. Upon receiving drought treatment, *C. pratensis* exhibited a significant increase in nocturnal O₂ consumption, whereas *C. toouchensis* exhibited a small, non-significant decrease in nocturnal O₂ consumption. Taken together, these data show that the ability to induce CAM in response to drought is associated with an increase in nocturnal O₂ consumption, whereas the C₃ drought response shows no such change to O₂ consumption.

6.3.4 Diel Malate and Citrate Concentrations

To assess the effect of drought on the diel turnover of organic acids in the two species, malate and citrate contents were measured at dawn, midday, dusk and midnight in *C. pratensis* and *C. toouchensis*, under well-watered and full drought conditions. Under well-watered conditions, whilst both species used C₃ photosynthesis (Fig. 6.2), no diel changes in leaf malate content were observed (Fig. 6.5). Upon treatment with full drought, steady-state malate content started to cycle in *C. pratensis* (Fig. 6.5B), in conjunction with the induction of CAM (Fig. 6.2A). A comparison of dawn and dusk levels of malate, using a one-tailed, independent t-test found that in drought treated *C. pratensis* plants, malate content increased significantly over the night. In contrast, in *C. toouchensis* plants under droughted conditions, there was no significant nocturnal increase in malate content (Fig. 6.5B). Fig. 6.5 only shows data standardised by fresh weight, for clarity, as standardising these data by dry weight or leaf area had no effect on the qualitative appearance of the data or the outcome of statistical tests performed. Taken together, these data show that the induction of CAM in *C. pratensis* is associated with a nocturnal accumulation of malate, and that this metabolic change is not present in the C₃ drought response.

In addition to malate, citrate contents were measured for both *C. pratensis* and *C. toouchensis*, under well-watered and droughted conditions. Under well-watered conditions, neither species showed a significant accumulation of citrate overnight, although *C. pratensis* did show a decrease in citrate content in the first 6 hours of the night (Fig. 6.6A). After drought

treatment, the total citrate content was lower for both *C. pratensis* and *C. tocochensis*, than in well-watered conditions. In addition, drought-treated *C. pratensis* plants exhibited a significant nocturnal increase in citrate, whereas no significant difference was seen between citrate at dawn and dusk in *C. tocochensis* (Fig. 6.6B). Together, these data show that the induction of CAM in *C. pratensis* is associated with a nocturnal accumulation of citrate, and that this metabolic change is not present in the C₃ drought response.

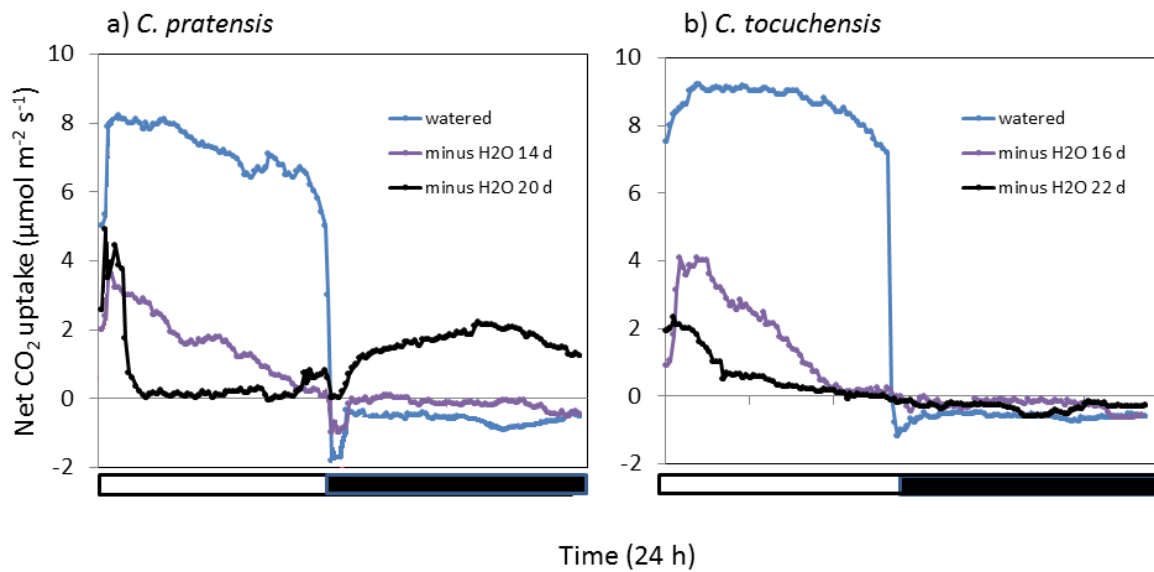


Fig. 6.2) Gas exchange profiles of *C. pratensis* and *C. tocuchensis* during drought. (A) *Clusia pratensis* employed C_3 photosynthesis in well-watered conditions. Fourteen days after the cessation of watering (intermediate drought), diurnal CO_2 assimilation decreased, and nocturnal CO_2 efflux became less negative. However, net positive CO_2 assimilation was not detected at this point. Twenty days after the cessation of watering (full drought), *C. pratensis* had completely switched into CAM; some CO_2 was assimilated in the morning, during phase II, but the majority of CO_2 assimilation was nocturnal. (B) *Clusia tocuchensis* employed C_3 photosynthesis in well-watered conditions. 16 days after the cessation of watering (intermediate drought), diurnal CO_2 assimilation decreased. Diurnal CO_2 assimilation had further decreased 22 days after the cessation of watering (full drought). CAM was not induced in *C. tocuchensis*. These data were measured by Professor Anne Borland, during the same dry-down experiment that was used to sample leaves for RNA-seq.

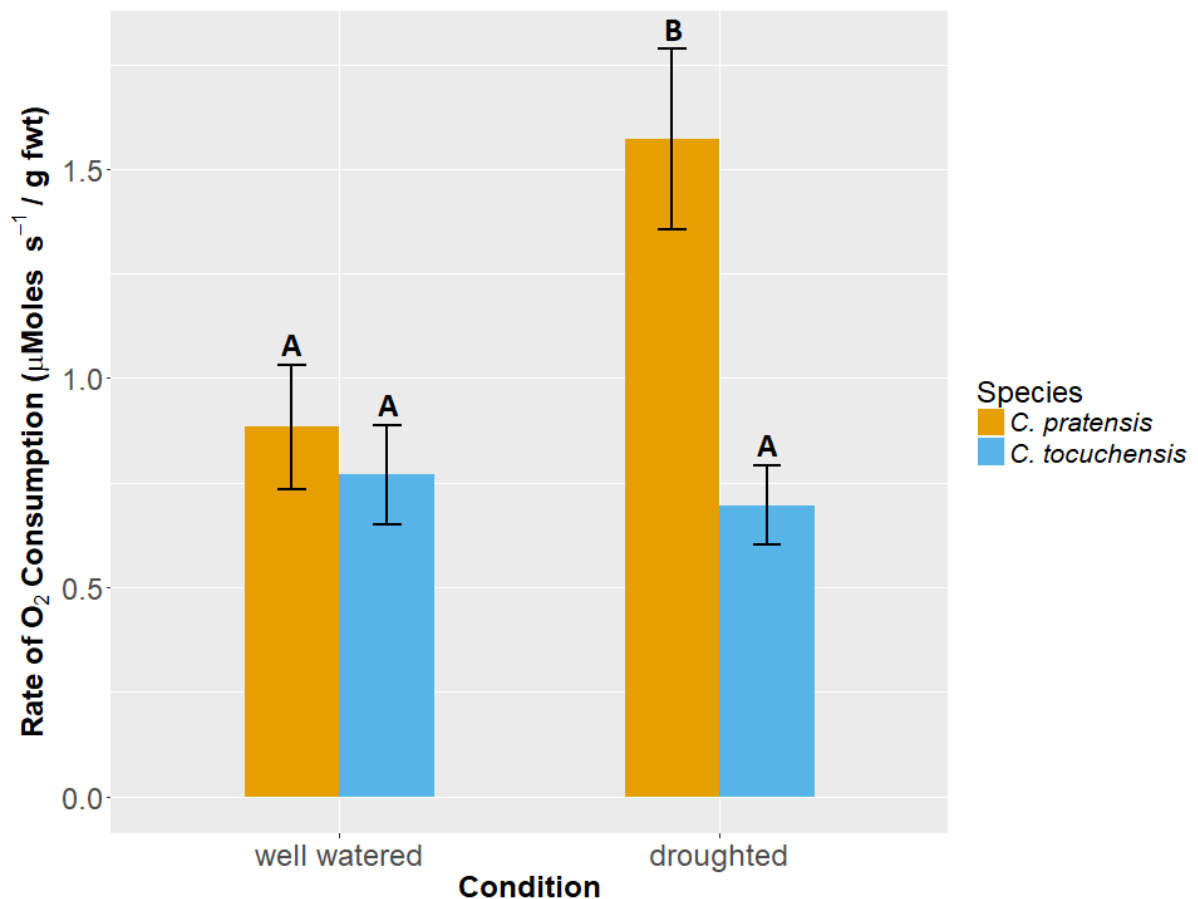


Fig. 6.3) The induction of Crassulacean acid metabolism during drought is accompanied by an increased nocturnal respiratory rate. Nocturnal oxygen consumption was measured in the facultative CAM species, *C. pratensis*, and the obligate C₃ species, *C. tocuchensis* under well-watered and drought-treated conditions. Data presented in this figure represents nocturnal O₂ consumption rate averaged on a per fresh weight basis. *Clusia pratensis* exhibited a large increase in nocturnal O₂ consumption when droughted, in conjunction with the induction of CAM. A two way ANOVA test found that O₂ consumption differed significantly between conditions ($p = 0.008$), and between species ($p < 0.001$). In addition, a significant interaction term between condition and species was found ($p = 0.002$). A post-hoc Tukey Kramer analysis found that the high O₂ consumption rate in the drought treated *C. pratensis* plants was significantly different from all other condition*species combinations. Groupings from the Tukey Kramer analysis are depicted as letters above each bar. For each bar, $n = 3$ and error bars represent ± 1 SD.

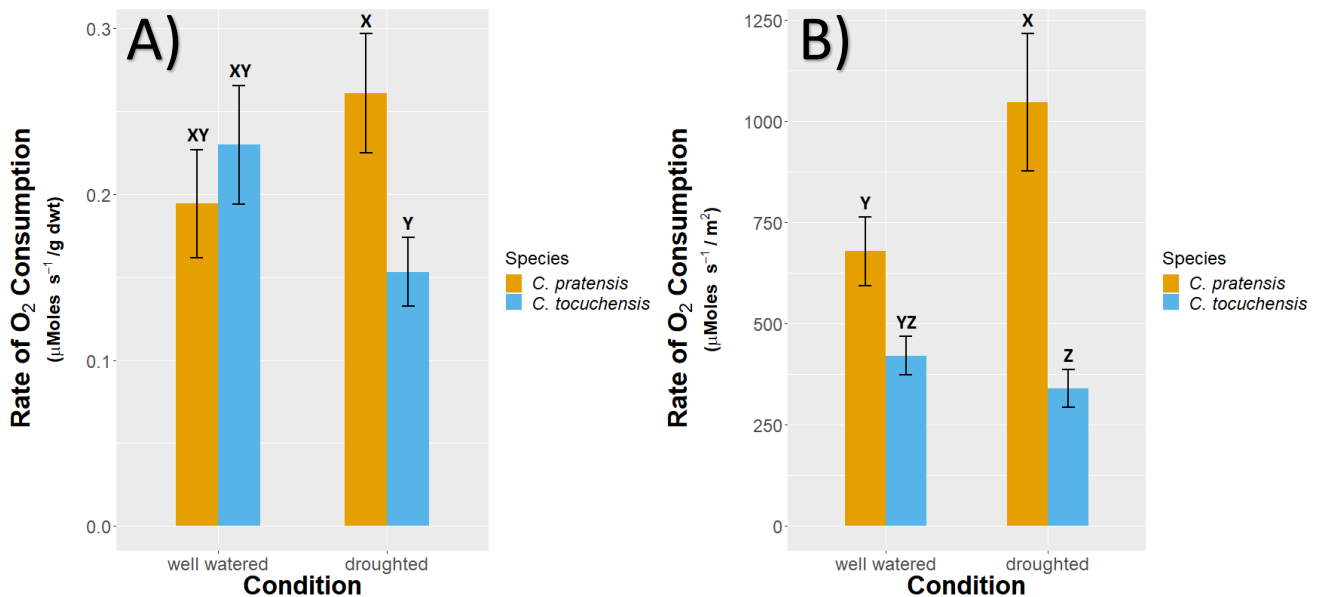


Fig. 6.4) The induction of Crassulacean acid metabolism during drought is accompanied by an increased nocturnal respiratory rate. Nocturnal oxygen consumption was measured in the facultative CAM species, *C. pratensis*, and the obligate C₃ species, *C. toouchensis*, under well-watered and drought-treated conditions. Data presented in this figure represents nocturnal O₂ consumption rate averaged (A) on a dry weight basis and (B) on a leaf area basis. (A) *Clusia pratensis* exhibited an increase and *C. toouchensis* exhibited a decrease in nocturnal O₂ consumption, averaged per dry weight, upon receiving drought treatment. A two way ANOVA test found that O₂ consumption did not differ significantly between conditions ($p = 0.794$), or between species ($p = 0.085$). However, a significant interaction term between condition and species was found ($p = 0.005$). A post-hoc Tukey Kramer analysis found that the high O₂ consumption rate did not differ between species under well-watered conditions, but upon drought treatment, *C. pratensis* exhibited a significantly higher O₂ consumption rate than *C. toouchensis*. (B) *Clusia pratensis* exhibited a large increase in nocturnal O₂ consumption, averaged per leaf area, when droughted. A two way ANOVA test found that O₂ consumption differed significantly between conditions ($p = 0.039$), and between species ($p < 0.001$). In addition, a significant interaction term between condition and species was found ($p = 0.005$). A post-hoc Tukey Kramer analysis found that in *C. pratensis*, the O₂ consumption rate was significantly higher when plants were drought-treated than when they were well-watered. In contrast, the same Tukey-Kramer analysis found that no significant difference could be detected between well-watered and droughted *C. toouchensis* leaves. For both graphs, groupings from the Tukey Kramer analyses are depicted as letters above each bar. For each bar, $n = 3$ and error bars represent ± 1 SD.

6.3.5 RNA-seq: Transcript Annotation

Of the three different methods employed for transcript annotation, each annotated a similar number of transcripts (Fig. 6.7). Both runs of OrthoFinder, as well as the Conditional Orthology Assignment were able to successfully annotate > 70 % of transcripts for each species. OrthoFinder was the preferred method of annotation, as it determines orthogroups (all paralogs and orthologs descended from a gene present in the last common ancestor of the species included in the OrthoFinder run), which can be used in downstream analyses (see GO enrichment analysis). However, the final annotation was completed by combining the OrthoFinder analysis (using 9 species in total) and the transcripts that were exclusively annotated by the conditional Orthology Assignment program, to maximise the annotation coverage. The end result of this annotation effort was that 84.87 % of *C. pratensis* transcripts and 83.97 % of *C. tocuchensis* transcripts were annotated.

6.3.6 Identification and Expression of 'Core-CAM Genes'

To dissect the putative CAM genes from those involved in a C₃ drought response, an in-house script was used to compare the differential expression in each species. This method identified genes that were more upregulated in *C. pratensis* than homologs in *C. tocuchensis* over the full drought treatment. These genes were cross referenced against genes that were more upregulated in the last 6 days of drought than the first 14 days of drought, in *C. pratensis*. The result of this was the identification of 584 transcripts. Manual inspection of the 584 genes found that it contains genes known to function in CAM, such as a gene encoding the carboxylation enzyme, phosphoenolpyruvate carboxylase (PEPC) (Fig. 6.8) and the decarboxylation enzyme PEP carboxykinase (PEPCK) (Fig. 6.9). In addition, the 'core-CAM genes' list contained the decarboxylation enzyme nicotinamide adenine dinucleotide phosphate (NADP-ME) (Fig. 6.10), and the aluminium activated malate transporter (ALMT) (Fig. 6.11), which are also known to function in CAM in other taxa (Wai et al., 2017; Heyduk et al., 2019a). Furthermore, many other genes known to be associated with CAM were present, such as 13 transcripts encoding malate dehydrogenase (MDH) and 2 encoding PEPC4, were present in the 'core-CAM genes'. The steady-state expression profiles of MDH and PEPC4 isoforms are not shown, for clarity, as they strongly resemble the gene

expression profiles depicted (Figs 6.8 to 6.11). Taken together, these data suggest that this analysis has been successful in identifying 'core-CAM genes' in *Clusia*.

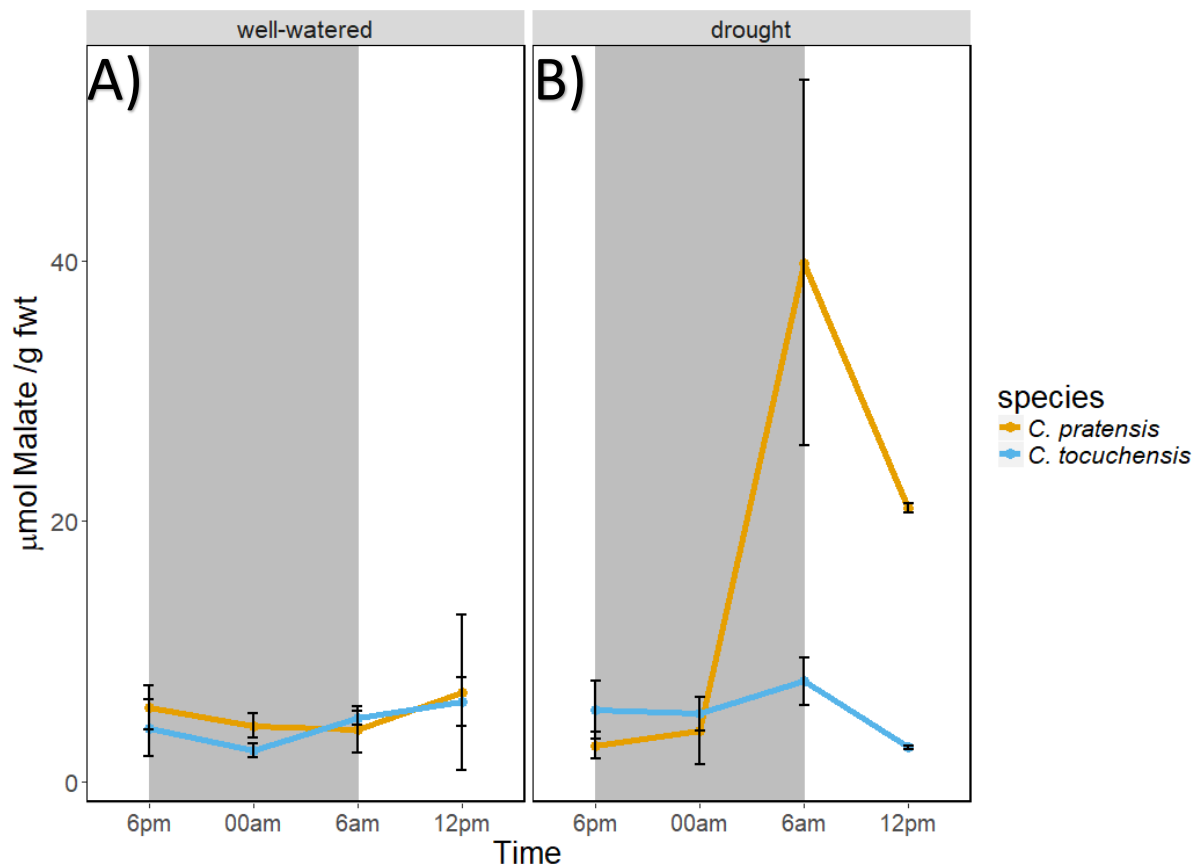


Fig. 6.5) Drought induces nocturnal malate accumulation in the facultative CAM species, *C. pratensis*. (A) Under well-watered conditions no accumulation of malate was detected in either *C. pratensis*, or the obligate C_3 species, *C. toouchensis*. A one-tailed, independent t-test comparing malate concentration at dusk (6pm) and dawn (6am) in well-watered *C. pratensis* plants found no significant difference ($p = 0.853$). Likewise, a one-tailed, independent t-test comparing malate concentration at dusk (6pm) and dawn (6am) in well-watered *C. toouchensis* plants found no significant difference ($p = 0.303$). (B) Under drought treatment, a significant nocturnal accumulation of malate occurred in *C. pratensis*, but not in *C. toouchensis*. A one-tailed, independent t-test comparing malate concentration at dusk (6pm) and dawn (6am) in drought-treated *C. pratensis* plants found a significant difference ($p = 0.022$). However, a one-tailed, independent t-test comparing malate concentration at dusk (6pm) and dawn (6am) in well-watered *C. toouchensis* plants found no significant difference ($p = 0.127$). For each species, $n = 3$ and error bars represent ± 1 SD.

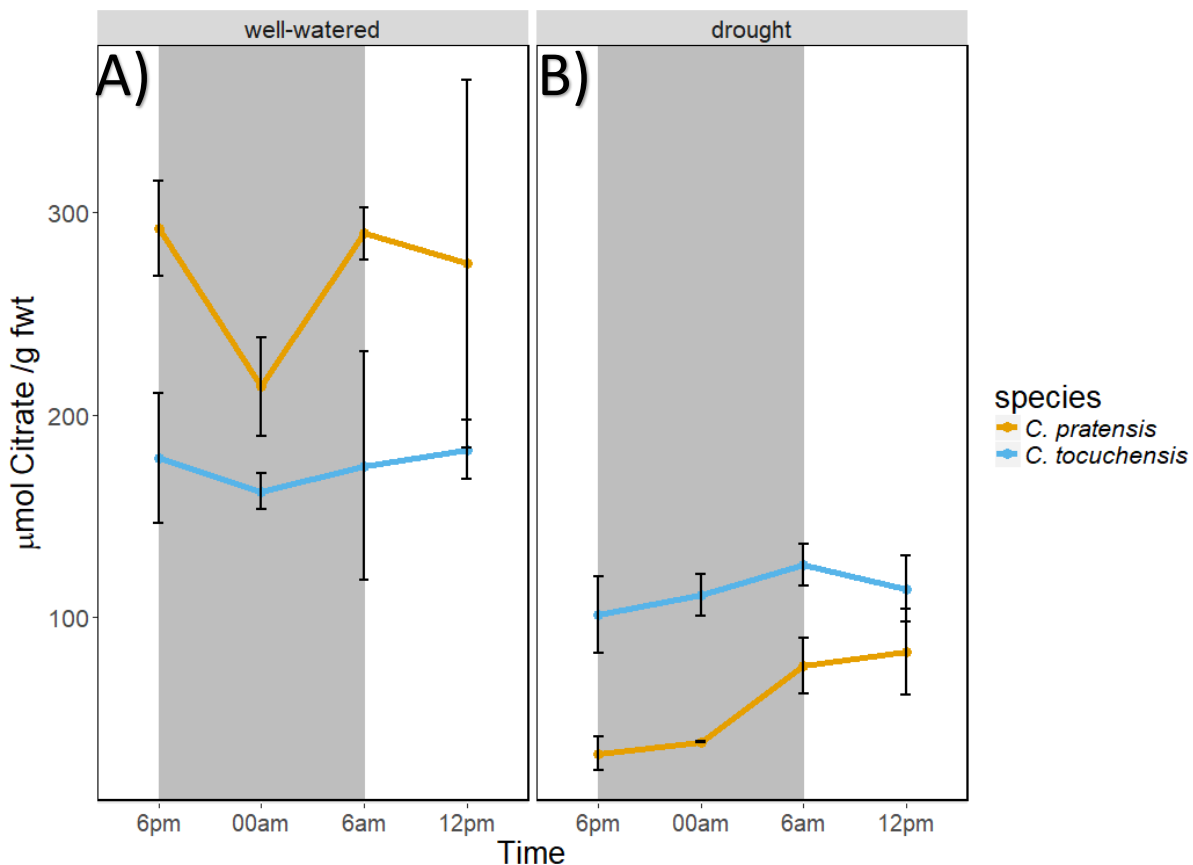


Fig. 6.6) Drought induces nocturnal citrate accumulation in the facultative CAM species, *C. pratensis*. Both species exhibited a drop in overall citrate concentrations in response to drought treatment. However, drought also caused *C. pratensis* (facultative CAM) to accumulate citrate overnight, whilst no such nocturnal accumulation of citrate was observed in *C. toouchensis* (obligate C_3). (A) Under well-watered conditions no accumulation of citrate was detected in either *C. pratensis*, or the obligate C_3 species, *C. toouchensis*. A one-tailed, independent t-test comparing citrate concentration at dusk (6pm) and dawn (6am) in well-watered *C. pratensis* plants found no significant difference ($p = 0.563$). Likewise, a one-tailed, independent t-test comparing citrate concentration at dusk (6pm) and dawn (6am) in well-watered *C. toouchensis* plants found no significant difference ($p = 0.538$). (B) Under drought treatment, a significant nocturnal accumulation of citrate occurred in *C. pratensis*, but not in *C. toouchensis*. A one-tailed, independent t-test comparing citrate concentration at dusk (6pm) and dawn (6am) in drought-treated *C. pratensis* plants found a significant difference ($p = 0.008$). However, a one-tailed, independent t-test comparing citrate concentration at dusk (6pm) and dawn (6am) in well-watered *C. toouchensis* plants found no significant difference ($p = 0.071$). For each species, $n = 3$ and error bars represent ± 1 SD.

6.3.7 Gene Ontology Enrichment

Initial GO enrichment was performed on the genes that were significantly upregulated between well-watered and full drought treatments. This was done separately for each species. For clarity, these lists of enriched GO terms are presented in Appendix A. Exploring the GO terms pertaining to the 'cellular compartment' (CC) of the gene product found that the upregulated genes in *C. pratensis* were enriched for 28 CC GO terms and the upregulated genes in *C. tocuchensis* were enriched for 22 CC GO terms (Table A.1 and A.2, respectively). Of these, 12 CC GO terms were enriched in the drought response transcriptomes of both species. CC GO terms that were enriched in both species included 'chloroplast', 'apoplast', 'nucleus' and 'plasma membrane'. Many of the CC GO terms that were uniquely enriched in *C. pratensis* related to mitochondrial locations, such as 'mitochondrial envelope', 'mitochondrial intermembrane space' and 'mitochondrial respiratory chain complex I'. In contrast, many of the CC GO terms that were exclusively enriched in the upregulated genes of *C. tocuchensis* related to chloroplastic locations, such as 'Chloroplast photosystem II', 'Chloroplast thylakoid lumen' and 'photosystem II antenna complex'. No CC GO terms relating to mitochondria were enriched in the upregulated *C. tocuchensis* genes.

Analysis of the GO terms pertaining to the 'biological process' (BP) of the gene product was also performed (Appendix A; Tables A. 3 and A. 4). Exploring the BP GO terms found that the upregulated genes in *C. pratensis* were enriched for 138 GO terms and the upregulated genes in *C. tocuchensis* were enriched for 72 BP GO terms (Table A.3 and A.4, respectively). Of these, 37 BP GO terms were enriched in the drought response transcriptomes of both species. BP GO terms that were enriched in both species included 'abscisic acid-activated signalling pathway', 'regulation of hydrogen peroxide metabolic process' and 'response to water deprivation'. The BP GO terms that were enriched exclusively in *C. pratensis* included 'aerobic respiration', 'mitochondrial electron transport, NADH to ubiquinone' and 'tricarboxylic acid cycle', amongst many others. The BP GO terms enriched exclusively in *C. tocuchensis* included 'wax biosynthetic process', 'cuticle development', 'leaf senescence' and 'stomatal movement'. In addition, a number of BP GO terms related to photosynthesis and chloroplastic repair/maintenance were enriched, such as 'thylakoid membrane organisation', 'nonphotochemical quenching', 'photosystem II repair' and 'photosystem II stabilisation'. No BP GO terms relating to mitochondria were enriched in the upregulated *C. tocuchensis* genes.

To provide a more refined analysis of the transcriptomic changes that occurred exclusively in the CAM drought response, a GO enrichment analysis was performed on the 'core CAM genes'; i.e. genes upregulated in the last 6 days of drought in *C. pratensis* that are also upregulated more in *C. pratensis* than *C. tocutensis*. It was predicted that the core CAM genes would be enriched in GO terms that relate to mitochondrial respiration, as this pattern was observed in initial GO enrichment analysis of upregulated *C. pratensis* genes. This prediction was confirmed, as the core-CAM genes were enriched in CC GO terms such as 'mitochondrial respiratory chain complex I', 'mitochondrial proton-transporting ATP synthase complex' and 'tricarboxylic acid cycle enzyme complex'. In fact, of the 27 CC GO terms enriched in the 'core-CAM genes', 12 relate to mitochondrial functions. Furthermore, of these 12 mitochondria-related enriched CC GO terms, 5 are enriched in the core-CAM genes, that were not identified in the GO enrichment done on just the upregulated *C. pratensis* genes. These 5 CC GO terms are 'mitochondrial matrix', 'mitochondrial proton-transporting ATP synthase complex', 'mitochondrial inner membrane', 'tricarboxylic acid cycle enzyme complex' and 'pyruvate dehydrogenase complex. Further analysis of the 'core-CAM' genes identified 'tricarboxylic acid cycle' as the most significantly enriched BP GO term. In addition, other BP GO terms, such as 'ATP synthesis coupled proton transport' and 'aerobic respiration' are significantly enriched ($p = 4.4 \times 10^{-12}$ & $p = 0.00644$, respectively, data not shown). Taken together, these data strongly suggest that genes involved in mitochondrial respiration undergo a greater upregulation during the CAM response to drought than in the C_3 drought response.

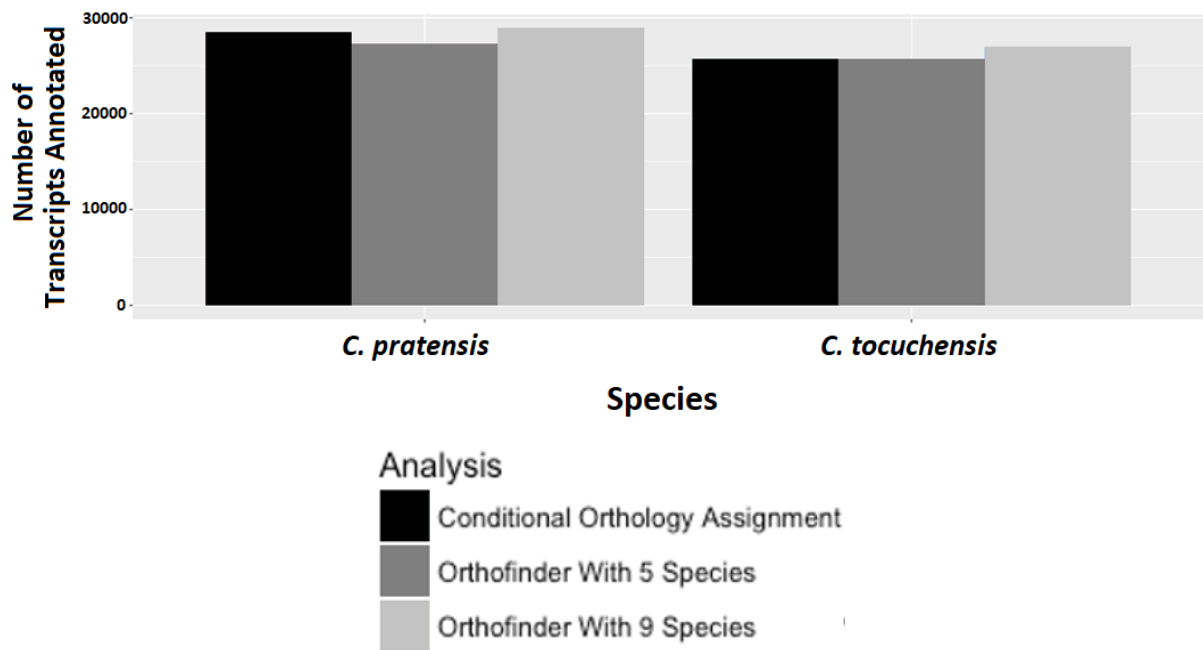


Fig. 6.7) Three annotation methods exhibited similar success rates, based on number of transcripts annotated. Transcripts were annotated using either a conditional orthology assignment tool, or using OrthoFinder with 5 or 9 species (including the two *Clusia* species in this study). Each method for annotation was able to annotate a similar number of genes, but using OrthoFinder with 9 species found the greatest number of annotations, for both species.

Table 6.1) Comparison of OrthoFinder (using 9 transcriptomes) with Conditional Orthology Assignment tool. Both tools were used to annotating transcripts in *C. pratensis* and *C. tocuchensis*.

Species	Annotation attempt	Percentage of transcriptome annotated (%)	Total transcripts annotated	Number of transcripts exclusively annotated
<i>C. pratensis</i>	OrthoFinder (9 species)	76.43	28889	2794
<i>C. tocuchensis</i>	OrthoFinder (9 species)	75.08	26947	1897
<i>C. pratensis</i>	Conditional Orthology Assignment	75.37	28491	3192
<i>C. tocuchensis</i>	Conditional Orthology Assignment	71.49	25658	3186

6.4 Discussion

6.4.1 Summary of Findings

The precise ecophysiological purpose of CAM in *Clusia* has stumped scientists over the last 20 years, due to the observation that CAM and C₃ physiotypes can often co-occur, in seasonally arid tropical dry forests (Grams et al., 1998; Lüttge 1999). For example, in Brazilian restinga the constitutive CAM species, *C. fluminensis* becomes deciduous during the dry season, whereas the sympatric weak CAM species, *C. lanceolata* keeps its leaves (Roberts et al., 1996). Early work explored if CAM was in fact an adaptation to tolerate dangerously high light levels, however this remained an unsatisfactory explanation (Roberts et al., 1996; Lüttge 2002; Kornas et al., 2009). To readdress the ecophysiological role of CAM in *Clusia*, this thesis has explored the role of CAM within the current framework of the causes of tree mortality; hydraulic failure and carbon starvation combining to lead to the death of a tree (Choat et al., 2018). Evidence from previous chapters found that, in *Clusia*, CAM is not associated with a higher TLP (Chapter 3), leaf capacitance (Chapter 2), nor does CAM affect vessel diameters (measured as a proxy for vulnerability to embolism) (Chapter 5). Thus, the hydraulic adaptations in *Clusia* show no signs that CAM is a typical drought avoidance strategy. Therefore, the primary ecophysiological role of CAM is unlikely to be the evasion of low water potentials that can cause hydraulic failure. This study aimed to investigate if CAM prevents metabolic rates from slowing during drought and thus to assess if the primary ecophysiological role of CAM is to prevent the symptoms of carbon starvation during drought. Whilst carbon starvation is defined as the partial loss of NSC reserves, this study focused on metabolic rates that are known to drop in the lead up to tree mortality (Sevanto et al., 2014). To this end, the data presented here showed that both photosynthetic and respiratory rates remained higher during the CAM response to drought than in C₃ species. Furthermore, RNA-seq data indicated that higher respiratory rates were the consequence of transcriptomic changes; as well as the upregulation of genes previously known to function in CAM, genes associated with mitochondrial respiration were more enriched in the CAM, and not the C₃ drought response. Taken together, these data demonstrate that the induction of CAM causes plants to maintain photosynthesis and also increase their respiratory metabolic rates during drought, thereby combatting the slowing down of metabolism that is symptomatic of carbon starvation.

6.4.2 Phenotypic Characterisation of *Clusia pratensis* and *C. tocuchensis*

To confirm that *C. pratensis* was employing CAM under drought stress (Holtum et al., 2004; Winter et al., 2008; Winter and Holtum, 2014), a combination of gas exchange and organic acid assays were employed. Gas exchange found that in both plant growth facilities, low light (Newcastle, UK) and higher light (ORNL, USA), the induction of all four phases of CAM could be triggered in *C. pratensis* after the cessation of watering. No such facultative employment of CAM was seen in *C. tocuchensis* (Borland et al., 1993). In addition, CAM was characterised at a metabolic level, by estimating the contents of malate and citrate in leaves, every 6 hours over a diel cycle (Fig. 6.5, Fig. 6.6). Under well-watered conditions, neither *C. pratensis* nor *C. tocuchensis* exhibited a significant increase in malate or citrate over the course of the night (Fig. 6.5A, Fig. 6.6A). However, upon drought treatment, *C. pratensis* alone exhibited a significant difference between dawn and dusk concentrations of malate; a metabolic phenotype that is integral to CAM (Fig. 6.5B). These data confirm that the gas exchange profiles presented (Fig. 6.2) are the consequence of flux through the CAM cycle. In addition, under drought, *C. pratensis*, but not *C. tocuchensis*, began to significantly accumulate citrate over the course of the night (Fig. 6.6B). Therefore, like *C. minor*, *C. major* and *C. alata* (Borland et al., 1992; Lüttge 1999; Kornas et al., 2009), the CAM cycle in *C. pratensis* is associated with a diel fluctuation in citric acid, although the precise role this metabolite plays in CAM remains enigmatic (Lüttge 2002; Kornas et al., 2009; Cheung et al., 2014). Taken together, both gas exchange and metabolite assays showed that *C. pratensis* exhibits a facultative CAM response typical of *Clusia*, and that *C. tocuchensis* is unable to facultatively induce CAM upon experiencing drought stress. Consequently, these species are ideal models for comparative analyses, to understand how CAM affects plant physiology during drought.

6.4.3 Maintenance of Photosynthetic Physiology During Drought

Gas exchange data used to phenotype the species in this study was also inspected, qualitatively, to assess the effect of drought on diel assimilation rates. An initial experiment in Newcastle, UK found that the C₃ species *C. tocuchensis* exhibited a considerable loss to integrated diel assimilation under drought conditions (Fig. 6.1A). In the facultative CAM

species, *C. pratensis*, the induction of CAM did coincide with a drop in diel assimilation (Fig. 6.1B). However, once drought had triggered a CAM phenotype, the diel assimilation rate remained relatively stable. By the end of the drought treatment, *C. pratensis* had a higher diel CO₂ assimilation than *C. tocuchensis*. In the constitutive CAM species, *C. fluminensis*, the drought treatment had very little effect on diel assimilation (Fig. 6.1C). In addition, a similar trend was observed in higher light growth rooms in ORNL, USA, as the diel assimilation of *C. tocuchensis* fell far below that of *C. pratensis* under full drought conditions. These data are congruent with findings from Borland et al., (1998) who showed that species with stronger CAM phenotypes exhibited a less severe drop in diel assimilation under droughted conditions. Taken together, these data strongly suggest that the ability to do CAM prevents photosynthetic metabolic rates from slowing during drought, in *Clusia*.

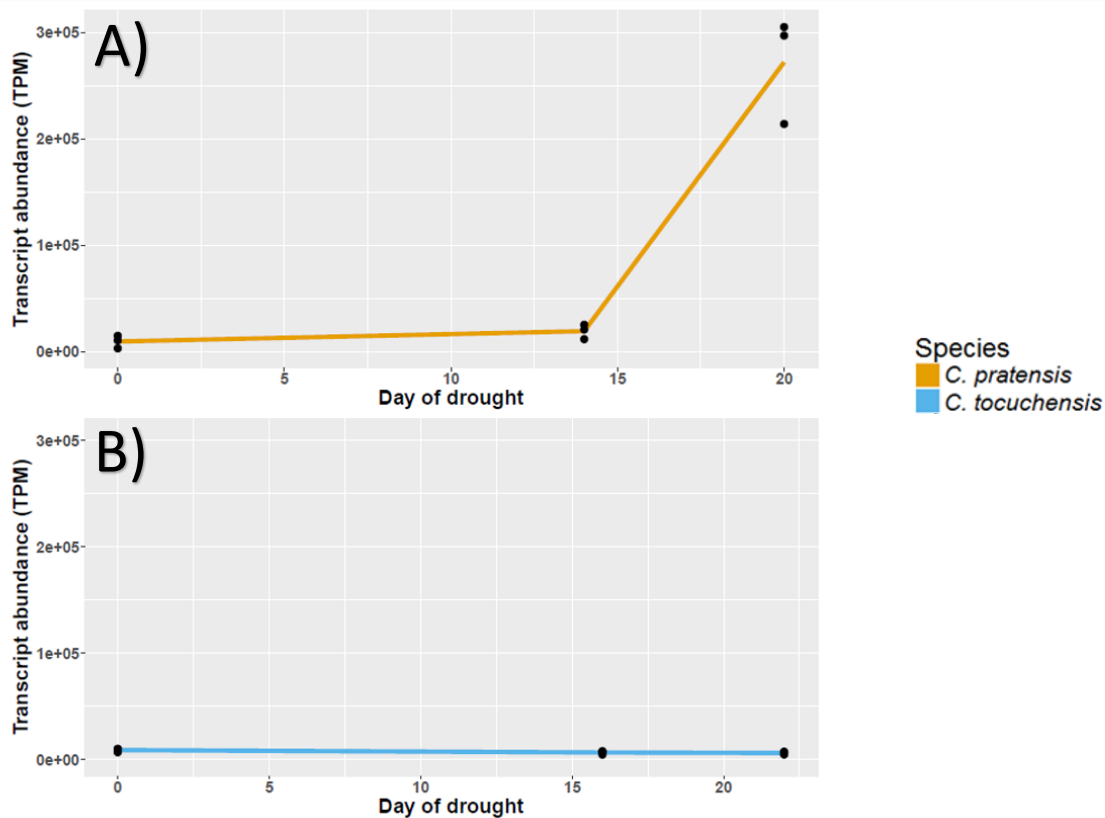


Fig. 6.8) PEPC transcript abundance increases with the induction of Crassulacean acid metabolism. Steady state mRNA transcript abundance was estimated using RNA-seq data. PEPC transcript abundance, estimated as transcripts per million, increased more over the entire drought treatment in (A) *C. pratensis* than in (B) *C. tocutensis*. In addition, PEPC steady state transcript abundance increased more in *C. pratensis* in the last 6 days of drought than in the first 14 days, coinciding with the induction of CAM in this species. For clarity, the steady state transcript level from only the most abundant *C. tocutensis* homologue is shown in this figure, although 3 isoforms were present. However, the *C. pratensis* PEPC transcript exhibited a greater fold change increase in steady-state transcript abundance than all 3 homologs in *C. tocutensis*. For each species, n = 3 and each individual data point is presented as a black dot.

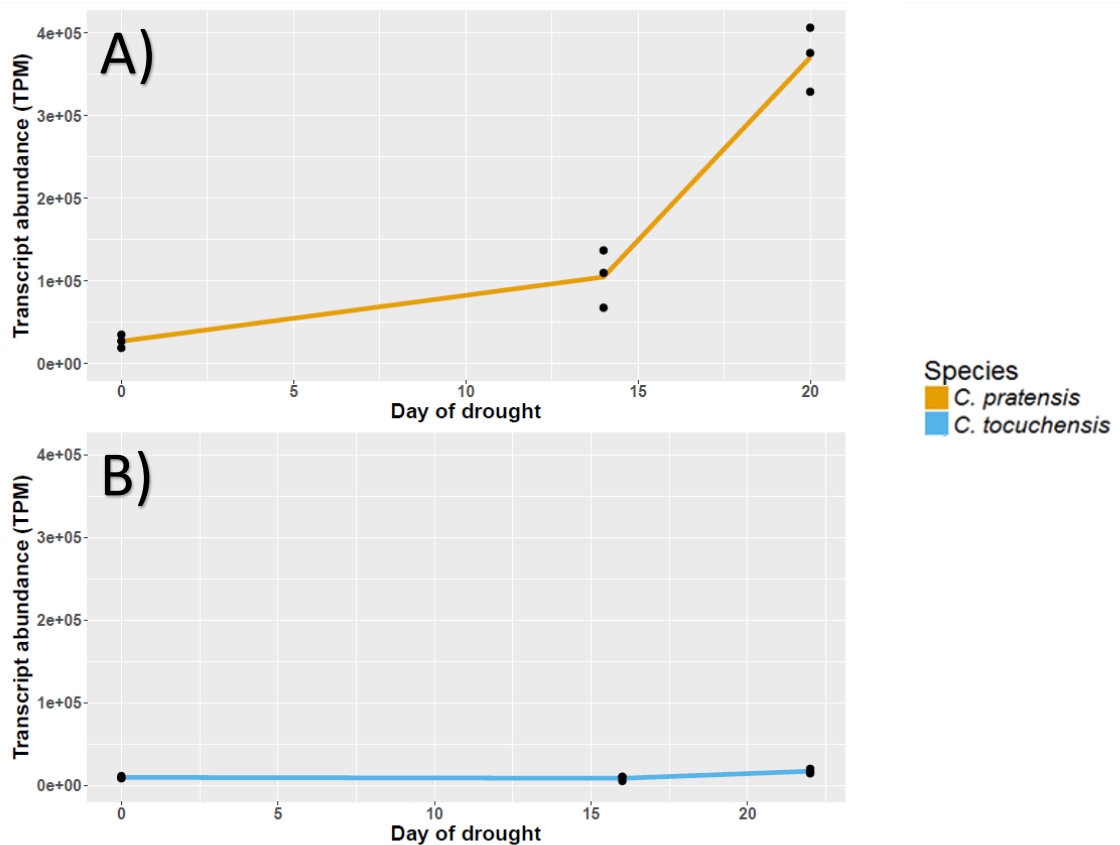


Fig. 6.9) PEPCK transcript abundance increases with the induction of Crassulacean acid metabolism. Steady state mRNA transcript abundance was estimated using RNA-seq data. PEPCK transcript abundance, estimated as transcripts per million, increased more over the entire drought treatment in (A) *C. pratensis* than in (B) *C. toouchensis*. In addition, PEPCK steady state transcript abundance increased more in *C. pratensis* in the last 6 days of drought than in the first 14 days, coinciding with the induction of CAM in this species. Only one PEPCK isoform was present in the transcriptome of *C. toouchensis*, which is displayed. For each species, n = 3 and each individual data point is presented as a black dot.

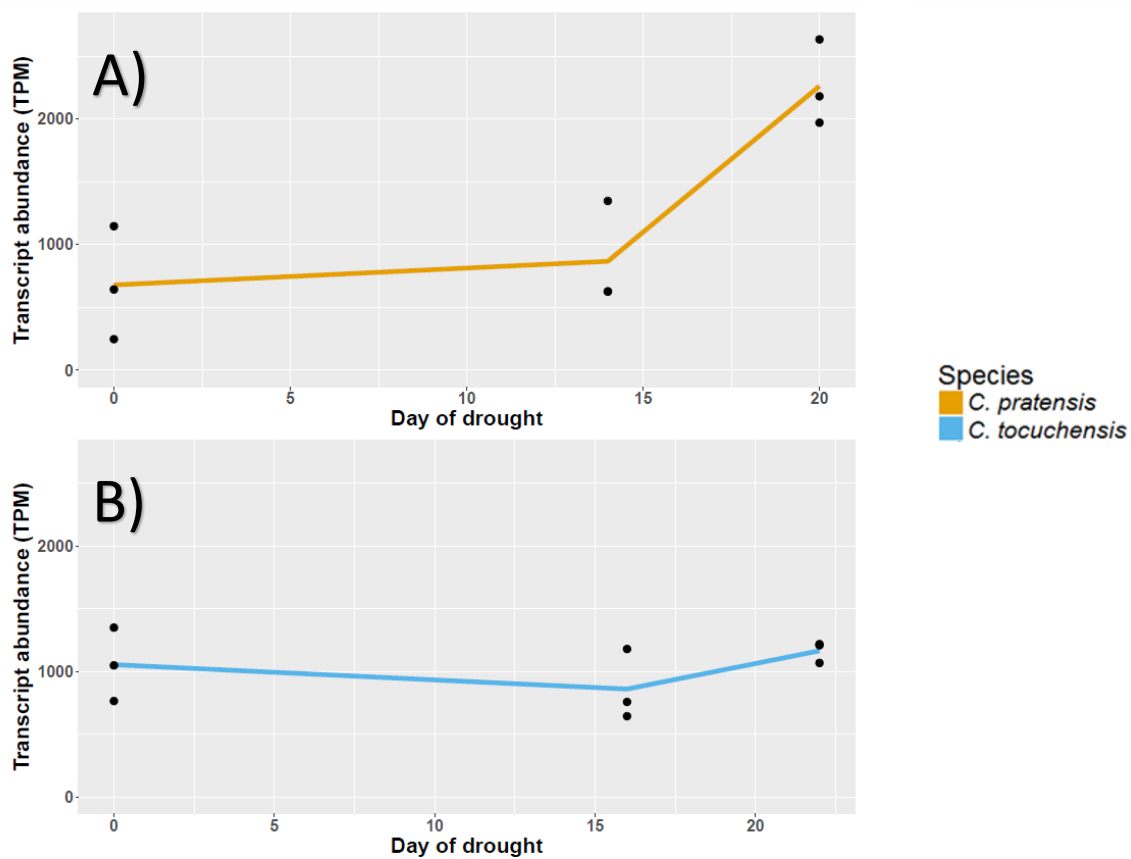


Fig. 6.10) NADP-ME transcript abundance increases with the induction of Crassulacean acid metabolism. Steady state mRNA transcript abundance was estimated using RNA-seq data. NADP-ME transcript abundance, estimated as transcripts per million, increased more over the entire drought treatment in (A) *C. pratensis* than in (B) *C. toouchensis*. In addition, NADP-ME steady state transcript abundance increased more in *C. pratensis* in the last 6 days of drought than in the first 14 days, coinciding with the induction of CAM in this species. For clarity, the steady state transcript level from only the most abundant *C. toouchensis* homologue is shown in this figure, although 2 isoforms were present. However, the *C. pratensis* NADP-ME transcript exhibited a greater fold change increase in steady-state transcript abundance than both homologs in *C. toouchensis*. For each species, $n = 3$ and each individual data point is presented as a black dot.

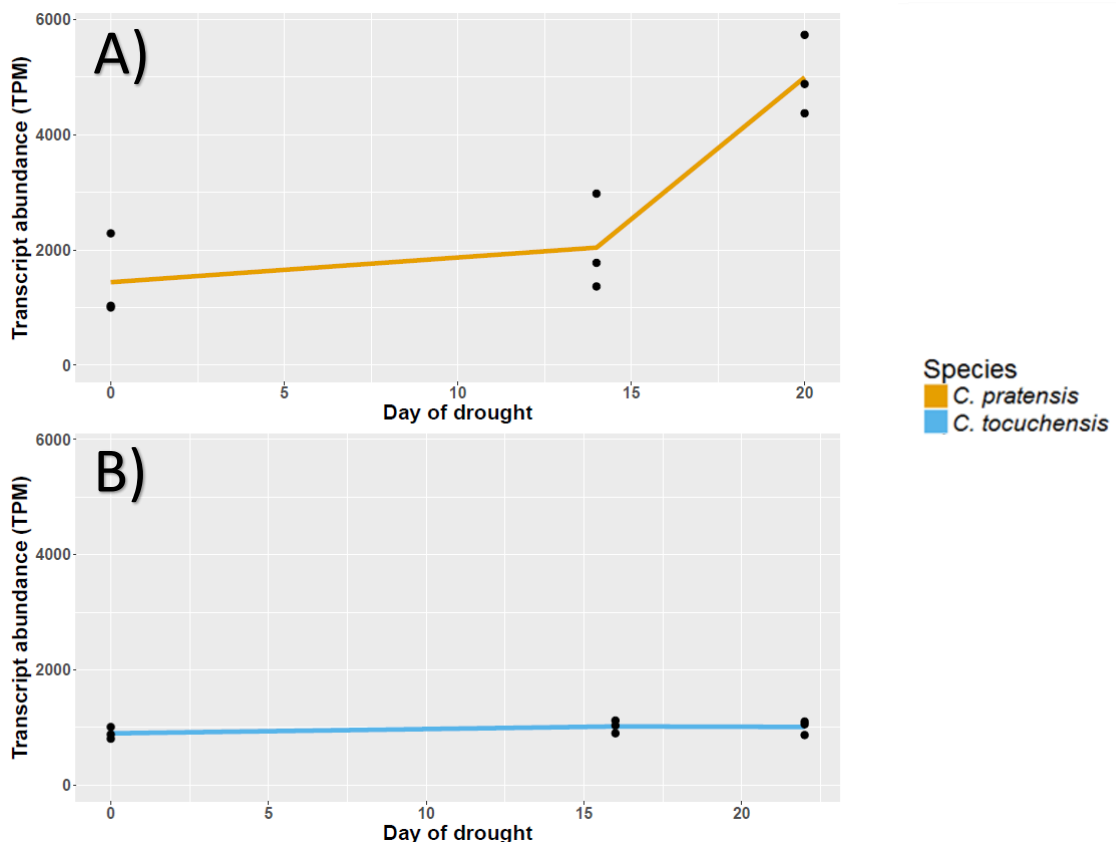


Fig. 6.11) ALMT transcript abundance increases with the induction of Crassulacean acid metabolism. Steady state mRNA transcript abundance was estimated using RNA-seq data. ALMT transcript abundance, estimated as transcripts per million, increased more over the entire drought treatment in (A) *C. pratensis* than in (B) *C. tocochensis*. In addition, NADP-ME steady state transcript abundance increased more in *C. pratensis* in the last 6 days of drought than in the first 14 days, coinciding with the induction of CAM in this species. For clarity, the steady state transcript level from only the most abundant *C. tocochensis* homologue is shown in this figure, although 2 isoforms were present. However, the *C. pratensis* ALMT transcript exhibited a greater fold change increase in steady-state transcript abundance than both homologs in *C. tocochensis*. For each species, $n = 3$ and each individual data point is presented as a black dot.

6.4.4 Maintenance of Respiratory Physiology During Drought

An indicator of carbon starvation during drought can be a drop in nocturnal respiration, as core metabolism slows when a plant's health declines (Sevanto et al., 2014). Therefore, measurements of nocturnal oxygen consumption were used to assess the effect of drought on respiratory rates in *C. pratensis* and *C. tocuchensis*. It was unlikely that the stress imposed in these experiments was severe enough to cause plants to approach mortality, and consequently the C₃ species, *C. tocuchensis*, exhibited no change in nocturnal respiration rate (Fig. 6.3, Fig. 6.4). However, *C. pratensis* exhibited an increase in nocturnal respiration during drought, coinciding with the induction of CAM (Fig. 6.3, Fig. 6.4B). The increase in oxygen consumption in *C. pratensis* is congruent with findings from flux balance analysis modelling, which predicted that CAM requires a higher nocturnal ATP consumption rate, and a subsequent increase to flux through mitochondrial ATP synthase (Shameer et al., 2018). It seems that, in contrast to the C₃ drought response, the induction of CAM causes plants to increase core respiratory metabolism during drought, in *Clusia*. Therefore, in conjunction with maintaining photosynthetic rates under water limited conditions, these data point towards CAM as a mechanism for sustaining, or even increasing core respiratory physiology during drought. Taken together, these results suggest that the 'CAM drought response' allows plants to maintain higher core metabolic rates than C₃ species, thereby minimising the symptoms of carbon starvation.

6.4.5 Identifying 'Core-CAM Genes' in the *Clusia* Transcriptome

As the CAM drought response is characterised by higher photosynthetic and respiratory metabolic rates than that seen in C₃ species, it was expected that this physiological drought response would be under genetic control. To explore the genetic regulation of CAM in *Clusia*, short-read RNA-seq was used to generate a *de novo* transcriptome assembly and quantitatively estimate the steady-state mRNA abundance of all expressed genes, during a dry-down experiment. Leaves were sampled under well-watered, intermediate and full drought treatments, and CAM was induced in *C. pratensis* in the latter conditions (Fig. 6.2). A set of 584 'core-CAM genes' were identified, by finding transcripts that were upregulated more in *C. pratensis* than in *C. tocuchensis*, and cross referencing these genes against those that were upregulated more in the final 6 days of drought than the first 14 days, in *C. pratensis*.

This approach was deemed successful due to the presence of many genes known to play a role in CAM in *Clusia* (Taybi et al., 2004), such as PEPC, PEPCK, NADP-ME and ALMT (Figs. 6.8 to 6.11), and are abundant in the transcriptomes of other species doing CAM (Wai et al., 2017; Heyduk et al., 2019a; Heyduk et al., 2019b; Wai et al., 2019).

6.4.6 Gene Ontology Enrichment Detects Signature of Increased Respiratory Rate

To investigate the transcriptomic response to drought with a more holistic approach, gene ontology (GO) enrichment was performed. Initial exploration of genes upregulated in each species showed distinctly different drought responses. The C₃ drought response in *C. tocuchensis* was characterised by GO terms describing the production of cuticular waxes and stomatal movement. As *C. tocuchensis* responds to drought by closing its stomata, its rate of water loss will approach that of cuticular transpiration (g_{\min}), which in turn will be critical for plant survival time (Blackman et al., 2019). Therefore, the upregulation of cuticle synthesis will be strongly deterministic of survival rates for this species. In addition, the genes that were upregulated in response to drought in *C. tocuchensis* were enriched in CC GO terms that describe chloroplastic locations. It seems that genes that control photosynthesis were upregulated, in conjunction with those that act to maintain and repair the photosynthetic machinery. For example, both BP GO terms ‘nonphotochemical quenching’ and ‘repair of photosystem II’ were enriched. These data suggest that the photosynthetic machinery is suffering damage due to drought stress, in *C. tocuchensis*. If stomatal closure is limiting the availability of CO₂ for photosynthesis (Fig. 6.1; Fig. 6.2), then it is possible that excess absorbed light energy is not being used by photochemical quenching, which would require greater turnover of chloroplastic genes as well as the repair of photosystems.

The facultative CAM species, *C. pratensis*, exhibited starkly different transcriptomic changes to those seen in *C. tocuchensis*. Namely, the drought response for *C. pratensis* was characterised by an upregulation of mitochondrial-functioning genes; as both ‘mitochondrial electron transport’ and ‘tricarboxylic acid cycle’ BP GO terms are enriched (Appendix A; Table A.3), as well as a number of CC GO terms related to mitochondrial locations (Appendix A; Table A.1). No such mitochondrial-related GO terms were enriched in the *C. tocuchensis* drought response (Appendix A; Table A.2 and A.4). To confirm that enriched mitochondrial GO terms

were associated with CAM, a GO enrichment analysis was performed on the 'core-CAM genes' (Table 6.2 and 6.3). The core-CAM genes were enriched in GO terms relating to mitochondrial respiration; this included both the tricarboxylic acid cycle and the electron transport chain, and even some GO terms that had not been enriched in the initial analysis of the upregulated *C. pratensis* genes (Appendix A; Table A.1 and A.3). These data are not able to determine if genes involved in mitochondrial respiration are upregulated to increase mitochondrial protein abundance, or because higher fluxes through mitochondrial respiration cause greater turnover of enzymes. Nevertheless, these data demonstrate that the increased oxygen consumption in the CAM drought response (Fig. 6.3) requires a reprogramming of genes involved in mitochondrial metabolism, in order to match the increasing respiratory needs of the plant.

Despite the prediction from flux balance analysis modelling that CAM requires a greater rate of nocturnal respiration (Shameer et al., 2018), the analysis outlined here is the first to show that the transcriptomic changes associated with CAM are characterised by changes to mitochondrial-functioning genes. This may be in part due to methodological differences, as other RNA-seq studies into the facultative CAM species *Talinum triangulare* (Talinaceae) and *Erycina pusilla* (Orchidaceae) performed GO enrichment on coexpression networks, rather than targeting nocturnally expressed genes that are upregulated following drought treatment. One study into the transcriptomic changes during drought in *Yucca aloifolia* (CAM), *Y. gloriosa* (C₃-CAM intermediate) and *Y. filamentosa* (C₃) found that upregulated genes in all three species were enriched in the GO term 'mitochondrion' (Heyduk et al., 2019). However, none of these *Yucca* species facultatively employ CAM, and therefore these transcriptomic changes may not be associated directly with CAM. Heyduk et al., (2019) do demonstrate that mitochondrial cytochrome-C expression is highest for the *Y. aloifolia*, with a peak at the beginning of the night, suggesting that some genetic upregulation of mitochondrial activity is associated with CAM. More work needs to be done to determine if high mitochondrial respiration rates are a feature of CAM across all taxa. It is possible that this feature is unique to forms of CAM that accumulate citrate overnight, as this metabolite requires greater flux through the tricarboxylic acid cycle, which would in turn drive the reduction of NAD⁺, and power mitochondrial electron transport. *Clusia* has long been known to accumulate high concentrations of citric acid through the CAM cycle (Borland et al., 1992; Lüttge 1999; Kornas et al., 2009). It is possible that nocturnal accumulation of citrate is an

adaptation to increase mitochondrial flux and thereby prevent respiratory decline; one of the symptoms of carbon starvation during drought.

Table 6.2) GO terms enriched in the core-CAM genes signify changes to mitochondria. 27

GO terms were enriched in the core-CAM gene set, many of which encode proteins that function in cellular compartments in the mitochondria.

GO Term	GO Term	Abundance of GO Term in <i>C. pratensis</i> Transcriptome	Abundance in Core-CAM genes	Expected Abundance in Core-CAM Genes	p-value
GO:0005747	mitochondrial respiratory chain complex I	55	24	1.1	1.5e-26
GO:0005759	mitochondrial matrix	196	30	3.93	3.00E-19
GO:0000275	mitochondrial proton-transporting ATP synthase complex, catalytic core F(1)	13	10	0.26	2.6e-15
GO:0005829	cytosol	4202	140	84.33	1.6e-12
GO:0005739	mitochondrion	2153	151	43.21	1.2e-11
GO:0005749	mitochondrial respiratory chain complex II, succinate dehydrogenase complex (ubiquinone)	8	5	0.16	1.7e-07
GO:0009570	chloroplast stroma	1286	56	25.81	2.5e-07
GO:0048046	apoplast	912	42	18.3	5.9e-07
GO:0005740	mitochondrial envelope	479	65	9.61	1.00E-06
GO:0005777	peroxisome	427	30	8.57	1.8e-06
GO:0005750	mitochondrial respiratory chain complex III	21	6	0.42	2.7e-06
GO:0005758	mitochondrial intermembrane space	37	7	0.74	7.7e-06
GO:0009507	chloroplast	4243	155	85.15	8.9e-06
GO:0005753	mitochondrial proton-transporting ATP synthase complex	33	15	0.66	3.5e-05
GO:0009941	chloroplast envelope	1288	46	25.85	5.8e-05
GO:0000015	phosphopyruvate hydratase complex	7	3	0.14	0.00026
GO:0005774	vacuolar membrane	1650	55	33.11	0.00038
GO:0005618	cell wall	1619	46	32.49	0.00049
GO:0009536	plastid	4376	165	87.82	0.00061
GO:0009514	glyoxysome	37	5	0.74	0.00082
GO:0005886	plasma membrane	5442	133	109.22	0.00119
GO:0005743	mitochondrial inner membrane	320	53	6.42	0.00129
GO:0045239	tricarboxylic acid cycle enzyme complex	13	4	0.26	0.00233
GO:0005737	cytoplasm	14393	402	288.86	0.00233
GO:0009346	citrate lyase complex	14	3	0.28	0.00248
GO:0009501	amyloplast	15	3	0.3	0.00305
GO:0045254	pyruvate dehydrogenase complex	7	2	0.14	0.0079

Table 6.3) GO terms enriched in the core-CAM genes signify changes to respiration. The 35 most enriched GO terms, of 71 significantly that were significantly enriched ($p < 0.01$) are displayed. The most enriched GO term is 'tricarboxylic acid cycle'. In addition, other GO terms pertaining to respiration are enriched, such as 'mitochondrial electron transport, succinate to ubiquinone' and 'acetyl-CoA biosynthetic process from pyruvate'.

GO ID	GO Term	Abundance of GO Term in <i>C. pratensis</i> Transcriptome	Abundance of GO Term in Core-CAM genes	Expected Abundance in Core-CAM Genes	p-value
GO:0006099	tricarboxylic acid cycle	93	36	1.85	1.00E-30
GO:0046686	response to cadmium ion	970	89	19.3	1.00E-30
GO:0006096	glycolytic process	149	30	2.96	1.1e-21
GO:0006108	malate metabolic process	57	15	1.13	2.5e-13
GO:0009651	response to salt stress	1375	70	27.36	4.2e-13
GO:0055114	oxidation-reduction process	1869	124	37.19	3.7e-12
GO:0015986	ATP synthesis coupled proton transport	57	14	1.13	4.4e-12
GO:1901006	ubiquinone-6 biosynthetic process	9	6	0.18	4.8e-09
GO:0015991	ATP hydrolysis coupled proton transport	83	13	1.65	9.7e-09
GO:0009413	response to flooding	21	7	0.42	1.1e-07
GO:1900039	positive regulation of cellular response to hypoxia	10	5	0.2	7.1e-07
GO:0006097	glyoxylate cycle	18	6	0.36	9.1e-07
GO:0031000	response to caffeine	11	5	0.22	1.3e-06
GO:0032355	response to estradiol	11	5	0.22	1.3e-06
GO:0009409	response to cold	833	36	16.57	1.6e-06
GO:0006102	isocitrate metabolic process	21	6	0.42	2.5e-06
GO:0005975	carbohydrate metabolic process	1794	87	35.69	4.3e-06
GO:0042128	nitrate assimilation	67	9	1.33	7.00E-06
GO:0006790	sulfur compound metabolic process	560	33	11.14	1.3e-05
GO:0010477	response to sulfur dioxide	4	3	0.08	3.1e-05
GO:0009594	detection of nutrient	4	3	0.08	3.1e-05
GO:0006121	mitochondrial electron transport, succinate to ubiquinone	4	3	0.08	3.1e-05
GO:0010439	regulation of glucosinolate biosynthetic process	5	3	0.1	7.6e-05
GO:0006007	glucose catabolic process	5	3	0.1	7.6e-05
GO:0006002	fructose 6-phosphate metabolic process	23	5	0.46	7.6e-05
GO:0035556	intracellular signal transduction	839	24	16.69	7.8e-05
GO:0006979	response to oxidative stress	899	34	17.89	0.00011

Table 6.3 – continued

GO:0005978	glycogen biosynthetic process	14	4	0.28	0.00013
GO:0006694	steroid biosynthetic process	220	12	4.38	0.00033
GO:0009094	L-phenylalanine biosynthetic process	18	4	0.36	0.00038
GO:0006086	acetyl-CoA biosynthetic process from pyruvate	18	4	0.36	0.00038
GO:0006105	succinate metabolic process	3	3	0.06	0.00039
GO:0006120	mitochondrial electron transport, NADH to ubiquinone	2	2	0.04	4.00E-04
GO:0009735	response to cytokinin	563	25	11.2	4.00E-04
GO:0019252	starch biosynthetic process	49	6	0.97	0.00041

6.5 Conclusions and Future Work

The findings presented in this study provide an initial insight into the role of CAM during the drought response, in *Clusia*. As carbon starvation is characterised by a drop in photosynthetic and respiratory rates, these core metabolisms were investigated during the drought response of a facultative CAM and an obligate C₃ species. CAM allowed *C. pratensis* plants to maintain a higher rate of both photosynthesis and respiration during drought. In addition, transcriptomic changes indicate that mitochondrial respiration was upregulated in association with CAM. This finding provides experimental evidence to reinforce the outcomes of flux balance analysis models, which predicted a 1.6-fold higher flux through mitochondrial ATP synthase than seen in C₃ plants (Shameer et al., 2018). Future work is needed to experimentally explore how CAM affects the anatomy, metabolic flux and proteome of mitochondria in *Clusia* and other taxa that employ CAM.

The data presented in this study is an initial attempt to characterise the effect of CAM on falling metabolic rates during drought. The findings suggest that CAM minimises drought-induced drops to metabolism. However, these data do not directly address how the NSC reserves in leaves are affected by drought in *C. pratensis* and *C. tocuchensis*. Future work should investigate how starch and soluble sugar stores are depleted during drought and explore how phloem loading and phloem turgor pressure is affected by drought in these two species. This will provide a more comprehensive picture of how CAM influences carbon balance and potentially negates carbon starvation in *Clusia*.

6.6 References

- Alexa, A., Rahnenführer, J., & Lengauer, T. (2006). Improved scoring of functional groups from gene expression data by decorrelating GO graph structure. *Bioinformatics*, *22*(13), 1600–1607. <https://doi.org/10.1093/bioinformatics/btl140>
- Aubry, S., Kelly, S., Kümpers, B. M. C., Smith-Unna, R. D., Hibberd, J. M., Carlier, M.-F., ... Didry, D. (2014). Deep Evolutionary Comparison of Gene Expression Identifies Parallel Recruitment of Trans-Factors in Two Independent Origins of C4 Photosynthesis. *PLoS Genetics*, *10*(6), e1004365. <https://doi.org/10.1371/journal.pgen.1004365>
- Blackman, C. J., Li, X., Choat, B., Rymer, P. D., De Kauwe, M. G., Duursma, R. A., ... Medlyn, B. E. (2019). Desiccation time during drought is highly predictable across species of Eucalyptus from contrasting climates. *New Phytologist*. <https://doi.org/10.1111/nph.16042>
- Borland, A. M., Griffiths, H., Broadmeadow, M. S. J., Fordham, M. C., & Maxwell, C. (1993). Short-term changes in carbon-isotope discrimination in the C3-CAM intermediate *Clusia minor* L. growing in Trinidad. *Oecologia*, *95*(3), 444–453. <https://doi.org/10.1007/BF00321001>
- Borland, A. M., Griffiths, H., Maxwell, C., Broadmeadow, M. S. J., Griffiths, N. M., & Barnes, J. D. (1992). On the ecophysiology of the Clusiaceae in Trinidad: expression of CAM in *Clusia minor* L. during the transition from wet to dry season and characterization of three endemic species. *New Phytologist*, *122*(2), 349–357. <https://doi.org/10.1111/j.1469-8137.1992.tb04240.x>
- Borland, A. M., Hartwell, J., Weston, D. J., Schlauch, K. a., Tschaplinski, T. J., Tuskan, G. a., ... Cushman, J. C. (2014). Engineering crassulacean acid metabolism to improve water-use efficiency. *Trends in Plant Science*, *19*(5), 327–338. <https://doi.org/10.1016/j.tplants.2014.01.006>
- Borland, A. M., Técsi, L. I., Leegood, R. C., & Walker, R. P. (1998). Inducibility of crassulacean acid metabolism (CAM) in *Clusia* species; physiological/biochemical characterisation and intercellular localization of carboxylation and decarboxylation processes in three

species which exhibit different degrees of CAM. *Planta*, 205(3), 342–351.

<https://doi.org/10.1007/s004250050329>

Borland, A. M., Wulschleger, S. D., Weston, D. J., Hartwell, J., Tuskan, G. a., Yang, X., & Cushman, J. C. (2015). Climate-resilient agroforestry: physiological responses to climate change and engineering of crassulacean acid metabolism (CAM) as a mitigation strategy. *Plant, Cell & Environment*, 38, 1833–1849. <https://doi.org/10.1111/pce.12479>

Bray, N. L., Pimentel, H., Melsted, P., & Pachter, L. (2016). Near-optimal probabilistic RNA-seq quantification. *Nature Biotechnology*, 34(5), 525–527.

<https://doi.org/10.1038/nbt.3519>

Brilhaus, D., Bräutigam, A., Mettler-Altmann, T., Winter, K., & Weber, A. P. M. (2016). Reversible Burst of Transcriptional Changes during Induction of Crassulacean Acid Metabolism in *Talinum triangulare*. *Plant Physiology*, 170(1), 102–122.

<https://doi.org/10.1104/pp.15.01076>

Brodersen, C. R., & McElrone, A. J. (2013). Maintenance of xylem network transport capacity: A review of embolism repair in vascular plants. *Frontiers in Plant Science*, 4(APR), 1–11. <https://doi.org/10.3389/fpls.2013.00108>

Brodersen, C. R., McElrone, A. J., Choat, B., Matthews, M. A., & Shackel, K. A. (2010). The dynamics of embolism repair in xylem: In vivo visualizations using high-resolution computed tomography. *Plant Physiology*, 154(3), 1088–1095.

<https://doi.org/10.1104/pp.110.162396>

Cheung, C. Y. M., Poolman, M. G., Fell, D. A., Ratcliffe, R. G., & Sweetlove, L. J. (2014). A Diel Flux Balance Model Captures Interactions between Light and Dark Metabolism during Day-Night Cycles in C3 and Crassulacean Acid Metabolism Leaves. *Plant Physiology*, 165(2), 917–929. <https://doi.org/10.1104/pp.113.234468>

Choat, B., Brodribb, T. J., Brodersen, C. R., Duursma, R. A., López, R., & Medlyn, B. E. (2018). Triggers of tree mortality under drought. *Nature*, 558(7711), 531–539.

<https://doi.org/10.1038/s41586-018-0240-x>

- Crous, K. Y., Zaragoza-Castells, J., Löw, M., Ellsworth, D. S., Tissue, D. T., Tjoelker, M. G., ...
Atkin, O. K. (2011). Seasonal acclimation of leaf respiration in Eucalyptus saligna trees:
Impacts of elevated atmospheric CO₂ and summer drought. *Global Change Biology*,
17(4), 1560–1576. <https://doi.org/10.1111/j.1365-2486.2010.02325.x>
- Duke, N. C., Kovacs, J. M., Griffiths, A. D., Preece, L., Hill, D. J. E., van Oosterzee, P., ...
Burrows, D. (2017). Large-scale dieback of mangroves in Australia. *Marine and
Freshwater Research*, 68(10), 1816. <https://doi.org/10.1071/mf16322>
- Emms, D. M., & Kelly, S. (2015). OrthoFinder: solving fundamental biases in whole genome
comparisons dramatically improves orthogroup inference accuracy. *Genome Biology*,
16(1), 1–14. <https://doi.org/10.1186/s13059-015-0721-2>
- Grams, T. E. E., Herzog, B., & Luttge, U. (1998). Are there species in the genus *Clusia* with
obligate C₃ photosynthesis? *Journal of Plant Physiology*, 152(1), 1–9.
[https://doi.org/10.1016/S0176-1617\(98\)80094-1](https://doi.org/10.1016/S0176-1617(98)80094-1)
- Hartmann, H. (2015). Carbon starvation during drought-induced tree mortality – are we
chasing a myth? *Journal of Plant Hydraulics*, 2(2008), 005.
<https://doi.org/10.20870/jph.2015.e005>
- Heyduk, K., Hwang, M., Albert, V., Silvera, K., Lan, T., Farr, K., ... Leebens-Mack, J. (2019).
Altered Gene Regulatory Networks Are Associated With the Transition From C₃ to
Crassulacean Acid Metabolism in *Erycina* (Oncidiinae: Orchidaceae). *Frontiers in Plant
Science*, 9(January), 1–15. <https://doi.org/10.3389/fpls.2018.02000>
- Heyduk, K., Ray, J. N., Ayyampalayam, S., Moledina, N., Borland, A., Harding, S. A., ...
Leebens-Mack, J. (2019). Shared expression of crassulacean acid metabolism (CAM)
genes pre-dates the origin of CAM in the genus *Yucca*. *Journal of Experimental Botany*,
(March). <https://doi.org/10.1093/jxb/erz105>
- Hohorst, H. (1970). L-malate estimation with malate dehydrogenase and NAD. In H.
Bergmeyer (Ed.), *Methods in Enzymatic Analysis* (pp. 1544–1548).

- Holtum, J. A. M., Aranda, J., Virgo, A., Gehrig, H. H., & Winter, K. (2004). $\delta^{13}\text{C}$ values and crassulacean acid metabolism in *Clusia* species from Panama. *Trees*, *18*, 658–668. <https://doi.org/10.1007/s00468-004-0342-y>
- Klepsch, M., Zhang, Y., Kotowska, M. M., Lamarque, L. J., Nolf, M., Schuldt, B., ... Jansen, S. (2018). Is xylem of angiosperm leaves less resistant to embolism than branches? Insights from microCT, hydraulics, and anatomy. *Journal of Experimental Botany*, *69*(22), 5611–5623. <https://doi.org/10.1093/jxb/ery321>
- Kornas, A., Fischer-Schliebs, E., Lüttge, U., & Miszalski, Z. (2009). Adaptation of the obligate CAM plant *Clusia alata* to light stress: Metabolic responses. *Journal of Plant Physiology*, *166*(17), 1914–1922. <https://doi.org/10.1016/j.jplph.2009.06.005>
- Lüttge, U. (1999). One morphotype, three physiotypes: Sympatric species of *Clusia* with obligate C3 photosynthesis, obligate CAM and C3-CAM intermediate behaviour. *Plant Biology*, *1*(2), 138–148. <https://doi.org/10.1111/j.1438-8677.1999.tb00237.x>
- Lüttge, U. (2002). CO₂-concentrating: consequences in crassulacean acid metabolism. *Journal of Experimental Botany*, *53*(378), 2131–2142. <https://doi.org/10.1093/jxb/erf081>
- Males, J., & Griffiths, H. (2018). Economic and hydraulic divergences underpin ecological differentiation in the Bromeliaceae. *Plant Cell and Environment*, *41*(1), 64–78. <https://doi.org/10.1111/pce.12954>
- Males, J., & Griffiths, H. (2017). Functional types in the Bromeliaceae: relationships with drought-resistance traits and bioclimatic distributions. *Functional Ecology*, *31*(10), 1868–1880. <https://doi.org/10.1111/1365-2435.12900>
- McDowell, N. G., Brodribb, T. J., & Nardini, A. (2019). Hydraulics in the 21st century. *New Phytologist*, *224*, 537–542. <https://doi.org/10.1111/nph.16151>
- McDowell, N., Pockman, W. T., Allen, C. D., David, D., Cobb, N., Kolb, T., ... Yezep, E. A. (2008). Mechanisms of plant survival and mortality during drought: why do some plants survive while others succumb to drought? *New Phytologist*, *178*, 719–739.

- Milburn, J. A. (1973). Cavitation studies on whole Ricinus plants by acoustic detection. *Planta*, 112(4), 333–342. <https://doi.org/10.1007/BF00390306>
- Möllering, H. (1985). Citrate Determination with Citrate Lyase, MDH and LDH. In H. Bergmeyer (Ed.), *Methods of Enzymatic Analysis* (pp. 2–12). Academic Press, New York.
- Nardini, A., Lo Gullo, M. A., & Salleo, S. (2011). Refilling embolized xylem conduits: Is it a matter of phloem unloading? *Plant Science*, 180(4), 604–611. <https://doi.org/10.1016/j.plantsci.2010.12.011>
- Niechayev, N. A., Pereira, P. N., & Cushman, J. C. (2019). Understanding trait diversity associated with crassulacean acid metabolism (CAM). *Current Opinion in Plant Biology*, 49, 74–85. <https://doi.org/10.1016/j.pbi.2019.06.004>
- Phillips, O. L., Aragão, L. E. O. C., Lewis, S. L., Fisher, J. B., Lloyd, J., López-gonzález, G., ... Torres-Lezama, A. (2009). Drought Sensitivity of the Amazon Rainforest. *Science*, 323(March), 1344–1347.
- Pimentel, H., Bray, N. L., Puente, S., Melsted, P., & Pachter, L. (2017). Differential analysis of RNA-seq incorporating quantification uncertainty. *Nature Methods*, 14(7), 687–690. <https://doi.org/10.1038/nmeth.4324>
- Popp, M., Kramer, D., Lee, H., Diaz, M., Ziegler, H., & Liittge, U. (1987). Crassulacean acid metabolism in tropical dicotyledonous trees of the genus Clusia. *Trees*, 1, 238–247.
- Richards, H. M. (1915). *Acidity and gas interchange in cacti*. Retrieved from <https://www.biodiversitylibrary.org/item/68027>
- Roberts, A., Griffiths, H., Borland, A. M., & Reinert, F. (1996). Is crassulacean acid metabolism activity in sympatric species of hemi-epiphytic stranglers such as Clusia related to carbon cycling as a photoprotective process? *Oecologia*, 106(1), 28–38. <https://doi.org/10.1007/BF00334404>
- Scoffoni, C., Albuquerque, C., Brodersen, C. R., Townes, S. V., John, G. P., Bartlett, M. K., ... Sack, L. (2017). Outside-Xylem Vulnerability, Not Xylem Embolism, Controls Leaf

- Hydraulic Decline during Dehydration. *Plant Physiology*, 173(2), 1197–1210.
<https://doi.org/10.1104/pp.16.01643>
- Scoffoni, C., Chatelet, D. S., Pasquet-Kok, J., Rawls, M., Donoghue, M. J., Edwards, E. J., & Sack, L. (2016). Hydraulic basis for the evolution of photosynthetic productivity. *Nature Plants*, 2(6), 1–8. <https://doi.org/10.1038/nplants.2016.72>
- Sevanto, S., Mcdowell, N. G., Dickman, L. T., Pangle, R., & Pockman, W. T. (2014). How do trees die? A test of the hydraulic failure and carbon starvation hypotheses. *Plant, Cell and Environment*, 37(1), 153–161. <https://doi.org/10.1111/pce.12141>
- Sheffield, J., & Wood, E. F. (2008). Global trends and variability in soil moisture and drought characteristics, 1950-2000, from observation-driven simulations of the terrestrial hydrologic cycle. *Journal of Climate*, 21(3), 432–458.
<https://doi.org/10.1175/2007JCLI1822.1>
- Tang, S., Dong, Y., Liang, D., Zhang, Z., Ye, C. Y., Shuai, P., ... Xia, X. (2015). Analysis of the Drought Stress-Responsive Transcriptome of Black Cottonwood (*Populus trichocarpa*) Using Deep RNA Sequencing. *Plant Molecular Biology Reporter*, 33(3), 424–438.
<https://doi.org/10.1007/s11105-014-0759-4>
- Taybi, T., Nimmo, H. G., & Borland, A. M. (2004). Expression of Phospho enol pyruvate Carboxylase and Phospho enol pyruvate Carboxylase Kinase Genes . Implications for Genotypic Capacity and Phenotypic Plasticity in the Expression of Crassulacean Acid Metabolism. *Plant Physiology*, 135(May), 587–598.
<https://doi.org/10.1104/pp.103.036962.1>
- Trueba, S., Pan, R., Scoffoni, C., John, G. P., Davis, S. D., & Sack, L. (2019). Thresholds for leaf damage due to dehydration: declines of hydraulic function, stomatal conductance and cellular integrity precede those for photochemistry. *New Phytologist*, 223(1), 134–149.
<https://doi.org/10.1111/nph.15779>
- Wai, C. M., VanBuren, R., Zhang, J., Huang, L., Miao, W., Edger, P. P., ... Ming, R. (2017). Temporal and spatial transcriptomic and microRNA dynamics of CAM photosynthesis in pineapple. *Plant Journal*, 92(1), 19–30. <https://doi.org/10.1111/tpj.13630>

- Wai, C. M., Weise, S. E., Ozersky, P., Mockler, T. C., Michael, T. P., & VanBuren, R. (2019). Time of day and network reprogramming during drought induced CAM photosynthesis in *Sedum album*. In *PLOS Genetics* (Vol. 15).
<https://doi.org/10.1371/journal.pgen.1008209>
- Williamson, V. G. (2017). "Listen to the Trees!" A tribute to the father of modern cavitation research, Professor John Milburn, on the 20th anniversary of his untimely death. *Journal of Plant Hydraulics*, 4(e005). <https://doi.org/10.20870/jph.2017.e005>
- Winter, K., Garcia, M., & Holtum, J. a. M. (2008). On the nature of facultative and constitutive CAM: environmental and developmental control of CAM expression during early growth of *Clusia*, *Kalanchoe*, and *Opuntia*. *Journal of Experimental Botany*, 59(7), 1829–1840. <https://doi.org/10.1093/jxb/ern080>
- Winter, K., Aranda, J., & Holtum, J. A. M. (2005). Carbon isotope composition and water-use efficiency in plants with crassulacean acid metabolism. *Functional Plant Biology*, 32(5), 381–388. <https://doi.org/10.1071/FP04123>
- Winter, K., & Holtum, J. A. M. (2014). Facultative crassulacean acid metabolism (CAM) plants: powerful tools for unravelling the functional elements of CAM photosynthesis. *Journal of Experimental Botany*, 65(13), 3425–3441.
<https://doi.org/10.1093/jxb/eru063>

Chapter 7. General Discussion

The experiments and approaches described in this thesis used the genus *Clusia* as a model to explore the ecophysiological role of succulence and Crassulacean acid metabolism (CAM) as adaptations to drought. *Clusia* contains species of remarkable physiological diversity (described below), which makes it an ideal model for comparative analyses. However, working with *Clusia* has some considerable limitations, due to the morphology and chemistry of tissue in this genus. The advantages and limitations of using *Clusia* as a model are discussed below.

7.1 Advantages of *Clusia* as a model genus

7.1.1 Physiological Diversity in *Clusia*

The main attraction of using *Clusia* as a model is the physiological diversity that is observed in this genus. It has long been documented that the photosynthetic physiology of *Clusia* species varies enormously; as this genus contains both C₃, C₃-CAM intermediate, facultative and constitutive CAM species (Popp et al., 1987; Lüttge 1999; Holtum et al., 2004; Barrera Zambrano et al., 2014). This level of photosynthetic diversity is unusual in the plant kingdom, as many genera, such as *Kalanchoë* or *Calandrinia* do not contain the entire range of C₃ to strong, constitutive CAM (Maxwell et al., 1997; Griffiths et al., 2008). Whilst other genera such as *Yucca* may contain this range of photosynthetic physiotypes, physiological characterisation of these genera is still somewhat in its infancy and cannot, therefore, benefit from over 20 years of research (Heyduk et al., 2016a; Heyduk et al., 2016b). The photosynthetic diversity of *Clusia* allows for the design of experiments to identify interspecific differences *within* a single genus, thereby reducing the chance that artefacts will arise from the phylogenetic distance between species studied (Scoffoni et al., 2016). In addition, the diversity of photosynthetic physiotypes in *Clusia* meant it was possible to choose the species with the cleanest C₃-to-CAM switch. To this end, *C. pratensis* was analysed, based on the advice of Dr. Klaus Winter, as it engages in little/no CAM under well-watered conditions, but can initiate a strong CAM phenotype upon receiving drought treatment (Winter et al., 2009; Winter and Holtum, 2014).

Beyond photosynthetic diversity, *Clusia* also displays a variety of leaf succulent adaptations across species (Popp et al., 1987; Barrera Zambrano et al., 2014). Both succulent anatomy in the hydrenchyma and chlorenchyma (so called water-storage and all-cell succulence) can be found in *Clusia*. Importantly, succulent anatomy in the hydrenchyma and chlorenchyma are independent, meaning that one can be present with or without the other. This was observed, indirectly, by Barrera Zambrano et al., (2014), who found that the strength of CAM correlates with palisade but not hydrenchyma cell size. Direct comparison of tissue depth in the hydrenchyma and chlorenchyma confirmed that these forms of succulent tissue do not correlate (Fig. 2.4). For example, *C. grandiflora* has little evidence of tissue succulence in either tissue. In contrast, *C. multiflora* has tissue succulence only in its hydrenchyma and *C. rosea* has it only in the chlorenchyma. Finally, *C. alata* has deep hydrenchyma and chlorenchyma tissue (Fig. 2.3). The independence of storage-succulence and all-cell succulence in *Clusia* makes it possible to statistically disentangle the effects that the hydrenchyma and chlorenchyma impose on plant physiology, as measures of both tissue types can be used as input for mixed-effect or multiple linear regression models (For example, Fig. 2.5; Fig. 2.8; Fig. 5.10). These approaches have proved valuable for providing novel insight on the specialised ways that these tissues each contribute to the plant drought response.

7.1.2 Dissecting Hydrenchyma and Chlorenchyma Tissues

The independence of hydrenchyma- and chlorenchyma-based succulence allowed more complex statistical models to be built, to try to understand the roles these tissues each have on the drought response. This approach was aided by the development of a method to manually dissect these tissues, in order to experimentally study each layer directly (Fig. 4.5). Only on the fifth attempt to develop a method to dissect these tissues (after attempting this about once every 4 months between February 2017 and October 2018) did it become clear that this could be done with the blunt edge of a razor blade. Dissections could be done rapidly, and tissue could be weighed instantly or frozen, thus minimising the effect that damage would have on the samples. *Clusia* appears to have a structurally weak point connecting the hydrenchyma and chlorenchyma; making these dissections possible, even in the 0.5 mm thick leaves of *C. tocuchensis*. Therefore, the structure of *Clusia* leaves provide a technical advantage that allowed for the direct physiological measurements of the hydrenchyma and chlorenchyma. Direct measurements of the hydrenchyma and chlorenchyma made it possible

to reinforce the findings of correlative comparative analyses; thus improving the robustness of conclusions made. For example, the finding that saturated water content (SWC) correlates with hydrenchyma, and not chlorenchyma depth (Fig. 2.5) is aided by the observation that hydrenchyma tissue has a higher SWC than chlorenchyma in *C. alata* and *C. tocuchensis* (Fig. 4.13).

7.2 Limitations of Using *Clusia* as a Model Genus

7.2.1 Latex

The weak connection between the hydrenchyma and chlorenchyma is an advantageous structural trait in *Clusia* leaves that allows for dissection of these tissue layers. However, there are many traits in *Clusia* leaves that substantially limit the range of experiments that are possible. One such limitation is caused by the presence of latex; a sticky liquid that exudes from any cut part of the leaf lamina or petiole. The presence of latex in *Clusia* prevents any measurement of hydraulic flow into a cut leaf (Melcher et al., 2012), which is a prerequisite for many measurements of hydraulic conductance (K). As a result, it was not possible to measure the maximal hydraulic conductance or the water potential that causes a 50 % drop in K (P50); two valuable traits for characterising the hydraulic physiology of plants.



Fig. 7.1) Latex exudate emerging from the cut petiole of a *Clusia rosea* leaf. Latex is sticky and prevents accurate measurements of hydraulic flow into the leaf.

7.2.2 Cuticular Wax

The abundance of cuticular wax causes *Clusia* leaves to have very low rates of transpiration when stomata are shut (g_{\min}) (Appendix B). As a result, the measurements for pressure volume curves took a long time to complete, as 24 hours would have to pass in order for leaf water potential to change, after reaching the turgor loss point (TLP). The low g_{\min} of *Clusia* leaves meant that constructing pressure volume curves for 11 species took over four months, and would be slow to replicate. In addition, the waxy cuticle meant that it was very difficult to infiltrate leaves with stains, to measure vein length per leaf area (VLA) (Chapter 5). Initial attempts to stain the vasculature were impeded as leaves could be cleared of pigments (Fig. 2), but Safranin-O would not enter the leaf. Pre-treatment of leaves with a nail file overcame this issue, but as a result, it was only possible to stain a small rectangle of leaf lamina, rather than whole leaves. Whilst the issues that arose from the wax in *Clusia* leaves were not insurmountable, they considerably slowed experiments and decreased the output that was achievable.



Fig. 7.2) Thick, impermeable waxy cuticles are difficult to infiltrate in *Clusia* leaves. For example, the *C. tocuchensis* leaf depicted had been treated with a stain (Safranin-O) to measure the vein density, but the stain did not reach the subcuticular tissue, so leaf remained white in appearance.

7.3 Conclusions

Despite the technical limitations associated with working on *Clusia*, the data generated throughout this project were able to address the main scope of this thesis, outlined in Chapter 1:

To investigate the effect of succulent anatomy on the hydraulic and metabolic physiology of leaves in the genus *Clusia*

Succulent anatomy can be found in two tissue layers in *Clusia*, the water storage hydrenchyma tissue and the photosynthetic chlorenchyma (specifically the palisade). The findings outlined in this thesis demonstrate that these tissue layers play distinctly different roles in the drought response. The distinct ecophysiological roles of succulent hydrenchyma and chlorenchyma tissues are outlined below:

7.3.1 The Ecophysiology of Succulent Hydrenchyma Tissue

Hydrenchyma in *Clusia* is an achlorophyllous, adaxial layer that ranges from approximately 0.05 mm (*C. grandiflora*) to 0.3 mm (*C. alata*) in depth (Fig. 4.4). The depth of the hydrenchyma is independent of CAM (Barrera Zambrano et al., 2014) as this tissue does not accumulate acids overnight (Fig. 4.6 and Fig. 4.7). Rather than providing space for organic acids synthesised in the CAM cycle, the primary role of succulent anatomy in the hydrenchyma is to increase the saturated water content (SWC) of leaves (Fig. 2.1; Fig. 2.5; Fig. 4.13), thereby providing hydraulic capacitance (Fig. 2.7). Despite hydrenchyma only making up a minority of total leaf depth, this tissue acts as a highly specialised water store; species with deeper hydrenchyma have higher absolute capacitance and are therefore able to effectively buffer the leaf against water loss (Fig. 2.8 and Fig. 2.9). The hydrenchyma layer is likely able to provide capacitance due to its low bulk modulus of elasticity (ϵ), which allows the cells to readily inflate and deflate in response to the water needs of the leaf (Fig. 2.10). In addition, capacitance may be aided by the high osmotic potential at full turgor (π_0) in the hydrenchyma, which establishes an osmotic gradient between this tissue layer and the chlorenchyma; thus driving the movement of water into the photosynthetic tissue as a leaf dehydrates (Fig. 4.8; Fig. 4.9; Fig. 4.12). However, the high π_0 in the hydrenchyma causes leaves to lose turgor at a less negative water potential, because their TLP is higher (Fig. 3.2 and Fig. 3.12). Therefore, a trade-off exists, where hydrenchyma buffers water potentials against dehydration, but as a

result makes the leaves more vulnerable to losing turgor, when dehydration does eventually occur. This trade-off may explain why hydrenchyma depth is not predicted by environmental water availability, as this drought avoidance strategy both prevents and makes leaves more vulnerable to low water potentials; two effects that would have antagonistic ecological consequences on species distributions (Fig. 4.1). It is possible that, due to this trade-off between capacitance and TLP, the primary ecological role of hydrenchyma is not to cope with long-term drought events over the course of weeks or months, but instead to dynamically buffer the leaf against diel changes in leaf water content that occur due to transpiration. More data is required to better understand if the ecophysiological function of hydrenchyma is to buffer the leaf over short time scales, but if this were true it may explain why hydrenchyma depth is higher in the humid, high elevation montane forests of Panama, which experience fluctuating cloud cover (Fig. 4.2 and Fig. 4.3).

7.3.2 The Ecophysiology of Succulent Chlorenchyma Tissue and Crassulacean Acid Metabolism

The chlorenchyma layer in *Clusia* is comprised of palisade and spongy mesophyll cells, although tissue succulence occurs predominantly in the former (Barrera Zambrano et al., 2014). Unlike hydrenchyma, greater tissue depth in the chlorenchyma, through the evolution of a deeper palisade layer, does not increase the SWC or capacitance of the leaf (Fig. 2.5; Fig. 2.6; Fig. 2.8; Fig. 2.9). This may be because species with greater tissue succulence in the chlorenchyma invest more in rigid cell walls, which would increase ϵ and prevent this form of succulence from providing capacitance to the leaf, although more data is needed to directly explore the cell wall anatomy associated with succulent chlorenchyma tissue. Nevertheless, it is clear that, in *Clusia*, chlorenchyma-based succulence does not confer capacitance, meaning the primary role of succulent anatomy in the chlorenchyma is to provide space for storage of organic acids required for the operation of CAM.

In *Clusia*, CAM involves the diel cycling of both malic and citric acids (Fig. 6.5 and Fig. 6.6) which are exclusively accumulated in the chlorenchyma (Fig. 4.6). The role of CAM is to minimise water loss, by restricting stomatal opening to the night, when vapour pressure deficits are lower (Fig. 4.11). As a result, the all-cell succulent species that engage in CAM experience lower rates of water loss (Fig. 2.11), and consequently require lower leaf VLA to

replace transpired water (Fig. 5.5). However, whilst CAM decreases the rate of water loss, species with this metabolic adaptation do not exhibit higher TLP values (Fig. 3.1), nor does their xylem vessel anatomy appear to be more vulnerable to embolism (Fig. 5.12 and Fig 5.13). Thus, the primary ecophysiological role of CAM is unlikely to be the prevention of hydraulic failure during drought; as CAM does not affect species' need to protect leaves against negative water potentials. If CAM did not evolve to prevent hydraulic failure in *Clusia*, it may instead be acting to minimise the symptoms of carbon starvation, as the employment of CAM allows plants to maintain higher core metabolic rates during drought. In *Clusia*, both photosynthetic and respiratory rates remain higher during drought if a plant can engage in CAM, compared to an obligate C₃ species (Fig. 6.1 to 6.4). In addition, the transcriptomic changes that accompany the induction of CAM are characterised by upregulation of genes that function in mitochondrial respiration (Table 6.2 and Table 6.3). This contrasts the transcriptomic C₃ drought response, which is characterised by maintenance and repair of photosystems (Appendix A; Table A.4). Therefore, the primary ecophysiological role of succulent chlorenchyma tissue in *Clusia* appears to be to facilitate CAM, which in turn prevents metabolic penalties from occurring during drought. Consequently, CAM is not a classic 'drought avoidance' strategy, as it can evolve without affecting the TLP (Fig. 3.1). In contrast to hydrenchyma, which prevents but also increases vulnerability to low water potentials, CAM confers a considerable metabolic benefit to plants during drought, without making leaf hydraulic physiology any more vulnerable to low water potentials. This may explain why CAM, and not hydrenchyma impacts the distribution of species into seasonally drier environmental niches (Fig. 4.1).

Taken together, the findings summarised above demonstrate that the two different succulent adaptations in the leaves of *Clusia* play distinctly different ecophysiological roles. These data confirm previous claims that succulence should not be considered a single trait, but rather a syndrome made up of multiple, non-overlapping adaptations, that each individually contribute to the drought response of a plant (Ogburn and Edwards, 2010).

7.4 Future work

More research is required both at an ecological, physiological and molecular level, to develop the findings outlined in this thesis. One question that remains open is the ecological role of hydrenchyma; as this tissue layer does not appear to be deeper in species from drier environmental niches. The data used to explore the ecological role of hydrenchyma did not distinguish between intraspecific trait variation and phenotypic plasticity. To overcome this, transplant experiments would be invaluable; by growing species where they naturally occur as well as in different ecosystems, it would be possible to explore the extent to which phenotypic plasticity affects hydrenchyma depth. The lowland tropical dry forests and montane cloud forests of Panama would be ideal sites to perform such transplant experiments, as species could be reciprocally grown in these two ecosystems to determine the extent to which phenotypic plasticity affects hydrenchyma development, and leaf capacitance.

From a physiological perspective, the role of cell wall elasticity in providing capacitance remains relatively unexplored. Whilst it was suggested that hydrenchyma have more elastic cell walls, this finding was inferred from an observation that species with a higher percentage of their leaf depth made up by hydrenchyma have lower values of ϵ (Fig. 2.10). It was not possible to directly measure ϵ in the different tissue layers, to confirm or refute this inference. Novel methods that use ultrasound signals to estimate ϵ in the different tissue layers of leaves would enable the comparison of cell wall properties in the hydrenchyma and chlorenchyma and would provide a more direct assessment of how ϵ varies in the different tissues of the leaf (Álvarez-Arena et al., 2018; Bidhendi and Geitmann, 2019). Furthermore, as the TLP can be calculated using just π_0 (Fig. 4.8 and Fig. 4.9) and ϵ (Equation 3.1), an estimate of the ϵ would allow for the calculation of the TLP in each tissue layer. It would be interesting to see if highly elastic cell walls in the hydrenchyma drive the TLP of this tissue up, as seems to occur in the central water storage tissue of *Agave*, *Pyrrhosia* and *Aloe* leaves (Schulte and Nobel, 1989; Ong et al., 1992; Ahl et al., 2019).

From a molecular perspective, the importance of nocturnal mitochondrial respiration for the functioning of CAM requires further work. Flux balance analysis modelling predicted that a greater flux through mitochondrial ATP synthase was required to drive the CAM cycle

at night (Shameer et al., 2018). This prediction was confirmed by physiological data, which showed an increased oxygen consumption rate in conjunction with the facultative induction of CAM (Fig 6.3 and Fig. 6.4). This increase in respiration appears to be under genetic control, as gene ontology enrichment analysis found that many of the genes upregulated concurrently with the induction of CAM function in the mitochondria (Table 6.2 and Table 6.3). To develop this work, isolation and analysis of the mitochondrial proteome would be invaluable, as this would demonstrate if proteins involved in mitochondrial respiration are more abundant in plants that do CAM.

7.5 References

- Ahl, L. I., Mravec, J., Jørgensen, B., Rudall, P. J., Rønsted, N., & Grace, O. M. (2019). Dynamics of intracellular mannan and cell wall folding in the drought responses of succulent Aloe species. *Plant Cell and Environment*, (March), 1–14. <https://doi.org/10.1111/pce.13560>
- Álvarez-Arenas, T. E. G., Sancho-Knapik, D., Peguero-Pina, J. J., Gómez-Arroyo, A., & Gil-Pelegrín, E. (2018). Non-contact ultrasonic resonant spectroscopy resolves the elastic properties of layered plant tissues. *Applied Physics Letters*, 113(25). <https://doi.org/10.1063/1.5064517>
- Barrera Zambrano, V. A., Lawson, T., Olmos, E., Fernández-García, N., & Borland, A. M. (2014). Leaf anatomical traits which accommodate the facultative engagement of crassulacean acid metabolism in tropical trees of the genus Clusia. *Journal of Experimental Botany*, 65(13), 3513–3523. <https://doi.org/10.1093/jxb/eru022>
- Bidhendi, A. J., & Geitmann, A. (2019). Methods to quantify primary plant cell wall mechanics. *Journal of Experimental Botany*, 70(14), 3615–3648. <https://doi.org/10.1093/jxb/erz281>
- Griffiths, H., Robe, W. E., Girnus, J., & Maxwell, K. (2008). Leaf succulence determines the interplay between carboxylase systems and light use during Crassulacean acid metabolism in Kalanchoë species. *Journal of Experimental Botany*, 59(7), 1851–1861. <https://doi.org/10.1093/jxb/ern085>
- Heyduk, K., Burrell, N., Lalani, F., & Leebens-Mack, J. (2016). Gas exchange and leaf anatomy of a C3-CAM hybrid, *Yucca gloriosa* (Asparagaceae). *Journal of Experimental Botany*, 67(5), 1369–1379. <https://doi.org/10.1093/jxb/erv536>
- Heyduk, K., McKain, M. R., Lalani, F., & Leebens-Mack, J. (2016). Evolution of a CAM anatomy predates the origins of Crassulacean acid metabolism in the Agavoideae (Asparagaceae). *Molecular Phylogenetics and Evolution*, 105, 102–113. <https://doi.org/10.1016/j.ympev.2016.08.018>

- Holtum, J. A. M., Aranda, J., Virgo, A., Gehrig, H. H., & Winter, K. (2004). $\delta^{13}\text{C}$ values and crassulacean acid metabolism in *Clusia* species from Panama. *Trees*, *18*, 658–668. <https://doi.org/10.1007/s00468-004-0342-y>
- Lüttge, U. (1999). One morphotype, three physiotypes: Sympatric species of *Clusia* with obligate C₃ photosynthesis, obligate CAM and C₃-CAM intermediate behaviour. *Plant Biology*, *1*(2), 138–148. <https://doi.org/10.1111/j.1438-8677.1999.tb00237.x>
- Maxwell, K., Von Caemmerer, S., & Evans, J. R. (1997). Is a low internal conductance to CO₂ diffusion a consequence of succulence in plants with crassulacean acid metabolism? *Australian Journal of Plant Physiology*, *24*(6), 777–786. <https://doi.org/10.1071/PP97088>
- Melcher, P. J., Holbrook, N. M., Burns, M. J., Zwieniecki, M. A., Cobb, A. R., Brodribb, T. J., ... Sack, L. (2012). Measurements of stem xylem hydraulic conductivity in the laboratory and field. *Methods in Ecology and Evolution*, *3*(4), 685–694. <https://doi.org/10.1111/j.2041-210X.2012.00204.x>
- Ogburn, R. M., & Edwards, E. J. (2010). The ecological water-use strategies of succulent plants. In J.-C. Kader & M. Delseny (Eds.), *Advances in Botanical Research* (1st ed., Vol. 55, pp. 179–225). <https://doi.org/10.1016/B978-0-12-380868-4.00004-1>
- Ong, B.-L., Koh, C. K.-K., & Wee, Y.-C. (1992). Changes in Cell Wall Structure of *Pyrrosia piloselloides* (L.) Price Leaf Cells During Water. *International Journal of Plant Sciences*, *153*(3), 329–332.
- Popp, M., Kramer, D., Lee, H., Diaz, M., Ziegler, H., & Liittge, U. (1987). Crassulacean acid metabolism in tropical dicotyledonous trees of the genus *Clusia*. *Trees*, *1*, 238–247.
- Schulte, P. J., & Nobel, P. S. (1989). Responses of a CAM Plant to Drought and Rainfall : Capacitance and Osmotic Pressure Influences on Water Movement. *Journal of Experimental Botany*, *40*(210), 61–70. Retrieved from <http://jxb.oxfordjournals.org/lookup/doi/10.1093/jxb/40.1.61>

- Scoffoni, C., Chatelet, D. S., Pasquet-Kok, J., Rawls, M., Donoghue, M. J., Edwards, E. J., & Sack, L. (2016). Hydraulic basis for the evolution of photosynthetic productivity. *Nature Plants*, 2(6), 1–8. <https://doi.org/10.1038/nplants.2016.72>
- Shameer, S., Baghalian, K., Cheung, C. Y. M., Ratcliffe, R. G., & Sweetlove, L. J. (2018). Computational analysis of the productivity potential of CAM. *Nature Plants*, 4(3), 165–171. <https://doi.org/10.1038/s41477-018-0112-2>
- Winter, K., Garcia, M., & Holtum, J. a. M. (2008). On the nature of facultative and constitutive CAM: environmental and developmental control of CAM expression during early growth of *Clusia*, *Kalanchoe*, and *Opuntia*. *Journal of Experimental Botany*, 59(7), 1829–1840. <https://doi.org/10.1093/jxb/ern080>
- Winter, K., & Holtum, J. A. M. (2014). Facultative crassulacean acid metabolism (CAM) plants: powerful tools for unravelling the functional elements of CAM photosynthesis. *Journal of Experimental Botany*, 65(13), 3425–3441. <https://doi.org/10.1093/jxb/eru063>

Appendix A. Gene Ontology Enrichment From Upregulated Genes in Each *Clusia* Species

Transcriptome data was interrogated to identify genes exhibiting a significantly higher steady state transcript abundance, in *C. pratensis* and in *C. tocuchensis*. For each species, these upregulated genes were analysed to find the gene ontology (GO) terms that were present more than expected by chance, based on the abundance of GO terms in the transcriptome assemblies. For each species, enriched GO terms pertaining to the cellular compartment (Table A.1 and A.2) and the biological process (Table A.3 and A.4) were identified. In each table, below, a column is present called 'Species' which describes whether that particular GO term is enriched in just the species being analysed, or if both *C. pratensis* and *C. tocuchensis*.

Table A.1) Significantly enriched 'Cellular Compartment' GO terms in genes upregulated after 20 days of drought in *C. pratensis*.

GO ID	GO Term	Abundance of GO Term in <i>C. pratensis</i> Transcriptome	Abundance in Upregulated <i>C. pratensis</i> Genes	Expected Abundance in Upregulated <i>C. pratensis</i> Genes	p-value	Species
GO:0048046	apoplast	92	26	10.28	1.30E-08	both
GO:0005618	cell wall	144	31	16.09	6.10E-08	both
GO:0005575	cellular_component	6843	1021	764.63	< 1e-30	both
GO:0009507	chloroplast	1508	261	168.5	1.20E-20	both
GO:0009941	chloroplast envelope	271	49	30.28	7.10E-07	both
GO:0009570	chloroplast stroma	309	64	34.53	3.60E-11	<i>C. pratensis</i>
GO:0009346	citrate lyase complex	2	2	0.22	0.00678	<i>C. pratensis</i>
GO:0005737	cytoplasm	4146	719	463.27	1.10E-30	both
GO:0005829	cytosol	793	162	88.61	2.40E-30	both
GO:0005783	endoplasmic reticulum	245	35	27.38	0.00101	both
GO:0005576	extracellular region	386	78	43.13	8.60E-08	both
GO:0005794	Golgi apparatus	383	52	42.8	0.00013	<i>C. pratensis</i>
GO:0016020	membrane	1774	311	198.22	1.10E-05	both
GO:0005740	mitochondrial envelope	106	44	11.84	0.00053	<i>C. pratensis</i>
GO:0005758	mitochondrial intermembrane space	2	2	0.22	0.00678	<i>C. pratensis</i>
GO:0000275	mitochondrial proton-transporting ATP synthase complex, catalytic core F(1)	3	3	0.34	0.00056	<i>C. pratensis</i>
GO:0005747	mitochondrial respiratory chain complex I	26	14	2.91	2.30E-09	<i>C. pratensis</i>
GO:0005749	mitochondrial respiratory chain complex II, succinate dehydrogenase complex (ubiquinone)	6	4	0.67	0.0006	<i>C. pratensis</i>
GO:0005750	mitochondrial respiratory chain complex III	6	5	0.67	2.10E-05	<i>C. pratensis</i>
GO:0005739	mitochondrion	997	216	111.4	4.00E-30	<i>C. pratensis</i>
GO:0005634	nucleus	2726	307	304.6	3.10E-10	both
GO:0005777	peroxisome	98	38	10.95	1.20E-17	<i>C. pratensis</i>
GO:0005886	plasma membrane	1156	196	129.17	1.10E-25	both
GO:0009506	plasmodesma	341	70	38.1	4.50E-13	<i>C. pratensis</i>
GO:0009536	plastid	1535	269	171.52	0.00015	<i>C. pratensis</i>
GO:0010319	stromule	15	5	1.68	0.0056	<i>C. pratensis</i>
GO:0005774	vacuolar membrane	226	55	25.25	2.20E-12	<i>C. pratensis</i>
GO:0005773	vacuole	365	87	40.78	1.40E-08	<i>C. pratensis</i>

Table A.2) Significantly enriched 'Cellular Compartment' GO terms in genes upregulated after 22 days of drought in *C. tocuchensis*.

GO ID	GO Term	Abundance of GO Term in <i>C. tocuchensis</i> Transcriptome	Abundance in Upregulated <i>C. tocuchensis</i> Genes	Expected Abundance in Upregulated <i>C. tocuchensis</i> Genes	p -value	Species
GO:0048046	apoplast	97	16	8.51	0.00179	both
GO:0005618	cell wall	150	28	13.15	0.0059	both
GO:0005575	Cellular component	6759	811	592.67	< 1e-30	both
GO:0009507	chloroplast	1575	197	138.11	1.30E-08	both
GO:0009941	chloroplast envelope	294	39	25.78	0.00014	both
GO:0030095	chloroplast photosystem II	11	6	0.96	5.20E-05	<i>C. tocuchensis</i>
GO:0009543	chloroplast thylakoid lumen	43	11	3.77	0.00021	<i>C. tocuchensis</i>
GO:0009535	chloroplast thylakoid membrane	197	39	17.27	1.50E-05	<i>C. tocuchensis</i>
GO:0005737	cytoplasm	3843	452	336.98	1.20E-11	both
GO:0005829	cytosol	610	64	53.49	0.00157	both
GO:0005783	endoplasmic reticulum	180	24	15.78	0.00532	both
GO:0005576	extracellular region	466	95	40.86	6.30E-19	both
GO:0030076	light-harvesting complex	14	6	1.23	0.00884	<i>C. tocuchensis</i>
GO:0016020	membrane	1675	195	146.87	0.00857	both
GO:0005634	nucleus	2696	312	236.4	3.20E-23	both
GO:0009783	photosystem II antenna complex	2	2	0.18	0.0054	<i>C. tocuchensis</i>
GO:0009654	photosystem II oxygen evolving complex	6	3	0.53	0.00669	<i>C. tocuchensis</i>
GO:0009505	plant-type cell wall	68	15	5.96	0.00025	<i>C. tocuchensis</i>
GO:0009705	plant-type vacuole membrane	29	7	2.54	0.00422	<i>C. tocuchensis</i>
GO:0005886	plasma membrane	1042	107	91.37	0.00033	both
GO:0010287	plastoglobule	39	11	3.42	7.90E-05	<i>C. tocuchensis</i>
GO:0009517	PSII associated light-harvesting complex II	2	2	0.18	0.0054	<i>C. tocuchensis</i>

Table A.3) Significantly enriched 'Biological Process' GO terms in genes upregulated after 20 days of drought in *C. pratensis*.

GO ID	GO Term	Abundance of GO Term in <i>C. pratensis</i> Transcriptome	Abundance in Upregulated <i>C. pratensis</i> Genes	Expected Abundance in Upregulated <i>C. pratensis</i> Genes	p-value	Species
GO:0009738	abscisic acid-activated signaling pathway	102	26	11.53	6.3E-07	both
GO:0006085	acetyl-CoA biosynthetic process	5	4	0.57	0.00022	<i>C. pratensis</i>
GO:0009060	aerobic respiration	28	19	3.16	4.3E-08	<i>C. pratensis</i>
GO:0007568	aging	62	15	7.01	0.00988	<i>C. pratensis</i>
GO:0043090	amino acid import	40	10	4.52	0.00313	<i>C. pratensis</i>
GO:0015696	ammonium transport	21	6	2.37	0.00576	<i>C. pratensis</i>
GO:0009072	aromatic amino acid family metabolic process	90	20	10.17	0.00267	<i>C. pratensis</i>
GO:0033345	asparagine catabolic process via L-aspartate	2	2	0.23	0.00682	<i>C. pratensis</i>
GO:0015802	basic amino acid transport	22	7	2.49	0.0044	<i>C. pratensis</i>
GO:0008150	biological_process	5945	892	671.88	< 1e-30	both
GO:0016132	brassinosteroid biosynthetic process	37	9	4.18	0.00259	both
GO:0006816	calcium ion transport	54	11	6.1	0.00407	<i>C. pratensis</i>
GO:0016117	carotenoid biosynthetic process	51	12	5.76	0.00504	<i>C. pratensis</i>
GO:0000902	cell morphogenesis	252	38	28.48	0.00156	<i>C. pratensis</i>
GO:0009932	cell tip growth	85	19	9.61	0.00228	both
GO:0043562	cellular response to nitrogen levels	17	6	1.92	0.00678	<i>C. pratensis</i>
GO:0016036	cellular response to phosphate starvation	61	14	6.89	0.00036	<i>C. pratensis</i>
GO:0015995	chlorophyll biosynthetic process	50	11	5.65	0.00215	<i>C. pratensis</i>
GO:0015996	chlorophyll catabolic process	34	15	3.84	2.1E-08	both
GO:0007623	circadian rhythm	58	15	6.55	0.0025	both
GO:0009108	coenzyme biosynthetic process	66	19	7.46	0.00497	<i>C. pratensis</i>
GO:0019344	cysteine biosynthetic process	67	15	7.57	0.0003	both
GO:0007010	cytoskeleton organization	240	25	27.12	0.00044	<i>C. pratensis</i>
GO:0042742	defense response to bacterium	158	33	17.86	0.000004	<i>C. pratensis</i>
GO:0006888	ER to Golgi vesicle-mediated transport	52	12	5.88	0.00088	<i>C. pratensis</i>
GO:0009873	ethylene-activated signaling pathway	50	15	5.65	0.000058	both
GO:0006635	fatty acid beta-oxidation	96	26	10.85	1.2E-07	<i>C. pratensis</i>
GO:0048444	floral organ morphogenesis	71	11	8.02	0.00922	<i>C. pratensis</i>
GO:0019375	galactolipid biosynthetic process	45	11	5.09	0.00085	<i>C. pratensis</i>
GO:0009450	gamma-aminobutyric acid catabolic process	2	2	0.23	0.00682	<i>C. pratensis</i>
GO:0006094	gluconeogenesis	102	28	11.53	7.9E-09	<i>C. pratensis</i>

GO:0010255	glucose mediated signaling pathway	2	2	0.23	0.00682	<i>C. pratensis</i>
GO:0019761	glucosinolate biosynthetic process	59	18	6.67	0.0000025	<i>C. pratensis</i>
GO:0006540	glutamate decarboxylation to succinate	2	2	0.23	0.00682	<i>C. pratensis</i>
GO:0006546	glycine catabolic process	22	8	2.49	0.00024	<i>C. pratensis</i>
GO:0006096	glycolytic process	115	43	13	2.6E-18	<i>C. pratensis</i>
GO:0006516	glycoprotein catabolic process	2	2	0.23	0.00682	<i>C. pratensis</i>
GO:0007030	Golgi organization	85	27	9.61	4.1E-10	<i>C. pratensis</i>
GO:0010286	heat acclimation	29	8	3.28	0.00188	<i>C. pratensis</i>
GO:0006972	hyperosmotic response	101	33	11.41	1.4E-09	<i>C. pratensis</i>
GO:0042538	hyperosmotic salinity response	54	14	6.1	0.000088	<i>C. pratensis</i>
GO:0006102	isocitrate metabolic process	5	4	0.57	0.00022	<i>C. pratensis</i>
GO:0019288	isopentenyl diphosphate biosynthetic process, methylerythritol 4-phosphate pathway	103	24	11.64	0.0000049	<i>C. pratensis</i>
GO:0009695	jasmonic acid biosynthetic process	54	13	6.1	0.00087	both
GO:0009867	jasmonic acid mediated signaling pathway	97	20	10.96	0.00018	<i>C. pratensis</i>
GO:0009106	lipoate metabolic process	19	7	2.15	0.00053	<i>C. pratensis</i>
GO:0000023	maltose metabolic process	77	21	8.7	0.0000018	<i>C. pratensis</i>
GO:0000165	MAPK cascade	78	14	8.82	0.00293	<i>C. pratensis</i>
GO:0008152	metabolic process	3459	547	390.92	0.000013	<i>C. pratensis</i>
GO:0019243	methylglyoxal catabolic process to D-lactate via S-lactoyl-glutathione	47	10	5.31	0.00436	<i>C. pratensis</i>
GO:0006120	mitochondrial electron transport, NADH to ubiquinone	5	3	0.57	0.00495	<i>C. pratensis</i>
GO:0007275	multicellular organism development	1341	177	151.55	0.00624	<i>C. pratensis</i>
GO:0043069	negative regulation of programmed cell death	76	14	8.59	0.00341	<i>C. pratensis</i>
GO:0009117	nucleotide metabolic process	359	83	40.57	0.00054	<i>C. pratensis</i>
GO:0055114	oxidation-reduction process	179	61	20.23	0.00092	<i>C. pratensis</i>
GO:0006733	oxidoreduction coenzyme metabolic process	208	67	23.51	0.00011	<i>C. pratensis</i>
GO:0031408	oxylipin biosynthetic process	12	6	1.36	0.00019	<i>C. pratensis</i>
GO:0019745	pentacyclic triterpenoid biosynthetic process	16	5	1.81	0.0077	<i>C. pratensis</i>
GO:0006098	pentose-phosphate shunt	66	19	7.46	9.1E-07	both
GO:0006817	phosphate ion transport	11	4	1.24	0.00953	<i>C. pratensis</i>
GO:0009853	photorespiration	79	39	8.93	3.5E-21	<i>C. pratensis</i>
GO:0015979	photosynthesis	113	14	12.77	0.00194	both

GO:0009638	phototropism	6	3	0.68	0.0093	both
GO:0009555	pollen development	119	18	13.45	0.00975	<i>C. pratensis</i>
GO:0010183	pollen tube guidance	4	3	0.45	0.00211	<i>C. pratensis</i>
GO:0000271	polysaccharide biosynthetic process	260	42	29.38	0.00723	both
GO:0009789	positive regulation of abscisic acid-activated signaling pathway	8	4	0.9	0.00247	<i>C. pratensis</i>
GO:0043085	positive regulation of catalytic activity	65	17	7.35	0.000024	<i>C. pratensis</i>
GO:0009939	positive regulation of gibberellic acid mediated signaling pathway	5	3	0.57	0.00495	<i>C. pratensis</i>
GO:0048578	positive regulation of long-day photoperiodism, flowering	2	2	0.23	0.00682	<i>C. pratensis</i>
GO:0010498	proteasomal protein catabolic process	111	26	12.54	0.000065	<i>C. pratensis</i>
GO:0043161	proteasome-mediated ubiquitin-dependent protein catabolic process	58	12	6.55	0.00348	<i>C. pratensis</i>
GO:0080129	proteasome core complex assembly	72	34	8.14	1.6E-18	<i>C. pratensis</i>
GO:0046777	protein autophosphorylation	65	18	7.35	0.0000033	<i>C. pratensis</i>
GO:0006457	protein folding	137	29	15.48	0.0000036	<i>C. pratensis</i>
GO:0006612	protein targeting to membrane	147	23	16.61	0.00211	<i>C. pratensis</i>
GO:0006508	proteolysis	408	94	46.11	0.0000019	both
GO:0010325	raffinose family oligosaccharide biosynthetic process	6	3	0.68	0.0093	<i>C. pratensis</i>
GO:0010359	regulation of anion channel activity	14	7	1.58	0.00019	<i>C. pratensis</i>
GO:0010310	regulation of hydrogen peroxide metabolic process	59	12	6.67	0.00279	both
GO:0019216	regulation of lipid metabolic process	24	9	2.71	0.00114	<i>C. pratensis</i>
GO:0010363	regulation of plant-type hypersensitive response	145	25	16.39	0.00068	both
GO:0032880	regulation of protein localization	20	6	2.26	0.00442	<i>C. pratensis</i>
GO:0010155	regulation of proton transport	27	10	3.05	0.000032	both
GO:0010029	regulation of seed germination	29	10	3.28	0.0008	<i>C. pratensis</i>
GO:0009737	response to abscisic acid	234	46	26.45	0.00296	<i>C. pratensis</i>
GO:0046685	response to arsenic-containing substance	14	8	1.58	0.000004	both
GO:0009733	response to auxin	127	24	14.35	0.000024	both
GO:0009617	response to bacterium	209	47	23.62	0.00089	<i>C. pratensis</i>
GO:0009637	response to blue light	39	11	4.41	0.00783	both
GO:0009741	response to brassinosteroid	30	6	3.39	0.00568	both
GO:0046686	response to cadmium ion	243	80	27.46	9.4E-29	<i>C. pratensis</i>
GO:0009409	response to cold	248	48	28.03	4.4E-10	both

GO:0009735	response to cytokinin	89	23	10.06	0.0000029	<i>C. pratensis</i>
GO:0034976	response to endoplasmic reticulum stress	149	28	16.84	0.000031	<i>C. pratensis</i>
GO:0009723	response to ethylene	124	31	14.01	0.0005	<i>C. pratensis</i>
GO:0010218	response to far red light	34	8	3.84	0.0055	both
GO:0009750	response to fructose	65	14	7.35	0.00071	<i>C. pratensis</i>
GO:0009620	response to fungus	174	32	19.66	0.00894	both
GO:0009739	response to gibberellin	43	14	4.86	0.00016	<i>C. pratensis</i>
GO:0009408	response to heat	122	32	13.79	2.9E-07	both
GO:0080027	response to herbivore	2	2	0.23	0.00682	<i>C. pratensis</i>
GO:0009644	response to high light intensity	100	24	11.3	0.0000014	both
GO:0042542	response to hydrogen peroxide	91	30	10.28	1.5E-11	both
GO:0001666	response to hypoxia	32	13	3.62	0.0000098	<i>C. pratensis</i>
GO:0080167	response to karrikin	49	12	5.54	0.00049	both
GO:0009416	response to light stimulus	494	81	55.83	0.00016	both
GO:0051788	response to misfolded protein	94	38	10.62	1.1E-17	<i>C. pratensis</i>
GO:0006979	response to oxidative stress	221	62	24.98	6.3E-08	both
GO:0010114	response to red light	31	9	3.5	0.00644	<i>C. pratensis</i>
GO:0009651	response to salt stress	334	85	37.75	3E-18	both
GO:0009744	response to sucrose	96	20	10.85	0.000091	both
GO:0009610	response to symbiotic fungus	19	7	2.15	0.00053	<i>C. pratensis</i>
GO:0009266	response to temperature stimulus	396	91	44.75	0.0000019	<i>C. pratensis</i>
GO:0009615	response to virus	101	8	11.41	0.00658	<i>C. pratensis</i>
GO:0009414	response to water deprivation	155	43	17.52	1.3E-12	both
GO:0009611	response to wounding	122	29	13.79	1.6E-07	both
GO:0010043	response to zinc ion	19	7	2.15	0.00053	<i>C. pratensis</i>
GO:0048767	root hair elongation	67	18	7.57	0.000024	both
GO:0019748	secondary metabolic process	229	59	25.88	0.00232	<i>C. pratensis</i>
GO:0010162	seed dormancy process	66	13	7.46	0.00554	<i>C. pratensis</i>
GO:0001887	selenium compound metabolic process	2	2	0.23	0.00682	<i>C. pratensis</i>
GO:0035725	sodium ion transmembrane transport	9	4	1.02	0.00416	<i>C. pratensis</i>
GO:0019252	starch biosynthetic process	90	26	10.17	8.4E-09	<i>C. pratensis</i>
GO:0005983	starch catabolic process	13	6	1.47	0.00032	<i>C. pratensis</i>
GO:0005982	starch metabolic process	106	33	11.98	0.00875	<i>C. pratensis</i>
GO:0016126	sterol biosynthetic process	63	13	7.12	0.00165	both
GO:0006790	sulfur compound metabolic process	250	60	28.25	0.00211	<i>C. pratensis</i>

GO:0009862	systemic acquired resistance, salicylic acid mediated signaling pathway	87	18	9.83	0.00022	<i>C. pratensis</i>
GO:0009407	toxin catabolic process	73	17	8.25	0.000071	<i>C. pratensis</i>
GO:0006099	tricarboxylic acid cycle	8	7	0.9	1.9E-07	<i>C. pratensis</i>
GO:0006511	ubiquitin-dependent protein catabolic process	159	53	17.97	6.1E-19	both
GO:0006636	unsaturated fatty acid biosynthetic process	30	12	3.39	0.0000098	<i>C. pratensis</i>
GO:0006212	uracil catabolic process	2	2	0.23	0.00682	<i>C. pratensis</i>
GO:0007033	vacuole organization	39	10	4.41	0.00098	<i>C. pratensis</i>
GO:0010189	vitamin E biosynthetic process	4	3	0.45	0.00211	<i>C. pratensis</i>
GO:0006766	vitamin metabolic process	41	13	4.63	0.00052	<i>C. pratensis</i>
GO:0006833	water transport	65	24	7.35	1.1E-09	<i>C. pratensis</i>

Table A.4) Significantly enriched 'Biological Process' GO terms in genes upregulated after 22 days of drought in *C. tocuchensis*.

GO ID	GO Term	Abundance of GO Term in <i>C. tocuchensis</i> Transcriptome	Abundance in Upregulated <i>C. tocuchensis</i> Genes	Expected Abundance in Upregulated <i>C. tocuchensis</i> Genes	p -value	Species
GO:0009738	abscisic acid-activated signaling pathway	90	17	8.04	0.00202	both
GO:0043447	alkane biosynthetic process	2	2	0.18	0.00559	<i>C. tocuchensis</i>
GO:0043481	anthocyanin accumulation in tissues in response to UV light	47	10	4.2	0.00211	<i>C. tocuchensis</i>
GO:0006914	autophagy	36	10	3.22	0.00052	<i>C. tocuchensis</i>
GO:0009926	auxin polar transport	39	8	3.49	0.00375	<i>C. tocuchensis</i>
GO:0008150	biological process	5876	720	525.08	< 1e-30	both
GO:0016132	brassinosteroid biosynthetic process	40	9	3.57	0.00613	both
GO:0009932	cell tip growth	91	16	8.13	0.00027	both
GO:0071555	cell wall organization	169	27	15.1	0.00527	<i>C. tocuchensis</i>
GO:0030003	cellular cation homeostasis	65	18	5.81	1.30E-08	<i>C. tocuchensis</i>
GO:0015996	chlorophyll catabolic process	39	13	3.49	2.70E-06	both
GO:0007623	circadian rhythm	72	16	6.43	0.00077	both
GO:0042335	cuticle development	20	8	1.79	0.00019	<i>C. tocuchensis</i>
GO:0019344	cysteine biosynthetic process	102	19	9.11	0.00017	both
GO:0070838	divalent metal ion transport	89	22	7.95	4.30E-07	<i>C. tocuchensis</i>
GO:0009819	drought recovery	4	3	0.36	0.00158	<i>C. tocuchensis</i>
GO:0009873	ethylene-activated signaling pathway	45	11	4.02	0.00028	both
GO:0010413	glucuronoxylan metabolic process	84	16	7.51	0.00042	<i>C. tocuchensis</i>
GO:0009695	jasmonic acid biosynthetic process	50	10	4.47	0.00341	both
GO:0010150	leaf senescence	31	8	2.77	0.00461	<i>C. tocuchensis</i>
GO:0009825	multidimensional cell growth	47	12	4.2	0.00019	<i>C. tocuchensis</i>
GO:0045892	negative regulation of transcription, DNA-templated	154	14	13.76	0.00127	<i>C. tocuchensis</i>
GO:0010196	nonphotochemical quenching	6	3	0.54	0.00703	<i>C. tocuchensis</i>
GO:0007389	pattern specification process	131	15	11.71	0.0026	<i>C. tocuchensis</i>
GO:0006098	pentose-phosphate shunt	106	16	9.47	0.00525	both
GO:0015979	photosynthesis	204	39	18.23	0.00845	both
GO:0019684	photosynthesis, light reaction	165	32	14.74	6.30E-05	<i>C. tocuchensis</i>
GO:0010206	photosystem II repair	6	3	0.54	0.00703	<i>C. tocuchensis</i>
GO:0042549	photosystem II stabilization	2	2	0.18	0.00559	<i>C. tocuchensis</i>
GO:0009638	phototropism	6	3	0.54	0.00703	both
GO:0009664	plant-type cell wall organization	86	16	7.68	0.00043	<i>C. tocuchensis</i>
GO:0000271	polysaccharide biosynthetic process	272	46	24.31	3.40E-07	both

GO:0009963	positive regulation of flavonoid biosynthetic process	40	10	3.57	0.00056	<i>C. tocuchensis</i>
GO:0045927	positive regulation of growth	3	3	0.27	0.00558	<i>C. tocuchensis</i>
GO:0006508	proteolysis	302	38	26.99	0.00178	both
GO:0008361	regulation of cell size	17	5	1.52	0.0067	<i>C. tocuchensis</i>
GO:0010310	regulation of hydrogen peroxide metabolic process	69	13	6.17	0.00159	both
GO:0010363	regulation of plant-type hypersensitive response	142	19	12.69	0.00934	both
GO:0035304	regulation of protein dephosphorylation	74	16	6.61	0.00027	<i>C. tocuchensis</i>
GO:0010155	regulation of proton transport	44	9	3.93	0.0046	both
GO:0006355	regulation of transcription, DNA-templated	665	78	59.42	6.30E-05	<i>C. tocuchensis</i>
GO:0046685	response to arsenic-containing substance	13	5	1.16	0.00179	both
GO:0009733	response to auxin	134	22	11.97	0.00277	both
GO:0009637	response to blue light	70	14	6.26	0.00248	both
GO:0009741	response to brassinosteroid	47	9	4.2	0.00198	both
GO:0010200	response to chitin	141	22	12.6	0.00075	<i>C. tocuchensis</i>
GO:0009409	response to cold	225	33	20.11	7.60E-07	both
GO:0010218	response to far red light	57	12	5.09	0.00086	both
GO:0009620	response to fungus	156	26	13.94	0.00054	both
GO:0009408	response to heat	114	19	10.19	0.00056	both
GO:0009644	response to high light intensity	97	23	8.67	7.60E-06	both
GO:0042542	response to hydrogen peroxide	75	16	6.7	0.00011	both
GO:0009753	response to jasmonic acid	165	27	14.74	9.70E-05	<i>C. tocuchensis</i>
GO:0080167	response to karrikin	46	12	4.11	0.0001	both
GO:0009416	response to light stimulus	497	81	44.41	2.50E-05	both
GO:0009612	response to mechanical stimulus	20	6	1.79	0.00268	<i>C. tocuchensis</i>
GO:0006979	response to oxidative stress	183	32	16.35	0.00122	both
GO:0009651	response to salt stress	297	46	26.54	3.00E-06	both
GO:0009744	response to sucrose	83	19	7.42	8.50E-06	both
GO:0009414	response to water deprivation	172	39	15.37	1.50E-07	both
GO:0009611	response to wounding	113	26	10.1	1.70E-07	both
GO:0048767	root hair elongation	74	16	6.61	0.00014	both
GO:0006364	rRNA processing	140	20	12.51	0.00737	<i>C. tocuchensis</i>
GO:0007165	signal transduction	531	84	47.45	0.0054	<i>C. tocuchensis</i>
GO:0016126	sterol biosynthetic process	53	11	4.74	0.00159	both
GO:0010118	stomatal movement	42	13	3.75	0.00173	<i>C. tocuchensis</i>
GO:0010027	thylakoid membrane organization	145	21	12.96	0.00253	<i>C. tocuchensis</i>
GO:0005992	trehalose biosynthetic process	9	5	0.8	0.00023	<i>C. tocuchensis</i>

GO:0006511	ubiquitin-dependent protein catabolic process	121	17	10.81	0.00268	both
GO:0000038	very long-chain fatty acid metabolic process	19	7	1.7	0.0003	<i>C. tocuchensis</i>
GO:0010025	wax biosynthetic process	10	5	0.89	0.00042	<i>C. tocuchensis</i>
GO:0045492	xylan biosynthetic process	84	16	7.51	0.00042	<i>C. tocuchensis</i>

Appendix B. *Clusia* Leaves Have Very Low Cuticular Conductance (g_{\min})

The minimal cuticular conductance (g_{\min}), when stomata are shut, was measured for 11 species of *Clusia*, to investigate if any relationship exists between CAM and g_{\min} . To measure g_{\min} , leaves were cut from the plant and hung up in a 25 °C constant-temperature room, under a fan, as outlined in (Sack and Scoffoni, 2010). Leaves were sequentially weighed every day, to determine the rate of water loss. The weight of leaves initially dropped quickly, due to water being lost through open stomata. However, after turgor was lost and the stomata shut, leaf weight fell in a linear fashion. Only data that fell on this linear portion of the line was used to calculate g_{\min} . For each species, $n = 12$. Upon completion of this experiment, no significant relationship was found between the percentage of photosynthesis done at night in well-watered plants and g_{\min} (Fig. A.1), suggesting that a species ability to do CAM does not affect its minimal cuticular conductance. Comparison of these data against measurements from other taxa shows that *Clusia* has very low g_{\min} . The range of g_{\min} values measured for *Clusia* was approx. 0.15 – 0.45 $\text{mmol m}^{-2} \text{s}^{-1}$, which falls in the low tail end of the distribution of g_{\min} values from a recent meta-analysis (Fig. A.2; from Duursma et al, 2018). Taken together, these data suggest that in *Clusia*, CAM has little effect on g_{\min} because g_{\min} is close to the physical minimum that plants can achieve.

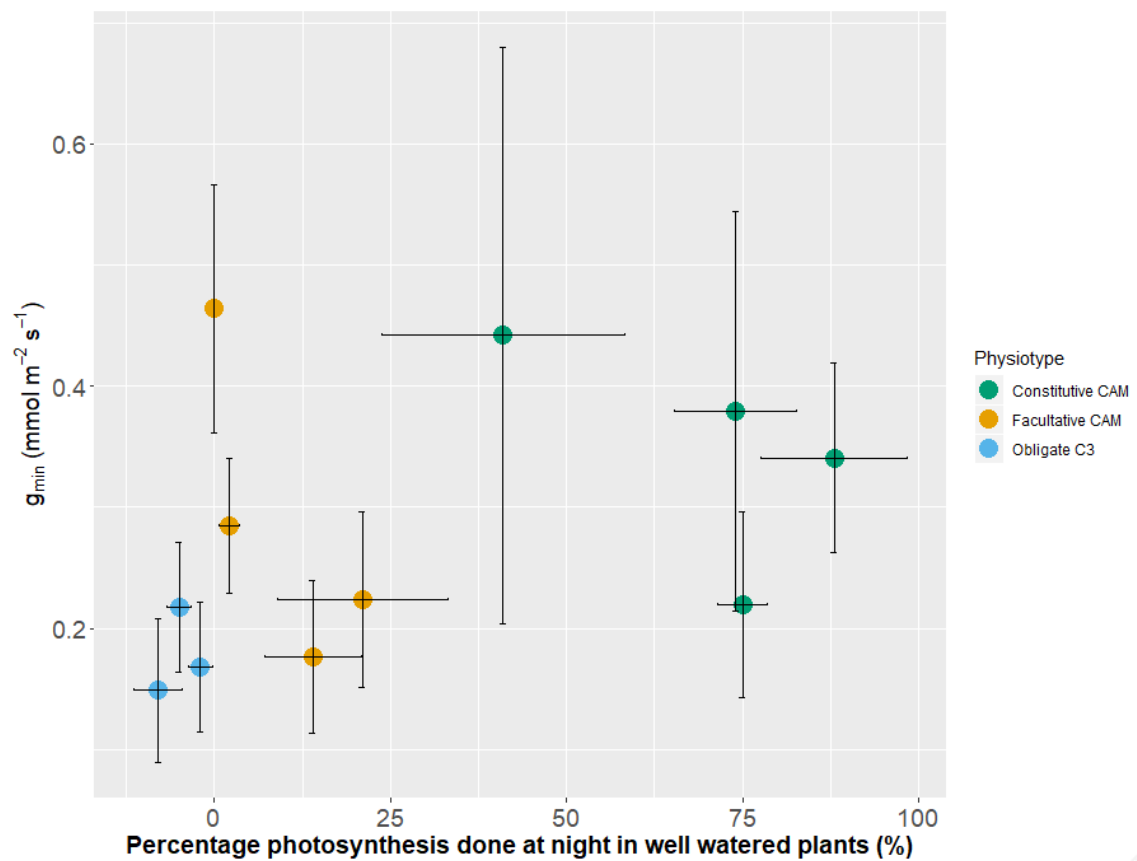


Fig. A.1) CAM does not affect cuticular conductance (g_{\min}) in *Clusia* leaves. No significant relationship was found between the percentage of CAM done in well-watered conditions and g_{\min} (Linear regression; $r^2 = 0.026$, $p = 0.290$). For each species, $n = 12$ and error bars represent ± 1 SD.

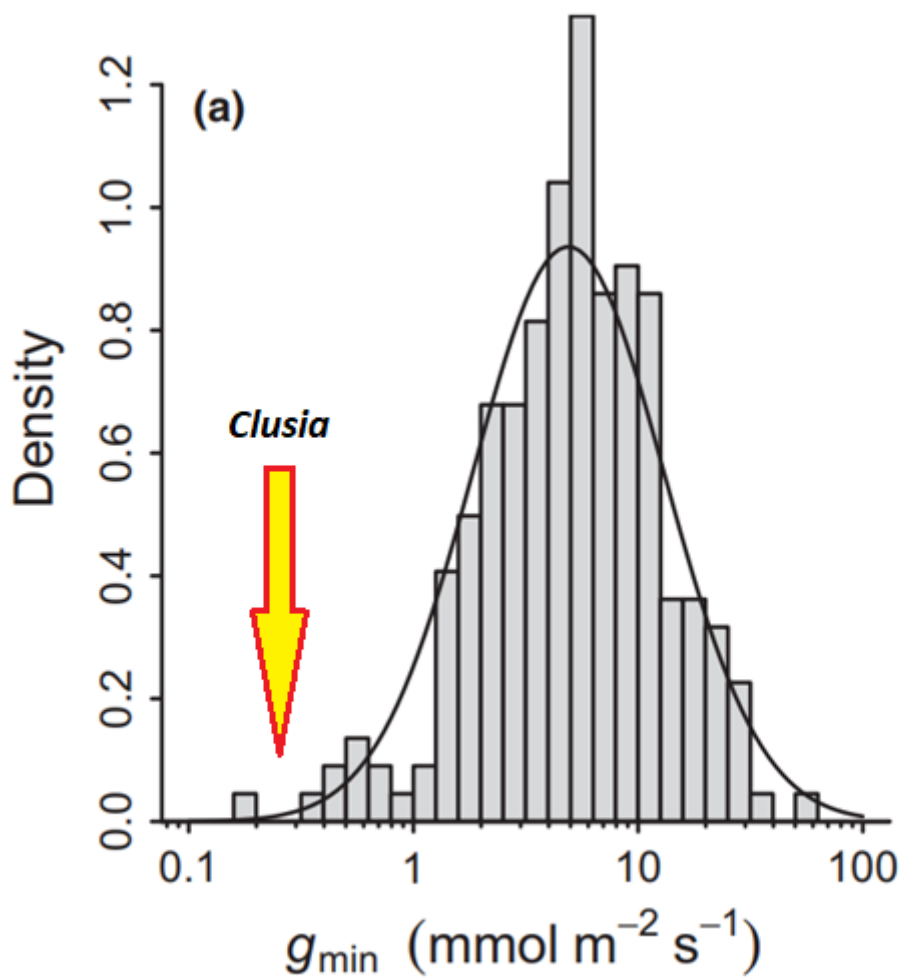


Fig. A.2) *Clusia* exhibits very low g_{\min} values, in comparison with data collected from a meta-analysis of all measured species. Graph shows the g_{\min} values from all measured species (adapted from Duursma et al, 2018), and arrow shows where the g_{\min} values for *Clusia* fall on this distribution.

References

- Sack, L., & Scoffoni, C. (2010). Minimum epidermal conductance (gmin, a.k.a. cuticular conductance). Retrieved August 15, 2017, from <http://prometheuswiki.publish.csiro.au/tiki-index.php?page=Minimum+epidermal+conductance+%28gmin,+a.k.a.+cuticular+conductance%29>
- Duursma, R. A., Blackman, C. J., López, R., Martin-StPaul, N. K., Cochard, H., & Medlyn, B. E. (2018). On the minimum leaf conductance: its role in models of plant water use, and ecological and environmental controls. *New Phytologist*. <https://doi.org/10.1111/nph.15395>